

**Short-Term Fluxes of Nitrous Oxide from Soil:
Measurement and Modelling**

by

**Conrad Philip Ashby
B.Sc., M.Sc.**

Thesis submitted to the University of Nottingham

for the degree of Doctor of Philosophy

September 1996



Dedication

To my parents

Acknowledgements

I would like to thank my supervisor Scott Young for his guidance and patience throughout the term of my PhD studies and beyond. Thanks are also due to John Corrie, Andrew Chester and Michael Gubbins for their technical assistance and to my friends and colleagues at Sutton Bonington who have always helped me where possible. In terms of non-academic support I would like to acknowledge the families Robb, Wilcock, Swift and Tarpey. Finally, I wish to express my gratitude to Fiona and my family, in particular Mum and Dad, for the continuous support, encouragement and understanding they have given over the years.

The financial assistance provided during the course of this study by the Natural Environmental Research Council is gratefully acknowledged.

Table Of Contents

List Of Figures.....	v
List Of Tables.....	x
Abstract.....	xiii

1. Introduction	1
1.1 Tiger Project	1
1.2 Aims And Objectives	1
1.3 The Greenhouse Effect	2
1.4 N₂O In The Atmosphere	4
1.4.1 N ₂ O Sinks	6
1.4.2 N ₂ O Sources	6
1.4.2.1 <i>Anthropogenic sources</i>	7
1.4.2.2 <i>Natural sources</i>	10
1.5 N₂O Emission From Soil	11
1.5.1 N ₂ O Emission From Denitrification	12
1.5.2 N ₂ O Emission From Nitrification	15
1.5.3 Effect Of N-Compounds On N ₂ O Evolution From Soil	18
1.5.4 Effect Of O ₂ Partial Pressure On N ₂ O Evolution From Soil	20
1.5.5 Effect Of Water Content On N ₂ O Evolution From Soil	22
1.5.6 Effect Of Organic Matter On N ₂ O Evolution From Soil	24
1.5.7 Effect Of Temperature On N ₂ O Evolution From Soil	26
1.5.8 Effect Of pH On N ₂ O Evolution From Soil	28
1.5.9 Effect Of Vegetation And Land Use On N ₂ O Evolution From Soil	31
1.5.10 Summary	33
1.6 Analysis Techniques For Quantifying N₂O Emission	35
2. General Materials And Methods	37
2.1 Automated Soil Headspace Gas Analyser	37
2.1.1 General Description Of The Gas Chromatograph	37
2.1.1.1 <i>The electron capture detector</i>	39
2.1.1.2 <i>GC column and column packing</i>	39
2.1.1.3 <i>Carrier and make-up gas supply</i>	40
2.1.1.4 <i>The automated gas sampling valve</i>	40
2.1.2 Soil Headspace Transfer Between Chambers And GC	41
2.1.2.1 <i>Circulation of chamber atmosphere</i>	41
2.1.2.2 <i>The incubator and gas tight chambers</i>	43
2.1.2.3 <i>Chamber-gas chromatograph link</i>	44
2.1.3 Calibration Of The Gas Chromatograph System	44
2.1.3.1 <i>Integration of the GC output</i>	44

2.1.3.2 GC-Integrator calibration.....	46
2.1.3.3 ECD calibration	47
2.1.4 Gas Tight Integrity Of The GC System.....	48
2.1.5 Co-ordination Of The GC Sampling Procedure	50
2.1.5.1 Gas Chromatograph-Integrator Link.....	50
2.1.5.2 Gas Chromatograph-Pump Link.....	50
2.1.6 Automated Continuous GC Running	51
2.1.7 Single Chamber Analysis	53
2.2 Soils	54
2.2.1 Soil Treatment And Storage	54
2.2.2 Re-packed Soil Core Construction	54
2.2.3 Soil Characteristics.....	56
2.2.4 Soil Analysis	57
2.2.4.1 Soil pH.....	57
2.2.4.2 Soil organic carbon content	57
2.2.4.3 Soil Moisture Characteristics	57
2.2.4.4 Particle size analysis.....	58
2.2.4.5 Nitrate and Ammonium determination.....	61
2.3 Earthworms.....	61
3. Modelling N₂O From Denitrification in Soil.....	62
3.1 Review Of N₂O Evolution Models	62
3.1.1 Introduction	62
3.1.2 Type Of Models Predicting Nitrogenous Gas Fluxes.....	63
3.1.3 Microscale Denitrification Models	64
3.1.4 Mesoscale Denitrification Models.....	67
3.1.5 Macroscale Denitrification Models	69
3.2 Model Principles And Assumptions	71
3.2.1 Model Aim.....	71
3.2.2 Model Principles	71
3.2.2.1 General model description	71
3.2.2.2 Soil water and gas filled porosity	73
3.2.2.3 N ₂ O equilibrium between water and gas phases.....	75
3.2.2.4 Initial N ₂ O concentration of the atmosphere.....	76
3.2.3 Enzyme Kinetic Theory	77
3.2.3.1 Denitrification rate	78
3.2.4 Diffusion Of Gases In Soil.....	80
3.2.4.1 Tortuosity.....	83
3.2.4.2 Compartment transfer of N ₂ O.....	84
4. Short-Term N₂O Flux Variability In Soil.....	90
4.1 The Effect Of Soil Aggregate Size On N₂O Fluxes.....	90
4.1.1 Introduction	90
4.1.2 Methods.....	91
4.1.2.1 Trial 1	91
4.1.2.2 Trial 2	92

4.1.3 Results	92
4.1.3.1 Trial 1	92
4.1.3.2 Trial 2	94
4.1.4 Discussion	96
4.2 The Effect Of Number And Size Of Soil Cores On N₂O Fluxes	104
4.2.1 Introduction	104
4.2.2 Method	104
4.2.2.1 5 core batch incubation	104
4.2.2.2 10 core batch incubation	105
4.2.3 Results	106
4.2.3.1 5 core batch incubation	106
4.2.3.2 10 core batch incubation	107
4.2.4 Discussion	109
4.3 The Effect Of Soil Core Water Content On N₂O Fluxes	116
4.3.1 Introduction	116
4.3.2 Method	116
4.3.3 Results And Discussion	117
4.3.3.1 General overview	117
4.3.3.2 Gaseous N ₂ O emissions from soil at different water contents.....	118
4.3.3.3 Gaseous CO ₂ emissions from soil at different water contents.....	120
4.3.3.4 Trends in mean gaseous emission rates from soil with increasing water content	121
4.4 Determination Of N₂O Source By Soil Core Dissection	129
4.4.1 Introduction	129
4.4.2 Method	129
4.4.3 Results And Discussion	130
4.5 The Effect Of Aggregate Homogenisation On N₂O Flux.....	133
4.5.1 Introduction	133
4.5.2 Method	133
4.5.3 Results And Discussion	134
4.6 Conclusions	137
5. Effect Of Faunal Residues On N₂O Flux	138
5.1 Effect Of Discrete Faunal Residues On N₂O Flux Under Unsaturated And Saturated Conditions.....	138
5.1.1 Introduction	138
5.1.2 Method	138
5.1.2.1 Unsaturated soil conditions	138
5.1.2.2 Saturated soil conditions	139
5.1.3 Results And Discussion	139
5.1.3.1 Unsaturated soil conditions:DFR amended & unamended soil cores	140
5.1.3.2 Saturated soil conditions: DFR amended & unamended soil cores....	142
5.2 Effect Of Discrete Faunal Residues And Fluctuating Water Table On N₂O Flux.....	149
5.2.1 Introduction	149
5.2.2 Method	149
5.2.3 Results And Discussion	152

5.2.3.1 General overview of N_2O and CO_2 emissions.....	152
5.2.3.2 Effect of soil water content on N_2O emission	153
5.2.3.3 Effect of soil water content on CO_2 emission	154
5.2.3.4 Effect of DFR incorporation on N_2O emission.....	158
5.2.3.5 Effect of DFR incorporation on CO_2 emission.....	164
5.2.3.6 Effect of DFR position on N_2O emission.....	164
5.2.3.7 Effect of DFR position on CO_2 emission.....	165
5.2.3.8 Effect of NO_3^- application on N_2O and CO_2 emission.....	165
5.2.3.9 N_2O and CO_2 concentration in soil water	167
5.2.3.10 N and C balance.....	169
5.3 Conclusions	173
6. Soil Water Content And N_2O Flux.....	174
6.1 Modelling The Effect Of Soil Flooding On N_2O Flux Rates.....	174
6.1.1 Introduction	174
6.1.2 Methods.....	174
6.1.3 Results And Discussion	178
6.1.3.1 Gaseous emissions from different aggregate sizes (Wick series)	178
6.1.3.2 Gaseous emissions from three contrasting soils (Wick series, Unclassified alluvium and Winton series; 2-5 mm aggregate size range)	183
6.2 Modelling The Effect Of Soil Flooding And Drainage On N_2O Emission Rates.....	192
6.2.1 Introduction	192
6.2.2 Method	192
6.2.2.1 Sequentially raising and lowering the soil core water table	192
6.2.2.2 Repetitive flooding and draining of soil on N_2O flux	193
6.2.3 Results And Discussion	194
6.2.3.1 N_2O and CO_2 emissions from soil cores affected by raising and lowering the water table.....	194
6.2.3.2 N_2O and CO_2 emissions from soil cores affected by repetitive flooding and draining	204
6.2.4 Modelling.....	210
6.3 Conclusions	214
General Discussion.....	216
Appendix.....	218
Bibliography.....	221

List Of Figures

- Figure 1.1 Simplified denitrification (dissimilatory nitrate reduction) pathway illustrating N transformations and the respective reducing enzymes..... 13
- Figure 1.2 Simplified autotrophic nitrification pathway illustrating the biochemical route to N₂O formation..... 16
- Figure 2.1 Experimental design of the soil headspace gas analyser..... 38
- Figure 2.2 Cross sectional view of the automatic gas sampling valve (GSV) labelled (9) in Fig. 2.1. Positions A and B show the configurations of the sampling loops and the sample lines. (----) represents the connective tubing between inlets and outlets of the GSV that undergo movement between positions A and B..... 42
- Figure 2.3 The two configurations of the 3-way taps (labelled (2) in Fig. 2.1). (a) = taps closed for circulation of chamber atmosphere; (b) = taps open for daily venting sequence..... 45
- Figure 2.4 Linearity of the ECD response to a range of standard concentrations of nitrous oxide (a, b and c) and carbon dioxide (d)..... 49
- Figure 2.5 Schematic of one of the smaller incubation chambers (*Kilner jars*)..... 53
- Figure 2.6 Schematic of manometer and water access tube construction, on core types *a* and *b*..... 55
- Figure 2.7 Soil moisture characteristic curves of the three test soils..... 60
- Figure 3.1 Schematic representation of the model showing four layers, each with a representative aggregate unit: (----) = N₂O diffusion pathway; (—) = denitrification pathway..... 74
- Figure 3.2 Initial velocity of reaction as a function of concentration of substrate S, for reactions (a) zero and (b) first order..... 78
- Figure 3.3 Schematic of in-situ transformations of NO₃⁻ and N₂O reduction and the flux of N₂O between the intra-aggregate pores in two shells through to the inter-aggregate pore (F_(A1,A2) and F_(A2,L1) respectively), (----) = N₂O diffusion pathway; (—) = denitrification pathway..... 81
- Figure 4.1 Cumulative N₂O flux from Trial 1 for soil cores re-packed with aggregates (Wick series) of diameter (a) 10-20 mm, (b) 5-10 mm and (c) 2-5 mm all with a bulk moisture content equivalent to 80 % F.C.. The arrow indicates the time of NO₃⁻ application. Closed symbols = replicate 1, open symbols = replicate 2..... 97

- Figure 4.2 Cumulative N₂O flux from Trial 2 for soil cores re-packed with aggregates (Wick series) of diameters (a) 10-20 mm, (b) 5-10 mm, (c) 2-5 mm and (d) < 2 mm, all with a bulk moisture content equivalent to 80 % F.C.. The arrow indicates the time of NO₃⁻ application. Closed symbols = replicate 1, open symbols = replicate 2.....98
- Figure 4.3 Cumulative CO₂ flux from Trial 2 for soil cores re-packed with aggregates (Wick series) of diameters (a) 10-20 mm, (b) 5-10 mm, (c) 2-5 mm and (d) < 2 mm, all with a bulk moisture content equivalent to 80 % F.C.. The arrow indicates the time of NO₃⁻ application. Closed symbols = replicate 1, open symbols = replicate 2.....99
- Figure 4.4 Mean of the average (a) N₂O and (b) CO₂ emission rates from Trials 1 and 2 expressed in table 4.1, for each aggregate size, at 80 % F.C.. Open symbols = - NO₃⁻, closed symbols = + NO₃⁻.....101
- Figure 4.5 Cumulative N₂O flux from replicate chambers each containing cores re-packed with different sized aggregates of the Wick series soil; (a) 5 cores in each chamber (2-5 mm), (b and c) 10 cores in each chamber (2-5 mm) and (d) 10 cores in each chamber (5-10 mm). The arrow indicates time of NO₃⁻ application. Closed symbols = replicate 1, open symbols = replicate 2.....110
- Figure 4.6 Cumulative CO₂ flux from replicate chambers each containing cores re-packed with different sized aggregates of the Wick series soil; (a) 5 cores in each chamber (2-5 mm), (b and c) 10 cores in each chamber (2-5 mm) and (d) 10 cores in each chamber (5-10 mm). The arrow indicates time of NO₃⁻ application. Closed symbols = replicate 1, open symbols = replicate 2.....111
- Figure 4.7 Cumulative N₂O flux from replicate gas-tight chambers each containing 10 re-packed cores containing 2-5 mm size aggregates from the Wick series, at different soil moisture contents. (a) = 49 % F.C.; (b) = 73 % F.C.; (c) = 87 % F.C.; (d) = 133 % F.C.. Closed symbols = replicate 1; open symbols = replicate 2. The arrow indicates time of NO₃⁻ application. (-----) = period of individual incubation.....122
- Figure 4.8 Cumulative CO₂ flux from replicate gas-tight chambers each containing 10 re-packed cores containing 2-5 mm size aggregates from the Wick series, at different soil moisture contents. (a) = 49 % F.C.; (b) = 73 % F.C.; (c) = 87 % F.C.; (d) = 133 % F.C.. Closed symbols = replicate 1; open symbols = replicate 2. The arrow indicates time of NO₃⁻ application. (-----) = period of individual incubation.....123
- Figure. 4.9 Mean chamber (a) N₂O and (b) CO₂ fluxes from 20 re-packed soil cores at different soil moisture contents, with and without NO₃⁻ application.....128
- Figure 4.10 Schematic of the progressive division of an unsaturated re-packed soil core to isolate the portion of soil core responsible for the bulk of the N₂O evolution.....130

- Figure 4.11 Illustration of the respective sections of the partitioned soil core volume: associated with (a) the relative proportion of total N_2O produced by the core as a whole after the final partitioning; and (b) the relative N_2O concentration per unit mass of soil per unit time..... 132
- Figure 4.12 Cumulative N_2O flux from 2 replicate chambers, each containing 10 cores of homogenized soil aggregates, with and without NO_3^- treatment. The arrow indicates the point at which the NO_3^- was applied. Closed symbols = replicate 1, open symbols = replicate 2 (67-134 hours = period of individual incubation).... 136
- Figure 5.1 Cumulative N_2O flux from soil cores re-packed with aggregates from the Wick series (< 2 mm diameter) at (a) 75 % F.C. and (b) under saturated conditions. Three cores are amended with dead Earthworms (W1,W2,W3) and three are unamended controls (C1, C2, C3)..... 145
- Figure 5.2 Cumulative CO_2 flux from soil cores re-packed with aggregates from the Wick series (< 2 mm diameter) at (a) 75 % F.C. and (b) under saturated conditions. Three cores are amended with dead Earthworms (W1,W2,W3) and three are unamended controls (C1, C2, C3)..... 146
- Figure 5.3 Schematic of core configurations (described in section 5.2.2) of 2 main treatments, with (+N) and without (-N) NO_3^- , each treatment containing 4 sub treatments including the control and 3 DFR amendments (W1 (1.0 g), W2 (2.0 g), and W3 (2.0 g))..... 151
- Figure 5.4 Cumulative N_2O flux from cores re-packed with aggregates from the Wick series soil (< 2 mm diameter) which were treated with DFR (W1,W2,W3) under variable soil water contents denoted as steps 1, 2, 3 and 4. (a) = unamended (- NO_3^-) and (b) = amended (+ NO_3^-) with KNO_3 155
- Figure 5.5 Cumulative CO_2 flux from cores re-packed with aggregates from the Wick series soil (< 2 mm diameter) which were treated with DFR (W1,W2,W3) under variable soil water contents denoted as steps 1, 2, 3 and 4. (a) = unamended (- NO_3^-) and (b) = amended (+ NO_3^-) with KNO_3 156
- Figure 5.6 Difference (Δ) between the cumulative N_2O flux from control cores and both W1 and W2. (a) = unamended (- NO_3^-) and (b) = amended (+ NO_3^-) with KNO_3 . Cores were re-packed with aggregates from the Wick series soil (< 2 mm diameter) and incubated under variable soil water contents denoted as steps 1, 2, 3 and 4..... 161
- Figure 5.7 Ratio of mean N_2O emission rates of control cores and DFR treatments. (a) = unamended (- NO_3^-) and (b) = amended (+ NO_3^-) with KNO_3 . Cores were re-packed with aggregates from the Wick series soil (< 2 mm diameter). Time periods (x-axis) are denoted as steps 1, 2, 3, 4, 5 and 6..... 162

Figure 5.8 Difference (Δ) between the cumulative CO₂ flux from control cores and both W1 and W2. (a) = unamended (-NO₃⁻) and (b) = amended (+NO₃⁻) with KNO₃. Cores were re-packed with aggregates from the Wick series soil (< 2 mm diameter) and incubated under variable soil water contents denoted as steps 1, 2, 3 and 4.....163

Figure 5.9 Difference between the cumulative gaseous emissions of (a) N₂O and (b) CO₂ from treatments W3 and W2 (W3-W2). Cores were re-packed with aggregates from the Wick series soil (< 2 mm diameter) and incubated under variable soil water contents, denoted as 1, 2, 3 and 4.....166

Figure 5.10 Difference (Δ) between the cumulative (a) N₂O and (b) CO₂ emissions from cores unamended (-NO₃⁻) and amended (+NO₃⁻) with KNO₃. Cores were re-packed with aggregates from the Wick series soil (< 2 mm diameter) treated with DFR under variable soil water contents denoted as 1, 2, 3 and 4.....168

Figure 5.11 Concentration of (a) N₂O and (b) CO₂ in soil water drained from unamended and NO₃⁻ amended cores (including the control, W1, W2 and W3 sub-treatments).....171

Figure 6.1 Observed mean cumulative and model predicted N₂O flux from replicate gas-tight chambers containing a single core re-packed with (a) < 2 mm, (b) 2-5 mm, (c) 5-10 mm and (d) 10-20 mm aggregates of the Wick series soil. The cores were incubated under variable soil water contents, denoted as 1, 2, 3 and 4. (***) = $P < 0.05$)......180

Figure 6.2 Observed cumulative CO₂ flux from replicate gas-tight chambers containing a single core re-packed with (a) < 2 mm, (b) 2-5 mm, (c) 5-10 mm and (d) 10-20 mm aggregates of the Wick series soil. The cores were incubated under variable soil water contents denoted as 1, 2, 3 and 4.....181

Figure 6.3 Cumulative N₂O (a and b) and CO₂ (c and d) emissions from replicate gas-tight chambers containing a single core re-packed with 2-5 mm size aggregates of the unclassified alluvium (a and c) and Winton series (b and d) soils. The soils were incubated under variable water contents denoted as 1, 2, 3 and 4. (***) = $P < 0.05$)......186

Figure 6.4 Relationship between N₂O flux rate from the three contrasting soils and (a) % clay fraction and (b) % organic matter, at 100 % F.C.....188

Figure 6.5 Relationship between N₂O flux rate from the three contrasting soils and pH under saturated conditions.....188

Figure 6.6 Relationship between CO₂ flux rate from the three contrasting soils and (a) % organic matter (at 100 % F.C.) and (b) pH (under saturated conditions).....189

Figure 6.7 Observed and predicted cumulative N₂O flux from soil under unsaturated and saturated conditions. The arrow represents the point of saturation.....190

Figure 6.8 Example of predicted cumulative N₂O flux from soil under unsaturated and saturated conditions. The arrow represents the point of saturation. (a) = model predictions with aggregates constructed with a different outer shell thickness (25 % of aggregate radius), (b) = model predictions with aggregates constructed with the same outer shell thickness.....190

Figure 6.9 Cumulative N₂O flux from (a) Wick series (b) Alluvium and (c) Winton series soil (cores re-packed with 2-5 mm diameter aggregates) under a water table (WT) of variable height denoted as steps 1-7.....198

Figure 6.10 Cumulative CO₂ emission from (a) Wick series (b) Alluvium and (c) Winton series soil (cores re-packed with 2-5 mm diameter aggregates) under a water table (WT) of variable height denoted as steps 1-7.....199

Figure 6.11 N₂O emission rate from (a) Wick series (b) Alluvium and (c) Winton series soil (cores re-packed with 2-5 mm diameter aggregates) which have been incubated under a water table (WT) of variable height.....202

Figure 6.12 CO₂ emission rate from (a) Wick series (b) Alluvium and (c) Winton series soil (cores re-packed with 2-5 mm diameter aggregates) which have been incubated under a water table (WT) of variable height.....203

Figure 6.13 Mean N₂O emission rates at each stage during the progressive flooding and subsequent draining events (excluding the initial 24 hours after each change in water table height) for the three contrasting soils.....204

Figure 6.14 Cumulative (a) N₂O and (b) CO₂ flux from cores re-packed with aggregates from the Wick series soil (2-5 mm diameter aggregates) which have been incubated during repetitive flooding and draining cycles (2 h sampling rate).....206

Figure 6.15 Rate of (a) N₂O and (b) CO₂ emissions from cores re-packed with aggregates from the Wick series soil (2-5 mm diameter aggregates) which have been incubated during repetitive flooding and draining cycles (2 h sampling rate).....207

Figure 6.16 Relationship between the peak emission rates of N₂O during the aggregate de-gassing events (period 2) and the time the core was (a) flooded and (b) drained. The graphs include regression lines with and without the anomalous rate that occurred at 560 h.....209

Figure 6.17 Observed and predicted cumulative N₂O flux from Wick series soil which has undergone a sequential rise and fall in the water table. (a) 4 layer model simulation (magnified) (b) 4 layer model simulation (c) 4 and 16 layer model simulations.....213

List Of Tables

Table 1.1 Summary of factors which affect the N ₂ :N ₂ O ratio from both denitrification and nitrification (adapted from Sahrawat and Keeney, 1986; Firestone and Davidson, 1989).....	34
Table 2.1 Timed events table of the GC during calibration and manual analysis of gas samples.....	47
Table 2.2 Parameter values of the GC during calibration and manual analysis of gas samples.....	47
Table 2.3 Timed events table for automated analysis of two chamber atmospheres....	52
Table 2.4 Characteristics of each of the three test soils.	56
Table 3.1 List of model parameters.....	72
Table 4.1 Mean hourly N ₂ O emission rates for each replicate re-packed core from Trials 1 and 2, with and without NO ₃ ⁻ amendment. Aggregate sizes include < 2 mm, 2-5 mm, 5-10 mm and 10-20 mm respectively.....	100
Table 4.2 Mean hourly CO ₂ emission rates for each replicate re-packed core from Trial 2, with and without NO ₃ ⁻ amendment. Aggregate sizes include < 2 mm, 2-5 mm, 5-10 mm and 10-20 mm respectively.	100
Table 4.3 Mean hourly N ₂ O and CO ₂ emission rates with and without NO ₃ ⁻ amendment from two replicate chambers containing either 5 or 10 cores re-packed with either 2-5 mm or 5-10 mm diameter aggregates.....	112
Table 4.4 Mean hourly N ₂ O emission rates from 10 individually incubated soil cores, that were previously 2 x 5 core batches. Each core was re-packed with aggregates from the Wick series (2-5 mm aggregate diameter)	112
Table 4.5 Mean hourly N ₂ O emission rates from 20 individually incubated soil cores, that were previously 2 x 10 core batches; I = 2-5 mm diameter aggregates II = 2-5 mm diameter aggregates III = 5-10 mm diameter aggregates.....	113
Table 4.6 Mean CO ₂ and N ₂ O emission rates from different sized re-packed cores as related to the related to the surface area to volume ratio of the cores within each chamber.....	113
Table 4.7 Mean emission rate of N ₂ O and CO ₂ from re-packed cores containing 2-5 mm diameter aggregates from the Wick soil series. Each replicate chamber contained 10 re-packed cores at different water contents, that were equivalent to 49 %, 73 %, 87 % or 133 % F.C. and treated with and without NO ₃ ⁻	124

Table 4.8 Mean N₂O emission rates from 2 x 10-cores incubated individually in 20 chambers with and without NO₃⁻. Each 2 x 10-core batch was incubated at water contents equivalent to either 49, 73, 87 or 133 % F.C.....125

Table 4.9 Mean CO₂ emission rates from 2 x 10-cores incubated individually in 20 chambers with and without NO₃⁻. Each 2 x 10-core batch was incubated at water contents equivalent to either 49, 73, 87 or 133 % F.C.....126

Table 4.10 Relative proportion of N₂O emitted from the successive soil sectioning of the bulk N₂O producing partitions of an unsaturated re-packed soil core.....132

Table 4.11 Mean N₂O emission rates from 20 cores of homogenized aggregates incubated in 2 batches, with and without NO₃⁻ (-NO₃⁻ = 0-67 h + NO₃⁻ = 134-201 h).....136

Table 4.12 Mean N₂O emission rates from 20 cores of slurried Wick soil incubated individually with and without NO₃⁻ (-NO₃⁻ = 67-134 h; + NO₃⁻ = 201-268 h)...136

Table 5.1 Mean N₂O emission rates from cores re-packed with Wick series soil (< 2 mm diameter aggregates) at 75 % F.C.. Three cores were amended with dead Earthworms (W1,W2,W3) and three were unamended (C1,C2,C3).....147

Table 5.2 Mean CO₂ emission rates from cores re-packed with Wick series soil (< 2 mm diameter aggregates) at 75 % F.C.. Three cores were amended with dead Earthworms (W1,W2,W3) and three were unamended (C1,C2,C3).....147

Table 5.3 Concentration of NO₃⁻-N and NH₄⁺-N in 6 soil cores re-packed with aggregates of the Wick series (< 2 mm diameter) that were treated with (W1,W2,W3) and without (C1,C2,C3) dead Earthworms under saturated and unsaturated conditions after 40 days incubation.148

Table 5.4 Sequence of events applied to each core as described in section 5.2.2151

Table 5.5 Mean emission rates of (a) N₂O and (b) CO₂ from cores treated with and without both DFR (W1,W2,W3) and NO₃⁻ amendments during sequential raising and lowering of the soil water content.....157

Table 5.6 Mean concentration of NO₃⁻-N and NH₄⁺-N from replicated soil cores, re-packed with aggregates of the Wick series soil (< 2 mm diameter) after about 36 days incubation at different soil water contents. The soils were treated with and without NO₃⁻ and with increasing mass of DFR (W1,W2,W3).....172

Table 5.7 Measured fractions of N from each soil core treatment that had undergone a sequential raising and lowering of the soil water content.....172

Table 5.8 Measured fractions of C from each soil core treatment that had undergone sequential raising and lowering of the soil water content.....172

Table 6.1 Mean (a) N₂O and (b) CO₂ emission rates from 2 replicate chambers, each containing a single core filled with one of four aggregate sizes, for 3 contrasting soils subjected to a progressive increase in soil water content.....182

Table 6.2 The mean NO₃⁻ concentration in the three test soils prior to and following each incubation.....187

Table 6.3 Parameter values derived from the literature and generated by optimization of the model for each of the three test soils.....191

Table 6.4 Mean (a) N₂O and (b) CO₂ emission rate from cores re-packed with 3 different soils, that have undergone changes in core water table height.....200

Table 6.5 The mean NO₃⁻ and NH₄⁺ concentration in all the test soils prior to and following each incubation.....201

Table 6.6 Mean N₂O and CO₂ emission rates from cores repacked with Wick series soil (2-5 mm diameter aggregates) that had undergone repetitive flooding and draining cycles (shaded areas represent the 24 hour period after the lowering of the water table).....208

Table 6.7 Mean of the average N₂O and CO₂ flux rates for the three periods defined during the repetitive flooding and draining of the soil. Periods 1, 2 and 3 represent flooded conditions, the 24 h following draining (encompassing *de-gassing*) and the remaining drained period respectively.....209

Abstract

Gaseous nitrous oxide (N₂O) undergoes physical and chemical reactions in the atmosphere, contributing to both global warming and the catalytic destruction of stratospheric ozone. This chemically reactive greenhouse gas is produced both naturally and anthropogenically. The greatest source of N₂O is from the microbial transformation of N compounds during the processes of nitrification and denitrification in natural and cultivated soils. However, there is some uncertainty in the strength of these emission sources. Therefore one of the directives of the *Terrestrial Initiative in Global Environmental Research* programme, of which the following work was a part, was to elucidate the factors which influence the emission rates of N₂O from these systems. It is essential that these factors are quantified, in order to correctly assess the effect of N₂O as an environmental determinant.

A reliable automated soil core headspace gas analyser system for the continuous measurement of N₂O at the laboratory scale was developed. The system determined N₂O evolution rates from reconstructed soil cores consisting of re-packed aggregates of known diameters, incubated under different environmental conditions. There was an increase in N₂O emission rate (range = 0.5-61 x 10⁻⁷ mol N m⁻² h⁻¹) with aggregate size, soil NO₃⁻ concentration and soil water content under unsaturated conditions. However, the extent of these trends was masked by the variability in emission rates. One source of variability in N₂O emissions from unsaturated soil, was related to localized organic (e.g. faunal) residues. Subsequent investigations involving the incorporation of discrete faunal residues, DFRs (dead Earthworms), was found to greatly stimulate N₂O emission from unsaturated re-packed soil cores. These N₂O emission rates approached those attained when the soil was under saturated conditions, which were up to 3 orders of magnitude greater than emission rates from unamended, unsaturated soil. There was no apparent influence of DFR on N₂O emissions from soil under saturated conditions suggesting that the effect of DFRs under aerobic conditions was the creation of localized anoxic zones.

N₂O emission rates increased with increasing soil water content reaching a maximum under fully saturated conditions for three different soils (range = 0.25-1.8 x 10⁻⁴ mol N m⁻² h⁻¹). The emissions of N₂O from the three soils were different under both unsaturated and saturated conditions and appeared to be related to soil parameters, specifically organic matter content, clay content and soil pH. The contrast in rates of N₂O emission from unsaturated and saturated soil prompted a test of the hypothesis that wetting/drainage cycles increase the total emission rate. During the saturated phase, N₂O is produced, but its egress is restricted by saturated transmission pores. Rapid drainage causes a flush of N₂O from saturated aggregates by providing open emission channels. The rapid increase in N₂O flux that was observed during the draining of saturated soil occurred in all three soil types (range = 1-5 x 10⁻³ mol N m⁻² h⁻¹). This almost instantaneous N₂O pulse, which in some cases lasted less than 2 hours, occurred repeatedly, emitting similar rates of N₂O during 10 cycles of flooding and draining.

An attempt was made to simulate N₂O emission using the results gained from these investigations to parameterize a reaction-diffusion model. The model successfully predicted N₂O emission from soil undergoing a transformation from unsaturated to saturated conditions. However, model deficiencies were found during simulations involving the sequential rise and fall in water table height. The inability of the model to accurately predict the rapid increase in flux that occurred following core drainage, exposed gaps in knowledge and areas of future research regarding the short-term fluxes of N₂O from soil.

Chapter 1: Introduction

1.1 TIGER PROJECT

The research undertaken was part of the Terrestrial Initiative in Global Environmental Research (TIGER). The TIGER programme had two main objectives: firstly, to understand in greater detail the structure and functioning of terrestrial ecosystems and to be able to predict their response to environmental change; secondly, to synthesise models which will link terrestrial systems to the atmosphere and so improve understanding of terrestrial feedback mechanisms in global change. TIGER was composed of four components: TIGER 1, Carbon cycling on land; TIGER 2, Trace greenhouse gas emissions; TIGER 3, Energy and water budget; and TIGER 4, Ecosystem impacts.

The following thesis was undertaken as part of the TIGER 2 programme. One of the principle aims of TIGER 2 was to elucidate the natural environmental factors which control nitrous oxide emissions.

1.2 AIMS AND OBJECTIVES

The main practical objective of the project was to develop a reliable automated soil headspace gas analyser system for continuous short-term measurement of N₂O at the laboratory scale. The principle aim of the research was to determine N₂O evolution rates from reconstructed soil cores incubated under different environmental conditions. The cores consisted of re-packed aggregates of known diameters from soil at Sutton Bonington and two other soils used by other workers from the TIGER 2 consortium. The results obtained from the investigations were used to develop and parameterize a model to predict N₂O evolution from soils.

1.3 THE GREENHOUSE EFFECT

The *Greenhouse effect* has been reviewed in detail in the literature, (Bouwman, 1990; Wild 1993; Houghton *et al.*, 1990; Houghton *et al.*, 1992; Houghton *et al.*, 1995) and will therefore only be described briefly.

The energy that drives the climate on Earth is derived primarily from the interception of solar radiation. The wavelengths of solar radiation is dictated by the surface temperature of the sun and range between 0.2 and 4 μm , which spans the near ultraviolet (9 %), visible (41 %) and near infra-red (50 %) parts of the spectrum (Wild, 1993; Monteith and Unsworth, 1990). Almost one third of this radiation is reflected back into space, with the rest being absorbed by the different components of the Earth's biosphere, such as the atmosphere, oceans and land. The energy absorbed from solar radiation is counterbalanced by the re-emission of radiation from the Earth and its atmosphere. This terrestrial outgoing radiation takes the form of long wave infra-red energy (5-100 μm) the intensity of which is determined by the temperature of the Earth-atmosphere system.

There are several factors of natural origin that can change the Earth's delicate energy balance of absorbance and emittance (Houghton *et al.*, 1995). These include the change in energy output from the sun, the amount of aerosols in the atmosphere which can absorb and reflect radiation, seasonal changes, and the *Greenhouse effect*.

The now widely accepted *Greenhouse theory* was first proposed in 1827 by French mathematician Jean Baptiste Fourier. The term *Greenhouse effect* conveys the idea that the Earth's surface would be considerably cooler than it would be without the atmosphere. However, it is really a misnomer as a greenhouse prevents convective heat loss, analogous to a cloud blanket preventing frost formation, which is quite separate from the radiative heating of the atmosphere.

Short wave solar radiation can pass through the atmosphere relatively unimpeded, while long wave terrestrial radiation emitted by the surface of the earth is partially absorbed and re-emitted by a number of trace or *greenhouse gases* in the atmosphere. Due to this energy

absorbance, both the atmosphere and the surface of the earth remain warmer than they would be without the greenhouse gases.

Without the current concentration of greenhouse gases the earth would act like a true *black body*, and the effective radiating temperature of the planet would be about $-18\text{ }^{\circ}\text{C}$ as opposed to its current $+15\text{ }^{\circ}\text{C}$. About 70-90 % of the terrestrial radiation emitted from the Earth's surface and the from clouds escapes through a wavelength band of 7-13 μm ; this is known as the *atmospheric window* (Badr and Probert, 1993). There is little absorbance by atmospheric components in this band width. However, if there is a sizeable increase in the atmospheric concentration of a gas that possesses strong absorption features in this spectral region, there will be an increase in the Earth-atmosphere temperature resulting in possible climatic catastrophes (Ramanathan *et al.*, 1987).

The greenhouse gases identified include, water vapour (H_2O), carbon dioxide (CO_2), methane (CH_4), nitrous oxide (N_2O) and chlorofluorocarbons (CFCs). All have significant natural and anthropogenic sources, except for the CFCs which are exclusively man-made. One of the most influential greenhouse gases is water vapour, which is active to a varying extent throughout the infra-red part of the spectrum and can account for about 80 % of the greenhouse effect (Houghton *et al.*, 1990; Stephens and Tjemkes, 1993). However the concentration of water in the atmosphere is determined internally within the global climate systems, and is subject to considerable variation. Furthermore, although water vapour traps long wave energy, clouds in turn reflect significant solar energy back into space. Hence it is doubtful whether an increase in the concentration of water vapour would be deleterious.

Omitting the influence of water vapour, satellite and other measurements indicate that currently, CO_2 accounts for about 55 % of the annual anthropogenic input of greenhouse gases, CFC's 24%, CH_4 15 % and N_2O accounting for 6 % (Lashof and Ahuja 1990; Hauglustaine *et al.*, 1994; Houghton *et al.*, 1995).

1.4 N₂O IN THE ATMOSPHERE

In the literature there have been several reviews of nitrous oxide in the atmosphere (Bouwman, 1990; Badr and Probert, 1993; Kroeze, 1994; Houghton *et al.*, 1995). The following is a summary of the current state of knowledge.

In 1772 Joseph Priestly conducted a series of experiments and discovered not only oxygen but also a gas he called *dephlogisticated nitrous air*, this was later renamed nitrous oxide (Badr and Probert, 1993). The presence of nitrous oxide in the atmosphere was established 150 years later by Adel (1938, 1939) who detected absorption bands corresponding to N₂O during investigations into the infra-red solar spectrum. Nitrous oxide is more commonly known as *laughing gas* and is associated with medical procedures due to its powerful anaesthetic properties. However, N₂O plays a significant role in both the global nitrogen cycle and in the atmosphere where it facilitates important reactions that influence the Earth's climate via global warming and ozone (O₃) destruction.

The current average concentration of N₂O in the atmosphere is about 311 ppbv (Houghton *et al.*, 1995), with the global trend increasing at about 0.27 % annually (Khalil and Rasmussen, 1992). Ice core analysis has demonstrated that the atmospheric concentration of N₂O has risen from between about 260-270 ppbv during the last century (Leuenberger and Siegenthaler, 1992; Crutzen, 1994; Machida *et al.*, 1995) to the current value; this is an increase of about 15 %. The rise in concentration was largely confined to the last 40 years, and is probably the result of human activities (Dibb *et al.*, 1993; Crutzen, 1994). There was no evidence from ice core studies of any other large concentration changes in the pre-industrial period extending back some 45,000 years (Leuenberger and Siegenthaler, 1992). However, it has been observed by Khalil and Rasmussen (1989) that there was a significant drop in atmospheric N₂O during the so called *little ice-age* of 1450-1750 AD, this may indicate that the natural source strength responds to changes in global temperature. An increase in N₂O emissions could therefore lead to a positive feedback reaction. It is estimated that global warming could enhance N₂O emission rates by 0.88 Tg N y⁻¹ for every 1 °C rise in global temperature (Kroeze, 1994).

Nitrous oxide may constitute a small proportion of the atmosphere, but it has an important role in global warming due to its *warming potential* which is considerably greater than that of CO₂ (Lashof and Ahuja, 1990; Houghton *et al.*, 1990; Houghton, 1991). On a molecule per molecule basis N₂O is about 200 times more effective at absorbing infra-red radiation than CO₂ (Rodhe, 1990; Lashof and Ahuja, 1990; Houghton *et al.*, 1990; Houghton, 1991).

Nitrous oxide molecules have three fundamental absorption bands within the infra-red part of the spectrum, the centre of each band lies at: 4.5 μm; 7.8 μm; and at 17 μm (Badr and Probert, 1993). The strongest absorption bands lie within the short wavelength section of the *atmospheric window*. The long wave infra-red radiation that is trapped by tropospheric N₂O is proportional to the square root of the atmospheric N₂O concentration. There is however, some overlapping of the two extreme N₂O spectral bands by both water vapour and CO₂, causing some reduction in the absorption potential of N₂O. At present the existence of N₂O molecules in the atmosphere contributes an additional 0.9-1.6 W m⁻² to the biospheric system (Dickinson and Cicerone, 1986).

N₂O is a relatively unreactive gas, which does not generally undergo chemical reaction with the ground, vegetation or any of the tropospheric components. Consequently N₂O is distributed evenly within the troposphere and has a residence time of some 120-150 years (Crutzen, 1994; Houghton *et al.*, 1995). However, upon diffusion into the stratosphere, N₂O reacts in two ways: firstly by reaction with activated oxygen atoms and secondly by photo-dissociation at wavelengths between 180-230 nm, both of which account for about 10 and 90 % of the total N₂O sink respectively (Badr and Probert, 1993; Houghton *et al.*, 1995).

Although N₂O is too inert to react directly with O₃ its reaction products are involved in various catalytic ozone destruction reaction chains that, in association with CFCs, largely determine the natural stratospheric ozone concentration and its anthropogenic downward trend. Each of the N₂O decomposition reactions can lead to the formation of NO_x compounds which facilitate ozone destruction, the mechanisms of which are reviewed by Badr and Probert (1993) and Crutzen (1994). If the currently observed rate of increase of

atmospheric N₂O concentration were to continue throughout the next 100 years, its level would rise about 20 % from 300 to 360 ppbv resulting in a 4 % reduction of O₃ concentration (Badr and Probert, 1993). It has been estimated that a 1 % decrease in ozone would increase the incidence of various skin cancers by about 2-10 % (Banin, 1986).

Atmospheric concentrations of N₂O will adjust slowly to changes in emissions. The longer emissions continue to increase at present day rates, the greater the reductions that will have to be made for concentrations to stabilize at an acceptable level. It is estimated that nitrous oxide would require an immediate reduction in emission from human activities of around 50 % to stabilize the concentration at the current level (Houghton *et al.*, 1995).

1.4.1 N₂O sinks

The only substantial sink for N₂O is in the stratosphere. It was recently calculated, based on existing atmospheric concentrations, that the specific removal rate by stratospheric reactions could account for as much as 16.2 Tg N y⁻¹ (Houghton *et al.*, 1995). The observed rate of increase in atmospheric N₂O concentration (0.27 %) corresponds to a net annual increase of about 3.9 Tg N, implying that the estimated reduction rate in the stratosphere is about 30 % less than the current atmospheric sources suggest (Houghton *et al.*, 1995).

The potential of soil and aquatic systems to consume N₂O has not been examined to any great length and could be of importance. However there is evidence that wetland ecosystems may contribute to the N₂O sink (Schiller and Hastie, 1994).

1.4.2 N₂O sources

It is only through atmospheric measurements and ice-core analysis, that the increase in N₂O is most likely to be related to human activities. Khalil and Rasmussen, (1992) using ice core data have estimated that the present global anthropogenic emissions are 7 ± 1 Tg y⁻¹. However, there is considerable uncertainty regarding the magnitude of N₂O sources

which, when combined, account for about 14.7 Tg N y⁻¹ (Houghton *et al.*, 1995; 9.2 Tg N y⁻¹: Crutzen, 1994). This represents a deficit from the estimated sink of about 10 %, which is probably due to the underestimation of existing identified sources, rather than an unidentified major source (Khalil and Rasmussen, 1992). The many small sources of N₂O, both natural and anthropogenic, are difficult to quantify accurately, hence estimates quoted in the literature vary significantly.

Accurate inventories of N₂O emissions are necessary to arrive at a more accurate global estimate. In order to obtain comparable international inventories a standard format was developed by the IPCC/OECD (Corfee-Morlott *et al.*, 1994) which facilitated comprehensive studies on the potential capacity of N₂O sources, both natural and anthropogenic.

1.4.2.1 Anthropogenic sources

Anthropogenic sources are well documented with countries around the globe able to produce an estimated N₂O emission inventory (Olivier *et al.*, 1994). The main anthropogenic sources of N₂O are agriculture, biomass burning and a number of industrial/combustion processes. The best estimate of the current global anthropogenic emission is 3-8 Tg N y⁻¹ (Houghton *et al.*, 1995).

Combustion and Industrial sources

Combustion sources include those evolved from refuse incineration, fossil fuel combustion and various other industrial processes. Hulgaard and Dam-Johansen (1992) measured N₂O emissions from various combustion systems using a GC grab sample procedure and an infra-red N₂O analyzer and determined that combustion systems are not as significant as previously thought. Until recently up to 30 % of the total emission of N₂O to the atmosphere had been attributed to combustion processes with 83 % of this due to coal combustion. This overestimation was due to an erratic

sampling procedure (Hao *et al.*, 1987). Only fluidized bed coal combustors emit quantities of N₂O of real significance (50 ppmv; Hayhurst and Lawrence, 1992).

The major combustion source is catalytic exhaust-gas clean up systems on cars which emit about 0.3-0.9 Tg N y⁻¹ (Blok and De Jager, 1994). One of the initial studies into the N₂O emission potential from cars was undertaken by Cicerone *et al.*, (1978) who determined the extent to which a catalytic converter promotes N₂O emission compared to that of a conventional exhaust system under different running conditions. The total combustion source is calculated by Blok and De Jager, (1994) as contributing about 0.5-1.4 Tg N y⁻¹ (0.3 Tg N y⁻¹, Olivier *et al.*, 1994; 0.75 Tg N y⁻¹, Kroeze, 1994; 0.3-0.9 Tg N y⁻¹, Houghton *et al.*, 1995). The various estimates reported in the literature highlight the uncertainty in the strength of this source.

Industrial processes such as *nylon-6,6* and N-fertilizer production emit significant amounts of N₂O to the atmosphere. For every kg of Adipic Acid produced during nylon production 300g of N₂O can be produced. Global N fertilizer production was recently estimated at 78.9 Tg N y⁻¹ (IFA, 1992); it is estimated that the N₂O emission during production of nitrogen-fertilizer is about 0.25 % (Kroeze, 1994). It has been estimated by Houghton *et al.*, (1995) that the total contribution from industrial sources is between about 0.5 and 0.9 Tg N y⁻¹, Olivier *et al.*, (1994) and Kroeze, (1994) estimated it at 0.6 Tg N y⁻¹.

Biomass burning

Biomass burning is estimated to account for between 0.2-1.0 Tg N y⁻¹ (Kroeze, 1994; Olivier *et al.*, 1994; Houghton *et al.*, 1995). However, there have been very few studies of these sources, particularly in the tropics, and thus uncertainties could be great. Furthermore, there is an added uncertainty regarding the *post burning effect* within tropical regions: it has been reported that there is significant increases in N₂O emissions following forest clearing especially within the first year (Keller *et al.*, 1993). There has been little attempt to separate the tropical soil source into natural and anthropogenic components.

Agriculture

Cultivated soils are by far the greatest sources of anthropogenic N₂O, emitting between 1.8-5.3 Tg N y⁻¹ (Houghton *et al.*, 1995). Nitrogen fertilizers are applied to about 11 % of the Earth's land surface and application rates have increased dramatically in recent years from 3.5 Tg in 1950 to 70 Tg in 1985, this trend is set to continue and is expected to reach about 100 Tg by the year 2000 (Aulakh *et al.*, 1992). Fertilized land, whether by mineral, manure or legume, is a significant source of N₂O with 0.2 to 4 % of fertilizer-N applied being emitted as N₂O (Olivier, 1993). Anhydrous ammonia fertilizers result in greater N₂O emissions than either ammonium or urea based fertilizers which in turn produce more N₂O than nitrate fertilizers (Kroeze, 1994). Almost 2/3 of the anthropogenic N₂O emission in 1990 was found to be related to anthropogenic N input to soils and oceans; the use of nitrogenous fertilizer has been calculated as directly contributing about 0.99 Tg N y⁻¹ (Kroeze, 1994). A comparable fertilizer-derived emission was estimated by Eichner (1990) from analysis of over 100 field experiments.

Tropical forest soils are probably the single most important source of N₂O, especially when undergoing a change in land use to agriculture (Houghton *et al.*, 1995). The flux of N₂O depends on the age of the tropical pasture. A pasture <10 years old can emit between 5-8 times more N₂O than the background rate from the natural forest; after about 10 years the emission rates decline linearly to sub-forest rates (Keller *et al.*, 1993). Therefore when applying tropical forest emission rates to global models, the land use history of the tropical pastures must be considered. Another important category related to cultivated soils, is animal excreta. It is estimated that, on a global scale, animals excrete in the region of about 100 Tg N y⁻¹ and which is tentatively calculated as contributing about 1.0 Tg N y⁻¹ to N₂O emission rates (Olivier *et al.*, 1994; Kroeze, 1994).

There are techniques available to reduce anthropogenic N₂O emissions: optimising combustion temperatures; use of N₂O reducing catalysts in industry; optimum N fertilization procedures (Blok and De Jager, 1994). However, the options for emission

reduction are not well quantified and further investigation is needed to determine the potential and cost of each.

1.4.2.2 Natural sources

Natural sources have been calculated as being twice the magnitude of anthropogenic sources. The estimate for natural emissions which are derived from both the oceans and soil is about 9 Tg N y^{-1} . This figure falls at the lower end of that needed to maintain pre-industrial concentrations of about 275 ppbv, (11 ± 3 Tg N y^{-1} ; Houghton *et al.*, 1995).

Natural sources from terrestrial eco-systems include soils under both tropical and temperate grasslands and forests, which are estimated to produce about 6 Tg N y^{-1} , with half of that amount being contributed by the tropical forest.

Oceans are reported to be super-saturated with respect to N₂O (Hayhurst and Lawrence, 1992) and are thus considered a source rather than a sink of N₂O, emitting between about 1.4-2.6 Tg N y^{-1} (Houghton *et al.*, 1995). However, there is considerable uncertainty regarding the magnitude of the ocean source. Banin (1986) reports that only localized areas are supersaturated and that the vast majority of the ocean surface is close to equilibrium with the atmospheric concentration.

Total N₂O emission from both cultivated and natural soils, regardless of vegetation/crop cover, has been calculated by Houghton *et al.*, (1995) as about 6-15 Tg N y^{-1} (7.5 Tg N y^{-1} , Olivier *et al.*, 1994). Soil can therefore be regarded as the principle source of atmospheric N₂O, and it has been estimated that soil in general may account for up to 90 % of the global source (Bouwman, 1990; Mosier and Schimel, 1991).

1.5 N₂O EMISSION FROM SOIL

The emission of N₂O from soil is ultimately derived from atmospheric N₂. The number of pathways through which N₂ can be converted into more complex compounds is limited, the principle routes being: fixation by symbiotic microbes; fixation by free living microbes; oxidation to NO_x caused by atmospheric electrical discharge; industrial production of ammonia, urea or nitrate for synthetic N fertilizers (Tisdale *et al.*, 1985). The subsequent microbial induced transformations of the natural or anthropogenically produced N-compounds, facilitate N₂O formation in soil (Alexander, 1977; Tate, 1995).

About 0.1 to 0.3 % of the top 15 cm of temperate soils exists as chemically combined N (Russell, 1988). The largest part of combined N in soil is in the organic matter/humus fraction which is unavailable to plants (Powlson, 1993). NO₃⁻ and readily exchangeable NH₄⁺, are the only forms of N that can be utilized by plants, and rarely constitute more than 1 % - 2 % of the total N present in soil (Russell, 1988). The NH₄⁺ that is released from the decomposition of organic matter by soil microbes, is the principle source of nitrogen for crops growing on land which does not receive fertilizer.

Soil N-compounds are susceptible to both volatilization and leaching, thus soil fertility may be compromised under intensive cropping without continual N conservation and maintenance (Russell, 1988). Consequently, much of the past research on the agronomic nitrogen cycle concerned the efficiency of N-fertilizers (Aulakh *et al.*, 1992). Allison (1955) reported that agronomic nitrogen balances revealed that the gaseous loss of N-compounds from soil accounted for, on average, about 15 % of applied fertilizer nitrogen. This has been confirmed with the use of ¹⁵N labelled fertilizers (Hauck, 1971; Dowdell and Webster, 1984). Nitrogen use efficiency studies led to the subsequent identification and study of a number of processes that contributed to gaseous loss of N from soil (Fillery, 1983; Sahrawat and Keeney, 1986). It was found that N₂O is produced naturally in soils primarily from the microbial reduction of nitrate and nitrite (denitrification), and by the microbial formation of nitrate and nitrite from the oxidation of

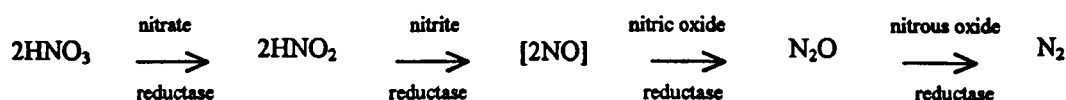
ammonium compounds (nitrification), (Mosier *et al.*, 1983; Tisdale *et al.*, 1985; Haynes, 1986 a, b; Sahrawat and Keeney, 1986; Aulakh *et al.*, 1992; Tate, 1995).

1.5.1 N₂O emission from denitrification

Aulakh *et al.*, (1992) estimated that N lost through denitrification can range from 0 to 100 kg N ha⁻¹. They also report that denitrification is responsible for 83 to 390 Tg N y⁻¹ being emitted to the atmosphere from the Earth. Estimates indicate that denitrification recycles from 52 % to 100 % of the total nitrogen input to terrestrial systems (Aulakh *et al.*, 1992).

The biological reduction of NO₃⁻ and NO₂⁻ to N₂O and ultimately N₂ is catalyzed by a diverse group of micro-organisms, primarily heterotrophic bacteria, which use organic carbon as an energy supply (Haynes and Sherlock, 1986). In the absence of O₂, these organisms use both NO₃⁻ and NO₂⁻ as terminal electron acceptors in their respiratory process, producing N₂O as an intermediary (Knowles, 1981 a, b; Fillery, 1983; Aulakh *et al.*, 1992; Tate, 1995). This sequential reduction of NO₃⁻ is mediated by enzymes (Fig. 1.1) and is known as *dissimilatory nitrate reduction*; this is the principle source of N₂O from soils (Sahrawat and Keeney, 1986). However, other relatively insignificant N₂O production pathways, relating to nitrate reduction reactions, are also active in soil. These include *assimilatory nitrate reduction*, which is the reduction of NO₃⁻ to NH₄⁺ for incorporation into cell biomass and usually occurs in aerobic conditions when reduced nitrogen is limiting, and *dissimilatory ammonium production*, which is the reduction of NO₃⁻ to NH₄⁺, using nitrate as a terminal electron source under long term anaerobic conditions (Tiedje *et al.*, 1981). The dissimilatory ammonium microbial population is reported to produce N₂O only in a side reaction (Tate, 1995). A true denitrifier, according to Tate (1995), must convert at least 80 % of assimilated NO₃⁻ to N₂O or N₂ via cytochrome cd, and this reduction must increase growth yield and be central to cellular metabolism rather than just a side reaction. Therefore all further references to denitrification will relate to *dissimilatory nitrate reduction* only.

Figure 1.1 Simplified denitrification (dissimilatory nitrate reduction) pathway illustrating N transformations and their respective reducing enzymes.



Nitric oxide is written in brackets because it is rarely detected in a free state and may possibly be just a side reaction and not a true intermediate (Tate, 1995). Each reduction step in the pathway is catalysed by its own specific enzyme, the biochemistry of which is described in the literature (Fillery, 1983; Lloyd, 1993; Tate, 1995). The specific N-reductase compounds, like other proteins, are greatly influenced by their environment. The overall denitrification rate is therefore dependent on the parameters which affect each individual N-reductase enzyme (Knowles, 1981 a, b; Fillery, 1983; Haynes and Sherlock, 1986; Davidson and Schimel, 1995; Tate, 1995). It follows that any alteration in the rate of N_2O production relative to the rate of N_2O consumption by the soil environment will affect the N_2O flux from soil.

Micro-organisms constitute less than 0.5 % (w/w) of the soil mass (Tate, 1995) with the bacterial population forming about half this amount (Foth, 1978). Denitrifiers, capable of anaerobic growth constitute about 20 % of the soil bacterial population, and 1 to 5 % of the total heterotrophs (Kaplan and Wofsey, 1985). *Pseudomonas spp.* and *Alcaligenes spp.* are the most dominant species capable of denitrification in soils (Firestone and Davidson, 1989; Kostina *et al.*, 1994). However, it has been recognized that a variety of heterotrophic prokaryotes and fungi are also capable of N_2O production via denitrification (Haynes and Sherlock, 1986; Shoun *et al.*, 1992). Ohyama and Kumazawa (1987) found that soybean bacteroides are capable of N_2O production via the reduction of NO_3^- . Sahrawat and Keeney (1986) and Haynes and Sherlock (1986) both report that *Rhizobium spp.* are also capable of reducing NO_3^- to N_2O . However, the rate of NO_3^- reduction by *Rhizobium spp.* is minimal compared to overall denitrification rates (Garcia-plazaola *et al.*, 1993).

However, not only are the individual bacterial strains of denitrifiers metabolically distinct, but the properties of the N-reductase enzymes are also highly variable. Tate (1995) compared the denitrifiers *Pseudomonas stutzeri*, *Pseudomonas aeruginosa* and *Paracoccus denitrificans* and found that the rates of anoxic growth of the organisms varied 1.5-fold, gas production varied over 8-fold and cell yield differed by a factor of 3.

Not all micro-organisms are capable of full dissimilatory nitrate reduction as some lack the full complement of enzymes to complete the pathway (Fillery, 1983; Robertson and Kuenen, 1990). Nitrate reductase and nitrous oxide reductase are the enzymes most frequently absent from microbes incapable of complete dissimilatory nitrate reduction (Haynes and Sherlock, 1986; Robertson and Kuenen, 1988, 1990). Consequently a variety of reduction products are apparent during anaerobic conditions in soil.

Denitrifying enzymes can persist in the soil for long periods of time without being used. This enables many denitrifiers to quickly switch their terminal electron acceptor from O_2 to NO_3^- during brief periods of anoxia following, for example, a rainfall event (Davidson and Schimel, 1995). Denitrifying enzymes have even been found in organisms that were growing aerobically in the absence of nitrate (Robertson and Kuenen, 1984). The enzymes associated with denitrification are robust, it was reported that a significant denitrifying enzyme capacity was still present in dry soils after 2 months storage (Smith and Parsons, 1985). Following periods of aerobiosis the N-reductase enzymes are de-repressed by the re-introduction of anoxic conditions (Dendooven and Anderson, 1995). Dendooven and Anderson (1994) found that the N-reductase enzymes are synthesised at different rates, NO_2^- -reductase is synthesised 5 hours after anaerobic conditions are imposed, while N_2O reductase was synthesised only after 16 hours. This may explain observed flushes of N_2O emissions upon rapid inducement of anaerobic conditions.

Because electrons are more readily transferred to molecular O_2 than to NO_3^- , denitrification can only occur under anoxic conditions (Tate, 1995). Tate (1995) noted that the primary difference between NO_3^- respiration and O_2 based respiration was that in the former electron transport process, NO_3^- is merely replacing O_2 as the final

electron acceptor. He therefore suggested that denitrifying organisms are not strictly anaerobic but are essentially obligate aerobes. However, denitrifiers possess different cytochrome sequences for both electron transfer situations (Tate, 1995).

There are however, contrary reports suggesting the possibility of *aerobic denitrification* (Robertson and Kuenen, 1984, 1990; Mateju *et al.*, 1992; Lloyd, 1993). Robertson and Kuenen (1984) found that a denitrifying microbe, *Thiosphaera pantotropha*, was capable of simultaneously utilizing both NO_3^- and O_2 as terminal electron acceptors during respiration in dissolved oxygen concentrations of up to 90 % of air saturation. However, this phenomenon was suggested as being the result of an error in methodology. Thomsen *et al.*, (1993) found that *T. pantotropha* does not utilize both O_2 and NO_3^- simultaneously, but that O_2 is the preferable electron acceptor, as it is more energy efficient.

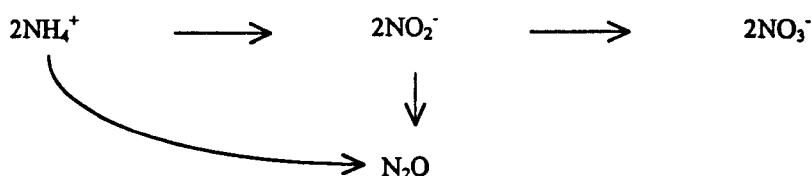
1.5.2 N_2O emission from nitrification

Nitrification is the oxidation of NH_4^+ (chemoautotrophic nitrification) or organic N compounds (heterotrophic nitrification) to NO_2^- or NO_3^- (Haynes, 1986 b; Tate, 1995). Nitrification involves the direct incorporation of molecular oxygen into N-compounds, changing NH_4^+ , the most reduced form of N (valency = -3), to NO_3^- , its most oxidized form (valency = +5). The complete oxidation of NH_4^+ , is a two stage process, which is undertaken primarily by two prolific chemoautotrophic genera; *Nitrosomonas spp.* transforms NH_4^+ to NO_2^- and *Nitrobacter spp.* oxidizes NO_2^- to NO_3^- (Fig. 1.2). In recent years, nitrifiers of other genera that oxidize both NH_4^+ and NO_2^- have been identified (Haynes, 1986 b; Sahrawat and Keeney, 1986; Tate, 1995).

Enzymes from chemoautotrophic nitrifying bacteria are the only means for nitrifiers to obtain energy. If substrate availability or some other factor limits nitrification, the nitrifiers effectively starve and in contrast to denitrification, the enzymatic capacity of the soil declines (Davidson and Schimel, 1995). Such instances can occur during rainfall when soil may become saturated and rapidly changes from aerobic to anoxic

conditions. Nitrifiers only recover between 5 and 15 % of the total energy released during nitrification; converting NH_4^+ to NO_2^- yields 66 kcal mol⁻¹, whereas NO_2^- oxidation produces 20 kcal mol⁻¹ (Tate, 1995). It follows that large quantities of ammonium and even larger quantities of nitrite must be oxidized to fix each carbon molecule. Ammonium oxidizers typically oxidize between 14 and 70 NH_4^+ molecules per carbon atom incorporated, whereas 76 to 135 NO_2^- molecules must be oxidized to achieve a similar rate of C (Tate, 1995).

Figure 1.2 Simplified autotrophic nitrification pathway illustrating the biochemical route to N_2O formation.



Nitrous oxide is an intermediate product between NH_4^+ and NO_2^- transformations, however the production mechanism is not clear. N_2O can also be formed from the chemical decomposition of NO_2^- in acid conditions and in anaerobic conditions by reduction of NO_2^- by nitrifying organisms (Firestone and Davidson, 1989). Possible NO_2^- decomposition and NH_4^+ oxidation pathways, resulting in N_2O production, have been reviewed in the literature (Chalk and Smith, 1983; Haynes, 1986 b).

Rates of N_2O production from nitrification are significantly lower than from dissimilatory nitrate reduction (Sahrawat and Keeney, 1986). However, nitrification, although subject to NH_4^+ concentration, was reported to be the dominant source of N_2O in aerobic soils (Bremner and Blackmer, 1978; Skiba *et al.*, 1993). Most topsoil's are well aerated, so that the production of N_2O through nitrification is believed to contribute significantly to the global flux (Bremner and Blackmer, 1981; Wild, 1993). It was estimated by Goodroad and Keeney (1984) that 0.1 to 0.2 % of nitrified N was emitted as N_2O , which is similar to measured field rates, that range from 0.03 to 0.6 % of applied N (Breitenbeck *et al.*, 1980; Seiler and Conrad, 1981; Aulakh *et al.*, 1984

a). In situ nitrification rate principally depends upon the population densities of the nitrifying bacteria present, the efficiency and degree of saturation of the respective nitrifying enzymes and the environmental limitations controlling nitrifier population development (Tisdale *et al.*, 1985; Tate, 1995).

The lack of species diversity in organisms involved in nitrification means that nitrifiers are consistently influenced by similar environmental factors. Nevertheless the diversity that does exist among nitrifying species and the adaptation of indigenous nitrifiers to their particular environment conditions mean that no definite constraints can be identified (Tate, 1995). Furthermore, heterotrophic nitrification may occur under environmental conditions that are apparently unsuitable for autotrophs, which can lead to complications in the understanding of N₂O emission from nitrification (Sahrawat and Keeney, 1986).

The factors that regulate the magnitude of N₂O from both denitrification and nitrification are well established under laboratory conditions (Sahrawat and Keeney, 1986; Tate, 1995). However, transposing this information into the soil environment has been difficult due to the heterogeneous nature of soil. N₂O emission rates from soils are usually characterised by large temporal and spatial variability because of the complex interactions between physical and biochemical factors that affect production and emission of N₂O.

Robertson (1989) presented a conceptual model of environmental regulation for both denitrification and nitrification using the terms *proximal* and *distal* to identify the cellular and environmental levels of control respectively. The *proximal* factors, including the organisms themselves, were recognized as: organic carbon, O₂ and NO₃⁻ availability, for denitrification; NH₄⁺ and O₂ availability for nitrification. These determinants are directly influenced by the *distal* factors: N availability; soil water content; soil organic matter content; soil temperature; soil chemical status; plant and land use. Notable reviews of both the proximal and distal factors controlling N₂O from soil, include: Fillery, (1983); Sahrawat and Keeney, (1986); Bouwman, (1990); Aulakh *et al.*, (1992); Tate, (1995). The following is a summary of knowledge to date.

1.5.3 Effect of N-compounds on N₂O evolution from soil

The primary prerequisites for both denitrification and nitrification pathways are NO₃⁻ and NH₄⁺ respectively (Sahrawat and Keeney, 1986). The application of NO₃⁻ and NH₄⁺ fertilizers has been shown to promote a N₂O flux from both processes (Bremner *et al.*, 1981; Cochran *et al.*, 1981; Conrad *et al.*, 1983; Tisdale *et al.*, 1985; Schuster and Conrad, 1992; Van Cleemput *et al.*, 1994; Flessa *et al.*, 1995). Sahrawat and Keeney, (1986) reported that soil fertilized with NH₄NO₃ showed increased emission of N₂O although emissions were small, ranging from 0.4 to 1.5 % of the fertilizer added. Bremner *et al.*, (1981) studied the effect of ammonia fertilization (250 kg N ha⁻¹) on N₂O emissions over a period of 139 days, and found that fertilized soils emitted nearly 10 times more N₂O than unfertilized plots. The fertilizer-induced emissions represented 4.0 to 6.8 % of the fertilizer N applied. Cochran *et al.*, (1981) observed N₂O emission via nitrification from a fallow field fertilized with 0, 55, 110, and 220 kg N ha⁻¹ and detected a positive correlation between the amount of fertilizer applied and N₂O flux.

The limiting factor in nitrification in most soils is the conversion of NH₄⁺ to NO₂⁻. Any NO₂⁻ found in soil is presumed to arise from NH₄⁺ oxidation and repression of *Nitrobacter spp.*, as NO₂⁻ is usually converted to NO₃⁻ as rapidly as it is formed (Haynes, 1986 b; Tate, 1995). However, elevated NH₄⁺ concentrations are toxic and can inhibit the second step of nitrification (Haynes, 1986 b). Tate (1995) reports that 200 µg g⁻¹ NH₄⁺-N supported rapid nitrification but elevation of NH₄⁺-N to 300 µg g⁻¹ inhibited the process. This inhibition could be due to the combined effect of low pH and increased salt content (Malhi and McGill, 1982). The NH₄⁺ oxidizing bacteria are characteristically less sensitive than NO₂⁻ oxidizing bacteria to high NH₄⁺ concentrations. Haynes (1986 b) reported that the rate of NO₃⁻ production increased with increasing NH₄⁺ concentration from 50 to 800 µg N g⁻¹ but at higher NH₄⁺ concentrations NO₂⁻ accumulated. Bergstrom *et al.*, (1994) reported that an increase in N₂O emission from denitrification following NH₄⁺ application in aerobic soils with high C levels, was probably due to the enhanced formation of NO₃⁻ during nitrification which was subsequently denitrified.

At NO_3^- concentrations of 40 to 100 $\mu\text{g N g soil}^{-1}$ the rate of denitrification has been shown to be independent of NO_3^- concentration and follows zero order kinetics. However, at concentrations less than 40 to 100 $\mu\text{g g soil}^{-1}$, diffusion constraints produce a first order reaction (Bowman and Focht, 1974; Fillery, 1983; Haynes and Sherlock, 1986). Any diffusional limitation of nitrate to denitrifiers may only apply to natural soils with a low NO_3^- concentration and poor structural development (Myrold and Tiedje, 1985). Ambus (1993) found that denitrification was limited by substrate diffusion in natural streamside soils. When the author removed this constraint by applying NO_3^- , the denitrification rate increased by factors of 10 to 25.

It has been reported by several workers that NO_3^- has an inhibitory effect on N_2O reduction, and thus there is a positive effect on the ratio of N_2O to N_2 , (Blackmer and Bremner, 1978; Firestone *et al.*, 1979; Firestone *et al.*, 1980; Haynes and Sherlock, 1986; Weier *et al.*, 1993; Tate, 1995). Firestone *et al.*, (1979, 1980) reported that an even stronger positive effect on the ratio of N_2O to N_2 was observed with NO_2^- application. These authors report that when the NO_3^- concentration was increased from 0 to 20 $\mu\text{g N g}^{-1}$ in field moist soil, the $\text{N}_2:\text{N}_2\text{O}$ ratio decreased from 76:1 to 4:1. It was found that when the concentration of NO_2^- was similarly increased, the $\text{N}_2:\text{N}_2\text{O}$ ratio decreased from 70:1 to 1:6 while the total gaseous production ($\text{N}_2 + \text{N}_2\text{O}$) was unchanged. It was suggested that the effect of NO_3^- addition was due to a microbial preference of NO_3^- as an electron acceptor, above that of N_2O , because the total gas produced increased with increasing NO_3^- concentration. It was also suggested that the effect brought about by NO_2^- may be due to the inhibition of N_2O -reductase rather than the use of NO_2^- as a preferential electron acceptor, because the total gaseous amount produced remained constant. Blackmer and Bremner (1978) found that the magnitude of N_2O reductase inhibition caused by NO_3^- or NO_2^- is greatly affected by water content (section 1.5.5) and pH (section 1.5.8). Sahrawat and Keeney (1986) reported that the effect of NO_3^- concentration on the reduction of N_2O is much less in organic soils due to a more complete reduction of NO_3^- (section 1.5.6). Van Cleemput *et al.*, (1988) stated that denitrification products are generally competitive inhibitors. However, the authors report that competition is only really clear with a large concentration of an N-oxide. A conflicting report from Betlach and Tiedje, (1981)

states that not all organisms that participate in denitrification are inhibited by additions of NO_3^- and NO_2^- .

The type of fertilizer N applied has also been found to influence N_2O flux emissions from soil. Anhydrous NH_3 produces greater fluxes than either NO_3^- or NH_4^+ sources although the water content (section 1.5.4) of soils in the study were very rarely in excess of field capacity (Breitenbeck *et al.*, 1980). The uptake of NO_3^- by plants is reported to be inhibited by NH_4^+ , thus denitrification may be enhanced in soil with high NH_4^+ concentrations. However, NO_3^- does not affect NH_4^+ uptake by plants (Tisdale *et al.*, 1985; Haynes and Sherlock, 1986). Haynes (1986 b) reported that an *end product repression* may exist during nitrification, where NO_3^- can inhibit both *Nitrosomonas* growth and *Nitrobacter* oxidation of NO_2^- .

1.5.4 Effect of O_2 partial pressure on N_2O evolution from soil

Nitrification is an obligatory aerobic process with O_2 directly incorporated into the final product. Nitrification can occur at O_2 concentrations as low as $0.3 \mu\text{g cm}^{-3}$ (Tate, 1995). Tisdale *et al.*, (1985) measured the production of NO_3^- -N in a soil with added $(\text{NH}_4)_2\text{SO}_4$, that was aerated with air-nitrogen mixtures with varying O_2 partial pressure, and showed that nitrification only begins to be limited at O_2 concentrations less than 5 %. It is reported by Robertson and Kuenen (1990) that under certain conditions anoxic nitrification by nitrifiers can occur.

The absence or restricted availability of O_2 in soils is one prerequisite for denitrification (Sahrawat and Keeney, 1986). It was shown by Parkin and Tiedje (1984) that decreasing O_2 content increased the ability of soil to denitrify. A reduction in O_2 content from 20 to 5 % of the gas circulating soil cores increased the denitrification rate by 4 fold.

The *de novo* synthesis of all N-reductases, and the pre-formed N-reductases used in denitrification are repressed by O_2 (Betlach and Tiedje, 1981; Haynes and Sherlock,

1986). Once O_2 is depleted from a microsite the synthesis of the denitrifier enzymes are induced. The development of a totally functional denitrifying system in a previously aerobic site requires about 40 minutes to 3 hours (Tate, 1995). Full induction of the pathway only occurs once all the O_2 has been exhausted.

Nitrous oxide reductase is more susceptible to O_2 than the preceding sequence of reductase enzymes. Thus, at slightly elevated O_2 concentrations, there may be an increase in the mole fraction of N_2O (Haynes and Sherlock, 1986; Fillery, 1983). Sabaty *et al.*, (1993) report that the ability of *Rhodobacter sphaeroides* (forma *denitrificans*) to reduce NO_3^- is impeded by increasing O_2 concentration: O_2 stopped nearly all NO_3^- and N_2O reductase and about 70 % of NO_2^- reductase activity. The inhibition of denitrification by O_2 is due to a diversion of the reducing power from the denitrifying chain to the respiratory chain (Sabaty *et al.*, 1993).

The $N_2:N_2O$ ratio is affected by the aeration state of soils, although denitrification rate increases with decreased aeration, the $N_2:N_2O$ ratio increases because of the greater rate of reduction of N_2O to N_2 under anaerobic conditions (Sahrawat and Keeney, 1986). The negative effect of an increase in the O_2 status of the soil on the $N_2:N_2O$ ratio might be an indirect effect of an increased N_2O production from nitrification.

Firestone *et al.*, (1980) reported that an increase in the O_2 concentration of soil slurries from 0 to 0.0163 atm. decreased the $N_2:N_2O$ ratio from about 2.3:1 to 1:1.4. Under very anoxic conditions it was found that the amount of N_2 produced was 20 times greater than the amount of N_2O ; this may suggest that soil can act as a sink for N_2O (Rolston *et al.*, 1978; Sahrawat and Keeney, 1986). Firestone *et al.*, (1980) reported a pattern of N_2 and N_2O production after the onset of anaerobic conditions. N_2 was the predominant product between 0 and 3 hours after the start of anaerobiosis, whereas the dominant product between 3 and 16 to 33 hours was N_2O . However, between 16 to 33 and 48 hours, the sole product of denitrification reverted to N_2 . Other workers also found temporal variation of the $N_2:N_2O$ ratio following treatment application (Letey *et al.*, 1980 a; Weier *et al.*, 1993). Under anoxic conditions, the variation in the ratio could be the result of a more rapid development of NO_3^- -reductase, compared to

N₂O reductase (Letey *et al.*, 1980a), rather than the result of a change in redox potential with time (Letey *et al.*, 1981).

Kralova *et al.*, (1992) and Masscheleyn *et al.*, (1993) found that at a redox potential of +400 mV, nitrification produced the highest N₂O emissions. At soil redox levels below +200 mV, N₂O was produced via denitrification. Under more reduced conditions, gaseous N emissions increased but the proportion of N₂O in the resulting gas was less. The maximum amount of N₂O evolved during denitrification reactions was observed at 0 mV (Kralova *et al.*, 1992). Smith *et al.*, (1983) found that the critical redox potential (Eh) for N₂O reduction and production during denitrification in soil water systems, varied with pH; at pH 6, 7 and 8.5, the Eh was +250 mV, while at pH 5 it was +300 mV. Sahrawat and Keeney (1986) report that when a soil is subjected to a fluctuating redox potential, caused by wetting and drying cycles, it can produce large N₂O emission rates. Aulakh *et al.*, (1992) suggest that this is probably due to release of available C and N substrates.

1.5.5 Effect of water content on N₂O evolution from soil

The main process in which O₂ moves through soil is by diffusion (Hillel, 1982), although there is also mass movement of oxygenated water into flooded soils or even transport of air through plants and into the rhizosphere, such as rice (Russell, 1988). The impact of soil moisture on the magnitude of both nitrification and denitrification is indirectly through its control of O₂ diffusion (Tate, 1995). Diffusion of a gas through water is 10,000 times slower than diffusion through air (Currie, 1961).

Sahrawat and Keeney, (1986) found that denitrification rate was proportional to the water content of soils and at low water contents the gaseous product was mainly N₂O. The authors also report that, in many investigations, N₂O fluxes from both mineral and organic soils were many times lower during dry periods than shortly after rainfall events when the soils were saturated. Mummey *et al.*, (1994) found that nitrification accounted for between 61-98 % of the N₂O produced from a steppe soil at water

contents less than saturation and that denitrification was the primary N_2O source at saturated water contents. Corre *et al.*, (1995) observed that N_2O emission from different ecosystems increased with increasing amounts of rainfall.

The water content of a soil is also important with respect to diffusion of substrates (NH_4^+ , NO_3^-) to organisms which are surrounded by water films and to diffusion of N_2O out of the soil (Tisdale *et al.*, 1985; Sahrawat and Keeney, 1986; Haynes and Sherlock, 1986). The greater the soil water content, the longer it takes for N_2O to leave the soil, hence the greater chance of further reduction to N_2 (Knowles, 1981 b; Drury *et al.*, 1992). The soil microbial community is essentially aquatic and thus requires a thin film of water on soil particles in which to grow. The greater the soil moisture, the greater the potential for microbial populations to expand. Thus the magnitude of both denitrification and nitrification will increase, subject to other environmental constraints. If this layer of moisture is absent then neither denitrification or nitrification will occur.

Weier *et al.*, (1993) examined the effect of soil water content on $N_2:N_2O$ ratios in soil at 60, 75 and 90 % water-filled porosity (θ_w/θ_T) and found that the ratio increased with water filled porosity (WFP) particularly at high levels of soil organic C. Davidson and Schimel, (1995) and Tate, (1995) suggest that nitrification is a more important source of N_2O than is denitrification when WFP is less than 60 %. The opposite is true when WFP is greater than 60 %; above this value the denitrifying rate increases with an increase in soil moisture. Low denitrification rates were observed continuously in a drained field soil system, with maximal activity associated to an increase in moisture due to rainfall (Sexstone *et al.*, 1985 a).

Fillery (1983) reports that denitrification in soil ceases when the soil becomes drier than field capacity. Rudaz *et al.*, (1991) detected N_2O after 30 minutes following water addition to a very dry soil. The source of the N_2O was from denitrification when the water content exceeded field capacity and from nitrification when the soil was below field capacity. Rudaz *et al.*, (1991) also showed that denitrifying organisms and their enzymes survive at very low matric potentials (< -9 MPa) and the resumption of

denitrifying activity occurs within minutes of soil wetting. Similar results were obtained by Davidson (1992).

Goodroad and Keeney (1984) report that nitrification increased with water content θ_w , from 0.1 to 0.3 m³ m⁻³. Generally the maximum rate of nitrification occurs at soil moisture potentials in the range of -0.01 to -0.033 MPa (Haynes, 1986 b). In this range, Tisdale *et al.*, (1985) report that the nitrification rate declines with decreasing soil moisture potential although appreciable nitrification can occur down to -1.5 MPa (permanent wilting point).

There have been reports that drying of soils increases the soil's capacity to denitrify, this is probably due to the enhancement of mineralizable soil organic matter that is made available to denitrifiers upon wetting of the soil (Tisdale *et al.*, 1985). When dry soils are re-wetted, even by small amounts of precipitation, there is a characteristic flush of mineralization of the native soil organic N accompanied by a flush of nitrification and an increased O₂ demand in the soil (Haynes, 1986 b; Mummey *et al.*, 1994). Smith and Patrick (1983) showed that alternate anaerobic-aerobic cycles of varying duration significantly increased N₂O emissions compared to either solely aerobic or sustained anaerobic conditions. Haynes and Sherlock (1986) state that fluctuating moisture contents produce an initial high flux of N₂O followed by a slow decline in emission rate. The authors suggest that this is probably due to a build up of NO₃⁻ during the aerobic phases of the wet dry cycle initially inhibiting N₂O reduction. However, this phenomenon may also be due to progressive exhaustion of the readily mineralizable C supply (section 1.5.6).

1.5.6 Effect of organic matter on N₂O evolution from soil

Most nitrifiers are not directly affected by the carbon content of soils due to their autotrophic nature, they fix CO₂ as a carbon source (Haynes, 1986 b). However, some nitrifiers, like the majority of denitrifiers, are heterotrophs and rely on the oxidation of a variety of photosynthetically fixed-carbon sources for growth (Haynes and Sherlock,

1986; Tate, 1995). Stimulation of denitrification or heterotrophic nitrification by carbon amendment suggests that the process is carbon limited (Weier *et al.*, 1993). Denitrification rates generally correlate with both total and *available* organic carbon in soils. Therefore any soil amendment that leads to an increase in available soil organic matter should increase denitrification (Sahrawat and Keeney, 1986; Haynes and Sherlock, 1986; Tate, 1995). Coyne *et al.*, (1994) found that the addition of poultry manure to soils caused a substantial increase in N₂O emission compared to untreated soil. However, the N₂O emitted only represented up to 0.7 % of the total N in the applied manure. Similarly, N₂O emissions were increased by a factor of 35 upon the application of sugarbeet residues (Flessa and Beese, 1995).

Any relationship between total organic C and denitrification is probably coincidental rather than mechanistic because only readily available C sources provide the electron donor sources for denitrification (Fillery, 1983; Haynes and Sherlock, 1986). This is emphasised by Paul *et al.*, (1993) who found that N₂O emissions were greater from soil following addition of manure slurries rather than composted manure. Tisdale *et al.*, (1985) report that 1 mg kg⁻¹ of *available* carbon is required for the production of 1.17 mg kg⁻¹ of N as N₂O or of 0.99 mg kg⁻¹ of N as N₂.

Aulakh *et al.*, (1992) report that the denitrification potential in field soils is closely related to biomass C. They speculated that biomass C may become readily available to denitrifiers following soil saturation. Alternatively, the availability of C to denitrifiers may be proportional to the active biomass mineralizing the organic matter, or part of the biomass C of facultative anaerobic denitrifiers is released by osmotic lysis of microbes that were unable to adjust to rapid increases in soil water content.

More available carbon is found in the surface layer than in sub-layers of soils, so it is expected that higher denitrification rates are found in surface soils. Denitrification activity and populations of denitrifiers generally decrease with soil depth (Parkin and Meisinger, 1989). However, McCarty and Bremner (1993) suggest that denitrification in the sub soil is not limited by small denitrifier populations but by the lack of available carbon; this is contrary to the findings of Parkin and Meisinger, (1989). McCarty and

Bremner (1993) speculated that plant residues are a major source of leachable organic C that is capable of promoting denitrification down the soil profile.

It is reported throughout the literature that the $N_2:N_2O$ ratio increases with increasing C availability (Sahrawat and Keeney, 1986; Haynes and Sherlock, 1986; Tate, 1995). Weier *et al.*, (1993) examined the effect of soil carbon on $N_2:N_2O$ ratios by treating soil with 0, 180, or 360 kg glucose-C ha⁻¹. The greatest $N_2:N_2O$ ratios were measured from the 360 C treatment, in conjunction with high levels of soil N. Increasing available carbon increases the $N_2:N_2O$ ratio because it results in more complete reduction of NO_3^- to N_2 (Haynes and Sherlock, 1986). Therefore, when the availability of NO_3^- exceeds the availability of carbon, the NO_3^- may be incompletely used and the $N_2:N_2O$ ratio will decrease (Firestone and Davidson, 1989; Tate, 1995).

The oxidation of organic compounds leads to the formation of CO_2 which may influence microbial processes. Keeney *et al.*, (1985) reported the effect of CO_2 concentration on both nitrification and denitrification and found that increasing CO_2 concentration from 0.3 % to 100 % progressively inhibited nitrification rate with no nitrification occurring at 100 % CO_2 . However N_2O production from nitrification increased with increasing CO_2 concentration, from 0.3 to 2.6 % and remained the major gaseous product up to a CO_2 partial pressure of 73 %; at 100 % CO_2 , no N_2O was produced. In the same study CO_2 was found to influence neither NO_3^- reduction nor N_2O production in *anaerobic* environments.

1.5.7 Effect of temperature on N_2O evolution from soil

Temperature affects the reaction rate of most biological processes. Goodroad and Keeney (1984) showed that increased nitrification was brought about by an increase in temperature from 10 to 30 °C. Ambus (1993) found a 4.4 fold increase in denitrification with a temperature change of 0 to 15 °C. Denitrification and nitrification both have a Q_{10} of 2, which indicates that the processes are sensitive to

temperature fluctuations both seasonally and diurnally (Goodroad and Keeney, 1984; Tisdale *et al.*, 1985; Haynes and Sherlock, 1986; Tate, 1995).

The minimum temperature for both denitrification and nitrification is generally 0 °C, however, denitrification has been shown to occur at -2 °C in supercooled water upon addition of an organic substrate (Dorland and Beauchamp, 1991). Somerfield *et al.*, (1993) and Burton and Beauchamp (1994) showed that both nitrification and denitrification are able to function, albeit slowly, under snow-covered soil. There have even been reports that freezing of soils increases the soils capacity to denitrify but this is probably due to the enhancement of the soil organic fraction that is made available to denitrifiers when the soil thaws (Tisdale *et al.*, 1985) and the release of surface-trapped N₂O from underlying unfrozen layers (Burton and Beauchamp, 1994). Flessa *et al.*, (1995) found that up to 46 % of the annual total amount of N₂O emitted was released during frost-thaw cycles, in December-January.

The maximum temperature for denitrification is approximately equivalent to that which limits the microbial population in general: about 60 to 70 °C. (Tisdale *et al.*, 1985; Sahrawat and Keeney, 1986; Tate, 1995). In the laboratory nitrification was found to occur up to a temperature of 65 °C and 45 °C for ammonium and nitrite oxidizers respectively (Tate, 1995).

The optimum temperature for each process varies due to the environment from which the soil was taken (Haynes, 1986 b). Powlson *et al.*, (1988) found that soils from different climatic zones responded differently to specific temperatures. However, the optimum temperature range for both processes in soils is generally between about 25 and 35 °C (Tisdale *et al.*, 1985). Bremner and Blackmer (1981) reported that an increase in the soil temperature from 5 to 30 °C increased N₂O emission from nitrification. Freney *et al.*, (1979) reported similar findings. Bailey (1976) found that during denitrification greater proportions of N₂O were evolved at low temperatures (below 15 °C) than at higher temperatures (above 30 °C). Keeney *et al.*, (1979) found that while the total rate of denitrification was low at temperatures less than 15 °C, the total amount of N₂O evolved could at least be equivalent to that produced at 25 °C.

The effect of temperature on the $N_2:N_2O$ ratio is not fully clear. Some studies showed an increase in the ratio with temperature (Keeney *et al.*, 1979) whereas in other investigations no significant effect of temperature was found (Bailey and Beauchamp, 1973; Skiba *et al.*, 1994). The effect of temperature probably results from a direct influence on the enzymatic reactions involved or an indirect result of increased microbial activity which will decrease O_2 availability (Smith and Arah, 1990). There is also some evidence that the temperature effect may be pH dependent. Nommick and Larsson (1989) reported that when the temperature dropped from 21 to 6 °C, the $N_2:N_2O$ ratio in a (forest) soil of pH 5.2 was unaffected, but in a (agricultural) soil of pH 6.9 the ratio decreased.

Temperature effects on N_2O production in soils may also be complicated by accumulation of NO_2^- at elevated temperatures which could subsequently be involved in chemical reduction to N_2O . Furthermore, in response to temperature change, differential organic matter mineralization may change the redox potential which further complicates prediction of N_2O production (Sahrawat and Keeney, 1986). An increase in temperature decreases the solubility of O_2 in water and increases the rate of diffusion of gases and solutes; both effects can have a profound influence on both nitrification and denitrification.

1.5.8 Effect of pH on N_2O evolution from soil

The optimum pH for autotrophic nitrifiers in cultures is between pH 7.0 and 9.0. In soils at pH >7.5, NH_3 may be present which is very toxic to *Nitrobacter spp.*. Thus NO_2^- may accumulate as NH_4^+ oxidizers remain active (Tate, 1995). The oxidation of NH_4^+ however, results in the acidification of the soil environment therefore suppressing nitrification (Haynes, 1986 b; Tate, 1995). In culture, both the rate of nitrification and the number of nitrifiers decline sharply below a pH of about 6.0 (Tate, 1995).

Goodroad and Keeney (1984) report that nitrification increased with increasing pH from 4.7 to 6.7. A similar observation was reported by Martikainen *et al.*, (1993).

These constraints apply mainly to autotrophic nitrification; heterotrophic nitrification can occur in acid soils such as under forests (Haynes, 1986 b), however the rate of nitrification is much lower than that of chemoautotrophs (Tate, 1995). Below a pH value of 5.5 aluminium toxicity could affect nitrification rates (Tisdale *et al.*, 1985; Haynes, 1986 b). Furthermore, aluminium immobilizes phosphate which enhances growth of NH_4^+ oxidizers (Sahrawat and Keeney, 1986; Russell, 1988). Generally, liming of soils stimulates nitrification, as CaCO_3 reduces the amount of available aluminium in the soil.

The optimum pH for denitrification occurs between 7.0 and 8.0, and the process is active within a pH range of about 3.9 to 9.0, however, denitrification is slow below pH 6.0. (Tisdale *et al.*, 1985; Sahrawat and Keeney, 1986). Weier and Gilliam (1986) showed that denitrification rate increased with pH, this was pronounced at pH values greater than 6.5. Similar results were found by Focht (1974). Blosl and Conrad (1992) state that pH greatly affects reduction of N-oxides. The authors found that pH changes the composition of the N-reducing bacterial community in soil, with NO_3^- reducers becoming more diverse with increasing pH.

The effect of pH on the $\text{N}_2:\text{N}_2\text{O}$ ratio is reported throughout the literature (Nommik, 1956; Wiljer and Delwiche, 1954; Blackmer and Bremner 1978; Firestone *et al.*, 1980; Koskinen and Keeney, 1982; Weier and Gilliam, 1986) with observations indicating that an increase in acidity decreased the $\text{N}_2:\text{N}_2\text{O}$ ratio. Firestone *et al.*, (1980) showed that the effect of pH on the $\text{N}_2:\text{N}_2\text{O}$ ratio was affected by the NO_3^- concentration. The authors found that, in the absence of measurable NO_3^- , there was no effect on the $\text{N}_2:\text{N}_2\text{O}$ ratio with changes in pH. However, when NO_3^- was added, the $\text{N}_2:\text{N}_2\text{O}$ ratio was about 16:1 at pH 6.5 and 1:2 at pH 9. The authors concluded that the effect of pH on the $\text{N}_2:\text{N}_2\text{O}$ ratio interacted with the effect of NO_3^- or NO_2^- concentration.

Weier and Gilliam (1986) also report that N_2O evolved from denitrification increased with an increase in acidity with maximum emission of N_2O (92.5 % of total gaseous product) at $\text{pH} \leq 5.8$. The total rate of denitrification however, either remained unchanged or decreased. Above this pH N_2O evolution ceased whereas total

denitrification increased. Similarly, Nommick and Larsson (1989) found that at pH 5.7 the $N_2:N_2O$ ratio was 1:3, while at pH 4.6 the ratio decreased to 1:20; at pH 4.3, N_2 production had ceased completely. It is suggested that N_2O reductase is more sensitive to low pH conditions, than the other N-oxide reductases (Knowles, 1981 b; Haynes and Sherlock, 1986).

Few studies have resolved whether denitrifier activity is limited by the direct effects of hydrogen ion activity or indirectly through nutrient deficiencies and/or toxicities induced by low pH. Koskinen and Keeney (1982), Davidson (1992) and Tate (1995) suggest that there are many interactions between pH and other factors such as temperature and organic matter that effect both denitrification and nitrification. Koskinen and Keeney (1982) report that at pH 4.6 and 5.4, the rate of N_2O production largely exceeded the rate of N_2O reduction, until more than 90 % of the soil NO_3^- had been reduced. At pH 6.9 the N_2O production rate exceeded the N_2O reduction rate only until 12 % of the soil NO_3^- had been reduced.

Haynes and Sherlock (1986) suggested, from laboratory studies, that an increase in pH may increase denitrifier activity by increasing the solubility of soil organic matter. Decreasing the pH reduces the availability of molybdenum which may limit the synthesis of NO_3^- -reductase, a molybdo-protein enzyme (Aulakh *et al.*, 1992). At pH values lower than 5.5 the denitrifier population may be inhibited by toxic concentrations of Mn and Al (Haynes and Sherlock, 1986).

It is recognised that in acid soils, chemical reduction of NO_2^- can also contribute to gaseous N production (Tate, 1995). Koskinen and Keeney (1982) suggested that, due to lower pH levels, NO_2^- concentrations may increase, thus affecting the $N_2:N_2O$ through a chemical reduction pathway.

1.5.9 Effect of vegetation and land use on N₂O evolution from soil

Different plant communities affect the soil in different ways, through their effect on soil humus, pH, water potential, nutrient availability and N cycling (Breitenbeck *et al.*, 1980; Russell, 1988). A recent study of the N₂O fluxes from different forest, grassland and agricultural ecosystems revealed large spatial variations (Ambus and Christensen, 1995). Haynes (1986 b) reviewed the effect of plants on nitrification rates and states that plant inhibition of nitrification is rather conflicting and inconclusive. He reports that the rate of nitrification decreases with increase in plant succession. Plants in the intermediate and climax stages of vegetative succession strongly inhibit nitrification, due to P limitations and production of various toxic organic compounds. Haynes (1986 b) also states that not only substances such as phenolic compounds derived from coniferous forest soils inhibit nitrification, but also root extracts from both forest trees and several grass species. However these studies are laboratory based and have not been proved in the field.

In the rhizosphere nitrifying and denitrifying heterotrophs may oxidize NH₄⁺ and reduce NO₃⁻ to a greater extent due to the profusion of readily available carbonaceous material. Klemedtsson *et al.*, (1991) reported that the increase in denitrification that occurred within rows of plants was greater than that between rows, due to the greater amount of available carbon produced in the rhizosphere. Similar results were found by Svensson *et al.*, (1991). In the rhizosphere the concentration of micro-organisms is up to 10 and 100 times greater than in the surrounding root-free soil (Haynes and Sherlock, 1986). This large microbial population, in conjunction with root respiration, can deplete the available O₂ thus changing the redox potential in the rhizosphere. A study on the effect of plant roots on the denitrification rate and the N₂:N₂O ratio showed that both the rate and the ratio were generally greater in the presence of plant roots this was explained as an indirect effect of the roots on the oxygen concentration in the soil (Klemedtsson *et al.*, 1987). The redox potential in the soil is also influenced by plant root systems which take up considerable amounts of water, dramatically altering the soil moisture potential.

Plants are also in direct competition with both denitrifiers and nitrifiers for NO_3^- and NH_4^+ respectively, thereby limiting the microbial processes (Tisdale *et al.*, 1985; Haynes, 1986 b; Bowden *et al.*, 1991). Preferences for specific N compounds exist in plant-microbial communities; nitrification may be limited, for example, as most plants and mycorrhizal fungi take up NH_4^+ in preference to NO_3^- (Haynes and Sherlock, 1986). Competition also exists between microbial communities. Bowman and Focht (1974) report that immobilization of NO_3^- although insignificant at high levels of NO_3^- application, appears to be more significant at lower NO_3^- concentrations, especially under aerobic conditions; thus competition between denitrifiers and immobilizing micro-organisms may be considerable when NO_3^- is limiting.

The choice of land use is a source of variability of N_2O emissions. For example, animals on land influence N_2O emissions with urine and faecal deposition (Colbourn, 1993; Monaghan and Barraclough, 1993; Ruz-Jerez *et al.*, 1994). The type of vegetation may also influence rates of N_2O production (Svensson *et al.*, 1991; Ambus and Christensen, 1995). In two Canadian prairies it has been shown that the total gaseous N loss was 2 to 5 times greater in summer-fallowed plots than from cropped plots (Aulakh *et al.*, 1982). Goodroad and Keeney (1984) showed that a coniferous forest floor produced significantly more N_2O than that from a deciduous forest floor. The same authors report that low N-grassland systems have lower N_2O emissions compared to managed ecosystems. Beauchamp *et al.*, (1996) recently reported that N_2O emission rates differed under different crops and under different cultivation practices.

Soil cultivation influences N_2O emissions through its capacity to influence the degree of soil compaction and pore geometry which have profound effects on the water-holding capacity of the soil and thus diffusion into and out of the soil as well as production rates (Linn and Doran, 1984; Sexstone *et al.*, 1985 b). It is reported that *no-till* soils have a greater loss of N by denitrification than is found from conventionally tilled agricultural systems (Linn and Doran, 1984; Aulakh *et al.*, 1984 a, b; Haynes and Sherlock, 1986; Stayley *et al.*, 1990; Rodriguez and Giambiagi, 1995). No-till soils tend to have higher levels of water soluble C promoting denitrification but

a lower rate of mineralization, hence lower nitrification and nitrifier populations (Haynes and Sherlock, 1986). Hilton *et al.*, (1994) compared no-till, chisel plough and mouldboard plough cultivation practices and found a decrease in denitrification emissions with increase in disturbance by cultivation. They also found that emission rates on corresponding treated soils, that were subsequently compacted by machinery were 1.6 times greater. A contrary report states that compaction of soils by farm machinery reduced emission rates from denitrification (Hansen *et al.*, 1993).

Colbourn and Harper (1987) reported that the drainage characteristics of soil play an important part in denitrification. They found that total denitrification rates were twice as great in undrained plots than in drained plots, but greater losses of N_2O (specifically) occurred in the drained plots. In fact all gaseous N emission was found to be in the form of N_2O in drained plots and as N_2 in undrained plots. The N_2O fraction in the drained plot decreased from 100 % of total gaseous N emission following a decrease in temperature in winter months, which caused an overall reduction in denitrification in both treatments (Colbourn and Harper, 1987).

1.5.10 Summary

All regulating factors except those influencing NO_3^-/NO_2^- concentration appear to have the same effect on the $N_2:N_2O$ ratio as on the total denitrification rate. Any factor that increases denitrification concurrently decreases the relative proportion of N_2O . Some conditions that favour a relatively higher proportion of N_2O production during denitrification, such as aerated soils and high NO_2^- concentrations, will also favour nitrification.

The results of numerous studies show a very consistent picture in considering whether a factor affects the N_2O production positively or negatively (Table 1.1). However, the mechanisms by which the factors affect this emission are seldom straightforward. Some mechanisms are associated with enzyme activity, whereas others affect the N_2O emission indirectly via soil or environmental conditions. The numerous variables

involved, the heterogeneous nature of soil, the apparent interaction between factors such as pH and NO_3^- and temperature and O_2 , and the fact that N_2O is produced during both denitrification and nitrification, hampers quantification of the mechanisms involved.

Table 1.1 Summary of factors which affect the $\text{N}_2:\text{N}_2\text{O}$ ratio from both denitrification and nitrification (adapted from Sahrawat and Keeney, 1986; Firestone and Davidson, 1989).

Factor	Effect on		
	$\text{N}_2:\text{N}_2\text{O}$ ratio	Denitrification rate	Nitrification rate
$\text{NO}_3^-/\text{NO}_2^-$	-	+	- / +
PO_2	-	-	+
soil water content	+	+	-
Carbon availability	+	+	
NH_4^+ availability	+		+
pH	+	+	+
Temperature	+	+	+

1.6 ANALYSIS TECHNIQUES FOR QUANTIFYING N₂O EMISSION

Collection and interpretation of data to unambiguously quantify gaseous losses of N produced by denitrification and nitrification has been a long-standing problem in soil N research. There are few methods that can directly quantify N₂O emissions from soil, the techniques currently available include gas chromatography (GC), infra-red (IR) gas analysis, and mass spectrometry (MS).

Gas Chromatography owes its popularity to several of its inherent advantages, including its capacity to separate multi-component mixtures and the fact that it can rapidly provide precise quantitative results from small samples. Since the development of GC techniques in the early 1950s a multitude of methods have been applied to measuring N₂O (Payne, 1973; Bailey and Beauchamp, 1973; Blackmer *et al.*, 1974; Ghoshal and Larsson, 1975; Blackmer and Bremner, 1977, 1978; Ryden *et al.*, 1979). Early analysis of N₂O by GC involved a wide array of instrument configurations due to insufficient sensitivity in the detectors used which were unable to measure ambient N₂O without prior concentration. Pre-concentration methods included the use of supercooled columns (Blackmer and Bremner, 1978), CO₂ traps (Mosier and Mack, 1980) or molecular sieves (Bailey and Beauchamp, 1973; Payne, 1973; Ryden *et al.*, 1978) in association with column coupling (Blackmer *et al.*, 1974) that was either in series (Burford, 1969) or in parallel that were connected to one or two different detectors (Smith and Dowdell, 1973). Currently the only GC detector sensitive enough to measure ambient N₂O without prior concentration is the ⁶³Ni-ECD, which was first used by Wentworth *et al.*, in 1971 and still continues to be widely used (Skiba *et al.*, 1994; Hargreaves *et al.*, 1994; Coolman and Robarge, 1995; Flessa *et al.*, 1995; Beauchamp *et al.*, 1996).

Infra-red (IR) gas analysis has been applied to measurement of N₂O concentration since the pioneering work of Arnold (1954) who first estimated N₂O loss from a soil surface. But was disregarded due to rapid developments in GC technology. However there has been a recent revival in its use for field scale measurements of N₂O emissions (Smith *et al.*, 1994 a; Smith *et al.*, 1994 b; Hargreaves *et al.*, 1994). Other recent developments include the tuneable diode laser which is used primarily for eddy

correlation determinations (Hargreaves *et al.*, 1994; Wiehnhold *et al.*, 1995). Groffman and Turner (1995) have used remote sensing techniques to quantify emission of gaseous N loss relative to plant productivity. Robertson *et al.*, (1993) used thermal infra-red emissions from remote sensing measurements to estimate denitrification in soil.

Mass spectrometry is the other main instrument capable of measuring ambient concentrations of N₂O. Knowles and Blackburn (1993) reviewed MS techniques with respect to soil N-studies. The majority of MS methods involve the application of ¹⁵N fertilizer to soils and measurement of the resultant labelled gaseous emission (Focht *et al.*, 1980; Mulvaney and Kurtz, 1982; Germon, 1985; Mosier *et al.*, 1986; Mulvaney and Vanden Heuvel, 1988; Monaghan and Barraclough, 1993; Arah *et al.*, 1993). ¹⁵N has also been recently measured using the *arc*ing method (Avalakki *et al.*, 1995) and by emission spectrometry (Murakami *et al.*, 1986; Erikson and Holtan-Hartwig, 1993) which are less complex and require less sophisticated instruments than mass spectrometry.

No instrument alone can differentiate between N₂O evolved from denitrification and that from nitrification, therefore various nitrification inhibitors have been used such as: low concentrations of acetylene (C₂H₂) (Klemedtsson *et al.*, 1987; Rudaz *et al.*, 1991; Martikainen and DeBoer, 1993; Chen *et al.*, 1994; Mummey *et al.*, 1994), nitrapyrin (Bronson *et al.*, 1992; Hutchinson *et al.*, 1993; Monaghan and Barraclough, 1993; Chen *et al.*, 1994), N-serve (Aulakh *et al.*, 1984a) methyl fluoride; (Miller *et al.*, 1993), dimethyl ether (Miller *et al.*, 1993), encapsulated calcium carbide (Bronson *et al.*, 1992) and dicyandiamide (Willison and Anderson, 1991; Eriksen and Holtan-Haertwig, 1993; Skiba *et al.*, 1993). Denitrification can be inhibited by O₂ (Robertson and Tiedje, 1987; Sabaty *et al.*, 1993) However, it has been found that the isotopic composition of N₂O emitted from soils from denitrification and nitrification can be differentiated. Isotopic characterisation is a relatively new technique and has been used by Webster and Hopkins (in press) to determine the source of N₂O from both cultures and soils under a range of experimental conditions.

Chapter 2: General Materials And Methods

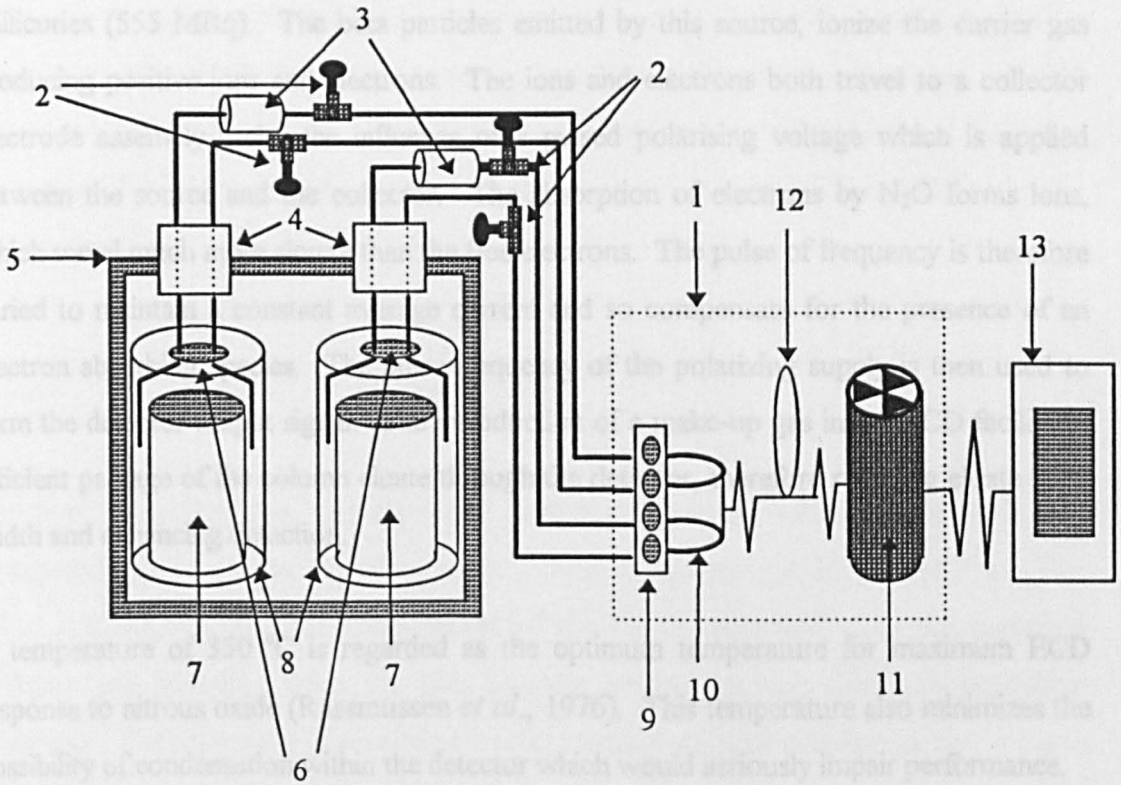
2.1 AUTOMATED SOIL HEADSPACE GAS ANALYSER

The initial aim of the work was to develop an automated soil headspace gas analyser for continuous short term measurement of nitrous oxide emission. The system constituted an incubator that housed gas tight chambers in which soil cores were contained. The atmosphere within each of the chambers was connected separately, via an air pump, to the sampling valve of a gas chromatograph. During a sampling event, the chamber atmosphere was first circulated through the GC sampling valve for 5 minutes to ensure assay of a representative aliquot. A volume (0.5 cm^3) of circulated atmosphere was then passed to the GC column for N_2O and CO_2 analysis. The following section describes the experimental design and configuration that was used throughout the study. The experimental design is illustrated in Fig. 2.1.

2.1.1 General description of the Gas Chromatograph

Analysis of the soil headspace was performed with a Perkin-Elmer 8410 series gas chromatograph fitted with a ^{63}Ni electron capture detector (ECD). The ECD was chosen as it possesses sufficient sensitivity for measuring ambient nitrous oxide without prior concentration using molecular sieves (Ryden *et al.*, 1978) or supercooled columns (Blackmer and Bremner, 1978). The GC possessed only one column which was down-line from a ten port heated gas sampling valve automated by a pneumatic actuator module (Valco Instruments Co. Inc.). High purity nitrogen was used as both the carrier and make-up gas streams through the GC system.

Figure 2.1 Experimental design of the soil headspace gas analyser.



1. Gas chromatograph
2. Aeration taps
3. Pumps
4. Incubator access port
5. Incubator
6. Gas tight chamber access port
7. Soil cores
8. Gas tight chambers
9. GSV
10. Sample loop
11. ECD
12. Column
13. Integrator

2.1.1.1 The Electron Capture Detector

The ECD is currently the most sensitive detector available for detection of electrophilic molecules, such as nitrous oxide (labelled 11 in Fig. 2.1). The ECD detector cell contains a nickel foil in a cylinder through which the carrier gas flows. The coating on the inner surface of the foil contains the radioactive isotope Nickel-63 at a nominal activity of 15 millicuries (555 MBq). The beta particles emitted by this source, ionize the carrier gas producing positive ions and electrons. The ions and electrons both travel to a collector electrode assembly under the influence of a pulsed polarising voltage which is applied between the source and the collector. The absorption of electrons by N_2O forms ions, which travel much more slowly than the free electrons. The pulse of frequency is therefore varied to maintain a constant average current and so compensate for the presence of an electron absorbing species. The pulse frequency of the polarizing supply is then used to form the detector output signal. The introduction of a make-up gas in the ECD facilitates efficient passage of the column eluate through the detector, therefore reducing eluate band width and enhancing detection.

A temperature of 350 °C is regarded as the optimum temperature for maximum ECD response to nitrous oxide (Rasmussen *et al.*, 1976). This temperature also minimizes the possibility of condensation within the detector which would seriously impair performance.

2.1.1.2 GC Column And Column Packing

Initially the column used was stainless steel 2 m in length with an outer diameter of 3.125×10^{-3} m and internal diameter of 2.2×10^{-3} m. The original column was filled with 'Porapak Q porous polymer' of size 50-80 mesh. However, this was found to give inadequate separation between the retention times of nitrous oxide and carbon dioxide which both have the same molecular weight (44). Following advice from Perkin Elmer it was decided to use a 2 m column packed with 'Porapak QS' (100-120 mesh) at an oven temperature of $55 \text{ °C} \pm 0.5 \text{ °C}$ for maximum separation of the two gases (labelled 12 in Fig. 2.1).

2.1.1.3 Carrier And Make-Up Gas Supply

The GC column was connected to a gas supply of high purity nitrogen (99.995%). This gas was filtered to extract both moisture and oxygen before entering the system using Chrompack 'Gas-clean' moisture and oxygen filters. Nitrogen gas was used for both the carrier and make-up gas supplies. The carrier gas is directed through the sampling port and picks up the gas sample while the make-up gas continually flows through the ECD. Calibration of both the carrier and make-up gas flows through the system was achieved with a soap bubble flow meter. The carrier gas pressure was set to 140 kPa, and the make-up gas to 190 kPa to give fluxes through the ECD and column of 40 and 25 cm³ min⁻¹ respectively.

2.1.1.4 The Automated Gas Sampling Valve

The sample injector used, was a ten port heated gas sampling valve (GSV), which was automated by a pneumatic actuator module (Valco Instruments Co. Inc.) labelled 9 in Fig. 2.1. The original ten port configuration of the GSV was modified to accommodate alternate gas sampling from the two separate streams coming from the incubation chambers. The procedure of alternate chamber analysis was advantageous as only a single carrier inlet, column and detector was needed. This reduced any systematic errors between chamber analyses. To increase reproducibility and maximize column efficiency, a low volume sample loop (0.5 cm³) was fitted to the GSV, labelled 10 in Fig. 2.1. A small volume in the sample loop decreases the sample fill time. Thus, the transfer of the sample from the loop to the column requires a lower carrier gas flow rate and a greater time is available for N₂O and CO₂ separation. The GSV-actuator is activated by relay switches labelled 1 and 0 on the gas chromatograph. These switches may be operated either via keyboard control or automatically set by the 'timed event' facility on the GC. The GSV operation is illustrated in Fig. 2.2.

Position A, (Fig. 2.2).

The fixed volume sample loop 1 is connected in series with the inlet and outlet of sample line 1. Meanwhile sample loop 2 links the carrier gas to the column and the inlet and outlet of sample line 2 remain dormant, in a closed circuit. At the appointed time the atmosphere from chamber 1 is circulated through sample line 1 purging the sample loop. The circulation of the chamber atmosphere is then stopped and the GSV switches to position B.

Position B, (Fig. 2.2).

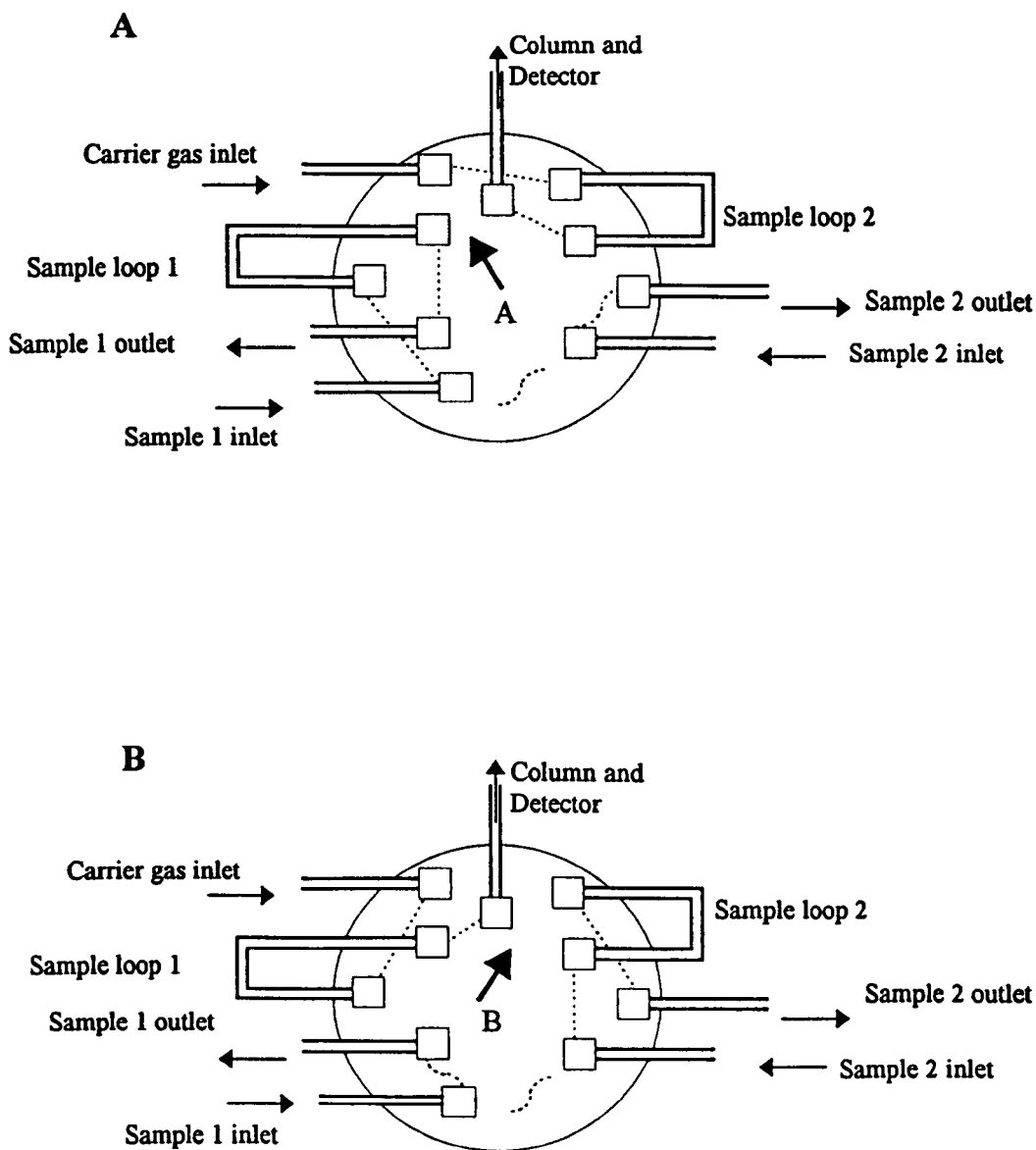
The switching of the GSV moves sample loop 1 to lie between the carrier gas inlet and the head of the column, whereupon the contents of the sample loop are driven onto the column by the carrier gas. At this point the inlet and outlet of sample line 1 lie dormant in a closed circuit. In this configuration sample loop 2 has moved into position between the input and output of sample line 2. At a designated time pump 2 is activated and the atmosphere from chamber 2 is circulated through the sample line effectively purging the sample loop. Gas circulation ceases prior to GSV activation and the return to position A. The contents of sample loop 2 are then forced onto the column when it is moved to link the carrier gas to the head of the column.

2.1.2 Soil headspace transfer between chambers and the Gas Chromatograph

2.1.2.1 Circulation of Chamber Atmosphere

Pumps were incorporated into the system (labelled 3 in Fig. 2.1) to circulate the atmosphere in each chamber via the gas sample loops. Two small diaphragm pumps were used (Charles Austin pumps Ltd. Model Capex II, Weybridge, Surrey), one for each sample line; this had the advantage of independent activation and deactivation. When the pumps were unrestricted by connecting pipe work they had a capacity of 4 litres min⁻¹ however when they were connected to the system the flow was 0.8 litres min⁻¹.

Figure 2.2 Cross sectional view of the automatic gas sampling valve(GSV) labelled 9 in Fig. 2.1. Positions A and B show the configurations of the sampling loops and the sample lines. (----) represents the connective tubing between inlets and outlets of the GSV that undergo movement between positions A and B.



Low power pumps were chosen because they would not compromise the gas tight integrity of the system, considering the narrow bore pipes of the GSV where there is potential for a build up of pressure. The pumps were up-line of the GC, pumping gas out of the chambers, and into the GSV. This configuration was chosen to reduce the risk of failure of the chamber seals caused by positive pressure. The internal surfaces of the pumps that were in contact with the flow of gas, were coated in unreactive silicone high vacuum grease. This was undertaken to ensure that the ECD was not contaminated by plasticisers or rubber volatiles from the pump.

2.1.2.2 *The Incubator and Gas Tight Chambers*

The incubator used was a Sanyo-Gallenkemp INL-421 model (Loughborough, UK), labelled 5 in Fig. 2.1. The incubator was programmed to maintain $15\text{ }^{\circ}\text{C} \pm 0.5\text{ }^{\circ}\text{C}$ throughout all of the trials. The chambers inside the incubator were connected to the GC via copper tubing. Light was excluded with a 'black out' screen over the incubator observation window. To avoid any effect of temperature variation within the incubator, the two chambers were positioned side by side. Therefore the size of the gas tight chambers were limited by the internal dimensions of the incubator. The internal volume of the incubator accommodated two large glass 25 cm diameter 'dry seal' desiccators (Jencons, Hemel Hempstead, UK) which were used as gas tight chambers. The lids of the chambers each possessed a service port, which enabled connection with the GC. The chamber service ports were closed with silicone rubber bungs with two holes drilled for the inlet and outlet gas lines. The bung and gas lines were made gas tight with silicone rubber sealant; the seal between the lid and base of the chamber was secured with silicone grease.

The air filled capacity of each sample line which included the volume of both the chambers (9147 cm^3 and 8980 cm^3) and gas transfer pipes (53 cm^3), were determined by water displacement and the sum of pipe internal dimensions respectively. The total volume of sample lines 1 and 2, with vacant chambers are 9.20 litres and 9.03 litres respectively.

2.1.2.3 Chamber-Gas Chromatograph Link

The gas lines connecting the chambers with the GC were GC grade copper tubing (Phase Separation Ltd, Queensferry, Clwyd, UK) with *Swagelok* brass joints and ferrules. Silicone rubber sealant was applied to every brass union and copper joint to make the system gas tight. The GC, chambers and air pumps were connected with piping of outer diameter 0.65 cm and internal diameter of 0.46 cm. Copper piping with an outer diameter of 0.31 cm and internal diameter of 0.22 cm and the respective *Swagelok* reducing unions were used to connect the 0.22 cm diameter 'male' GC sample input and output ports to the larger bore piping. The two gas sample lines were of equal length.

The inlet and outlet ports of each pump were connected to the piping via a jacket of polyurethane tubing which was clamped with 'jubilee clips'. Brass *Swagelok* 3-way taps, facilitated periodic (daily) pumped aeration of the chambers. The two sets of 3-way taps located on each line effectively isolates the GC sample loops, therefore only the chambers and the large bore tubing underwent daily venting. The taps had to be turned manually to open (Fig. 2.3 b) and close (Fig 2.3 a) the system and the pumps were switched on and off via the GC keyboard.

2.1.3 Calibration of the gas chromatograph system

2.1.3.1 Integration of the GC output

The output from the ECD was recorded by a Perkin-Elmer Personal Integrator, model 1020X, labelled 13 in Fig. 2.1. The integrator records information upon the start of a GC run for a designated time period. The information from each GC run was stored on the hard disc of the integrator and simultaneously sent to a printer (Kodak Diconix 150+ printer). The integrator was used to determine the area of both CO₂ and N₂O chromatogram peaks. However, it was necessary to manually designate the start and end of each peak using the on-screen editing facility .

Figure 2.3 The two configurations of the 3-way taps (labelled (2) in Fig. 2.1). (a) = taps closed for circulation of chamber atmosphere; (b): taps open for daily venting sequence.

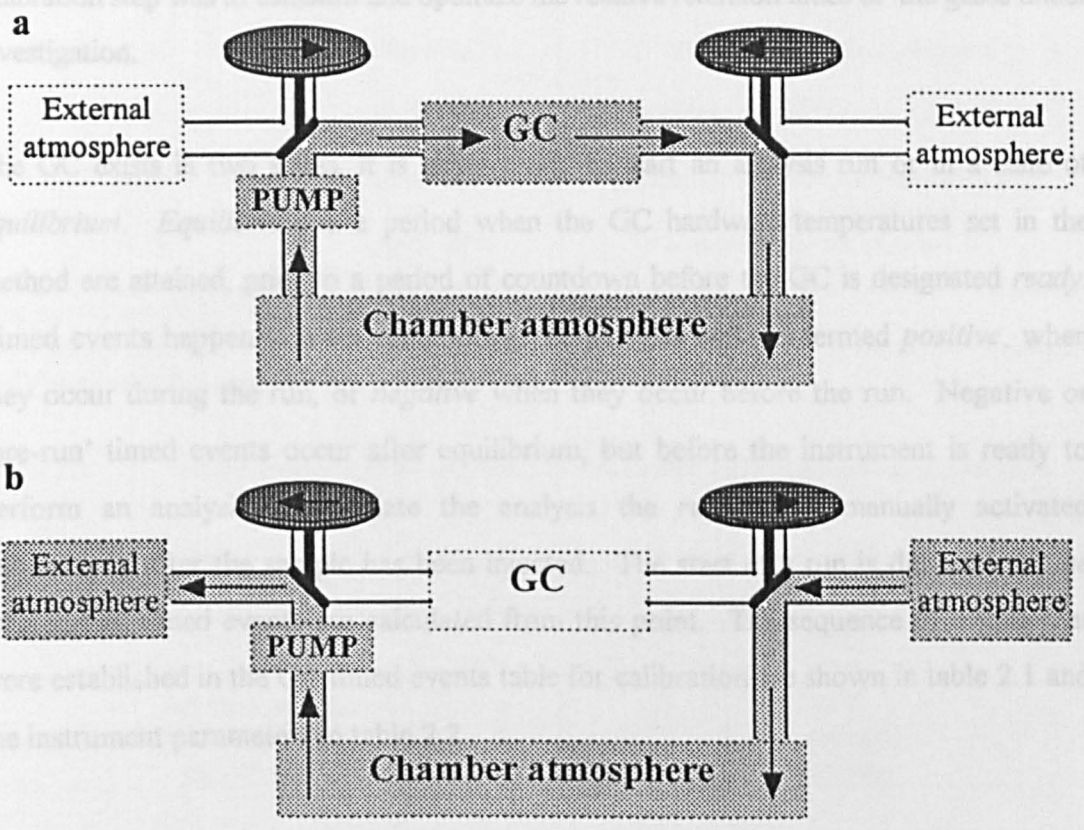
Prior to any instrument analysis, the GC was configured (i.e. information about the hardware fitted was provided) and a method was generated (the establishment of hardware temperatures and pressures, a countdown period and a 'timed events' table). The initial calibration step was to establish and optimize the relative retention times of the gases under investigation.

Equilibrium was reached when the GC hardware temperatures set in the method are attained, and a period of counting before the GC is designated ready. Timed events happen sequentially, and are designated positive, when they occur during the analysis, and negative, when they occur during the 'pre-run'.

Timed events occur after equilibrium, but before the instrument is ready to perform an analysis. Before the analysis the instrument is manually activated. The instrument parameters are set, and the events table for calibration, shown in table 2.1 and the instrument parameters are set.

Calibration includes the manual injection of nitrous oxide from a standard cylinder of known concentration via a 10 cm³ syringe. The standard is used to purge sample loop 1 before being swept onto the column by GSV activation. The signal sent from the PCD for each gas was calibrated by the integrator using the on-screen editing facility. Sample loop 2 was calibrated with the same method as described in tables 2.1 and 2.2, however, relay 0 was used to switch the GSV from position B to position A.

Once the system has been calibrated, the timed events given in table 2.1, can be used for manual analysis of individual gas samples, using a syringe.



2.1.3.2 GC-Integrator Calibration

Prior to any instrument analysis, the GC was *configured* (i.e. information about the hardware fitted was provided) and a *method* was generated (the establishment of hardware temperatures and pressures, a countdown period and a 'timed events' table). The initial calibration step was to establish and optimize the relative retention times of the gases under investigation.

The GC exists in two states, it is either *ready* to start an analysis run or in a state of *equilibrium*. *Equilibrium* is a period when the GC hardware temperatures set in the method are attained, prior to a period of countdown before the GC is designated *ready*. Timed events happen at a set time during the analysis and are termed *positive*, when they occur during the run, or *negative* when they occur before the run. Negative or 'pre-run' timed events occur after equilibrium, but before the instrument is ready to perform an analysis. To initiate the analysis the *run key* is manually activated immediately after the sample has been injected. The start of a run is designated *time zero* and all timed events are calculated from this point. The sequence of events that were established in the GC timed events table for calibration are shown in table 2.1 and the instrument parameters in table 2.2.

Calibration includes the manual injection of nitrous oxide from a standard cylinder of known concentration via a 10 cm³ syringe. The standard is used to purge sample loop 1 before being swept onto the column by GSV activation. The signal sent from the ECD for each gas was calibrated by the integrator using the on-screen editing facility. Sample loop 2 was calibrated with the same method as described in tables 2.1 and 2.2, however, relay 0 was used to switch the GSV from position B to position A.

Once the system has been calibrated, the timed events given in table 2.1, can be used for manual analysis of individual gas samples, using a syringe.

Table 2.1 Timed events table of the GC during calibration and manual analysis of gas samples.

Time (minutes)	Events	Action
<-3.00	equilibrium	temperature attainment
-3.00	countdown	countdown
-0.01	Set Zero	detector signal calibrated to zero
0.00	press Run	initiates GC run/ integrator recording
+0.01	relay 1 ON †	pneumatics activated; GSV switched from position A to position B*
+0.06	relay 1 OFF †	pneumatics de-activated in GSV

*contents of sample loop in GSV transferred to GC column

†calibration of sample loop 2 used the activation and de-activation of relay 0 which corresponded to GSV movement from position B to position A.

Table 2.2 Parameter values of the GC during calibration and manual analysis of gas samples.

Parameter	Value
Oven temperature	55 °C
Injection temperature	75 °C
Detection temperature	280 °C
Isothermal time	10.0 minutes
Equilibration time	3.0 minutes

The difference in retention times between carbon dioxide (1.914 minutes) and nitrous oxide (2.437 minutes) was greatest with an oven temperature of 55 °C.

To calibrate the system for both CO₂ and N₂O the ECD temperature was set to 280 °C. The optimum analysis temperature of each gas is different, however, the accuracy of both determinations was only marginally reduced at this temperature.

2.1.3.3 ECD Calibration

The linearity of the ECD response to both gases was assessed using dilutions from commercial standards (10 and 200 ppmv N₂O; 50000 ppmv CO₂). Standard dilutions of

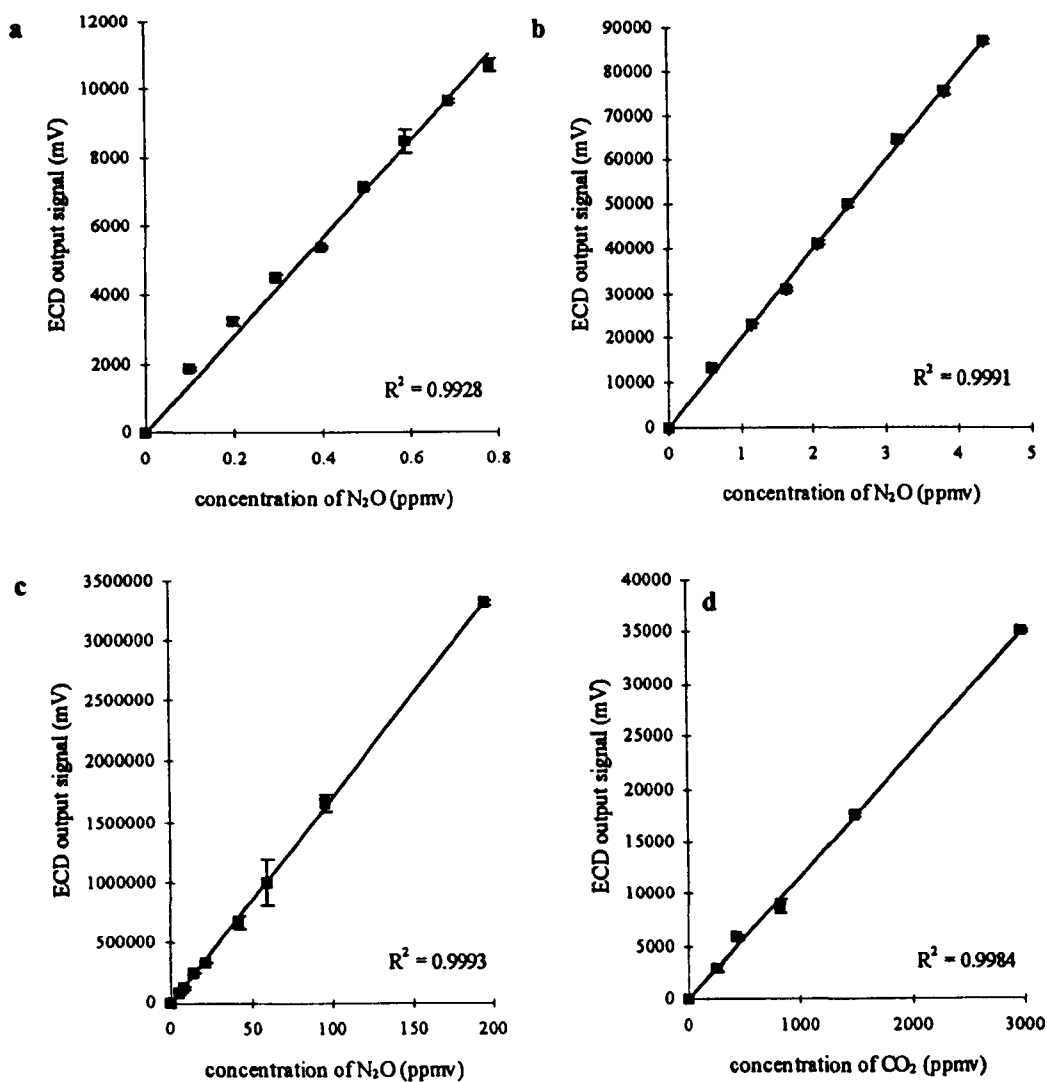
N₂O were made with a 500 cm³ gas sampling bulb. The bulb was first purged with ultra pure N₂ gas from which a known volume was extracted using a syringe. The extracted volume was then replaced with an equivalent volume of the stock gas (10 ppmv N₂O), to give a minimum N₂O standard of 0.02 ppmv N₂O. Following triplicate analysis of the first standard, a second aliquot of the N₂O stock (10 ppmv) was introduced to the gas sampling bulb to give a second standard. The dilution and analysis procedures were repeated until the GC was calibrated with 2 sets of 8 N₂O standards over the ranges 0-1 and 0-5 ppmv N₂O (Fig. 2.4, a and b). A third set covering the range 0-200 ppmv was calibrated using a 200 ppmv N₂O stock (Fig. 2.4, c). The same technique was used with the CO₂ standard (50000 ppmv) for the range of 0-3000 ppmv CO₂ (Fig. 2.4, d). All changes in gas composition in the gas sampling bulb were accounted for in the calculations of the sequential standard concentrations.

Prior to simultaneous measurement of both N₂O and CO₂ by the GC at 280 °C, gaseous emission rates of N₂O alone were measured by the GC at 350 °C and CO₂ was analysed with an ADC-CO₂ infra-red (IR) gas analyser (Analytical Development Company Ltd., Hoddesdon, UK). The IR apparatus was used only in experiments described in section 4.1-4.4. A sample of the headspace atmosphere was extracted via a septum in the gas-tight chambers using a syringe and injected into the IR gas analyser for quantification of CO₂.

2.1.4 Gas tight integrity of the GC system

Once the ECD was calibrated and the two gas tight chambers and pumps were connected in series, a check on the gas tight integrity of the GC system was undertaken. The pumps were simultaneously activated and the brass connecting unions inspected for major breaches in the gas tight integrity by applying a soapy solution. Each union and connection, on each line was inspected in turn for bubble formation which indicates a gas leak. However, no major leak was detected. A further check on the gas tight integrity was to inject a standard amount of N₂O into each sample line via a rubber septum, this was situated in the lid of each gas tight chamber. The known amount of N₂O introduced into each sample line was left to be pumped around the system, periodically being analysed. The subsequent chamber

Figure 2.4 Linearity of the ECD response to a range of standard concentrations of nitrous oxide (a, b and c) and carbon dioxide (d).



concentrations of N_2O would indicate whether a subtle leak was taking place in the system or not. The quantity of gas extracted during the analysis was taken into account during calculation of the chamber N_2O concentration.

2.1.5 Co-ordination of the GC Sampling Procedure

The equipment shown in Fig. 2.1 was linked by terminal blocks on the GC. The GC terminal blocks were activated by 4 on/off relay drivers (0,1, 2 and 3) controlled by the GC timed events schedule. There are 3 terminal blocks located on the side of the GC and 1 block on the side of the integrator, each block contains 10 terminals.

2.1.5.1 Gas Chromatograph-Integrator Link

The GC was linked to the integrator, so that the analogue output signal from the ECD was constantly displayed on the integrator VDU. This was facilitated by connecting terminals 9 and 10 on terminal block 1 of the GC to terminals 1 and 2 respectively, on the integrator terminal block.

The automatic recording of a sample run, was accomplished by activation of the integrator recording system at the start of the GC run. This was achieved by connecting terminals 5 and 6 on terminal block 2 of the GC with terminals 7 and 8 on the integrator. Thus, when the GC run was initiated, the integrator would start to record the output signal from the GC. The length of the recording period was determined by a designated 'end time' in the integrator software.

2.1.5.2 Gas Chromatograph-Pump Link

Two pumps were used to circulate the chamber atmospheres through sample loops A and B. The pumps were incorporated into the system using a custom built dual channel relay control box activated via the GC terminal blocks. The relay box possessed two 3-pin

sockets, A and B, corresponding to pumps A and B respectively. The relay box was linked to terminal block 3 on the GC with socket A connected to terminals 3 and 4 and socket B connected to terminals 7 and 8. Terminals 3 and 4 were activated by relay switch 2 on the GC while terminals 7 and 8 corresponded to relay switch 3. These relay switches were either operated manually via the keyboard or automatically by the timed event facility on the GC. The activation of the pumps had to be carefully co-ordinated, so that sufficient gas from the chamber was circulated through each respective sample loop to take a representative sample prior to analysis. After the deactivation of the pumps adequate time was needed before the change in GSV pathway in order to disseminate any build up of pressure that may have occurred in the sample loop back into the incubation chambers.

2.1.6 Automated Continuous GC Running

Once the system had been calibrated and connected, a timed event table that allowed continuous automated running of the GC was constructed. This required that both pumps were activated and de-activated in co-ordination with the sampling and recording of each run. In manual operation, the GC was started by pressing the RUN button. For the system to sample automatically, a short circuit was introduced between terminals 2 and 9 and terminals 3 and 10 respectively on terminal block 2. This caused the system to start automatically, immediately following the countdown, as soon as the GC was designated *ready*.

To determine the sampling rate, precise co-ordination between the length of both the countdown and the run was necessary. A 2 hour sampling rate with 5 minutes of pre-run events, required a countdown time of 90 minutes (including 5 min. equilibrium time), and a run time of 30 minutes. However, although total run time was 30 minutes, the integrator only recorded output for 13 minutes, after which all the gases of interest were eluted. The general timed events table used for automated analysis of N₂O and CO₂ from 2 chambers every 2 hours is shown in table 2.3. The values used for temperature and gas flow parameters remain the same as previously reported.

2.1.7. Single Chamber Analysis

Table 2.3 Timed events table for automated analysis of two chamber atmospheres.

Time (minutes)	Event	Action
-90.00	countdown	countdown
-5.00	relay 3 ON	pump A activation
-0.06	relay 3 OFF	pump A de-activation
-0.01	Set zero	detector signal calibrated to zero
0.00	run starts	initiates GC run and integrator recording for 13 minutes
0.01	relay 1 ON	pneumatics activated; GSV switched from position A to position B *
0.06	relay 1 OFF	pneumatics de-activated in GSV
2.94	relay 2 ON	pump B activation
7.94	relay 2 OFF	pump B de-activation
6.00	relay 0 ON	pneumatics activated; GSV switched from position B to position A **
6.05	relay 0 OFF	pneumatics de-activates in GSV
30.00	end GC run	start countdown

* contents of sample loop 1 transferred to GC column

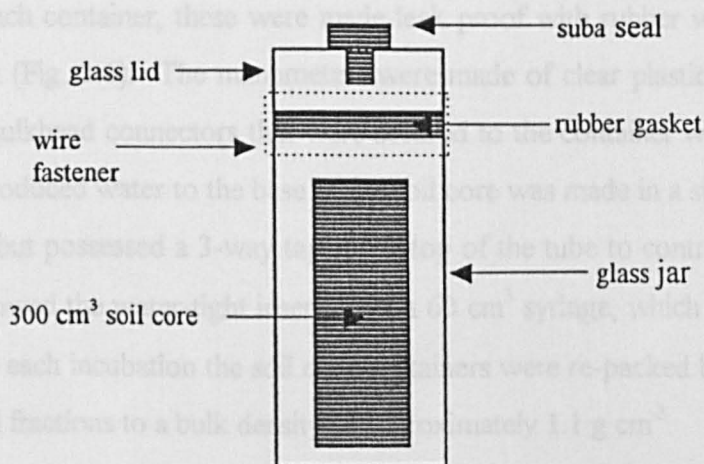
**contents of sample loop 2 transferred to GC column

2.1.7 Single Chamber Analysis

Incubation chambers for individual soil cores (25 cm³, 300 cm³ and 510 cm³ volume) were constructed from *Kilner* jars with a capacity of 1500 cm³ (Fig. 2.5). The jar lids were made gas tight with a rubber gasket. In the lid of each jar a hole was drilled (10 mm in diameter) in which was placed a rubber *Suba-seal* septum; the septum was made gas tight with the use of silicone rubber sealant.

Up to 24 jars could be accommodated within the incubator. The temperature was maintained at 15 °C in a light free environment and the clear glass jars were covered with a cardboard jacket to minimise any effect of light on the cores whilst analysis was undertaken. The headspace in the individual chambers was periodically analysed, as for the automated system. The gas was manually extracted through the rubber septum in the lid with a 10 cm³ syringe and injected into sample port 1. The timed events method used in the GC is described in table 2.1. When a sample of soil headspace gas was extracted from these chambers for analysis, an equivalent volume of high purity N₂ was injected back into the chamber, to avoid the development of any pressure gradients. Usually a sample was taken at the start and end of the individual incubation period, from which the mean flux rate of gases was calculated.

Figure 2.5 Schematic of one of the smaller incubation chambers (*Kilner jars*).



2.2 SOILS

2.2.1 Soil treatment and storage

There were three soil types used to study gas fluxes, a local sandy loam, and two from Lothian, Scotland, a sandy clay loam and a clay loam (table 2.4). Each of the soil samples were taken to a depth of 15 cm and gently hand sieved in the field-moist state, into four size fractions (<2 mm, 2-5 mm, 5-10 mm and 10-20 mm diameter). Visible particulate organic matter and pebbles were removed. The sieved fractions were stored in the dark in 12 cm deep covered trays that were lined with plastic sheeting, at a temperature of $2\text{ }^{\circ}\text{C} \pm 1\text{ }^{\circ}\text{C}$.

2.2.2 Re-packed soil core construction

Four different sizes of re-packed soil core were used, contained in heavy duty plastic cylinders: (*a*: 13.0 cm diameter and 16.3 cm in height; *b*: 7.0 cm diameter and 13.0 cm in height; *c*: 5.2 cm diameter and 15.0 cm in height; *d*: 5.2 cm diameter and 5.0 cm in height). The first core type was made from a general purpose wide neck container with straight sides. The second type (*b*) was made from a polypropylene narrow neck bottle, the rounded shoulder was taken off to give a straight sided cylinder. The last two cores (*c* and *d*) were cut from plastic drainage pipe, and the base covered with a fine nylon mesh to contain the soil. Cores *a* and *b* had manometers and tubes to introduce water inserted at the base of each container, these were made leak proof with rubber washers and silicone rubber sealant (Fig. 2.6). The manometers were made of clear plastic tubing attached to right-angled bulkhead connectors that were secured to the container with brass nuts. The tubes that introduced water to the base of the soil core was made in a similar fashion to the manometers, but possessed a 3-way tap at the top of the tube to control water flow. The 3-way tap allowed the water-tight insertion of a 60 cm³ syringe, which was used to deliver the water. In each incubation the soil core containers were re-packed by hand with one of the sieved soil fractions to a bulk density of approximately 1.1 g cm⁻³.

Figure 2.6 Schematic of manometer and water access tube construction on core types a and b.

Table 2.4 Characteristics of each of the three test soils

Location	Soil Name	Soil Class	Latitude
Grid reference			
Elevation			
Soil Series			
Texture			
Land Use			
Particle Size Analysis			
% Sand			
% Silt			
% Clay			
% Organic Matter			
% Organic Carbon			
pH (H ₂ O) 1:2.5			
pH (CaCl ₂) 1:2.5			
% moisture content at Field Capacity (0.005 MPa)			

2.2.3 Soil Characteristics

Table 2.4 Characteristics of each of the three test soils.

Location	Sutton Bonington Leicestershire	Bush (Crofts) Lothian	Bush (Cowpark) Lothian
Grid reference	507 261	245 653	238 627
Elevation	157m	190m	180m
Soil Series	Wick	unclassified alluvium	Winton
Texture	Sandy Loam	Sandy Clay Loam	Clay Loam
Land Use	fallow	winter barley	grass
Particle Size Analysis			
% Sand	70	49	35
% Silt	19	32	38
% Clay	11	19	27
% Organic Matter	2.1	4.7	5.5
% Organic Carbon	1.2	2.7	3.2
pH (H ₂ O) 1 : 2.5	5.7	6.4	5.2
pH (CaCl ₂) 1 : 2.5	4.9	6.0	4.8
% moisture content at Field Capacity (0.005 MPa)	30	36	43

2.2.4 Soil Analysis

2.2.4.1 Soil pH

The pH was determined by the method of Page *et al.*, (1982), using a Philips PW9409 digital pH meter. Two 10 g sub-samples of air dry soil were transferred to 50 cm³ beaker and either 25 cm³ of de-ionized water or 25 cm³ of 0.01 M calcium chloride were added. The soil slurries were stirred intermittently for 30 minutes and left to stand for 1 hour before the pH values of the settled soil suspensions were measured.

2.2.4.2 Soil organic carbon content

Soil organic matter content was determined by the Walkley-Black method (Page *et al.*, 1982). A 5 g sub-sample of air dried soil was ground and sieved to <0.5 mm then oven dried at 105 °C. Sub-samples (0.25 g) of the oven dried soil were weighed into 500 cm³ conical flasks and 10 cm³ of 0.167 M K₂Cr₂O₇ solution added. Concentrated H₂SO₄ (20 cm³) was then added and the suspensions were mixed and allowed to stand for 30 minutes. Following this, 200 cm³ of de-ionized water, 10 cm³ concentrated H₃PO₄, and 2 cm³ barium diphenylamine sulphonate solution (0.16 g dm⁻¹) were added. The flasks were then cooled under running water and the contents titrated against 0.5 M ammonium iron (II) sulphate in H₂SO₄ (0.5% v/v) to a bright green end point. A reagent blank was also titrated for the control; the quantity of oxidised organic carbon was found by difference between blank and sample titres.

2.2.4.3 Soil Moisture Characteristics

A restricted range of the soil moisture characteristic of each soil was determined with the 'Haines' suction apparatus. This is essentially a porous sintered glass funnel connected to a burette with a length of pressure tubing, forming a flexible U-tube. The apparatus is pre-filled with de-ionized water and arranged on a stand. 100 cm³ of air

dried soil (<2 mm) was distributed evenly in the funnel to form a level bed. The soil was then allowed to wet up by capillary action, raising the burette to shorten the connecting U-tube as necessary. The funnel was covered by a polythene sheet to minimize evaporation. When the soil surface was damp, the sample was flooded by raising the burette such that free water existed around the sample.

A note was made of the height of the soil surface from the floor, the meniscus reading in the burette and its height from the floor. The burette was then lowered about 1 cm and when the equilibrium was re-established both the new meniscus reading in the burette and its height from the ground were noted. Up to suctions of 0.002 MPa, equilibration was rapid but from 0.002 - 0.005 MPa it was necessary to allow 24 hours for equilibrium. This procedure was repeated until the meniscus was about 50 cm below the floor of the funnel. The moisture characteristics of each soil are shown in Fig. 2.7.

2.2.4.4 Particle size analysis

Soil particle size analysis was determined by the pipette method (Page *et al.*, 1982).

A 10 g sample of air dried soil was placed in a 500 cm³ tall beaker with 10 cm³ of de-ionized water. To remove the organic matter, 10 cm³ of 30 % H₂O₂ was added and the suspension was stirred. The soil mixture was allowed to stand until the rapid effervescence of the oxidation reaction had subsided. Excess frothing was washed down with distilled water and additional H₂O₂ was added until effervescence had ceased completely. The contents of the beaker were then diluted with approximately 40 cm³ of de-ionized water and placed on a hotplate at 90 °C for 1 hour, where the volume of the suspension was reduced to approximately 25 cm³. This suspension volume was maintained at 25 cm³ by adding de-ionized water for the duration of the heating. Once the beakers were removed from the hotplate and cooled, 10 cm³ of dispersing agent (5 g sodium hexametaphosphate and 0.7 g anhydrous sodium carbonate in 100 cm³ de-ionized water) was added. The suspensions were then diluted with distilled water to approximately 150 cm³, and then transferred to a 250

cm³ bottle which was shaken overnight. The soil suspension was passed through a 63 μm sieve to remove the sand fraction which was oven dried (105 °C) overnight and the weight noted, (*A*). The proportion of sand was determined using equation 2.2. The sieved suspension was then transferred to a 500 cm³ cylinder and diluted to the (500 cm³) mark and stirred thoroughly. A 25 cm³ pipette was used to extract a sample of the homogenized suspension from a depth of 20 cm. This sample was oven dried overnight and weighed to determine the silt and clay fraction (*B*; g in 25 cm³). The proportion of silt in the sample was determined using equation 2.3. The suspension in the cylinder was re-stirred and left to stand for 8 hours at 20 °C to allow the clay fraction (< 2 μm) to settle to a depth of 10 cm. At the appropriate time a 25 cm³ pipette was used to extract a sample at exactly 10 cm depth which was again oven dried overnight and weighed to determine the clay fraction (*C*, g in 25 cm³). The proportion of clay in the sample was determined using equation 2.4. The mass of peroxide treated soil, *M* (g) was determined using equation 2.1. *M* is defined as the sum of the mass of the extracted sand fraction, *A* (g) and the mass of the silt and clay fraction in the measuring cylinder, (*B* (g in 25 cm³) × 20), minus the weight of dispersant.

mass (g) peroxide treated soil (*M*) =

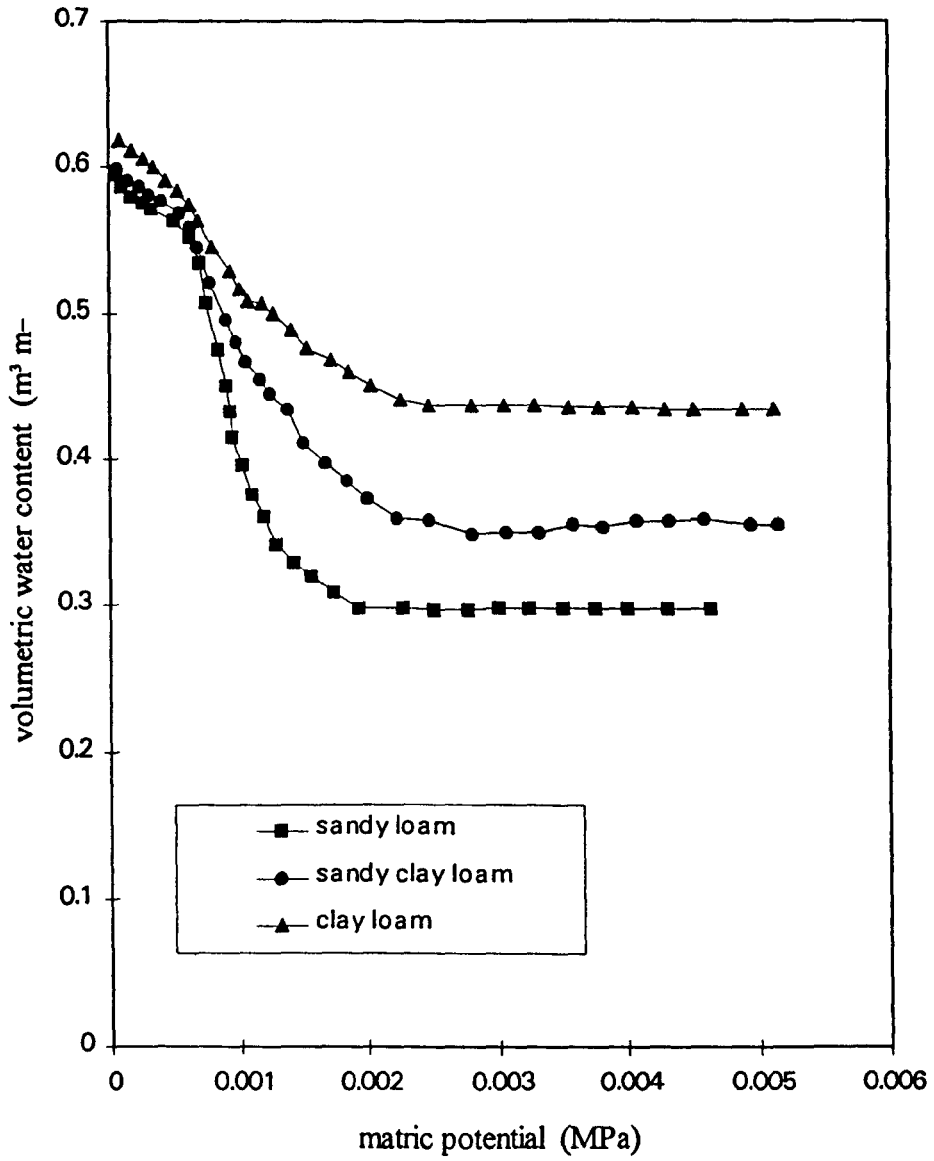
$$\left[(20 \times B) + A - wt \text{ of dispersant} \right] \quad (2.1)$$

$$\% \text{ sand (63 } \mu\text{m} - 2 \text{ mm)} = \left[\frac{A \times 100}{M} \right] \quad (2.2)$$

$$\% \text{ silt (2 } \mu\text{m} - 62 \mu\text{m)} = \left[\frac{20 \times (A - C) \times 100}{M} \right] \quad (2.3)$$

$$\% \text{ clay (<2 } \mu\text{m)} = \left[\frac{(20 \times C - wt \text{ of dispersant}) \times 100}{M} \right] \quad (2.4)$$

Figure 2.7 Soil moisture characteristic curves of the three test soils.



2.2.4.5 Nitrate and Ammonium determination

Inorganic N assay was conducted on incubated soil cores periodically using the colorimetric analysis method (Page *et al.*, 1982). A 50 g soil sample (of known moisture content) was shaken with 150 cm³ of 1 M potassium chloride in a 250 cm³ screw top bottle for 2 hours. The resulting suspension was filtered and analysed for NO₃⁻ and NH₄⁺ by automated colorimetric analysis. The nitrate analytical method is based on the reduction of nitrate to nitrite by a hydrazine-copper reagent which subsequently forms an azo dye with sulphanilamide and naphthylethylenediamine. Absorbance is measured at a wavelength of 520 nm. A stock solution of potassium nitrate (1000 mg N dm⁻³) was used to make up standard solutions in 1 M potassium chloride to give concentrations of 5, 10, 20, and 30 mg dm⁻³ NO₃⁻-N.

Nitroprusside is used as a catalyst for ammonium to react with sodium salicylate and sodium dichloroisocyanurate to form a blue indophenol. Absorbance is measured at 650 nm. A stock solution of ammonium chloride (1000 mg N dm⁻³) was used to make standard solutions in 1 M potassium chloride to give concentrations of 1, 2, 4, and 8 mg dm⁻³ NH₄⁺-N. The ammonium and nitrate analysis was corrected for instrument drift by periodic inclusion of a mid-range standard in sample runs at a rate of 1 in 5.

2.3 EARTHWORMS

Earthworm species *Aporrectodea spp.* and *Lumbricus spp.* were extracted from the Wick soil sampling site at Sutton Bonington using a spade. The earthworms were placed in liquid nitrogen for 30 minutes prior to deep freeze storage. The N content of freeze dried samples of each species was determined by Kjeldahl digestion. The nitrogen contents of the dry tissue of *Aporrectodea spp.* and *Lumbricus spp.* were about 10 % and 11 % respectively. Prior to use in any investigations, the frozen Earthworms were allowed to defrost for 30 minutes at room temperature in the laboratory.

Chapter 3: Modelling N₂O From Denitrification In Soil

3.1 REVIEW OF N₂O EVOLUTION MODELS

3.1.1 Introduction

Modelling is a means by which scientists from all disciplines communicate over spatial and temporal domains of mutual interest. These cross-discipline interactions are the drivers for progress in process modelling and extrapolation of N₂O fluxes from cellular to global levels (Schimel and Potter, 1995). Groffman (1991) reviews the factors controlling both denitrification and nitrification at different scales of investigation. The understanding of the ecological controls of microbial processes at large scales is important for the identification of environments that are likely to produce significant N₂O fluxes, and for the understanding of how these fluxes may change, in response to climatic changes. The production and emission of N₂O occurs on a microscopic scale which is mediated by the physical properties of soil and by the physiological processes of plants and micro-organisms. Pure culture and enzyme studies have elucidated both the N-pathways and their constraining factors. These factors are well known and are reflected in the complexity of microscale N₂O production models; however this complexity is difficult to translate into changes in the environment due to the spatial heterogeneity of soil. The models at the cellular and aggregate scale generally emphasise N reduction kinetics and their respective response to changes in soil parameters, which are quantified with relatively fine temporal resolution. However, these models are not easily extrapolated up to annual or longer cycles because of problems in expressing episodic events in terms of average climate drivers for N₂O emissions.

3.1.2 Type of models predicting nitrogenous gas fluxes

Generally, models of N_2O evolution from soils are empirical or mechanistic in nature. Mechanistic models of N_2O production require detailed information of the range of reaction rate constants, substrate diffusion coefficients and pore-solute velocities from comparative field and laboratory experiments. Empirical approaches require a large body of data that include N_2O flux values and the determining soil properties upon which a multifactorial regression analysis may be employed to derive a relationship. However, this empirical approach is limited because the N_2O flux is derived from two separate processes, nitrification and denitrification, that are influenced quite differently by changes in soil conditions. Empirical models describing N_2O generation and movement are seldom universal and are limited to the parameters defined in the data set. Hybrids of the two model types are also essentially site specific and tend to neglect soil heterogeneity. The spatial variability of denitrification has been attributed to the presence in the soil of denitrifying *hot-spots* (Parkin, 1987). Some attempts have been made to model these hot-spots using a stochastic approach. Hot-spots may be treated as featureless points in a simulated log-normal distribution of denitrification rates observed in macroscopic samples (Parkin and Robinson, 1989), or associated with soil aggregates (Leffelaar, 1979; Smith, 1980) or as particulate organic matter (Parkin, 1987). Once the hot spot has been recognised and attributed a size and structure, the knowledge of the mechanisms governing N_2O emission could be employed such that a hybrid mechanistic/stochastic model may be developed. However, this approach has not been developed or tested to any great extent.

The pathways for N_2O production from nitrification are still uncertain, therefore few models have been constructed that can simulate this process. However, Grant (1995) has attempted to develop a mathematical model based on the hypothesis that NO_2^- is used as an alternative acceptor for electrons not absorbed by O_2 during C oxidation for growth by NH_3 oxidizers. The model is governed by O_2 and substrate concentration, temperature and water content. To avoid the problem of modelling the joint effect of two different N_2O production processes the majority of models predicting N_2O production are derived from denitrification simulations only. However, models

predicting denitrification, predict NO₃⁻ reduction to N₂ with no reference to N₂O production or emission. These models generally contain a deterministic element based on a prior understanding of the biological mechanisms responsible for denitrification and tend to treat soil as a homogenous medium. Many models produced are purely theoretical and have not been tested with observed data from different soils, and at best they provide only indications of the influential parameters.

3.1.3 Microscale denitrification models

At the cellular and aggregate scale, mathematical models of varying complexity have been developed, from simple, zero order reaction terms to complex equations based on competitive substrate limitation. Focht (1974) devised a zero order model with respect to NO₃⁻ reduction that included the sequential reduction of NO₃⁻ as affected by a linear function of both pH and O₂ status and an exponential function of temperature and air-filled porosity. The N₂O:N₂ ratio was dependent on the aeration and pH of the system. Cho and Mills (1979) also modelled the reduction of NO₃⁻ as a zero order process, although the subsequent reduction of the N-species were found to be best described by competitive Michaelis-Menton kinetics. First order kinetic descriptions were used by Mehran and Tanji (1974) to describe all nitrogen transformations including nitrification, denitrification, mineralization, immobilization, plant uptake of N and NH₄⁺ exchange. All N-transformations were assumed to be independent of organic matter decomposition and the quality of carbon substrates.

Van Veen and Frissel (1979) modelled both C and N cycles inter-dependently, with micro-organisms central to N dynamics, which included nitrification, denitrification, mineralization and immobilization. The decay of various C and N pools were driven by first order or Monod kinetics, in association with multiplicative reduction factors, that were used to reduce reaction rates when suboptimal conditions were imposed. However this model only considers total denitrification which is influenced by the diffusion of O₂ and NO₃⁻. There is no reference to nitrous oxide.

A useful model for N analysis in pure cultures which described sequential NO_3^- reduction with competitive Michaelis-Menten kinetics was created by Betlach and Tiedje (1981). The extent of denitrification was controlled by O_2 concentration, with each reduced N-species possessing individual transformation rate constants. Myrold *et al.*, (1981) also developed a model using dual Michaelis-Menten kinetics with competitive inhibition of NO_3^- reduction by O_2 ; mass flow and diffusion described the macroscale transport of solutes. This was further developed by Myrold and Tiedje (1985) who modelled the effect of NO_3^- diffusion on anaerobic reduction sites in unsaturated re-packed soil cores.

Dendooven and Anderson (1994, 1995) developed a mechanistic model that linked C mineralization and denitrification. Competitive Michaelis-Menten kinetics were used to simulate the sequential reduction of NO_3^- which is dependent on the concentration of each N-species and an associated weighting factor describing electron acceptor competition. Therefore a description of the inhibitory effects from NO_3^- and NO_2^- , pH and O_2 concentration on N_2O reductase were not required. The model incorporated C substrate availability and composition changes coupled with reduction of N-oxides. These models simulated N_2O production from artificial soil slurries which obviates micro-spatial factors which act under field conditions.

Molina *et al.*, (1983) modelled the total rate of denitrification as a constant fraction of decomposition of organic matter. The model included descriptions of short term dynamics of organic residue decomposition associated with two defined carbon pools each containing labile and non-labile components. The decomposition was limited by N availability which was dependent on residue decomposition, mineralization, immobilization, nitrification and denitrification. This model was extended to simulate the potential rate of nitrification by Clay *et al.*, (1985), who coupled it with a layered soil sub-model that was subject to water flow, temperature effects, plant growth and tillage.

A transient microsite modelling approach was described by McConnaughey and Bouldin (1985 a, b). They combined processes that influence trace gas production via

the sequential reduction of NO_3^- at the aggregate level in saturated conditions, with transient diffusion of all N species throughout the saturated soil. The model accounted for the formation of anaerobic microsites and transient anaerobiosis in homogenous, structureless soil. Additionally, the model accounted for temporal changes in substrate availability and enzyme activity using both double Monod and Michaelis-Menten kinetic approaches.

The modelling of anaerobic sites within unsaturated aggregates was undertaken by Leffelaar (1988). A homogenous, unsaturated cylindrical soil aggregate model was constructed which could predict the spatial and temporal variation in NO_3^- reduction parameters within the aggregate, caused by microbial activity. The model did not include any descriptions of gaseous transport out of the aggregates. The model was extended by Leffelaar and Wessel (1988) to describe a homogenous soil layer possessing microbial respiration and denitrification in an unsaturated soil. However, like the previous model, transport only occurred within the model aggregates. The major processes within the model included growth and maintenance of the denitrifier biomass and sequential reduction of NO_3^- . Growth of biomass was modelled using first order kinetics with the relative growth rate linked to N-oxide reduction by a double Monod description that encompasses rate limiting factors for the availability of C and N substrates. The authors used the Pirt equation to calculate the consumption rates of electrons by the substrates.

Another soil aggregate model was devised by Smith (1980) based on the work of Currie (1961) which was similar to that constructed by Leffelaar (1979) which calculated the size of anaerobic microsites within soil crumbs. N_2O production in Smith's model (1980) was formulated using an empirical description. The extent of simulated N_2O production is influenced by aggregate size limitations on O_2 diffusion within an aggregate, throughout a log-normally distributed population of soil aggregates. However, the values obtained from this model have not been fitted to any data. This work was extended by Arah and Smith (1989) in a model of steady state NO_3^- reduction in aggregates using Michaelis-Menten kinetics. Within the anaerobic zone of a spherical aggregate the NO_3^- concentration profile was calculated by a

numerical solution and used to determine the aggregate denitrification rate. The assembly denitrification rates from aggregates of different sizes were then estimated by integration over log-normal probability distributions of aggregate radius and respiration potential. The model did not allow for variation in water content.

3.1.4 Mesoscale denitrification models

Whereas a number of models have estimated N₂O gas flux rates from soils based on microbial metabolism few have included descriptions of spatial and temporal variability in controlling factors such as temperature, moisture, texture and organic matter availability. By contrast N₂O models relating to ecosystems generally contain comparatively little detail about substrate dynamics and gas transport processes. When expanding mechanistic models from the organism to landscape/ecosystem scale, the environmental cycles must integrate short and long term soil processes encompassing all temporal changes to be of any practical use. However, most simulations of N₂O production from ecosystems use empirical models.

N₂O production from urea-treated and untreated short-grass prairie soil was modelled by Mosier and Parton (1985) and Parton *et al.*, (1988) via nitrification and denitrification. N₂O production was controlled by soil temperature, moisture, NH₄⁺, and NO₃⁻ levels which are described empirically. In this model relationships between N₂O production and environmental variables were developed from an extensive grasslands database. However, the model did not simulate the underlying enzyme kinetics and microbial growth processes. The primary data driver requirements for the models developed by Mosier and Parton (1985) and Parton *et al.*, (1988), were mean monthly or weekly climate parameters, soil texture and management.

Johnsson *et al.*, (1991) described a field scale model of total denitrification as a function of potential denitrification rate, soil temperature, soil O₂ status and NO₃⁻ availability. Soil temperature, moisture content and potential denitrification rate were modelled as a function of soil type. The potential denitrification rate was also a

function of cropping system. The denitrification part of the model included the major processes determining inputs, transformations and outputs of N in arable soils. Denitrification was not carbon limited. The interaction of determining processes that occur on a microscale in the soil are integrated in the model to represent the macroscale level. However, the model had difficulty explaining periodic spatial and temporal variations in N loss due to wet-dry and freeze-thaw cycles.

Li *et al.*, (1992 a, b) produced a complex field scale model of denitrification and decomposition (DNDC) that was controlled by agricultural practices, soil properties and soil climate. First order kinetics described the daily decomposition of several soil carbon pools that were linked to rainfall-driven denitrification and were dependent on growth and maintenance of the denitrifier and nitrifier populations which affect N_2O production. In the DNDC model there was a description of the flow of substrates with water up and down the soil profile. This model was designed to simulate agro-ecosystem level N_2O and N_2 fluxes with explicit consideration of enzyme kinetic and microbial biomass dynamics. N_2O emission from soil is described by an empirical function, based on soil moisture and the clay content of soil. It was assumed that the N_2O flux is restricted to such an extent, due to low diffusion rates in water during saturated conditions, that emission is negligible and is thus ignored.

Grant (1991) and Grant *et al.*, (1993 a, b) modelled total denitrification as affected by temperature, water content and NO_3^- concentration. The model involved the simulation of denitrification at the horizon layer, based on aggregate level studies. This model used double Monod equations to describe denitrification within anaerobic microsites of a layered soil and first order kinetic descriptions for both C and N decomposition dynamics. Denitrification was made dependent on water content, temperature and diffusion of both O_2 and substrates. The effect of plant roots on O_2 uptake and production of C was also incorporated into the model. The model simulated the transformation and transfer of reaction substrates and products within and between aqueous and gaseous phases of a simulated layered profile.

IMAGING SERVICES NORTH

Boston Spa, Wetherby
West Yorkshire, LS23 7BQ
www.bl.uk

**PAGE MISSING IN
ORIGINAL**

models, which translated air temperature and precipitation records into model variables. However, few data sets exist to test the model.

One aspect of N₂O emission from soil that is frequently neglected is the physical constraints imposed on gaseous transport through soil. The transport of N₂O, generally modelled using Fick's law, interacts with production and consumption to influence total exchange. Transport is important because the residence time of the N₂O in soil water, influences the time during which it is vulnerable to further reduction to N₂.

The following model is based on quantitative relationships between specific processes and environmental variables derived from experiments, coupling both biological and physical components. Therefore the model is capable of depicting denitrification over temporal and spatial scales relevant to water status and fertilizer use.

3.2 MODEL PRINCIPLES AND ASSUMPTIONS

3.2.1 Model aim

The aim was to develop a reaction-diffusion based model to predict rates of nitrous oxide evolution from denitrification in soil subject to rapid environmental changes. The model was validated by examining the effect of changes in soil aggregate size, water content and nitrate concentration on N₂O evolution from re-packed soil cores.

3.2.2 Model principles

The reduction of nitrate to nitrogen gas results in the formation of an intermediary product, nitrous oxide. The specific factors that influence the production of nitrous oxide from soil have been reviewed in the introduction. The principle factors governing N₂O evolution within the model include diffusion coefficients through gas and water phases, the size of the anaerobic zone, volumetric water content and the reduction rate of nitrate and nitrous oxide. It is assumed that there is an equal distribution of NO₃⁻ throughout the model soil, and therefore no movement of N within the profile other than N₂O.

3.2.2.1 General model description

Simulation modelling software called *ModelMaker* (SB Technology, 1993) was used to construct the model. *Modelmaker* uses a 4th order Runge Kutta procedure to solve the differential equations used to describe diffusive transfers (Press *et al.*, 1986) and a Marquardt error minimization process to parameterize the model. The model principally describes the effect of soil water status on the reduction of NO₃⁻ to N₂O and N₂, and evolution of nitrous oxide from soil columns.

Table 3.1 List of model parameters.

parameter	definition	units
t	time	s
$[X]_j^i$	concentration of soil compartment species; where $X = N_2O, N_2$ or NO_3 ; $i =$ aggregate (A) layer (L) or atmosphere (o) compartment; $j =$ solution phase (s), air phase (a) or total compartment volume (T)	mol m^{-3}
$\Delta [X]_j^i$	change in concentration of soil compartment species; X ; where $X = N_2O, N_2$ and NO_3 ; $i =$ aggregate (A) or layer (L) compartment; $j =$ solution phase (s), air phase (a) or total compartment volume (T)	$\text{mol m}^{-3} \text{ s}^{-1}$
$D_j^{N_2O}$	diffusion coefficient of N_2O in phase j ; where $j =$ solution phase (s) or air phase (a)	$\text{m}^2 \text{ s}^{-1}$
D_j^*	effective diffusion coefficient of N_2O in phase j ; where $j =$ solution phase (s) or air phase (a); $D_j^* =$ (diffusion coefficient x area x tortuosity)	$\text{m}^2 \text{ s}^{-1} \text{ m}^2$
β	Bunsen absorption coefficient for nitrous oxide at 15 °C	
$F_{(i,i+1)}$	diffusive flux between compartments i and $i+1$; where $i =$ aggregate (A) or layer (L) compartment	mol s^{-1}
k_i	rate constant for reduction of species i ; where $i = N_2O$ or NO_3	s^{-1} , $\text{mol m}^{-3} \text{ s}^{-1}$
θ'_j	porosity of compartment i ; where $i =$ aggregate (A) or layer (L) and $j =$ air phase (a), solution phase (s) or total compartment volume (T)	$\text{m}^3 \text{ m}^{-3}$
f'_j	phase tortuosity in compartment i ; where $i =$ aggregate (A) or layer (L) compartment and $j =$ solution phase (s) or air phase (a)	
R_i	radius of i ; where $i =$ aggregate (A) or layer (L) compartment	m
Δd	diffusive distance between compartments	m
d_i	depth of i ; where $i =$ aggregate (A) or layer (L) compartment	m
V_i	volume of i ; where $i =$ aggregate (A) or layer (L) compartment	m^3
SA_i	surface area of i ; where $i =$ aggregate (A) or layer (L) compartment	m^2

The model soil core is constructed of several layers, each with a single aggregate size (Fig. 3.1). The representative aggregate in each layer is assumed to be spherical and constructed of homogeneous *shells*. The pore space is deemed continuous throughout each of the aggregate *shell* and layer compartments. Diffusion and enzyme kinetics are the principle mechanisms that govern nitrous oxide concentration in the model soil. The diffusion of N₂O occurs through both water and gas filled pores. The reduction rate of NO₃⁻ and N₂O is determined by zero and first order enzyme kinetics, respectively.

3.2.2.2 Soil water and gas filled porosity

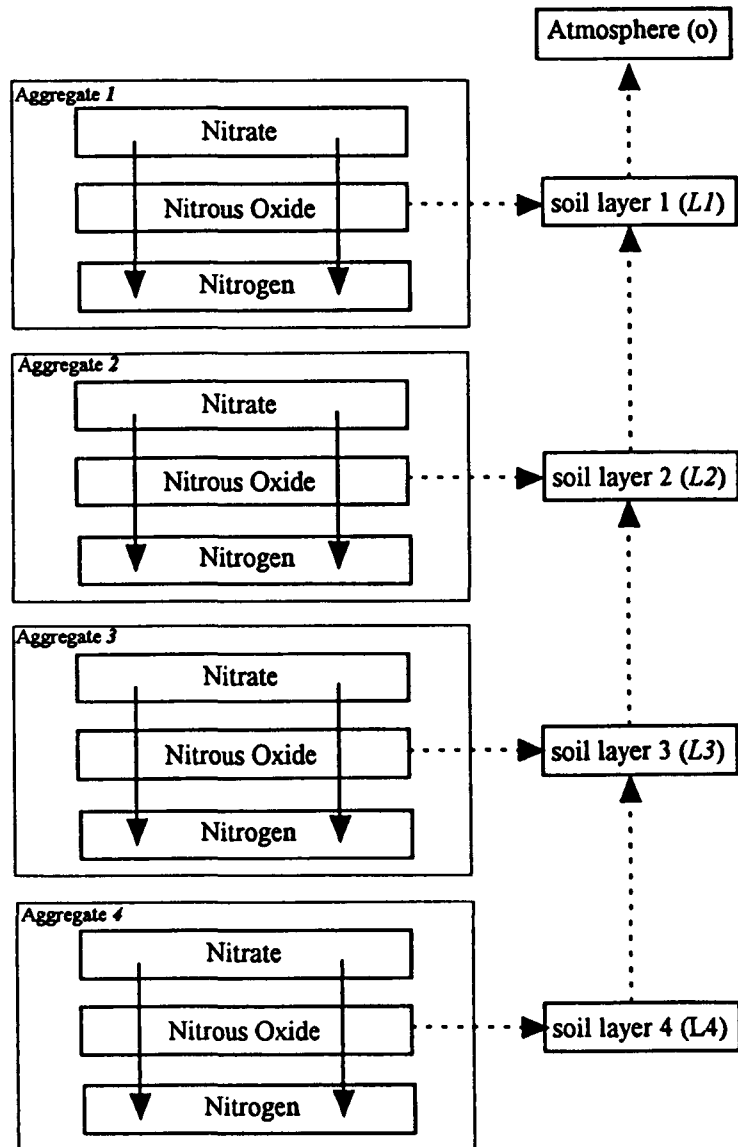
Soil particles are considered to be assembled into spherical aggregates of radius, R. Consequently, the soil has two types of pore space, the *intra-aggregate* (within the aggregate) and *inter-aggregate* (between aggregate) porosity. At saturation all available pore space is filled with water. However, at field capacity only the *intra-aggregate* pore space is considered saturated. Field capacity is deemed equivalent to the water content at 0.005 MPa suction. The *inter-aggregate* pore space at field capacity is assumed to be gas-filled. At water contents less than field capacity the *intra-aggregate* pore space contains both solution and gas phases.

The air filled porosity and the volumetric water content are two of the most important variables within the model soil; the former is a function of the latter (equation 3.1; table 3.1);

$$\theta_a^i = (\theta_T^i - \theta_s^i) \quad (3.1)$$

Field capacity was determined from the moisture characteristic of the test soils (section 2.2.4.3; Fig. 2.7). Soil moisture contents could therefore be calculated in the model as a % of F.C., and the volumetric proportion of solution to gas phase determined. It is assumed that any addition of water to a model compartment occurs instantly, resulting in immediate equilibrium throughout that compartment.

Figure 3.1 Schematic representation of the model showing four layers, each with a representative aggregate unit: (--->) = N_2O diffusion pathway; (--->) = denitrification pathway.



Gas diffusion through soil depends on the water content of the soil (Nye and Tinker, 1977). Diffusion in air and water differ by a factor of 10^4 (Currie, 1961), therefore any alteration in water status will have a significant effect on the rate of nitrous oxide evolution. It is therefore assumed that movement of N_2O in any soil compartment that possesses an air fraction will be through the air phase exclusively. However, both the air and solution phases in each soil compartment are in constant dynamic equilibrium with respect to gas concentrations (section 3.2.2.3).

3.2.2.3 N_2O equilibrium between water and gas phases

The concentration of a gas in solution at equilibrium (dm^3 (s.t.p.) dm^{-3}) depends upon temperature, pressure and its intrinsic solubility in water. The term used to express the degree of solubility of a gas in a liquid, at fixed temperature and pressure is the *Bunsen absorption coefficient*, β . This is defined as the volume of gas in dm^3 at s.t.p dissolved in 1 dm^3 of liquid when it is present at the reported temperature and at a pressure of 1.01325×10^{-2} MPa (1 atmosphere).

Equilibrium between the solution and air phase is assumed at all times to be controlled by the appropriate Bunsen coefficient (equation 3.2). At 15°C and standard pressure, the concentration ratio of N_2O in the solution and air phase ($[N_2O]_s^i / [N_2O]_a^i$) is 0.743 (Tiedje, 1982).

$$[N_2O]_s^i = ([N_2O]_a^i \beta) \quad (3.2)$$

The total N_2O concentration ($[N_2O]_T^i$; mol m^{-3} whole soil) within a soil compartment is therefore split into equivalent concentrations in the air phase (mol m^{-3} soil air) and solution phase (mol m^{-3} soil water) respectively. Each phase concentration can then be calculated from $[N_2O]_T^i$, β and the appropriate capacity terms (θ_a^i, θ_s^i), using equations 3.2 and 3.3 respectively.

$$[N_2O]_a^i = \left[\frac{[N_2O]_T^i}{(\beta \theta_s^i) + \theta_a^i} \right] \cdot \theta_T^i \quad (3.3)$$

The overall diffusion equation that describes movement between two compartments does not use the total soil concentration difference for each compartment, but the difference in phase concentrations within each soil compartment ($\Delta [N_2O]_a^i, \Delta [N_2O]_s^i$).

3.2.2.4 Initial N₂O concentration of the atmosphere

The concentration of N₂O within all compartments is expressed in units of mol m⁻³; determination of gas concentration requires a knowledge of partial pressure and temperature. According to Avogadro's hypothesis 1 mole of gas occupies 0.0224 cubic metres at standard temperature and pressure (273.15 K and 0.101325 MPa). If it is assumed that the partial pressure of N₂O in the atmosphere is 3.1×10^{-7} then, substituting into equation 3.4, the composition of the model atmosphere at s.t.p. can be calculated, ($[N_2O]_r^p$). To determine the appropriate gas concentration at temperature T , the composition at s.t.p, is multiplied by ΔT , a temperature conversion factor (equation 3.5).

$$[N_2O]_r^p = \left(\frac{3.1 \times 10^{-7}}{0.0224} \right) \Delta T, \quad (3.4)$$

and

$$\Delta T = \left(\frac{273.15}{(273.15 + T^{\circ}C)} \right) \quad (3.5)$$

3.2.3 Enzyme kinetic theory

The denitrification process has been reviewed in the introduction, however, the kinetics that govern the reduction of nitrate to nitrous oxide and dinitrogen gas have only been briefly mentioned.

For two molecules to react they must first meet, therefore if concentrations of reactants increase, the velocity (v) of a reaction usually increases. This concept can be expressed through a constant k which is the rate of a reaction when unit concentrations of reactants are present (equation 3.6):

$$\text{rate or velocity of reaction} = k [\text{reactant}(s)]^n \quad (3.6)$$

The value of the exponent (n) is the *order* of the reaction. Reactions can be classified according to the value of n in their rate equations; for simple reactions, n is a small integral number. Fig. 3.2 shows how the order of a reaction can be deduced from a graph of the initial velocity v , against concentration of substrate, S .

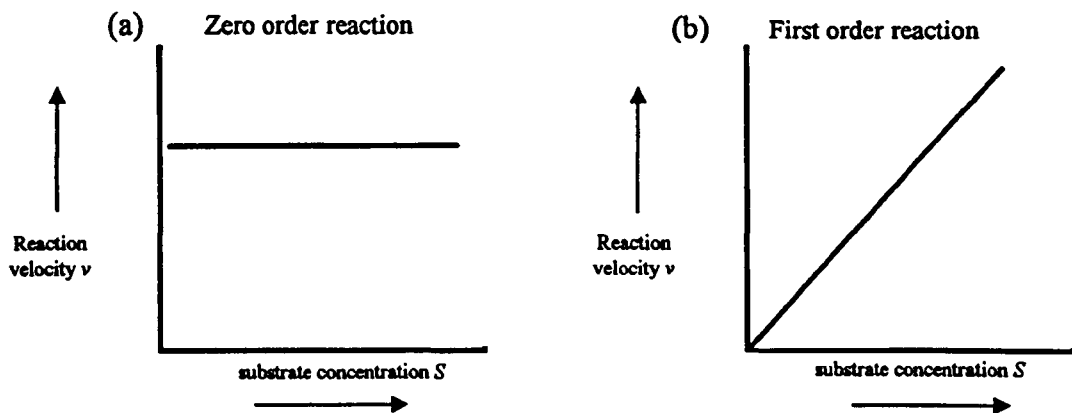
The velocity (mol s^{-1}) for a zero order reaction is constant, as described by equation 3.7. The rate constant in a zero order reaction is independent of substrate concentration and is therefore proportional only to enzyme concentration or surface area. By contrast, the velocity of a first order reaction (equation 3.8) is proportional to the concentration of the substrate.

The initial and transformed substrate concentrations of S are represented by s^0 and s^t respectively, so that after time t the remaining concentration of S is represented by $[s^0 - s^t]$. The velocity v , has units of concentration time^{-1} ; thus for the zero order reactions k also has units of concentration time^{-1} , while in the first order reaction, k is in units of time^{-1} .

$$\text{zero order with respect to } S, \quad v = k \quad (3.7)$$

$$\text{first order with respect to } S, \quad v = k [s^o - s^f] \quad (3.8)$$

Figure 3.2 Initial velocity of reaction as a function of concentration of substrate S , for reactions (a): zero and (b): first order.



3.2.3.1 Denitrification rate

Denitrification in the model occurs only within aggregates and uses zero- and first-order enzyme kinetics to describe nitrate and nitrous oxide reduction respectively. It is known that anaerobic conditions are a precursor to denitrification, but, nitrous oxide can be produced in seemingly aerobic soils (Bremner and Blackmer, 1981). Therefore, for both NO_3^- and N_2O reduction, the model assumes two different reaction rates, for unsaturated and saturated conditions respectively. Each soil compartment uses the rate constant that corresponds to its current aeration status, which is determined using equation 3.1 (section 3.2.2.2).

The reduction of NO_3^- to N_2O

The reduction of nitrate to nitrous oxide is the first irreversible N transformation. The nitrate concentration in the soil aggregate is assumed to be subjected only to losses by denitrification and not by vertical transport within the soil profile solution phase.

The reduction of nitrate occurs only in the solution phase of the aggregates. However the rate of reduction is governed by the air-filled porosity of that compartment. There are two rate constants that represent the microbial variability that occurs in the soil under different oxygen regimes: under saturated conditions $k1$ operates and when the soil is unsaturated a lower rate ($k2$), is applied.

The loss from the nitrate pool corresponds to an increase in concentration of the N_2O pool, and is denoted by the following zero order equation:

$$\frac{d[NO_3]_s^A}{dt} = -(k_{NO_3}), \quad (3.9)$$

where the following qualifications apply:

$$\theta_a^A = 0 ; k_{NO_3} = k1 \quad \text{and} \quad \theta_a^A > 0 ; k_{NO_3} = k2$$

N_2O reduction to N_2

The reduction of nitrous oxide to nitrogen gas is described by first order kinetics. The reduction of N_2O occurs within the aggregate water phase, the rate of which is dependent on the air-filled porosity of the compartment. Under saturated conditions the rate constant $k3$ operates and when the soil is unsaturated the lower rate ($k4$), is applied (equation 3.10).

$$\frac{d[N_2O]_s^A}{dt} = -[N_2O]_s^A k_{N_2O}, \quad (3.10)$$

where the following qualifications apply:

$$\theta_a^A = 0 ; k_{N_2O} = k3 \quad \text{and} \quad \theta_a^A > 0 ; k_{N_2O} = k4$$

The model does not describe the evolution of N_2 gas. Once the nitrogen molecule has reached the nitrogen gas pool it plays no further part in the model. It was not possible to quantify nitrogen gas emission, therefore it was not modelled.

3.2.4 Diffusion of gases in soil

Diffusion results from the random motion of ions, atoms or molecules. In the case of gases, a gradient of partial pressure causes the molecules of the unevenly distributed gas to migrate from a zone of high concentration to a zone of low concentration even though the gas phase as a whole may remain isobaric.

In general, the diffusion of gases through the air phase of soil maintains the exchange of gases between the atmosphere and the soil while diffusion through the solution phase ensures movement of gases to and from hydrated organisms (Hillel, 1982). However, during periods of rainfall the soil may become partially or totally saturated in which case the only exchange route for gases is through the solution phase. For both saturated and unsaturated pathways, the diffusion process can be described by Fick's first law (equation 3.11).

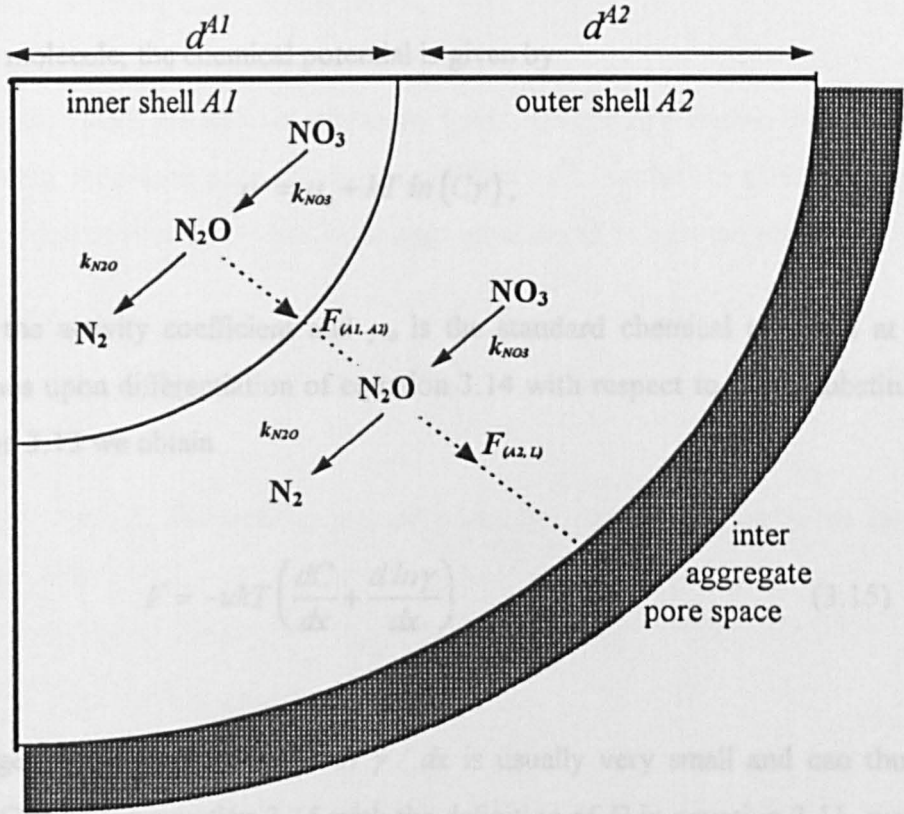
$$F = -D \frac{dC}{dx}, \quad (3.11)$$

where F is the diffusive flux ($\text{mol m}^{-2} \text{s}^{-1}$), D is the diffusion coefficient ($\text{m}^2 \text{s}^{-1}$) and dC/dx is the concentration gradient, ($\text{mol m}^{-3} \text{m}^{-1}$). The negative sign arises because movement is from a large to a small concentration and thus denotes a loss from the area of large concentration.

The diffusion coefficient of molecules is directly proportional to their absolute mobility, u , which is the limiting velocity they attain under unit force. D and u are related by the Nernst-Einstein equation:

$$D = ukT, \quad (3.12)$$

Figure 3.3 Schematic of in-situ transformations of NO_3^- and N_2O reduction and the flux of N_2O between the *intra*-aggregate pores in two shells and through to the *inter*-aggregate pores ($F_{(A1,A2)}$ and $F_{(A2,L)}$ respectively): (---) = diffusion pathway; (—) = denitrification pathway.



where k is the Boltzman constant, and T is the temperature in Kelvin. The Nernst-Einstein equation is derived as follows. For a system with concentration gradients in the x direction only, the force on a molecule is the gradient of its chemical potential $d\mu/dx$ (Nye and Tinker, 1977). Thus the flux across a plane normal to the x axis is:

$$F = -C \left(\frac{d\mu}{dx} \right) u \quad (3.13)$$

For a single molecule, the chemical potential is given by

$$\mu = \mu_o + kT \ln(C\gamma), \quad (3.14)$$

where γ is the activity coefficient and μ_o is the standard chemical potential at unit activity. Thus upon differentiation of equation 3.14 with respect to x and substituting into equation 3.13 we obtain

$$F = -ukT \left(\frac{dC}{dx} + \frac{d \ln \gamma}{dx} \right) \quad (3.15)$$

For uncharged particles the term, $d \ln \gamma / dx$ is usually very small and can thus be neglected. Comparing equation 3.15 with the definition of D in equation 3.11, we find $D = ukT$.

Diffusion in soil depends on the total volume and tortuosity of the soil pore space and is not affected by pore size distribution. Diffusion is unaffected by the pore size because the mean free path of molecules in thermal motion (the distance an average molecule in random motion travels before it collides with another) is of the order of $10^{-6} - 10^{-7}$ m; which is considerably smaller than the radii of the pores which generally account for most of a soil's porosity (Hillel, 1982).

3.2.4.1 Tortuosity

Since soil pores are not straight tubes but follow tortuous paths around the soil particles, the actual distance between two points in a path is greater than the straight line distance between them. The effect of this is to decrease the apparent diffusion coefficient in the soil by a factor which is known as the tortuosity factor, f'_j (table 3.1). Nye and Tinker (1977) give a comprehensive account of how to describe tortuosity through both gas and water phases.

Each soil compartment has its own tortuosity factor governing diffusion in each phase. Under saturated conditions only, the tortuosity factor f'_s , applied to diffusion through the solution phase of both *intra*- and *inter*-aggregate pores, is denoted as:

$$f'_s = (\theta'_s)^n \quad (3.16)$$

The tortuosity through the *inter*-aggregate pores in unsaturated conditions takes a similar form:

$$f'_a = (\theta'_a)^n \quad (3.17)$$

The exponent, n , is dictated by particle shape. The more complicated a particle shape the larger the value (Currie, 1960); spheres are given a value of 0.5 (Bruggeman, 1935).

When θ'_i is less than field capacity, however, the description of tortuosity through *intra*- aggregate pores is more complicated (equation 3.18). As the soil wets up, at water contents less than field capacity, the ratio of water to air increases and the mean path length of the air-filled pore increases, thus the tortuosity factor f_a^A decreases. The decrease in gas tortuosity factor with increasing water content has been described by Currie (1961):

$$f_a^A = \theta_a^A \left[\frac{\theta_a^A}{(\theta_a^A + \theta_s^A)} \right]^{2.5} \quad (3.18)$$

In all the model diffusion equations, the diffusion coefficient is multiplied by the tortuosity factor f_j^i , and the fraction of the soil volume occupied by that phase, θ_j^i . This, combined with the diffusive surface area (SA_i) accounts for the tortuous diffusion through the diffusional cross sectional area of the respective phase. The term D_j^* is used to describe this effective diffusion coefficient.

3.2.4.2 Compartment transfer of N₂O

As N₂O production proceeds, a concentration gradient develops between the aggregates and the external atmosphere so that N₂O diffuses out of the aggregate. The production, reduction and diffusion of N₂O are modelled as simultaneous processes within each aggregate compartment.

There are a considerable number of working flux equations within the model, however they can all be generalised to the form expressed in equation 3.19 (table 3.1);

$$F_{(i,i+1)} = \left(\frac{-D_j^* \left([N_2O]_j^i - [N_2O]_j^{i+1} \right)}{\Delta d} \right), \quad (3.19)$$

where:

$F_{(i,i+1)}$ = flux between adjacent compartments i and $i+1$; (mol s⁻¹)

D_j^* = effective diffusion coefficient of phase j ; where $D_j^* = (D_j^{N_2O} \theta_j^i f_j^i SA_i)$;
(m² s⁻¹ m²)

$([N_2O]_j^i - [N_2O]_j^{i+1})$ = difference in N_2O concentration between adjacent compartment phases; (mol m^{-3})

Δd = diffusive distance; (m)

Diffusion through the pore space of all model compartments is dependent on the state of the air-filled porosity: The generalized flux equation (3.19) is used to describe any one of three possible diffusion processes (A, B and C) that can occur within each respective model compartment, subject to the state of the air-filled porosity of each compartment.

A. gas phase to gas phase transfer when $\{\theta_a^i > 0; \theta_a^{i+1} > 0\}$

$$F_{(i,i+1)} = \left(\frac{-D_a^* ([N_2O]_a^i - [N_2O]_a^{i+1})}{0.5 (d_i + d_{i+1})} \right)$$

B. solution phase to solution phase transfer when $\{\theta_a^i = 0; \theta_a^{i+1} = 0\}$

$$F_{(i,i+1)} = \left(\frac{-D_s^* ([N_2O]_s^i - [N_2O]_s^{i+1})}{0.5 (d_i + d_{i+1})} \right)$$

C. solution phase to gas phase transfer when $\{\theta_a^i = 0; \theta_a^{i+1} > 0\}$

$$F_{(i,i+1)} = \left(\frac{-D_s^* ([N_2O]_s^i - ([N_2O]_a^{i+1} \beta))}{0.5 (d_i)} \right)$$

(θ_a^{i+1} is the air-filled phase of an adjacent compartment)

When the two compartments involved in N_2O transfer, possess the same air-filled porosity, either unsaturated (A) or totally saturated (B), diffusion naturally occurs within the same phase; during these events the diffusion equation follows the conventional approach describing transfer as that from the centre of compartment i to the centre of compartment $i+1$. However, in condition C, the porosity of both compartments possess a different air-filled content; i is saturated while $i+1$ is unsaturated. Consequently the description of the transfer between the two phases is different from diffusion through one medium. Due to the different solubilities of N_2O in the air and solution phases, $[N_2O]_a^i$ in the compartment with a gaseous phase is multiplied by the Bunsen coefficient to calculate the equivalent value of $[N_2O]_s^i$ and so establish the correct concentration gradient between the two compartments. In effect, the gas filled pores described in C, possess a dual character as they behave as a *pseudo* water compartment when undergoing transfer with a neighbouring saturated compartment, while simultaneously existing as a gas phase allowing aerobic transfers with other adjacent, unsaturated compartments.

There are three occasions when condition C applies: when the soil is at field capacity (transfer between the saturated *intra*-aggregate pores and the unsaturated *inter*-aggregate pores); when the soil core water table rises, (unsaturated soil compartments overly saturated layer compartments); when the whole soil core is saturated and diffusion is between saturated soil and the atmosphere above the soil core surface.

In each diffusion equation the denominator term is the path length (Δd , equation 3.19) and a conventional description of diffusion regards the distance as being the sum of half the thickness of both compartments i and $i+1$. However, where diffusion is between two different media the diffusive distance attributed, is that from the centre of the rate limiting compartment to its interface (Crank *et al.*, 1981). This occurs during diffusion between *intra*- and *inter*-aggregate compartments, diffusion between gas and solution phases, and diffusion between the top soil compartment and the atmosphere.

It is always assumed that the diffusive path length for diffusion from the *intra*- to *inter*-aggregate pores is through the *intra*-aggregate pores only. This assumption arises as

both media are capable of possessing a different air-filled porosity at any one time, this is especially apparent at field capacity (C). Diffusion through the *intra*-aggregate pores is slower than that through the *inter*-aggregate network due to greater tortuosity, and is thus the rate limiting step of the diffusive process out of the aggregates. It is assumed that once N_2O has reached the outer aggregate interface it is in equilibrium with the *inter*-aggregate layer compartment.

A similar feature applies to diffusion between different phases in *inter*-aggregate pores of adjacent layer compartments. Diffusion through water is considerably slower than that through air, thus the rate limiting part of the transfer between the two layers is through the water saturated pores. Hence only diffusion through the solution phase is described, and the diffusional distance is from the centre of the saturated layer to the interface of the two layers (i.e. half the thickness of the saturated layer). It is also assumed that once N_2O has reached the interface, it is in equilibrium with the gas filled *inter*-aggregate pores of the above compartment.

The other occasion when the diffusive path length is dictated by a single compartment is transfer between the soil surface and the atmosphere. Diffusion through soil is greatly influenced by a change in air-filled porosity, which profoundly affects both tortuosity and the apparent diffusion coefficient. The atmosphere however is not subject to changes in air-filled porosity, hence the rate limiting part of any diffusion between the two media is transfer through the soil. It is this step that is used to describe diffusion from the uppermost soil layer to the atmosphere. Hence the diffusive distance is from the centre of the top layer to the soil-atmosphere interface.

The diffusive steps in the model can be generalized into four categories:

- i diffusion between aggregate compartments;
- ii diffusion between aggregate and layer compartments;
- iii diffusion between layer compartments;
- iv diffusion between the top layer compartment and the atmosphere.

The change in N_2O concentration with time in model compartments corresponding to the above categories are presented in the following equations 3.20 - 3.23. The change

in total concentration for an aggregate compartment (Fig. 3.3; $A1$), is given in equation 3.20; where;

$$\frac{d[N_2O]_T^{A1}}{dt} = k_{NO_3} - \left(\theta_{,s}^{A1} [N_2O]_{,s}^{A1} k_{N_2O} \right) - \left(\frac{D_j^* \Delta [N_2O]_j^{A1,A2}}{\Delta d V_{A1}} \right) \quad (3.20)$$

Diffusion between the *intra*- and *inter*-aggregate pore space takes place from the outer aggregate compartment only, (Fig. 3.3); the subsequent change in total N_2O concentration in an outer aggregate type compartment ($A2$) with time, is shown in equation 3.21.

$$\frac{d[N_2O]_T^{A2}}{dt} = k_{NO_3} - \left(\theta_{,s}^{A2} [N_2O]_{,s}^{A2} k_{N_2O} \right) + \left(\frac{D_j^* \Delta [N_2O]_j^{A1,A2}}{\Delta d V_{A2}} \right) - \left(\frac{D_j^* \Delta [N_2O]_j^{A2,L}}{\Delta d V_{A2}} \right) \quad (3.21)$$

The change in total N_2O concentration in the *inter*-aggregate pore space of a layer type compartment is given by equation 3.22; where L_{-1} is the *inter*-aggregate pore space within the layer compartment below and L_{+1} , the *inter*-aggregate pore space within the layer compartment above compartment L ;

$$\frac{d[N_2O]_T^L}{dt} = \left(\frac{D_j^* \Delta [N_2O]_j^{A2,L}}{\Delta d V_L} \right) + \left(\frac{D_j^* \Delta [N_2O]_j^{L-1,L}}{\Delta d V_L} \right) - \left(\frac{D_j^* \Delta [N_2O]_j^{L,L+1}}{\Delta d V_L} \right) \quad (3.22)$$

The ultimate step in the diffusive process is diffusion from the top soil compartment to the atmospheric compartment, represented by equation 3.23.

$$\frac{d[N_2O]_T^o}{dt} = \left(\frac{D_j^* \Delta [N_2O]_j^{L1,o}}{\Delta d} \right) \quad (3.23)$$

The change in the total amount of N_2O in the atmosphere, is dependent only on the flux between the top soil layer compartment ($L1$) and the atmospheric compartment (σ ; Fig. 3.1). The output in the atmospheric compartment is the net cumulative concentration of N_2O evolved from the soil which is converted to a flux (mol m^{-2}), this is directly comparable to the observed flux readings discussed in chapter 6.

Chapter 4: Short-term N₂O Flux Variability In Soil

4.1 THE EFFECT OF SOIL AGGREGATE SIZE ON N₂O FLUXES

4.1.1 Introduction

Denitrification and nitrification rates in soil are influenced by many factors that are well understood at the microbial level (Tate, 1995). However, the heterogeneous nature of soil makes the interpretation of this knowledge at the field level difficult. This is especially relevant with respect to the reported variability of N₂O fluxes from soil (Burton and Beauchamp, 1985; Parkin, 1987; Parkin and Robinson, 1989; Colbourn, 1993). In temperate regions, denitrification is considered the greatest source of N₂O emissions from soil (Bouwman, 1990). Such emissions are the product of spatial and temporal variability of denitrification zones within the soil (Christensen *et al.*, 1990 a, b). Variation in the incidence of these denitrification zones was thought to be directly related to soil aggregates. A common supposition to explain variation in rates of denitrification in apparently well-drained soils, was the existence of anaerobic microsites within soil aggregates of different size (Dowdell and Smith, 1974). This concept is based on work by Greenwood (1961) and Currie (1961) which described the factors influencing the aeration status of soil aggregates. Mathematical models of denitrification within soil, which incorporated this concept were subsequently developed (Leffelaar, 1979; Smith, 1980; Arah and Smith, 1989). Sexstone *et al.*, (1985 b) made direct measurements of the O₂ concentration within soil aggregates of different size, using an O₂ micro-electrode. Their results confirmed the existence of anaerobic zones within aggregates that were incubated in an aerobic environment. An investigation by Seech and Beauchamp, (1988) found a 12 fold difference in the rate of denitrification between aggregates in the size ranges of < 0.25 mm and 10-20 mm.

There have been very few investigations into the effect of aggregate size on N₂O emissions alone. The aim of the following investigation was to determine, for re-

packed soil cores under realistic field conditions, the effect of aggregate diameter on N₂O emission rates.

4.1.2 Methods

4.1.2.1 Trial 1

Two replicate core containers with dimensions of 13.0 cm diameter and 16.3 cm height, were re-packed with different aggregate sizes of Wick series soil, at a bulk density of 1.1 g cm⁻³. This bulk density was intended to simulate that commonly encountered in conventionally managed agricultural soils (Linn and Doran, 1984). The aggregate size fractions used were 2-5 mm, 5-10 mm and 10-20 mm diameter respectively (section 2.2.1). Prior to core re-packing, the water content of the soil was determined gravimetrically. If necessary, sufficient de-ionised water was added to the soil aggregates, to give a soil water content equivalent to 80 % field capacity. The water was sprayed on, to achieve an even application throughout the sub-sample. Once re-packed, the cores were pre-incubated at 15 °C ± 0.5 °C, for 72 hours, to establish isothermal conditions. The quantification of N₂O was undertaken using the automated continuous GC configuration described in section 2.1, with a sampling interval of 2 hours, for approximately 220 hours. The incubation temperature was set at 15 °C ± 0.5 °C; which approximates the highest temperature attained in the field at 2 cm depth from the soil surface at Sutton Bonington, during the seasons of Spring and Autumn when the soil is in a moist state (Meteorological station, Sutton Bonington). Once the N₂O flux from re-packed soil cores had been determined for approximately 50 hours, a KNO₃ solution (100 kg N ha⁻¹) was applied to the surface of each replicate core. To establish an even application, the KNO₃ solution was applied using a syringe. The depth of solution applied to each core, was equivalent to a 2 mm rainfall event, which approximates the mean daily rainfall for Sutton Bonington. Throughout the incubation period the gas analysis system was vented every 24 hours (section 2.1.2.3).

4.1.2.2 Trial 2

The experimental procedure in trial 2 was identical to that in trial 1, but cores repacked with < 2 mm sized aggregates, were also included in the incubation study. In addition to N_2O analysis, CO_2 emission rates for each replicate chamber were recorded using an ADC- CO_2 gas analyzer (section 2.1.3.3). A 10 cm^3 headspace gas sample was periodically extracted with a 20 cm^3 syringe, via a rubber septum located on the top of each gas tight chamber for CO_2 analysis. To avoid any artificial pressure gradients, the volume of gas extracted, was replaced with a corresponding volume of high purity N_2 , using a syringe. At the start of a trial, or following a chamber venting procedure, the CO_2 concentration within the chamber was determined to establish a baseline from which the cumulative flux could be calculated.

4.1.3 Results

4.1.3.1 Trial 1

General overview of Trial 1

All mean replicate N_2O emission rates quoted, are derived from the gradient of the cumulative gaseous emissions from each of the replicate chambers. The gradient is calculated via a regression analysis which also provides the associated standard error. Apart from replicate 2 containing the 5-10 mm size aggregates, there was an increase in the mean rate of N_2O emission from all aggregate sizes, following the application of the NO_3^- solution (Fig. 4.1). However, throughout the incubation period, the mean rate of N_2O emission from each pair of replicate chambers, was noticeably different from each other in each size category, whether amended with NO_3^- or not. However, there was an apparent increase in N_2O emission rates with aggregate size (table 4.1).

10-20 mm diameter aggregates (Trial 1)

When the largest aggregate size (10-20 mm) was incubated it was clear from the start that replicate chamber 2 had a greater N_2O emission rate than replicate chamber 1 (Fig. 4.1 a; table 4.1). After NO_3^- application, rates of N_2O emission from both replicate chambers, increased in the same ratio. However, after 150 hours incubation, the N_2O emission rates decreased from chambers 1 and 2, by factors of about 2 and 3, respectively.

5-10 mm diameter aggregates (Trial 1)

For the incubation of 5-10 mm diameter aggregates, replicate chamber 2 initially had double the rate of N_2O emission compared to replicate 1 (Fig. 4.1 b; table 4.1). After NO_3^- application the N_2O emission rate increased in replicate chamber 1 by a factor of about 1.5, while that from replicate chamber 2 remained unchanged. However, there was a significant reduction in the rate of N_2O emission (factor of 3) in replicate chamber 2, after 120 hours incubation of the re-packed cores containing 5-10 mm diameter aggregates. Consequently this led to an overall reduction in the mean N_2O emission rate in replicate 2, despite the initial increase in N_2O emission directly following addition of NO_3^- . Replicate 1 maintained an increasing N_2O flux rate, following NO_3^- addition.

2-5 mm diameter aggregates (Trial 1)

Replicate chamber 1 produced an N_2O emission rate that was a factor of 1.3 greater than replicate chamber 2, during the unamended incubation of the 2-5 mm aggregates (Fig. 4.1 c; table 4.1). After NO_3^- addition, the N_2O emission rate from replicate chamber 1 increased more than that of replicate chamber 2, by a factor of 2.

It was initially thought that the significant difference observed for replicate cores must be either an artefact of the core re-packing operation or a gas leak in the system. The experiment was therefore repeated (Trial 2), following a successful check on the gas-

tight integrity of the analysis system, as described in section 2.1.4, to ensure that any variation observed was a consequence of soil spatial variability and not experimental procedure.

4.1.3.2 Trial 2

General overview of Trial 2

The N₂O emission rates from each aggregate size in Trial 1 were similar to the corresponding mean rates in Trial 2. For all four aggregate diameters used, the mean emission rate increased upon application of the NO₃⁻ solution (Fig. 4.2). However, there were noticeable differences between the N₂O emission rates from the two replicate chambers, for all four aggregate sizes. Fig. 4.4 illustrates the positive trend in the mean rates of N₂O emission and increasing aggregate size. The 10-20 mm aggregate size produced the greatest N₂O emission rate and the < 2 mm aggregate size the lowest emission rates.

10-20 mm aggregate diameter (Trial 2)

Prior to NO₃⁻ amendment, the N₂O emission rate from replicate chamber 2 was greater than that from replicate chamber 1, by a factor of 3.7 (Fig. 4.2 a). Once the cores had been amended, the difference between the N₂O emission rates from the two chambers reduced to a factor of about 2.5 (table 4.1). Following the increase in N₂O emission rate resulting from NO₃⁻ amendment, there was a significant reduction (factor of 2) in N₂O emission rates from both replicate chambers containing 10-20 mm size aggregates after approximately 120 hours total incubation; this was similar to the trend observed in Trial 1. The N₂O emission rate from replicate 2 was reduced to less than the rate prior to NO₃⁻ application.

5-10 mm aggregate diameter (Trial 2)

The N₂O emission rates from the two replicate chambers containing cores re-packed with 5-10 mm size aggregates, differed by 2 orders of magnitude in the unamended state (Fig. 4.2 b; table 4.1). Despite an increase in N₂O emission rates from both chambers after treatment with NO₃⁻, replicate chamber 1 maintained a rate that was still greater than that of replicate chamber 2, differing by a factor of about 3.

2-5 mm aggregate diameter (Trial 2)

During the incubation of the 2-5 mm size aggregates, the N₂O emission rate from chamber 1 was greater than that of chamber 2, by a factor of 2, prior to NO₃⁻ amendment (Fig. 4.2 c; table 4.1). After treatment with NO₃⁻ both replicate N₂O emission rates increased; the N₂O emission rate doubled from replicate chamber 1. After a total of 150 hours incubation, there was a sharp increase in the N₂O emission rate from chamber 2 which surpassed that from chamber 1 several fold. However, the rate given in table 4.1 is the gradient for the whole incubation period.

< 2 mm aggregate diameter (Trial 2)

The replicate chambers containing cores re-packed with < 2 mm size aggregates, differed in N₂O emission rates prior to NO₃⁻ application, by a factor of about 1.3 (Fig. 4.2 d; table 4.1). After NO₃⁻ treatment the rate from replicate chamber 1 increased by a factor of about 1.44, while that from chamber 2 increased by a factor of 1.14.

CO₂ emissions from Trial 2

In contrast to N₂O emission rates, the mean CO₂ emission rates from the replicate chambers for each incubated aggregate size were very similar (table 4.2; Fig. 4.3). Although there were too few points to calculate the effect of NO₃⁻ application, it appeared to have very little influence on the emission rates of CO₂ from each aggregate size. Throughout the separate trials the CO₂ emission rate has approximated a zero

order relationship compared to that of N₂O. The apparent stability of the CO₂ emissions regardless of aggregate size is illustrated in Fig. 4.4 b.

4.1.4 Discussion

Following the first trial it was surmized that the variability observed between replicate cores could be due to a gas leak. However, a testing procedure (section 2.1.4) proved the gas-tight integrity of the incubation system. The integrity of the chambers was supported by the low variability in CO₂ emission rates, both between replicates and between treatments in trial 2. Further evidence disproving a leak in the system, was the fact that no one chamber continually possessed greater N₂O emissions than the other. The results obtained in the two trials, were unlikely to be due to differences in the core re-packing procedure, because all the cores were reconstructed with the same bulk density throughout the two trials. Thus the N₂O flux results obtained can be assumed to be a result of soil variability rather than an artefact of the experimental procedure.

The increase in N₂O emissions following NO₃⁻ addition (Fig. 4.4), could be due to either the application of the NO₃⁻ itself, or the local increase in moisture content increasing denitrification, or a combination of both factors (Linn and Doran, 1984). The NO₃⁻ amendment led to an almost immediate increase in N₂O emission, this could possibly be due to denitrifying enzymes already in existence within the soil (Rudaz *et al.*, 1991). At 80 % field capacity, the N₂O emission rates from the range of aggregate sizes investigated was between 10⁻⁶ and 10⁻⁷ mol N₂O-N m⁻² h⁻¹. Similar rates have been reported by Christensen *et al.*, (1990 a) for soils at the same moisture content. These rates are at the lower end of reported levels; rates measured in both the laboratory and field, have been quoted as low as 10⁻⁸ mol N₂O-N m⁻² h⁻¹ and as high as 10⁻⁴ mol N₂O-N m⁻² h⁻¹ (a range of N₂O emission rates from the literature, are shown in the Appendix).

Figure 4.1

Cumulative N_2O flux from Trial 1 for soil cores re-packed with aggregates (Wick series) of diameters (a) 10-20 mm, (b) 5-10 mm and (c) 2-5 mm, all with a bulk moisture content was 80 % of F.C.. The arrow indicates the time of NO_3^- application. Closed symbols = replicate 1, open symbols = replicate 2.

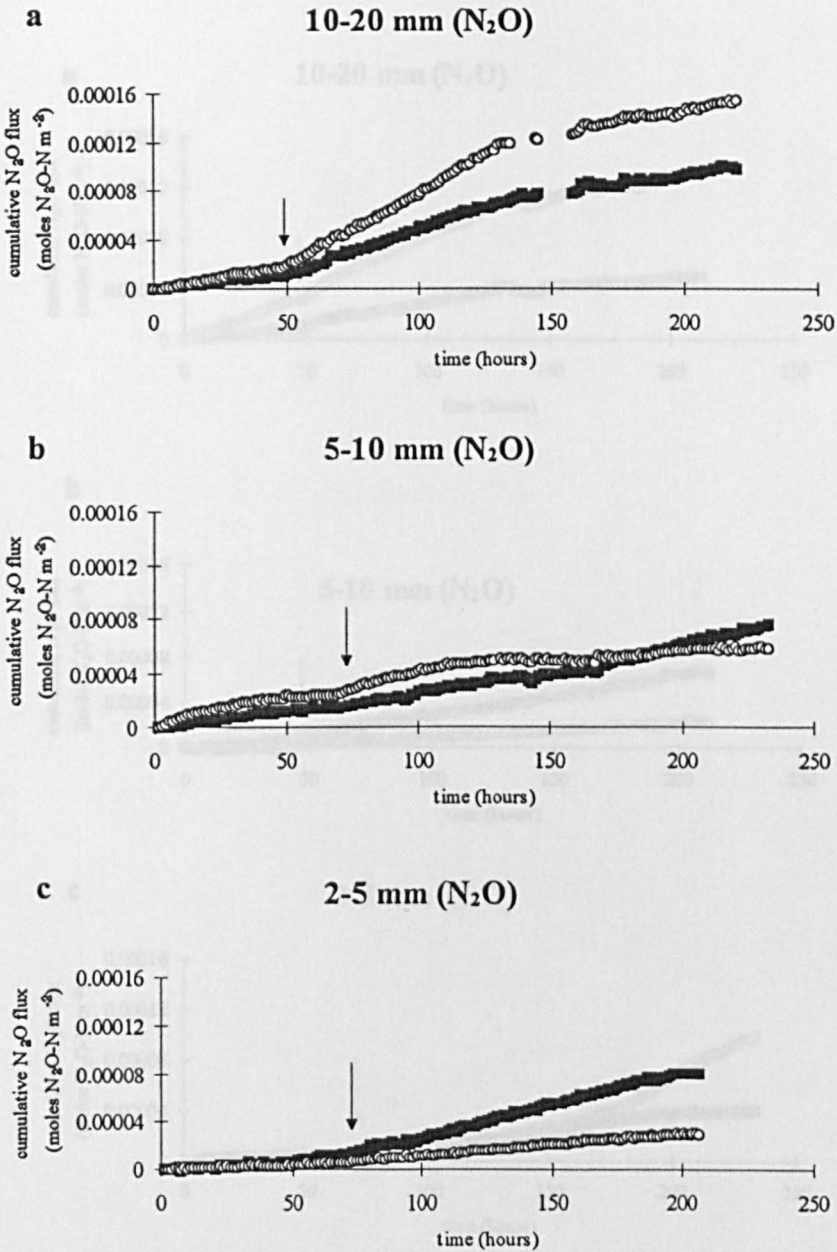


Figure 4.2

Cumulative N_2O flux from Trial 2 for soil cores re-packed with aggregates (Wick series) of diameters (a) 10-20 mm, (b) 5-10 mm (c) 2-5 mm and (d) <2 mm, all with a bulk moisture content was 80 % of F.C.. The arrow indicates the time of NO_3^- application. Closed symbols = replicate 1, open symbols = replicate 2.

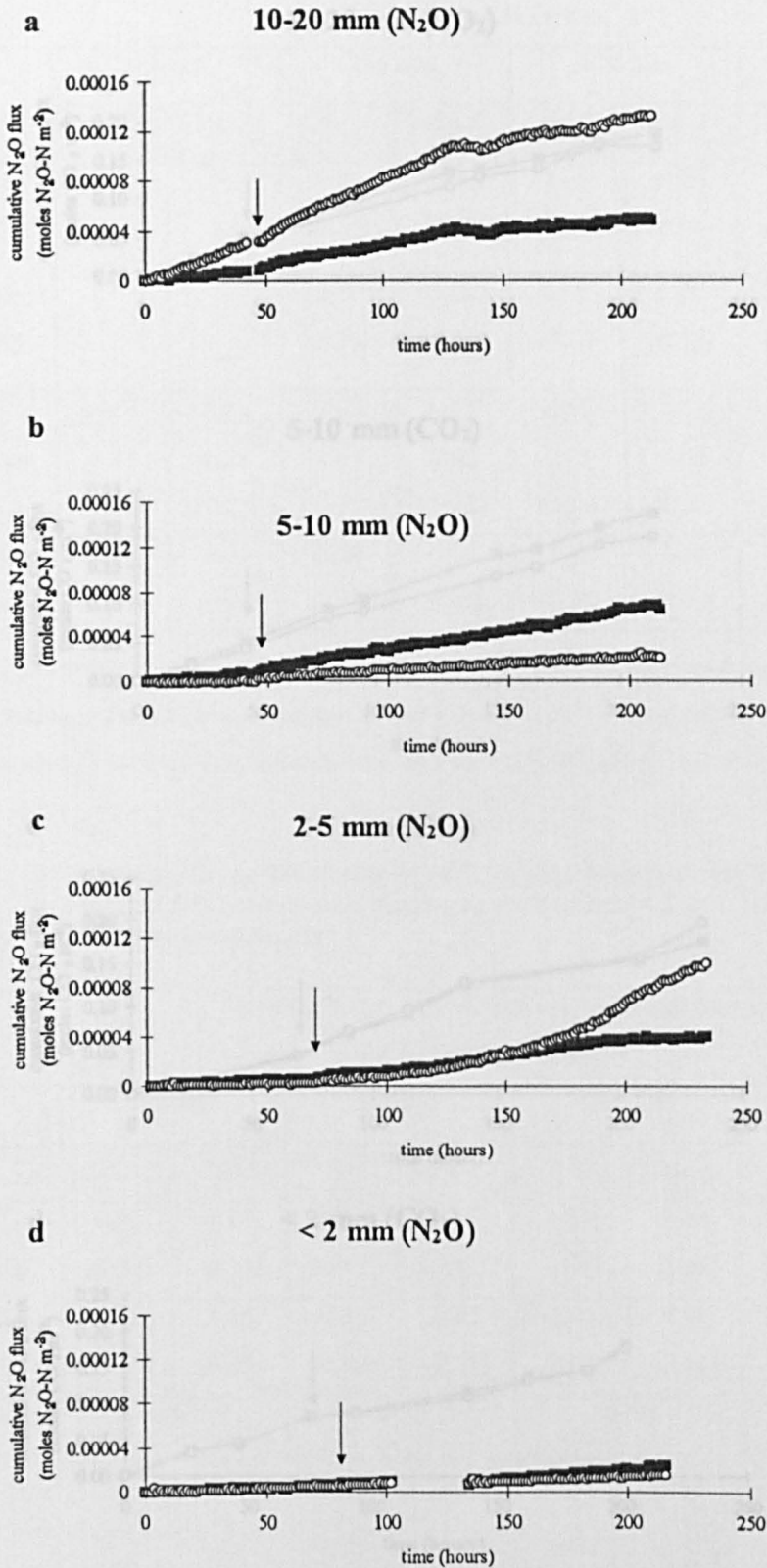


Figure 4.3

Cumulative CO_2 flux from Trial 2 for soil cores re-packed with aggregates (Wick series) of diameters (a) 10-20 mm, (b) 5-10 mm (c) 2-5 mm and (d) <2 mm, all with a bulk moisture content was 80 % of F.C.. The arrow indicates the time of NO_3^- application. Closed symbols = replicate 1, open symbols = replicate 2.

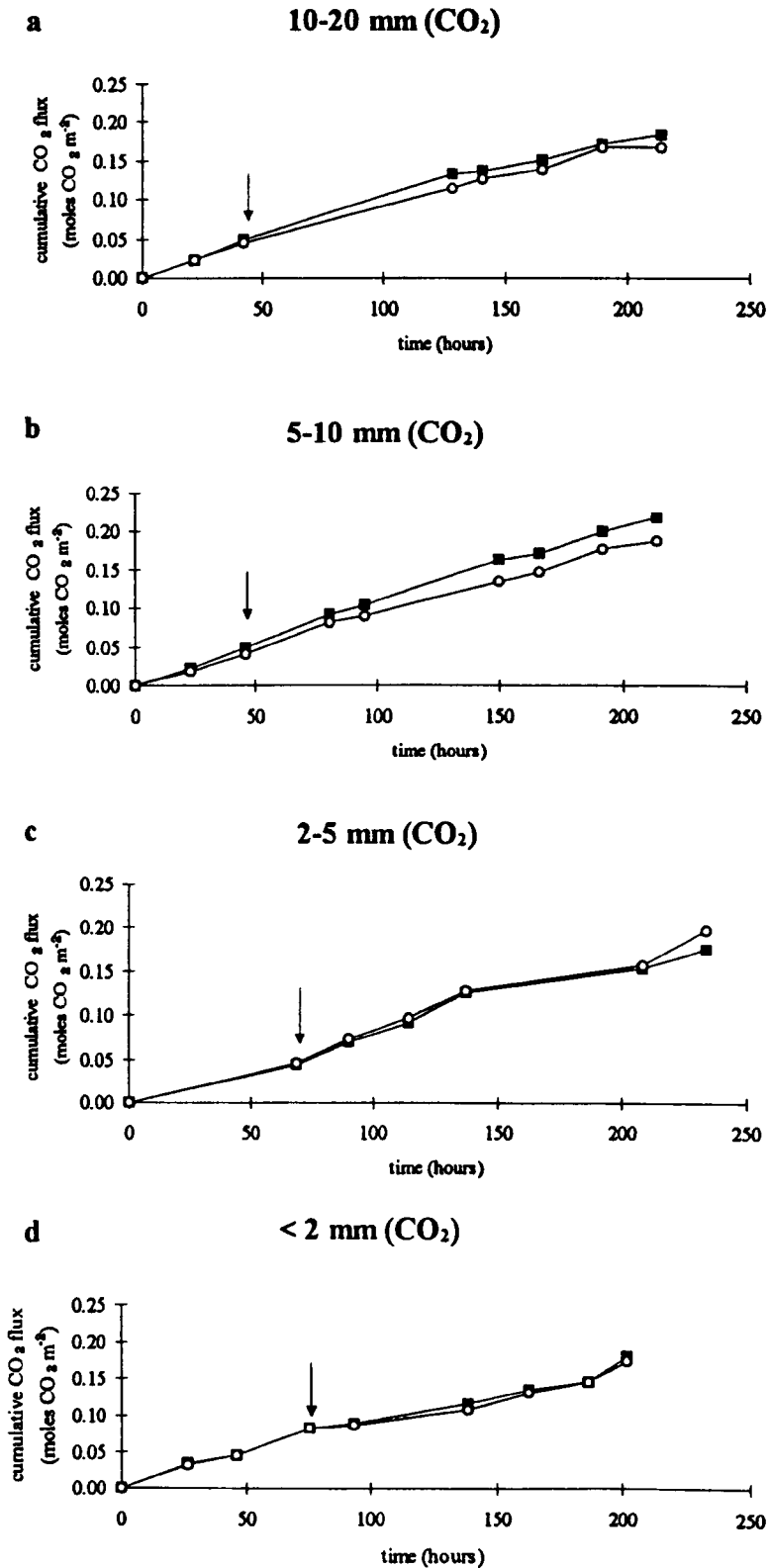


Table 4.1 Mean hourly N₂O emission rates for each replicate re-packed core from Trials 1 and 2, with and without NO₃⁻ amendment. Aggregate sizes include < 2 mm, 2-5 mm, 5-10 mm and 10-20 mm respectively.

Mean N ₂ O flux rate of each aggregate size fraction ($\times 10^{-7}$ moles N ₂ O-N m ⁻² h ⁻¹)									
		< 2 mm		2-5 mm		5-10 mm		10-20 mm	
<i>Trial 1</i>		rep 1	rep 2	rep 1	rep 2	rep 1	rep 2	rep 1	rep 2
-NO ₃ ⁻	mean			1.12	0.78	2.39	4.49	2.28	3.70
	(SD)	-	-	(0.30)	(0.19)	(0.22)	(0.84)	(0.27)	(0.21)
+NO ₃ ⁻	mean			5.14	1.78	3.48*	4.48*	7.39**	12.11**
	(SD)	-	-	(0.39)	(0.16)	(0.57)	(0.72)	(0.45)	(0.54)
<i>Trial 2</i>		rep 1	rep 2	rep 1	rep 2	rep 1	rep 2	rep 1	rep 2
-NO ₃ ⁻	mean	0.75	0.57	1.03	0.42	1.75	0.02	1.87	6.84
	(SD)	(0.23)	(0.21)	(0.16)	(0.12)	(0.28)	(0.28)	(0.37)	(0.40)
+NO ₃ ⁻	mean	1.08	0.65	2.24	5.91	3.42	1.20	3.20***	8.28***
	(SD)	(0.29)	(0.13)	(0.35)	(1.81)	(0.26)	(0.14)	(0.42)	(0.36)

*mean rate for the period 60-120 h; the emission rate from 120-220 h was 4.14×10^{-7} (for rep 1) and 1.10×10^{-7} (for rep 2) mol N₂O-N m⁻² h⁻¹.

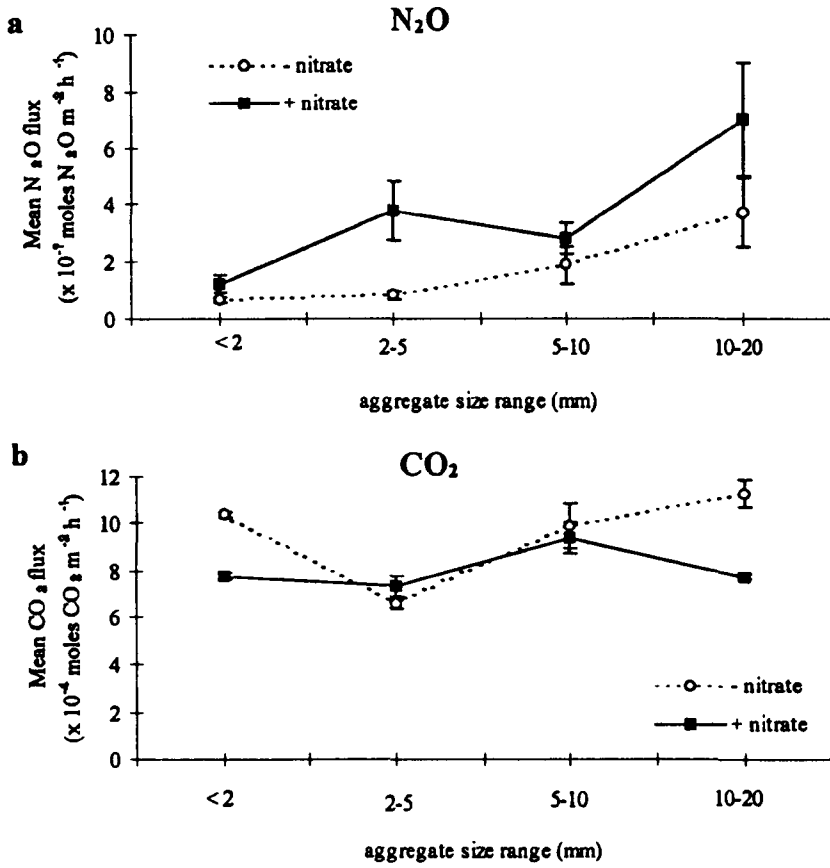
**mean rate for the period 50-150 h; the emission rate from 150-220 h was 3.10×10^{-7} (for rep 1) and 4.15×10^{-7} (for rep 2) mol N₂O-N m⁻² h⁻¹.

***mean rate for the period 60-120 h; the emission rate from 120-220 h was 1.21×10^{-7} (for rep 1) and 3.38×10^{-7} (for rep 2) mol N₂O-N m⁻² h⁻¹.

Table 4.2 Mean hourly CO₂ emission rates for each replicate re-packed core from Trial 2, with and without NO₃⁻ amendment. Aggregate sizes include < 2 mm, 2-5 mm, 5-10 mm and 10-20 mm respectively.

Mean CO ₂ flux rate of each aggregate size fraction ($\times 10^{-3}$ moles CO ₂ m ⁻² h ⁻¹)									
		< 2 mm		2-5 mm		5-10 mm		10-20 mm	
<i>Trial 2</i>		rep 1	rep 2	rep 1	rep 2	rep 1	rep 2	rep 1	rep 2
-NO ₃ ⁻	mean	0.99	0.97	0.64	0.67	1.07	0.87	1.16	1.071
	(SD)	(0.26)	(0.26)	(1×10^{-16})	(1×10^{-16})	(0.03)	(0.06)	(0.07)	(0.01)
+NO ₃ ⁻	mean	0.79	0.76	0.75	0.83	1.00	0.86	0.78	0.76
	(SD)	(0.16)	(0.15)	(0.18)	(0.18)	(0.07)	(0.10)	(0.12)	(0.12)
overall mean (0-200 h)		0.88		0.72		0.95		0.94	

Figure 4.4 Mean of the average gaseous emission rates (a) N₂O from Trials 1 and 2 and (b) CO₂ from Trial 2 only expressed in table 4.1, for each aggregate size, at 80 % F.C.. Open symbols = -NO₃⁻, closed symbols = +NO₃⁻.



The large variation in denitrification rates from different sized aggregates found by Seech and Beauchamp (1988) was greater than that encountered in these investigations, which showed a maximum difference of about 7 fold between the smallest and largest aggregate sizes (table 4.1). However, the variation in N_2O emission rates reported by Seech and Beauchamp (1988) was between a wider range of aggregate sizes (< 0.25 mm and 10-20 mm), which were incubated at greater moisture contents and a higher temperature (25 °C). The results from this investigation support the theory proposed by Leffelaar (1979) and Smith (1980), that the greatest denitrification rate occurs in the largest aggregate, due to the relatively larger anaerobic volume in the aggregate interior. The anaerobic volume is thought to arise from limitations in O_2 diffusion. Contrary to model predictions (Leffelaar, 1979; Smith, 1980) and the results obtained in this investigation, the smallest aggregate size in the investigations of Seech and Beauchamp (1988) emitted the greatest amount of N_2O . Seech and Beauchamp (1988) concluded that their results were due to carbon limitation in the larger aggregates, which were not as *microbially dynamic* as the smaller aggregates.

At 80 % field capacity, the trend in N_2O emissions with increasing aggregate size was not significant, possibly because of the large error associated with variability between replicate emissions. However, there was a positive trend between the mean N_2O emission rates of all the replicates from the two trials and aggregate size, whether amended with NO_3^- or not (Fig. 4.4 a). The relationship was less clear in the NO_3^- amended state, as the mean N_2O emission rates from the 2-5 mm size aggregates were apparently greater than the mean N_2O emission rates from the 5-10 mm size fraction. Another reason for the lack of a significant trend may have been due to the low water content, which may not have facilitated the potential maximum rates of N_2O emissions from the respective aggregate sizes.

In contrast to N_2O , CO_2 emission rates appeared unaffected by aggregate size (Fig. 4.4b). However, the slight reduction in the mean CO_2 emission rate observed from soil cores following NO_3^- amendment, may have been due to the increase in soil water content. Addition of solution to the core surface may have either decreased aerobic,

heterotrophic respiration, or restricted CO₂ diffusion. The restriction in diffusion may not have been observed in the N₂O emission rates due to a relatively greater increase in the N₂O emission rate. Contrary findings were reported by Corre *et al.*, (1995), where there was an increase in both N₂O and CO₂ production following the application of simulated rainfall events to incubated cores. However, the work of Corre *et al.*, (1995) involved the use of *dry* cores and not field moist cores that were used in this investigation. Seech and Beauchamp (1988) found that CO₂ evolution rates were greatest with the smaller aggregate size possibly due to a higher level of microbial activity. However, they found, that there was no clear relationship between aggregate size and CO₂ production, similar to the findings presented here.

The principle feature of these results, is the variability of N₂O emission rates compared to that of CO₂. The rates of CO₂ emission are very stable throughout the incubation of each aggregate size, there is great similarity between replicate rates of each aggregate size and across the range of aggregate sizes used. The N₂O emission rates on the other hand vary not just between aggregate sizes, but also spatially and temporally within replicates.

4.2 THE EFFECT OF NUMBER AND SIZE OF SOIL CORES ON N_2O FLUXES

4.2.1 Introduction

There have been several investigations of the variability of N_2O emission rates from apparently identical soil cores. Most of these have found log-normal distributions of N_2O flux (Folorunso and Rolston, 1985; Parkin *et al.*, 1987; Christensen *et al.*, 1990 a; Ambus and Christensen, 1993; Colbourn, 1993; Van Cleemput *et al.*, 1994). In section 4.1 it was shown that the N_2O emission rates of replicate chambers, containing one core each, were significantly different for all the aggregate sizes studied. Better agreement may be found between replicate chambers, by increasing the number of re-packed cores within each chamber. Although a large volume of soil ($\sim 10^5$ aggregates) was used in the single cores in each chamber, there may have been a subtle difference between the two cores that were responsible for the variation in the N_2O fluxes encountered. Sources of heterogeneity may be internal cracks within the large cores, or anoxic areas within the soil that may be eradicated by using an increased number of smaller cores within each chamber. Thus both the aggregates and the larger core structure are replicated. The following section, investigates whether the variable emissions of N_2O present in the previous investigation are encountered during the incubation of increased numbers of smaller re-packed cores within each chamber.

4.2.2 Method

4.2.2.1 5 core batch incubation

Due to the fixed size of the incubation chambers, an increase in the number of cores within each chamber, required a reduction in core size. Ten cores of diameter 5.2 cm and height 16.5 cm (section 2.2.2) were re-packed with 2-5 mm size aggregates of the Wick series soil, at a bulk density of 1.1 g cm^{-3} . The base of each plastic core was covered with polythene and secured with PVC tape, so that gaseous emission from the

re-packed soil occurred through the upper surface only. The water contents of the soil cores were adjusted, as necessary, to 80 % field capacity. Prior to analysis, all the re-packed cores were pre-incubated at 15 °C for 72 hours to achieve isothermal conditions. The 10 re-packed cores were randomly split into two batches of 5, for incubation in the two chambers: cores 1-5 in replicate chamber 1 and cores 6-10 in replicate chamber 2. Measurement of N_2O (at 2 h intervals) and CO_2 (at 24 h intervals) emission was with the continuous, automated GC and manual ADC procedures, respectively. After approximately 50 hours incubation, a KNO_3 solution (100 kg N ha^{-1}) was applied to the surface of each of the re-packed cores in both chambers with a syringe. The depth of water applied was equivalent to 2 mm of rainfall. Following the NO_3^- treatment, the analysis of both N_2O and CO_2 emission rates from the incubation of the two batches of 5 cores was resumed.

Individual incubation of cores

Once the automated analysis was completed (~ 220 hours) each of the 10 cores were placed in individual chambers (section 2.1.7) and incubated for a period of 72 hours. The atmosphere from each chamber was extracted at the end of the incubation period using a 10 cm^3 gas-tight syringe and manually injected into the GC, for analysis of N_2O alone. No measurement of CO_2 was taken following individual incubation of soil cores.

4.2.2.2 10 core batch incubation

These experiments were identical to the 5 core batch experiment, except that 10 smaller cores were incubated in each replicate chamber. The cores had a diameter of 5.2 cm and height of 5.5 cm (section 2.2.2) re-packed with aggregates from the Wick series soil. Two sizes of aggregates were used: 2-5 mm and 5-10 mm diameter. Cores were randomly selected: cores 1-10 were placed in chamber 1, while cores 11-20 were placed in chamber 2. Again, the period of individual incubation for each core was for 72 hours.

4.2.3 Results

4.2.3.1 5 core batch incubation

The mean rates of N₂O emission from the chambers containing 5 cores (Fig. 4.5 a), were comparable to the range of values recorded in the previous set of investigations (section 4.1), which used a similar volume of soil in one core. However, a significant difference in mean N₂O emission between the 2 replicate chambers was observed again. In both the untreated and NO₃⁻ amended state, the cores in chamber 1 produced an N₂O emission rate which was approximately, 1 order in magnitude greater than that from chamber 2. After NO₃⁻ application, the N₂O emission rate remained virtually unchanged although a small decrease in the mean emission rate from both 5 core batches was observed (table 4.3). The marked contrast in N₂O emission rates from the two chambers required a further check on the gas tight integrity of the system. To verify that the difference in N₂O emission rates between replicate chambers was solely due to the soil, the 5 cores in replicate chamber 1 (cores 1-5) were exchanged with those from replicate chamber 2 (cores 6-10). This was undertaken 24 hours after NO₃⁻ application (marked on Fig. 4.5 a), once N₂O emission rates had been established. The N₂O emission rates from each respective group of 5 cores resumed their original flux rates, following the batch exchange, confirming the validity of the headspace analysis.

When the cores were individually incubated, it was found that the N₂O emission rate of two separate cores, numbers 2 and 5 from replicate chamber 1, were about 30 and 6 times greater (6.29×10^{-6} and 1.24×10^{-6} moles N₂O-N m⁻² h⁻¹, respectively) than that from any other core in the two batches (table 4.4). The remaining 8 cores had a mean emission rate of 2.02×10^{-7} N₂O-N m⁻² h⁻¹.

In contrast to the N₂O results, measurement of CO₂ fluxes showed excellent agreement between the two replicate chambers (Fig. 4.6 a). The flux rates of CO₂ from the two replicate chambers were similar to those emitted in the previous investigations (table 4.3).

4.2.3.2 10 core batch incubation

10 core batch incubation (I)

The previous experiment was repeated with the same aggregate size, but with 10 cores in each chamber (Fig. 4.5 b). However, in contrast to the previous results, N₂O emission rates from the replicate chambers were apparently not significantly different. However there was a significant increase in N₂O emission rates from both replicate chambers, following the addition of NO₃⁻. The N₂O emission rates from both replicate chambers increased by a factor of about 2, following NO₃⁻ amendment.

Emission rates from the 2 batches of 10 individually incubated cores reflected the similarity in N₂O emission rates from the two replicate chambers (table 4.5 I). There was no significant difference ($P > 0.05$) between the mean of the 2 batches of individually incubated cores, (1-10 and 11-20). Both the mean and standard deviation of the N₂O emission rates from the 2 batches, were very similar. The mean N₂O emission rates from the respective core batches 1-10 and 11-20, increased by factors of 1.4 and 1.5 respectively, during the individual core analysis at the end of the batch incubations.

The emissions of CO₂ from the two replicate chambers were not significantly different from one another either with or without NO₃⁻ amendment (Fig. 4.6b; table 4.3). Mean CO₂ emission rates from replicate chamber 1 increased, while replicate chamber 2 decreased upon NO₃⁻ amendment, but this was a very minor effect (table 4.3).

10 core batch incubation (II)

The previous trial was repeated to try and resolve the contradicting results shown in Figs 4.5 a and b. The N₂O emission rates for the repeated trial (Fig. 4.5 c; table 4.3), indicated that the observed similarity between the two replicate chambers containing the 10 core batches, may have occurred by chance. In the repeated trial the N₂O emission rates from the replicate chambers were similar in the untreated state, but

significantly diverged after NO₃⁻ amendment. The mean N₂O emission rates from both replicate chambers, increased significantly after NO₃⁻ amendment. However, the mean N₂O emission rate from chamber 2, was approximately one order of magnitude greater than that from chamber 1, following the application of NO₃⁻ (table 4.3). The variation between the rates of N₂O emission from the replicate chambers was quickly established, therefore the incubation was terminated after 92 hours.

Again the individual analysis of the cores reflected the different rates of N₂O emission from each chamber (table 4.5 II). The mean of the individual N₂O emission rates from cores 1-10 was less than that from cores 11-20. This was probably the result of 3 cores (numbers 12,15 and 16; table 4.5 II) from replicate chamber 2, which had N₂O emission rates approximately 5 times greater than the remaining 7 cores from this batch. The mean N₂O emission rate from cores 11-20 had decreased nearly 5 fold during the individual analysis, whereas cores 1-10 had decreased by a factor of only 0.7.

The mean CO₂ emission rates (Fig. 4.6c; table 4.3) were similar to those measured in the previous 2 x 10 core batch trial. The rates of CO₂ emission from both the replicate batches were not significantly different from each other, either prior to, or after NO₃⁻ amendment. Furthermore, the CO₂ emission rate from both replicate chambers were not significantly affected by the application of NO₃⁻ (Fig. 4.6c)

10 core batch incubation (III)

The experiment was repeated once more, but with a different aggregate size (5-10 mm) to confirm that the variation previously observed from the 10 core batches was not aggregate size specific (Fig. 4.5 d). Again, the mean N₂O emission rates from each replicate chamber were significantly different from one another, both with and without the NO₃⁻ amendment (table 4.3). From the start of the incubation, the N₂O emission rates from replicate chamber 1 were more than 3 times greater than from chamber 2. The difference between N₂O emission rates continued after NO₃⁻ amendment, although, the mean N₂O emission rates from both chambers decreased each by a factor

of about 0.5. The mean N₂O emission rates from the individual core incubation reflected the disparity between cores 1-10 and 11-20 (table 4.5). The mean N₂O emission rates from cores 1-10 were significantly ($P < 0.05$) greater than the corresponding mean from cores 11-20, by a factor of 2. The mean N₂O emission rates from both sets of cores (table 4.5), were, respectively, 1.25 and 3 times greater than from the batch incubation (table 4.3).

The results presented in table 4.6 are the mean of all N₂O and CO₂ emission rates from the large cores in trial 2 (tables 4.1 and 4.2; section 4.1) and the mean of all N₂O and CO₂ emission rates from the chambers containing 5 and 10 cores respectively (table 4.3; section 4.2). The CO₂ emission rates from the 5-10 mm aggregates (III) were similar to the previous two 10 core trials (I, II); emission rates were relatively constant throughout the entire incubation period and very similar for both replicate chambers. The 10 cores in each chamber possessed a surface area:volume ratio that was 1/3 of that from 5 cores in each chamber. Similarly, all the 10 core incubation CO₂ emission rates (I, II, III) were approximately 1/3 of that from the 5 core incubation trial (table 4.6). The 5 cores had a very similar surface area:volume ratio to the single large cores described in section 4.1 and similar CO₂ emission rates. The results suggest a fairly uniform rate of microbial decomposition throughout the soil volume, regardless of aggregate size and core geometry. In contrast N₂O emission rates were highly variable, as described previously.

4.2.4 Discussion

The rates of N₂O emission from the incubation of an increased number of smaller cores within each chamber (section 4.2.3) appeared to be as variable as those from chambers containing one core (section 4.1.3). However, the variability was not an artefact of the analysis system or the method of core construction. This was confirmed by several methods: the leak test on the GC analysis system (section 2.1.4); exchange of the (5) cores incubated in each chamber (section 4.2); examination of N₂O emission rates from individual cores (table 4.5); comparison with CO₂ emission rates (table 4.3).

Figure 4.5

Cumulative N_2O flux from replicate chambers each containing cores re-packed with aggregates of the Wick series soil. (a) 5 cores in each chamber (2-5 mm diameter aggregates), (b and c) 10 cores in each chamber (2-5 mm diameter aggregates), (d) = 10 cores in each chamber (5-10 mm diameter aggregates). The solid arrow = time of NO_3^- application. Closed symbols = chamber 1, open symbols = chamber 2.

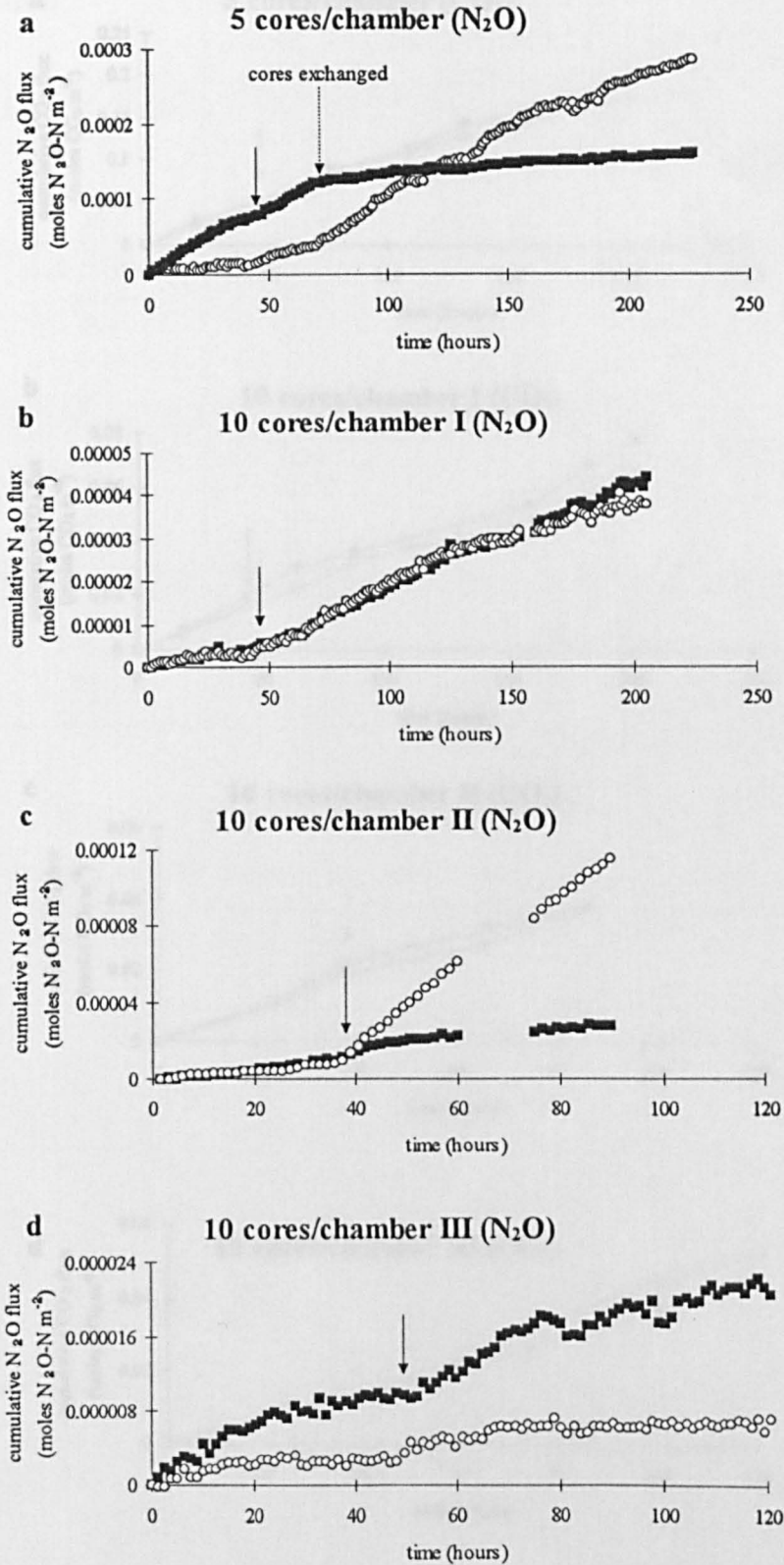


Figure 4.6

Cumulative CO_2 flux from replicate chambers each containing cores re-packed with aggregates of the Wick series soil. (a) 5 cores in each chamber (2-5 mm diameter aggregates), (b and c) 10 cores in each chamber (2-5 mm diameter aggregates), (d) = 10 cores in each chamber (5-10 mm diameter aggregates). The arrow indicates time of NO_3^- application. Closed symbols = chamber 1, open symbols = chamber 2.

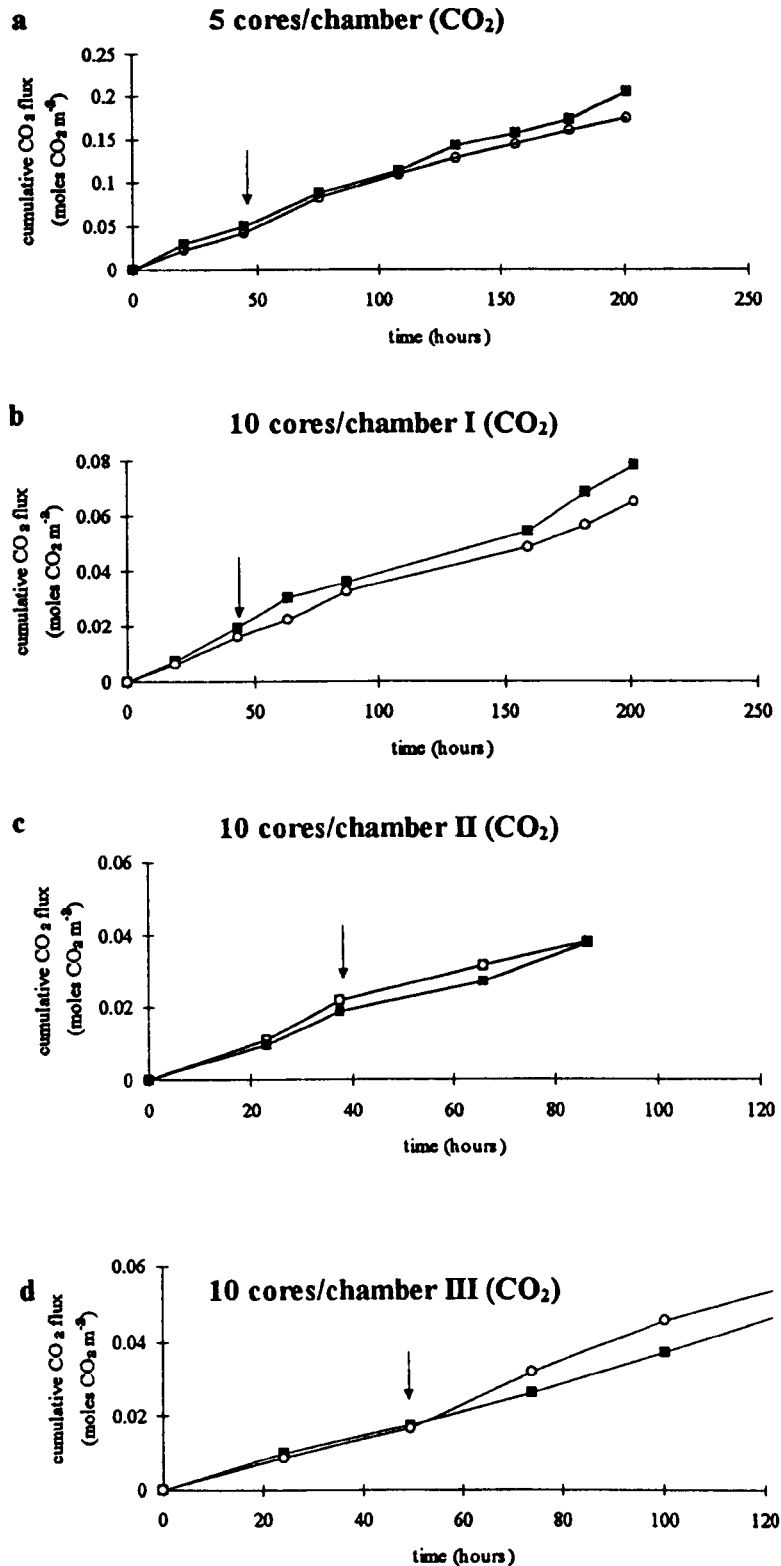


Table 4.3 Mean hourly N₂O and CO₂ emission rates with and without NO₃⁻ amendment from two replicate chambers containing either 5 or 10 cores re-packed with either 2-5 mm or 5-10 mm diameter aggregates.

Treatment		Mean rate of N ₂ O and CO ₂ emission			
		N ₂ O (x 10 ⁻⁷ moles N ₂ O-N m ⁻² h ⁻¹)		CO ₂ (x 10 ⁻³ moles CO ₂ m ⁻² h ⁻¹)	
		chamber 1	chamber 2	chamber 1	chamber 2
2-5 mm	(2 x 5 cores)	(cores 1-5)	(cores 6-10)	(cores 1-5)	(cores 6-10)
-NO ₃	mean	19.60	3.88	1.14	0.95
	(SD)	(1.50)	(1.23)	(0.14)	(0.06)
+NO ₃	mean	16.67	2.76	0.97	0.85
	(SD)	(2.09)	(0.68)	(0.10)	(0.12)
2-5 mm	(2 x 10 cores I)	(cores 1-10)	(cores 11-20)	(cores 1-10)	(cores 11-20)
-NO ₃	mean	0.99	0.92	0.30	0.43
	(SD)	(0.25)	(0.32)	(0.06)	(0.10)
+NO ₃	mean	2.46	2.23	0.36	0.30
	(SD)	(0.21)	(0.40)	(0.09)	(0.03)
2-5 mm	(2 x 10 cores II)	(cores 1-10)	(cores 11-20)	(cores 1-10)	(cores 11-20)
-NO ₃	mean	2.90	2.33	0.56	0.49
	(SD)	(0.34)	(0.32)	(0.05)	(0.04)
+NO ₃	mean	2.21	19.39	0.33	0.38
	(SD)	(0.64)	(0.96)	(0.02)	(9x10 ⁻¹⁶)
5-10 mm	(2 x 10 cores III)	(cores 1-10)	(cores 11-20)	(cores 1-10)	(cores 11-20)
-NO ₃	mean	2.46	0.76	0.35	0.34
	(SD)	(0.47)	(0.26)	(0.05)	(0.09)
+NO ₃	mean	1.57	0.33	0.40	0.51
	(SD)	(0.58)	(0.26)	(0.02)	(0.06)

Table 4.4 Mean hourly N₂O emission rates from 10 individually incubated soil cores that were previously 2 x 5-core batches. Each core was re-packed with aggregates from the Wick series (2-5 mm diameter).

Mean N ₂ O flux rate (x 10 ⁻⁷ moles N ₂ O-N m ⁻² h ⁻¹)			
core no.		core no.	
1	2.38	6	0.85
2	62.87	7	2.02
3	3.22	8	2.24
4	0.38	9	2.16
5	12.44	10	2.99
mean	16.25	mean	2.05
(SD)	(26.47)	(SD)	(0.77)

Table 4.5 Mean hourly N₂O emission rates from 20 individually incubated re-packed soil cores that were previously 2 x 10-core batches; I = 2-5 mm diameter aggregates, II = 2-5 mm diameter aggregates, III = 5-10 mm diameter aggregates.

Mean N ₂ O flux rate (x 10 ⁻⁷ Moles N ₂ O-N m ⁻² h ⁻¹)											
I				II				III			
core no.	N ₂ O	core no.	N ₂ O	core no.	N ₂ O	core no.	N ₂ O	core no.	N ₂ O	core no.	N ₂ O
1	2.28	11	4.12	1	1.16	11	2.19	1	3.64	11	0.71
2	1.67	12	3.01	2	0.64	12	7.58	2	2.76	12	2.02
3	4.43	13	8.00	3	7.14	13	1.33	3	2.51	13	0.71
4	3.32	14	2.36	4	1.58	14	1.45	4	0.97	14	0.72
5	8.31	15	3.36	5	0.95	15	10.70	5	4.02	15	0.67
6	2.67	16	1.62	6	0.70	16	7.35	6	2.36	16	0.78
7	3.64	17	2.11	7	0.78	17	2.17	7	1.33	17	1.21
8	1.93	18	4.10	8	1.15	18	1.85	8	1.08	18	1.32
9	2.42	19	3.52	9	1.07	19	1.41	9	0.73	19	1.23
10	4.41	20	1.71	10	0.83	20	2.40	10	0.31	20	0.52
mean	3.51	mean	3.39	mean	1.59	mean	3.85	mean	1.97	mean	0.99
(SD)	(1.95)	(SD)	(1.86)	(SD)	(1.97)	(SD)	(3.38)	(SD)	(1.27)	(SD)	(0.46)

Table 4.6 Mean CO₂ and N₂O emission rates from different sized re-packed cores as related to the relative surface area to volume ratio of the cores within each chamber.

		1 x core / chamber	5 x core / chamber	10 x core / chamber
SA : VOL ratio of soil core/s		1:16	1:15	1:5
CO ₂ flux rate (x 10 ⁻⁴ moles CO ₂ m ⁻² h ⁻¹)				
-nitrate	mean	9.3	10.45	4.12
	(SD)	(1.90)	(1.34)	(1.00)
+nitrate	mean	8.2	9.1	3.8
	(SD)	(0.83)	(0.85)	(0.73)
N ₂ O flux rate (x 10 ⁻⁷ moles N ₂ O-N m ⁻² h ⁻¹)				
-nitrate	mean	1.66	11.74	1.73
	(SD)	(2.19)	(11.12)	(0.94)
+nitrate	mean	3.25	9.72	4.70
	(SD)	(2.65)	(9.84)	(7.24)

The N₂O emission rates recorded from the individual cores highlighted the extent of spatial variability. The majority of the cores emitted low N₂O emissions, while a few cores exhibited unexpectedly high N₂O fluxes. Similar findings have been reported by Christensen *et al.*, (1990 a), Van Cleemput *et al.*, (1994) and Svensson *et al.*, (1991) and suggest the existence of sporadic N₂O-production hot-spots within soil; even in soil cores constructed with apparently uniform aggregates.

In contrast to the N₂O emission rates, the CO₂ emission rates from each replicate chamber remained stable during each of the incubation trials. The CO₂ emission rates were not affected by treatment with NO₃⁻, but were significantly related to core size (table 4.6). The CO₂ emission rate declined proportionally with a reduction in soil volume which suggests that CO₂ was produced at relatively uniform rates throughout the soil volume. Because of the high degree of variability there was no apparent trend in N₂O emission with surface area:soil volume ratio (table 4.6). Similar findings were reported by Parkin *et al.*, (1987).

The rates of N₂O and CO₂ emission differ from one another, for several possible reasons. N₂O produced throughout the core, may be further reduced to N₂ as it diffuses to the soil surface. This could explain the absence of a relationship between N₂O emission rates and soil core volume but not the high degree of variability shown. However, heterogeneity in the soil core may result in local concentrations of mineralizable organic carbon; which would lead to variable denitrification rates throughout the core due to variation in redox conditions, without significantly affecting the rate of CO₂ emission. Localized areas of compaction could impede O₂ diffusion and hence induce anoxic areas within the core, contributing to the variability in N₂O emission rates. Correspondingly, localized areas of compaction could impede N₂O diffusion thus increasing the chances of further reduction to N₂. The variability observed in N₂O emission rates may have also arisen because a moisture content equivalent to 80 % field capacity, could be close to the point between high and low rates of denitrification. Hence, any localized increase in water content could facilitate large changes in N₂O flux.

The application of NO₃⁻ to soil cores of all sizes usually enhanced N₂O emission rates. This suggests that the rate of N₂O emission in the soil used was generally NO₃⁻ limited. This could also be a source of variability in N₂O emission rates from unamended cores. The addition of NO₃⁻ solution may also have induced greater anaerobism in the surface layers of the soil core. Typically, NO₃⁻ spiking increased soil water content from 80 % to 93 % of field capacity in the smallest core and to 84 % of field capacity in the other size cores.

4.3 THE EFFECT OF SOIL CORE WATER CONTENT ON N_2O FLUXES

4.3.1 Introduction

Reports in the literature state that soils above field capacity, generally evolve N_2O entirely from denitrification, while below field capacity nitrification is the dominant process (Mulvaney and Kurtz, 1984; Linn and Doran, 1984). In previous investigations (sections 4.1 and 4.2) all cores underwent incubated analysis at the same moisture content, 80 % field capacity. The demarcation between a high and low N_2O emission rate from the Wick series, may be close to 80 % field capacity. Hence, a small localized, change in the moisture content at this level may significantly promote increased rates of N_2O via denitrification. The aim of the following investigation is to elucidate whether 80 % F.C. is close to the boundary between high and low N_2O emission rates; which could help to explain the variability so far encountered. Additionally the investigation will generally evaluate the effect of different moisture contents on N_2O emission rates.

4.3.2 Method

Four batches of 20 cores (diameter 5.2 cm and height 5.5 cm) were re-packed with 2-5 mm diameter aggregates of Wick series soil, at a bulk density of 1.1 g cm^{-3} . The base of each core was covered with a fine nylon mesh to prevent soil loss, but allow the passage of water into and out of the core. Each core was allowed to slowly wet up from the core base, until the surface aggregates were covered by a film of water. Then each of the four batches of 20 cores were placed on one of four sand baths maintained at suctions of either 30, 8, 5 or 0 kPa for 21 days at $15 \text{ }^\circ\text{C}$; the cores were covered to minimize evaporation from the soil surface. Following the period of moisture equilibration, the base of each core was then sealed with polythene and PVC tape to ensure that gaseous emission was via the core surface only. Prior to analysis of gaseous emissions, each batch of 20 cores was pre-incubated for 24 hours at $15 \text{ }^\circ\text{C} \pm 0.5 \text{ }^\circ\text{C}$ to achieve isothermal conditions. Each batch of 20 cores was then randomly

split into 2 groups of 10, labelled and placed in incubation chambers 1 and 2 respectively. Incubated analysis was undertaken for about 80 hours. N₂O and CO₂ emission rates were measured with the automated GC and the manual ADC procedures, respectively. Following the chamber analysis, the cores were taken out and incubated individually for a further 80 hours. The mean emission rate of N₂O and CO₂ for each core was manually determined as described in section 2.1.4. Headspace gas samples were extracted using a 10 cm³ syringe and manually injected into the GC and ADC analyzer respectively. Following the analysis of individual core emission rates, a treatment of KNO₃ (100 kg N ha⁻¹) was applied to the surface of every core. To achieve an even distribution of NO₃⁻, the solution, equivalent to 1 mm rainfall, was applied with a syringe. Once each core had been treated, it was replaced back into its original batch of 10, in the two incubation chambers. The core batches then underwent a further 80 hour period of incubated analysis, followed by another period of individual incubation for a similar length of time. N₂O and CO₂ emission rates were determined throughout. This sequential procedure was undertaken for all cores at each of the four soil moisture contents.

4.3.3 Results and discussion

4.3.3.1 General overview

The field capacity of the soil is generally defined (section 2.2.4.3) as being equivalent to the water content of the soil at 5 kPa suction. The soil water potentials applied by the sand baths corresponded to soil moisture contents equivalent to 49, 73, 87 and 133 % field capacity.

The results obtained from this investigation support the findings of the previous trials. N₂O emission rates were highly variable between replicates and with variation in water content and NO₃⁻ concentration. The emission rates of N₂O were stimulated by NO₃⁻ application at all moisture contents. By contrast, CO₂ emission rates were relatively stable throughout the incubations, regardless of water content or NO₃⁻ concentrations.

Replicate chambers containing cores at 133 % field capacity, emitted N₂O at a rate one order of magnitude greater than the rates from cores below field capacity. Similar changes in N₂O emission rates from above and below field capacity, have been reported in the literature (Aulakh *et al.*, 1991; Davidson, 1992; Weier *et al.*, 1993). Some selected examples of the range of N₂O emission rates from soils of different moisture contents, observed by different authors, are shown in the Appendix.

4.3.3.2 Gaseous N₂O emissions from soil at different water contents

N₂O emissions from soil at 49 % F.C.

The two replicate chambers containing (10) soil cores at 49 % F.C., had similar N₂O emission rates until the addition of the NO₃⁻ solution (Fig. 4.7 a). Once the NO₃⁻ solution was applied, the N₂O emission rates from both chambers 1 and 2 increased, however they were noticeably different from one another. The mean N₂O emission rate from replicate chamber 1 increased by a factor of approximately 7, while the N₂O emission rate for chamber 2, only increased by a factor of 2 (table 4.7). The individual analysis revealed that core number 8 from replicate chamber 1 produced a rate nearly 5 times greater than any of the other 9 cores following NO₃⁻ amendment (table 4.8). The individual analysis results generally confirmed the increase in N₂O emission rates upon addition of the NO₃⁻ solution. Again, it appeared that a single core dominated the batch rate of N₂O emission.

N₂O emissions from soil at 73 % F.C.

The replicate chambers containing soil cores that were incubated at 73 % field capacity, showed significantly different mean N₂O emission rates throughout the trial (Fig. 4.7 b). After NO₃⁻ application the mean N₂O emission rates from the replicate chambers did not appear to change significantly, although there was a small increase from chamber 2 (table 4.7). This trend was reflected in the individual core analysis (table 4.8). The individual incubations highlighted that the variation observed in the

batch rate of N₂O emission was dominated by a single core (number 6). It appeared that 19 of the individual core N₂O emission rates were greater following NO₃⁻ amendment.

N₂O emissions from soil at 87 % F.C.

At 87 % field capacity the mean N₂O emission rates from the two replicate chambers were again very different prior to NO₃⁻ amendment (Fig. 4.7 c; table 4.7). In the untreated state, replicate chamber 2 had an N₂O emission rate 3 times greater than that in replicate chamber 1 (table 4.7). This difference was reflected in the individual analysis (table 4.8); in this case, the disparity was due to core number 19, which had an N₂O emission rate that was greater than any other core in the batch, by a factor of about 20. The independent analysis of the cores revealed, that emission from core number 19 decreased by about 5 times, following NO₃⁻ application. By contrast, emission from the remaining 19 cores increased following NO₃⁻ application.

N₂O emissions from soil at 133 % F.C.

All the cores with a water content equivalent to about 133 % field capacity, had N₂O emission rates which were 1 order of magnitude greater than any of the emission rates from cores at the other soil water contents (Fig. 4.7 d; table 4.7). The N₂O emission rates from both replicate chambers appeared to be very similar in both the untreated and NO₃⁻ amended state. The mean N₂O emission rates from chambers 1 and 2 were significantly greater after NO₃⁻ application, they increased by factors of 5.5 and 3.3 respectively. The apparent similarity between the two chambers prior to NO₃⁻ amendment was reflected in the individual core analysis, although the variability between cores differed up to one order of magnitude in each chamber (table 4.8). The individual analysis also revealed that the N₂O emission rate from all 20 cores increased, following NO₃⁻ application. Following NO₃⁻ application core number 10, developed an emission rate nearly 400 times greater than the mean N₂O emission rate prior to NO₃⁻ application and more than 2 orders of magnitude greater than the average of the other 19 individual cores (table 4.8). The large increase in emission rate occurred 80 hours

after NO_3^- treatment. The addition of the N-solution may have supplied the limiting *ingredient* to conditions that already favoured denitrification in this core. The large N_2O flux was possibly facilitated by microbial activity, as there was a noticeable difference between the CO_2 emission rate from that particular core and the other 19 cores. The N_2O emission rates were so large that this core was taken as the subject of further investigation (section 4.5). The individual analysis of core N_2O emissions again highlighted the high degree of spatial variability that exists between replicate cores, at all soil moisture contents.

4.3.3.3 Gaseous CO_2 emissions from soil at different water contents

General overview of CO_2 emissions

The emission rates of CO_2 from the two replicate chambers containing cores at all the moisture contents were similar to one another, in both the unamended and NO_3^- amended states (Fig. 4.8). However, there was a slight reduction in mean CO_2 emission rate from the replicate chambers at 47 %, 73 % and 83 % F.C. following NO_3^- application (table 4.7). However, unlike the cores at lower moisture contents the rate of CO_2 emission from cores at 133 % F.C. increased slightly when amended with NO_3^- (Fig. 4.8). In contrast to N_2O , the emission rates of CO_2 from cores that were at 133 % F.C., were similar to those from cores at lower water contents (Fig. 4.8; table 4.7).

The decrease in CO_2 emission rates from cores at 73 % and 87 % field capacity (but not 47 % F.C) upon NO_3^- amendment, was reflected in the individual core analysis (table 4.9). At 133 % F.C. the individual core analysis did not reflect an increase in CO_2 emission rates from the replicate batches after NO_3^- application. All but cores numbered 10 and 15 from the group of 20, that were at 133 % field capacity, had decreased rates of CO_2 emission upon NO_3^- application. This may be due to the limited supply of available carbon within the cores for heterotrophic denitrification, or

the general demise of aerobic respiration with time due to the gradual onset of anaerobic conditions.

4.3.3.4 Trends in mean gaseous emission rates from soil with increasing water content

The mean of the replicate chamber N₂O emission rates (Fig. 4.9 a) show a general trend of increasing N₂O emissions from soil cores with increasing water content, both unamended and treated with NO₃⁻. The corresponding representation of mean CO₂ emissions (Fig. 4.9 b) shows contradicting trends. In the unamended state the CO₂ emission declines with increasing water content, however in the NO₃⁻ amended state there is an increase in emission rates with increasing soil water content.

The positive trend found between N₂O emission rates and increasing soil moisture content (Fig. 4.9 a) was similar to that found by Linn and Doran (1984) and Aulakh *et al.*, (1991). However, the trend between N₂O emission rates and increasing soil moisture content was less consistent upon NO₃⁻ amendment; due to the anomalous (high) emission rate from one of the cores at 49 % F.C.. The N₂O emission rate appeared to increase continuously up to 133 % F.C. in both unamended and NO₃⁻ amended states (Fig. 4.9 a). In contrast, Schuster and Conrad (1992) found that N₂O production rate reached a peak at 47 % water holding capacity (approximating 100 % F.C.), before declining. This was despite an overall increase in total denitrification rate with increasing water content, from 4 %-68 % water holding capacity; (47 % and 133 % field capacity in the Wick series soil is equivalent to 25 % and 67 % water holding capacity). Linn and Doran (1984) found that up to a water filled porosity of 60 %, microbial activity and therefore CO₂ production increased, but above 60 % aerobic microbial activity decreased due to reduced aeration. Corre *et al.*, (1995) found that simulated rainfall to dry soils increased rates of both ambient N₂O and CO₂ emission. Linn and Doran (1984) found linear relationships between CO₂ and N₂O production between water filled porosity's of 30 % and 70 %. In this study, a similar relationship was found between the N₂O emission rates and CO₂ emission rates from NO₃⁻ amended cores, but not for unamended cores (Fig. 4.9 b).

Figure 4.7

Cumulative N_2O flux from replicate gas-tight chambers each containing 10 re-packed cores containing 2-5 mm size aggregates from the Wick series soil, at different soil moisture contents. a = 49 % F.C.; b = 73 % F.C.; c = 87 % F.C.; d = 133 % F.C.. Closed symbols = replicate 1; open symbols = replicate 2. The arrow indicates time of NO_3^- application. ---- = period of individual incubation.

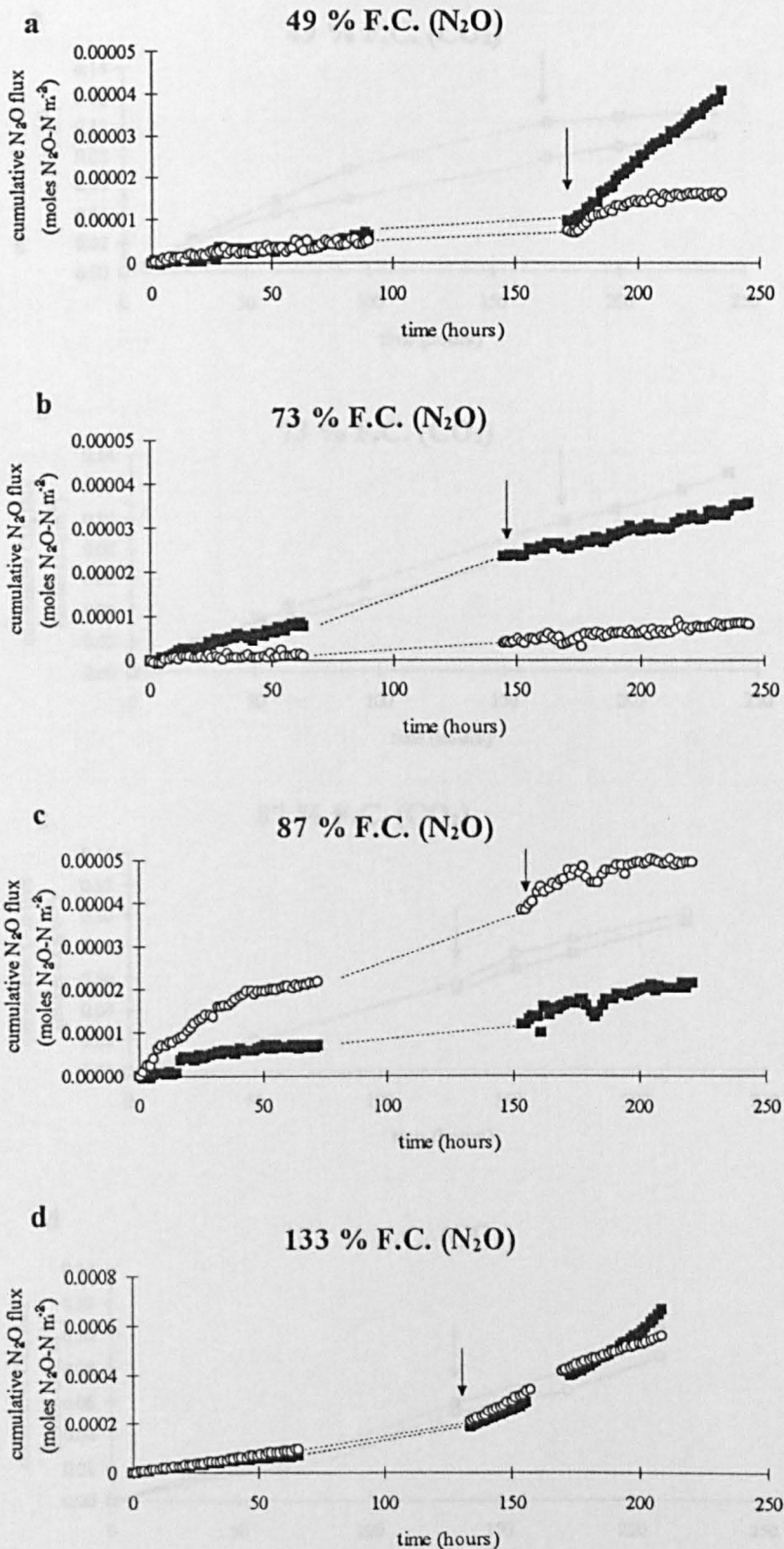


Figure 4.8

Cumulative CO_2 flux from replicate gas-tight chambers each containing 10 re-packed cores containing 2-5 mm size aggregates from the Wick series soil, at different soil moisture contents. a = 49 % F.C.; b = 73 % F.C.; c = 87 % F.C.; d = 133 % F.C.. Closed symbols = replicate 1; open symbols = replicate 2. The arrow indicates time of NO_3^- application. ----- = period of individual incubation.

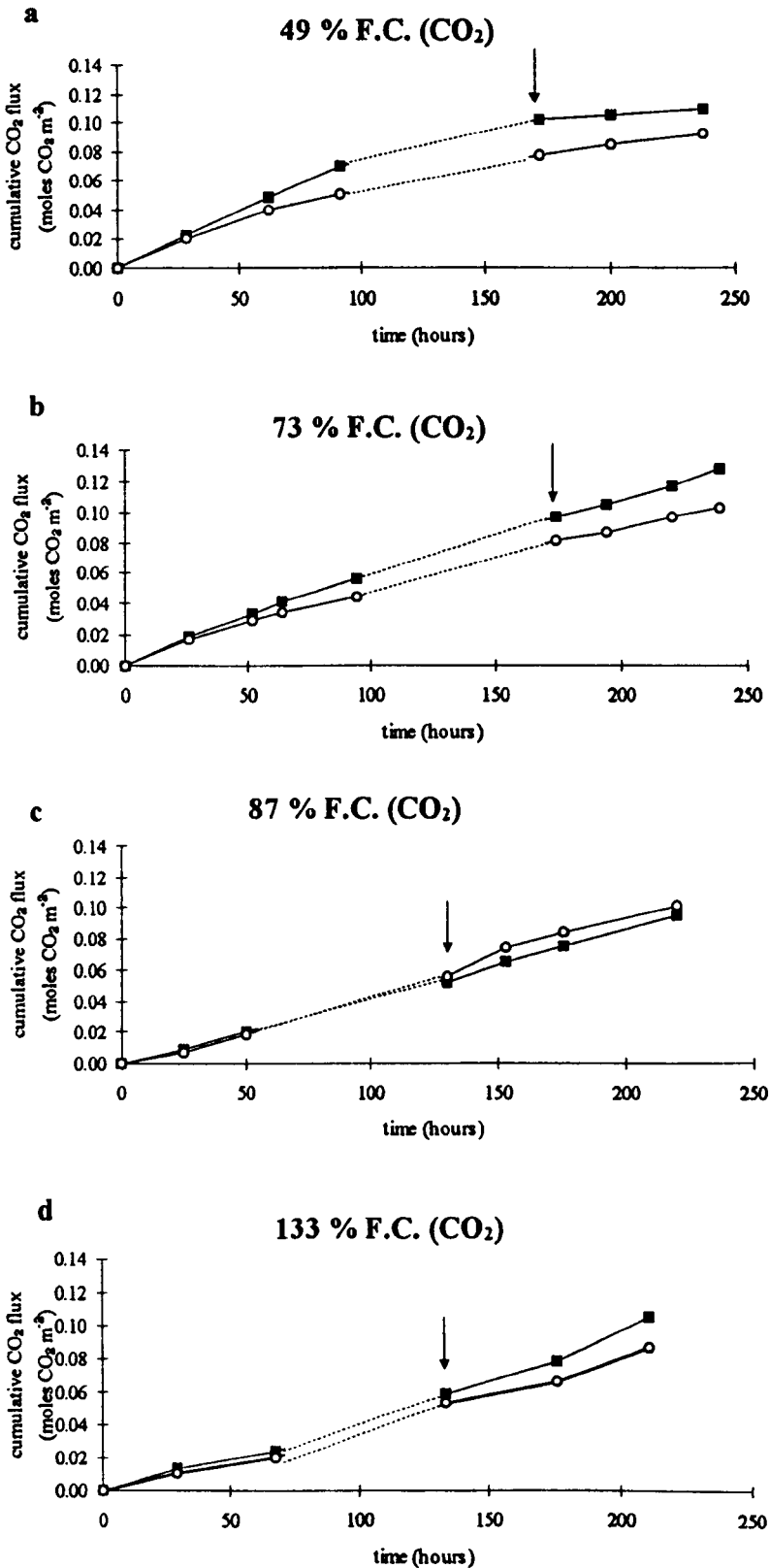


Table 4.7 Mean emission rate of N₂O and CO₂ from re-packed cores containing 2-5 mm diameter aggregates from the Wick soil series. Each replicate chamber contained 10 re-packed cores at different water contents, that were equivalent to 49 %, 73 %, 87 % or 133 % F.C. and treated with and without NO₃⁻.

Treatment		Mean emission rate of N ₂ O and CO ₂			
		N ₂ O (x 10 ⁻⁷ moles N ₂ O-N m ⁻² hr ⁻¹)		CO ₂ (x 10 ⁻⁴ moles CO ₂ m ⁻² hr ⁻¹)	
		(cores 1-10)	(cores 11-20)	(cores 1-10)	(cores 11-20)
49 % field capacity					
-NO ₃	batch mean	0.67	0.64	7.77	5.79
	(SD)	(0.02)	(0.02)	(0.17)	(0.25)
+NO ₃	batch mean	4.97	1.41	1.15	2.24
	(SD)	(0.05)	(0.10)	(0.11)	(0.15)
73 % field capacity					
-NO ₃	batch mean	1.38	0.25	6.20	5.06
	(SD)	(0.03)	(0.02)	(0.13)	(0.24)
+NO ₃	batch mean	1.17	0.46	4.15	3.13
	(SD)	(0.03)	(0.03)	(0.12)	(0.09)
87 % field capacity					
-NO ₃	batch mean	1.22	3.76	4.22	4.35
	(SD)	(0.04)	(0.10)	(0.16)	(0.42)
+NO ₃	batch mean	1.34	1.40	4.03	4.61
	(SD)	(0.09)	(0.12)	(0.28)	(0.01)
133 % field capacity					
-NO ₃	batch mean	11.26	14.64	3.53	2.99
	(SD)	(0.08)	(0.04)	(0.01)	(0.04)
+NO ₃	batch mean	61.54	47.95	5.90	5.32
	(SD)	(0.82)	(0.80)	(0.32)	(0.41)

Table 4.8 Mean N₂O emission rates from 2 x 10-cores incubated individually in 20 chambers. Each 2 x 10-core batch was incubated at water content equivalent to either 49, 73, 87 or 133 % F.C., with and without NO₃⁻.

Mean N ₂ O flux rate (x 10 ⁻⁷ moles N ₂ O-N m ⁻² h ⁻¹)								
core number	49 % F.C.		73 % F.C.		87 % F.C.		133 % F.C.	
	- nitrate	+ nitrate	- nitrate	+ nitrate	- nitrate	+ nitrate	- nitrate	+ nitrate
1	0.22	0.78	0.18	0.43	0.62	0.57	12.46	37.61
2	0.17	0.53	0.53	0.71	0.45	0.66	3.48	29.50
3	0.36	0.74	0.42	0.40	0.54	0.73	21.31	41.67
4	0.03	0.51	0.44	0.40	1.04	0.86	14.95	26.51
5	0.23	0.54	0.32	0.61	0.76	2.52	1.91	20.03
6	0.08	0.56	15.35	1.64	0.49	0.93	22.49	20.50
7	0.21	0.50	0.44	0.52	0.39	1.18	14.70	21.14
8	0.33	2.75	0.26	0.84	0.50	0.68	35.35	61.74
9	1.22	0.90	0.53	0.89	0.61	0.96	23.81	79.98
10	0.25	0.43	0.40	0.61	0.44	0.93	20.70	8032.89
mean	0.31	0.82	1.89	0.71	0.58	1.00	17.11	837.2
(SD)	(0.34)	(0.70)	(4.73)	(0.37)	(0.20)	(0.56)	(9.92)	(2528)
11	0.17	0.66	0.15	0.64	0.64	6.81	15.07	59.92
12	0.04	0.61	0.32	0.85	0.61	1.26	29.88	62.84
13	0.14	0.61	0.28	0.57	0.40	0.67	5.58	26.77
14	0.13	0.38	0.28	0.72	0.52	0.66	14.53	82.83
15	0.13	0.40	0.54	0.57	0.56	1.02	3.53	20.48
16	1.11	0.80	0.21	0.79	0.65	0.69	9.78	36.66
17	0.04	0.88	0.46	0.75	0.52	0.77	45.89	87.38
18	0.24	0.31	0.24	0.90	0.49	0.67	17.53	54.83
19	0.18	0.66	0.52	0.54	15.61	3.60	2.62	18.00
20	0.24	0.42	0.50	0.42	0.47	0.80	25.65	51.77
mean	0.24	0.57	0.35	0.68	2.05	1.70	17.01	50.15
(SD)	(0.31)	(0.19)	(0.14)	(0.15)	(4.77)	(2.01)	(13.57)	(24.44)

Table 4.9 Mean CO₂ emission rates from 2 x 10-cores incubated individually in 20 chambers. Each 2 x 10-core batch was incubated at water content equivalent to either 49, 73, 87 or 133 % F.C., with and without NO₃⁻.

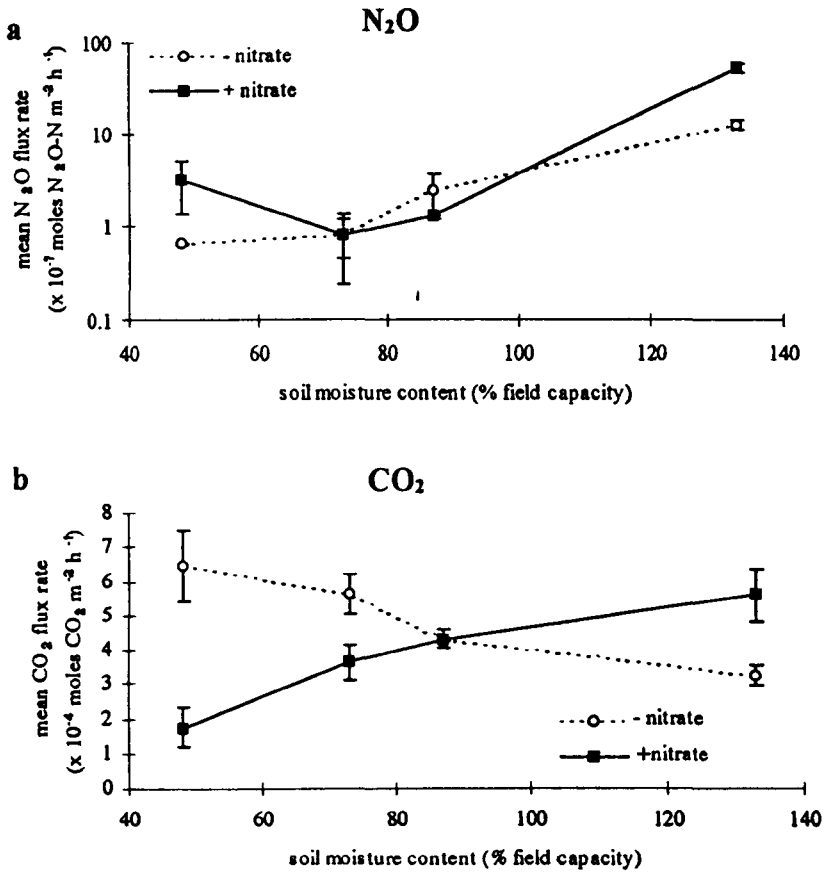
Mean CO ₂ flux rate (x 10 ⁻⁴ moles CO ₂ m ⁻² h ⁻¹)								
core number	49 % F.C.		73 % F.C.		87 % F.C.		133 % F.C.	
	- nitrate	+ nitrate	- nitrate	+ nitrate	- nitrate	+ nitrate	- nitrate	+ nitrate
1	3.51	3.95	4.52	3.06	*	4.14	5.74	3.77
2	4.02	6.21	4.52	4.23	4.27	3.89	4.43	3.58
3	4.27	4.71	7.66	3.94	5.02	3.39	4.43	3.95
4	4.02	3.20	4.52	3.64	3.51	4.14	4.24	3.01
5	3.77	3.95	4.52	2.48	2.76	3.89	6.68	3.39
6	7.28	3.95	4.13	0.73	5.02	3.64	4.99	3.39
7	5.02	3.58	6.09	3.64	2.51	3.39	5.37	3.20
8	3.77	4.71	4.52	3.94	5.02	3.89	4.80	3.95
9	3.77	4.71	5.31	3.64	*	3.14	4.24	3.39
10	1.26	4.33	4.13	3.94	*	3.64	5.37	6.59
mean	4.07	4.33	4.99	3.32	4.02	3.72	5.03	3.82
(SD)	(0.15)	(0.83)	(1.11)	(1.04)	(1.31)	(0.34)	(0.73)	(1.02)
11	4.52	3.58	4.52	3.94	2.76	4.90	4.80	3.95
12	2.51	5.08	4.52	4.52	3.26	4.14	4.24	2.82
13	4.27	3.58	5.31	3.94	5.77	4.14	4.80	3.58
14	3.26	3.20	4.91	2.77	4.02	3.39	4.43	4.14
15	3.51	3.95	4.91	3.94	6.28	4.14	4.24	4.71
16	2.76	4.71	4.91	3.64	5.52	3.39	5.37	4.14
17	4.02	6.21	4.91	3.35	4.52	3.14	5.93	3.58
18	3.01	4.33	5.70	3.35	5.52	3.64	5.74	3.95
19	3.77	5.08	5.70	3.94	*	3.89	5.37	3.77
20	2.51	3.58	4.13	4.52	*	2.89	4.99	4.33
mean	3.41	4.33	4.95	3.79	4.71	3.77	4.99	3.90
(SD)	(0.72)	(0.94)	(0.51)	(0.54)	(0.14)	(0.60)	(0.60)	(0.51)

* missing data

The reduction in CO₂ emission rates in unamended cores with increasing moisture content, was probably due to the general reduction in aerobic respiration. The cores at 133 % field capacity had the lowest CO₂ emission rate in the unamended state, possibly because it had the lowest aerobic activity. However, the addition of NO₃⁻ increased CO₂ production in these soil cores, probably due to the further stimulation of the denitrifying population with NO₃⁻ (Fig. 4.9 b). The CO₂ flux from soils less than field capacity all decreased upon NO₃⁻ amendment, possibly due to a local reduction in aerobic respiration (greater anaerobism) in the surface layers of the soil core. Typically, NO₃⁻ spiking increased the soil water content by only 3 % at each moisture level. However, there is an inconsistency between the huge effect of a 3 % increase in water content caused by NO₃⁻ addition to cores at 47 % F.C. and the relatively small effect of water content shown by the unamended cores in Fig. 4.9 b. The opposing trends of CO₂ emission observed in unamended and NO₃⁻ amended soil cores in the large chambers was not reflected in the individual core analysis. Although the individual core emissions were relatively consistent, it does not discount the fact that an anomalous core may be responsible for the observed results.

However, the point at which the two CO₂ emission rates in the amended and unamended state crossover (Fig. 4.9 b) could signify the junction between aerobic and anaerobic dominance in microbial activity. This point approximates to 87 % F.C. and may be the demarcation between high and low rates of N₂O emission. This would help to explain some of the variability between N₂O emissions in prior experiments that had taken place at 80 % F.C..

Figure. 4.9 Mean chamber (a) N_2O and (b) CO_2 fluxes from 20 re-packed soil cores at different soil moisture contents with and without NO_3^- application.



4.4 DETERMINATION OF N₂O SOURCE BY SOIL CORE DISSECTION

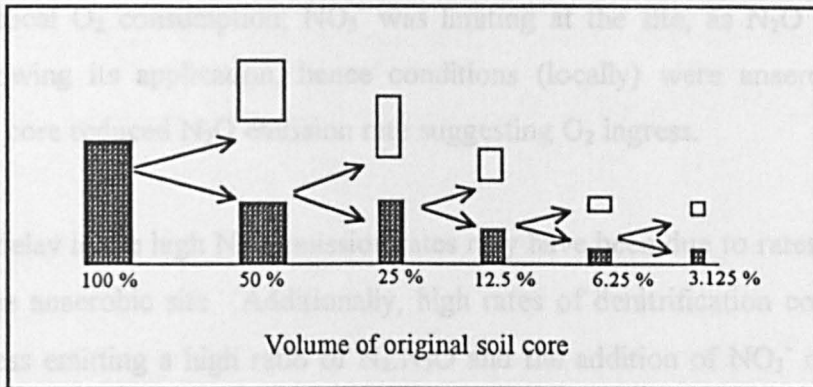
4.4.1 Introduction

The re-packed soil core that emitted N₂O at an unexpectedly high rate, described in section 4.3, (core number 10; 133 % F.C.) was isolated following the completion of the work in section 4.3. The N₂O emission rate of the core was 8.033×10^{-4} moles N₂O-N m⁻² h⁻¹, which was far in excess of any other N₂O emission rate so far encountered. In this investigation the core was subject to further examination to determine the source of this large N₂O emission. This was achieved with a series of successive, sectioning-incubation procedures (Fig. 4.10).

4.4.2 Method

Following the completion of the preceding experiment, the soil core, assumed to be still at 133 % F.C., was incubated for 24 hours in an individual incubation chamber. The mean emission rate of N₂O for the core was manually determined as described in section 2.1.7. Once the 24 hour incubation period was completed, the soil was sectioned into 2 equal parts, with the point of division being at half the core length. Each section was then separately incubated for a further 24 hours. The change in the chamber N₂O concentration over the subsequent incubation period was measured for each soil section. The soil section that produced the bulk of the N₂O evolution was again cut in half, this time along the core section diameter. The core section that produced the lower N₂O emission rate was left intact. All three sections of the former whole soil core, then underwent a further period of incubation for 24 hours and the amount of N₂O produced from all three sections quantified. This procedure of partitioning the core section responsible for the bulk of the N₂O emission was then repeated (Fig. 4.10). Each time all sections were incubated and assayed in a similar manner. Prior to each incubation stage, all of the individual chambers were vented to establish ambient concentrations.

Figure 4.10 Schematic of the progressive division of an unsaturated re-packed soil core to isolate the portion of soil responsible for the bulk of the N_2O evolution.



4.4.3 Results and discussion

Following the first partitioning of the core, it was evident that the soil core was emitting N_2O disproportionately throughout its volume (table 4.10). Throughout the partitioning sequence, the section that contained the source of the bulk flux constituted between 97 % and 56 % of the combined flux from all sections, at each partitioning stage (table 4.10). However, as the partitioning of the source sections proceeded, the total amount of N_2O emitted by all the sections combined was markedly reduced. This reduction in total N_2O emission was probably due to the increased aeration of the soil. Removal of the core sheath and sectioning of the soil core exposed new surfaces, which would have considerably increased access of O_2 .

After several partitionings of the core, the bulk source of the N_2O production was identified as the remains of an Earthworm. This *discrete faunal residue* (DFR) was part of a soil mass that represented about 3 % of the original core volume (Fig. 4.11 a) and which accounted for 56 % of the N_2O produced from the whole soil core (table 4.10). The extent of N_2O emitted by the 3 % volume of soil, relative to the other soil portions, is clearly seen when the amount of N_2O emitted is plotted relative to the respective soil volume (Fig. 4.11 b).

The DFR was probably a site of intense microbial respiration which induced local anaerobic conditions, producing unexpectedly high N₂O emissions from the core. The evidence supporting this includes: that DFR is a source of mineralizable carbon, which will promote local O₂ consumption; NO₃⁻ was limiting at the site, as N₂O emission increased following its application, hence conditions (locally) were anaerobic; the division of the core reduced N₂O emission rate suggesting O₂ ingress.

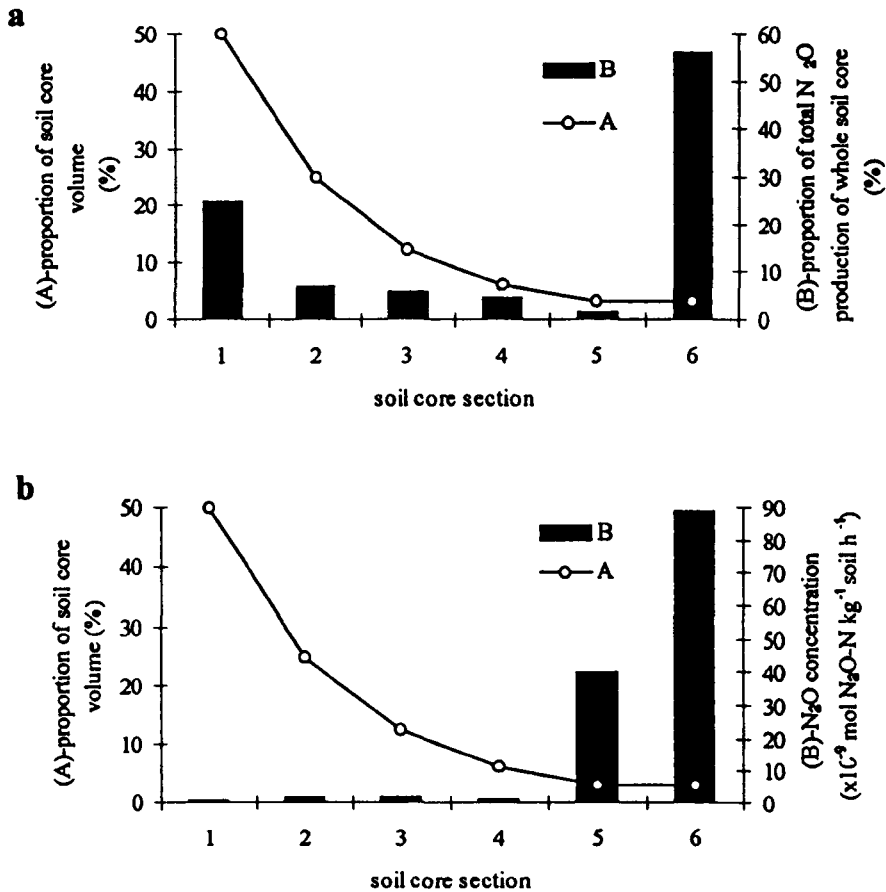
The apparent delay in the high N₂O emission rates may have been due to rates of NO₃⁻ diffusion to the anaerobic site. Additionally, high rates of denitrification could have been in progress emitting a high ratio of N₂:N₂O and the addition of NO₃⁻ may have reduced the action of N₂O-reductase, thus considerably lowering the ratio (Blackmer and Bremner, 1978).

The discovery that the remains of an Earthworm was possibly responsible for the bulk of the N₂O production in a re-packed soil core, supports the literature findings that spatial variation in gaseous N₂O emissions may be the specific result of variation in organic carbon supply (Parkin, 1987; Christensen *et al.*, 1990 a). Parkin (1987), isolated samples with high denitrification activity and sectioning these samples into distinct soil layers of different denitrification activity. The author discovered that a particulate organic fraction (decaying leaves) was responsible for all the activity observed in the top 1 cm of the soil core. Few literature results surpassed a rate of 8.033×10^{-4} moles N m⁻² h⁻¹ observed in this investigation. However comparable flux values were reported by Christensen *et al.*, (1990 a) and Weier *et al.*, (1993) from soils containing plant residues and from soils amended with organic carbon respectively; these rates are shown in the Appendix.

Table 4.10 Relative proportion of N₂O emitted from the successive soil sectioning of the bulk N₂O producing partitions of an unsaturated re-packed soil core.

proportion of core emitting bulk N ₂ O flux (%)	proportion of total N ₂ O flux emitted by the core section containing the bulk source (%)	total N ₂ O emission from all core sections after each partitioning stage (x 10 ⁻⁹ moles N ₂ O-N cm ⁻³ soil h ⁻¹)
100	100	16.76
50	97	7.89
25	85	3.96
12.5	77	1.63
6.25	65	1.24
3.125	56	0.43

Figure 4.11 Illustration of the respective sections of the partitioned soil core volume: associated with (a) the relative proportion of total N₂O produced by the core as a whole after the final partitioning; and (b) the relative N₂O concentration per unit mass of soil per unit time.



4.5 THE EFFECT OF AGGREGATE HOMOGENISATION ON N₂O FLUX

4.5.1 Introduction

In section 4.4 it was shown that N₂O emission variability could be due to discrete faunal residues. This investigation was to establish whether homogenization of the aggregate structures reduced N₂O emission variability that was thought to be related to the disproportionate distribution of decaying organic matter.

4.5.2 Method

Soil aggregates of size 5-10 mm from the Wick soil series were thoroughly homogenized with de-ionized water, at a soil:solution ratio of 2:1, in a *Kenwood* food mixer for 5 minutes. Prior to mixing, the soil aggregates and the de-ionized water were pre-incubated for 48 hours at a temperature of 15 °C, to avoid any possible effects resulting from differences in temperature. Sub-samples (100 g) of the resulting saturated slurry were transferred to 20 x core containers of diameter 5.2 cm and height 5.5 cm. The cores were then randomly separated into 2 groups of 10, labelled and placed in 2 gas-tight replicate chambers, for incubation at 15 °C. The automated GC procedure, was used to quantify the emission of N₂O alone. Following 68 hours incubation, the cores were taken out and placed in individual incubation chambers for a further 68 hours and analysed for individual N₂O emission rates using the manual GC procedure. Following the individual core headspace assay a KNO₃ solution was added to each core (100 kg N ha⁻¹). The applied NO₃⁻ solution, equivalent to 2 mm depth of liquid, was stirred throughout the whole core using a spatula. The two batches of 10 cores were then replaced back into their respective replicate chambers and incubated for a further 68 hours, after which each of the cores underwent another 68 hour individual incubation with determination of N₂O emission rate.

4.5.3 Results and discussion

The mean N_2O emission rates from the replicate chambers, containing 10 cores of homogenized soil aggregates, were almost identical throughout the experimental period (Fig. 4.12; table 4.11). This similarity is reflected in the individual analysis of the 20 cores both before and after NO_3^- addition (table 4.12). The similarity between the 20 homogenized replicates suggests that the difference observed between the unsaturated aggregated soil cores (section 4.3) was due to local conditions associated with DFRs, and which was removed by the mixing process. Low variability in N_2O emission rates from the homogenized cores, could be the result of the high water content of the slurries which would have stimulated denitrification throughout the whole core. This would raise the background N_2O emission rate and effectively mask any localized emissions from DFRs. Additionally, the mixing process may have distributed any local concentrations of organic carbon evenly throughout the slurry. Mixing would eliminate local O_2 depletion and N mineralization which would otherwise arise from DFRs in aerobically incubated cores with intact aggregate structures.

The rate of N_2O evolution from both chambers significantly increased by a factor of about 4, after 30 hours incubation and was maintained linearly, for another 40 hours until individual incubation (Fig. 4.12; table 4.11). The lag-time prior to the increase in emission rate at 30 hours could be due to the time taken to establish anaerobic conditions within the soil and the subsequent synthesis of new denitrifying enzymes by the developing denitrifying population. Alternatively the enhanced denitrification could be due to a carbon based substrate becoming available as a result of a microbial succession or the death of the aerobic microbial population. The limited availability of carbon could account for the subsequent reduction in mean N_2O emission rate, between 134 and 201 hours incubation (Fig. 4.12; table 4.11). The application of easily metabolizable organic carbon has been shown to rapidly promote soil denitrification rates, which decline when the C-source has been utilized (Christensen *et al.*, 1990 b).

The N₂O emission rates from the saturated slurries were about 2 to 3 orders of magnitude greater than the general emission rates encountered in the unsaturated aggregate investigations because of the increased water content in the slurried soil. Similar differences in magnitude between emission rates from unsaturated soil and saturated slurries have been reported in the literature (Christensen *et al.*, 1990 a; see Appendix). However, the rate of N₂O emission from the slurried soil was 5 times less than the N₂O emission rate from the aerobic, aggregated core that contained the Earthworm (DFR) remains (section 4.4). There are several possible explanations for this occurrence. In the aggregated core containing the DFR, there was intense local anaerobism caused by O₂ consumption by the carbon source. This would promote denitrification in association with conditions of minimal restriction on N₂O diffusion out of the core (low water content). Additionally the aggregated core possessed a local source of inorganic N from mineralization of the DFR. Following local nitrification, this would further promote denitrification. Furthermore, one would expect greater N₂O production from DFR than soil alone, as denitrification rate increases with decreasing C:N ratio (Bowman and Focht, 1974). Generally, Earthworms have a C:N ratio of about 5:1 (Lee, 1985) and soil, a ratio of 10:1 (White, 1981). Another reason is that the single aggregated core possessed a DFR, which may not have been the case for the 20 homogenized cores. Therefore the homogenized cores may not have possessed any local hot-spots of anaerobism or NH₄⁺/NO₃⁻ cycling. In addition, the homogenization process destroyed aggregate structures and increased the soil water content, which would restrict N₂O diffusion despite potentially increasing its rate of production. Mulvaney and Kurtz (1984) and Aulakh and Doran (1990) showed that N₂O diffusion out of soil cores can be significantly impeded by soil water. A relatively minor consideration is the reduced viability of N₂O-reductase in the aggregated core containing the DFR, due to greater diffusion of O₂ into the core. This may have promoted a higher N₂O:N₂ ratio compared to that in the slurried cores.

Figure 4.12 Cumulative N₂O flux from 2 replicate chambers, each containing 10 cores of homogenized soil aggregates, with and without NO₃⁻ treatment. The arrow indicates the point at which the NO₃⁻ was applied. Closed symbols = replicate 1, open symbols = replicate 2. 67-134 hours = period of individual incubation.

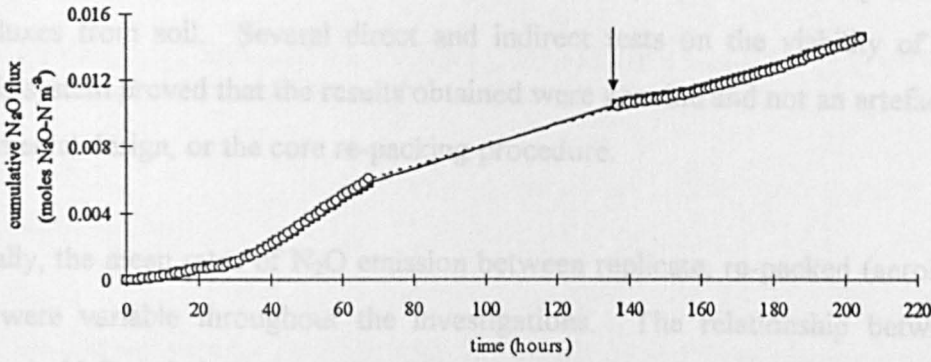


Table 4.11 Mean N₂O emission rates from 20 cores of homogenized aggregates incubated in 2 batches, with and without NO₃⁻ (-NO₃⁻ = 0-67 h; +NO₃⁻ = 134-201 h)

Treatment		Mean rate of N ₂ O emission (x 10 ⁻⁵ moles N ₂ O-N m ⁻² hr ⁻¹)	
		cores 1-10	cores 11-20
-NO ₃ ⁻ (0-30 hours)	batch mean	3.07	3.01
	(SD)	(0.32)	(0.31)
(30-67 hours)	batch mean	13.38	14.10
	(SD)	(0.57)	(0.62)
+NO ₃ ⁻ (134-201 hours)	batch mean	6.08	6.20
	(SD)	(0.79)	(0.62)

Table 4.12 Mean N₂O emission rates from 20 cores of slurried Wick soil incubated individually with and without NO₃⁻ (-NO₃⁻ = 67-134 h; + NO₃⁻ = 201-268 h).

N ₂ O emission flux (x10 ⁻⁵ moles N ₂ O-N m ⁻² h ⁻¹)					
core number	- nitrate	+ nitrate	core number	- nitrate	+ nitrate
1	6.87	6.46	11	6.93	6.67
2	7.18	6.74	12	7.54	7.07
3	6.80	5.86	13	7.14	6.94
4	8.27	7.46	14	7.09	6.70
5	7.21	6.39	15	6.48	5.99
6	7.19	6.74	16	6.76	6.25
7	6.48	6.15	17	6.18	5.92
8	6.84	6.37	18	6.25	6.12
9	6.52	6.13	19	6.62	6.17
10	6.62	6.15	20	6.47	6.10
mean (SD)	7.00 (0.52)	6.45 (0.45)	mean (SD)	6.75 (0.43)	6.39 (0.41)

4.6 CONCLUSIONS

The automated soil headspace gas analyser proved successful in accurately determining N₂O fluxes from soil. Several direct and indirect tests on the viability of the gas analysis system proved that the results obtained were genuine and not an artefact of the experimental design, or the core re-packing procedure.

Generally, the mean rates of N₂O emission between replicate, re-packed (aerobic) soil cores were variable throughout the investigations. The relationship between the increase in N₂O emission rate with aggregate size and moisture content, was masked by the variability between replicate chambers. However, relative to N₂O, there was virtually no difference between mean CO₂ emissions from replicate chambers, from different aggregate sizes or when the soil was amended with NO₃⁻. Thus, despite the variable nature of N₂O emissions, the replicate cores containing the Wick soil series appeared very consistent in terms of microbial activity.

The variability in N₂O emission rates was most probably related to the heterogeneous distributions of organic residues leading to localized concentrations of NO₃⁻ and available organic carbon, within and between the aggregates. The identification of *discrete faunal residues* as the source of very high N₂O emission and the fact that NO₃⁻ addition stimulated N₂O emission, supports this theory. However, in contrast to N₂O, CO₂ emission rates were not profoundly affected by the DFR, which strongly suggests that the mechanism involved in variable denitrification rates was due to an effect on local conditions, rather than stimulation of microbial activity *per se*.

Denitrification was apparently the primary mechanism for N₂O production, as N₂O emission rates generally increased with NO₃⁻ addition, aggregate size and soil moisture content. Both water and increasing aggregate volume impedes O₂ diffusion, thus inducing anaerobic conditions.

Chapter 5: Effect Of Faunal Residues On N₂O Flux

5.1 EFFECT OF DISCRETE FAUNAL RESIDUES ON N₂O FLUX UNDER UNSATURATED AND SATURATED CONDITIONS

5.1.1 Introduction

One of the prerequisites for denitrification is a supply of readily available carbon (Tate, 1995). Considerable work has been undertaken involving the effects of different carbon substrate concentrations on denitrification (Weier *et al.*, 1993). Generally, these studies involve soil amendment with glucose (Bowman and Focht, 1974; Seech and Beauchamp, 1988; Dendooven and Anderson, 1995), but other workers have introduced suspensions of dead microbes (Christensen *et al.*, 1990 b), vegetative matter (Aulakh *et al.*, 1991) and cattle slurry (Egginton and Smith, 1986; Hansen *et al.*, 1993), to observe the effects on denitrification. However, there has been very little research into the effects of faunal residues on N₂O emissions from soil. It was found in a previous investigation (section 4.5) that the decaying remains of an Earthworm was responsible for extremely high N₂O emission rates in an aggregated, aerobic soil. The following section investigates the effect of adding dead Earthworms to the N₂O emission rates from both unsaturated and saturated soil.

5.1.2 Method

5.1.2.1 Unsaturated soil conditions

Six cores (diameter 5.2 cm and height 5.5 cm) were re-packed with 100 g of the Wick series soil (< 2 mm diameter). The base of each plastic core was sealed with polythene and secured with PVC tape, to permit gaseous emission from the soil surface only. Prior to core re-packing, the water content of the soil was adjusted (as necessary) to

75 % field capacity and pre-incubated at 15 °C for 72 hours, to achieve isothermal conditions. During the re-packing process, 3 cores were randomly selected and discrete faunal residues (DFR) were placed in each core at half the soil depth. The DFRs were dead Earthworms (section 2.3) of different weights (W1: 0.45 g; W2: 0.83 g; W3: 1.85 g). The remaining 3 cores were left unamended to act as a control (C1,C2,C3). Each of the 6 cores was individually incubated (section 2.1.7) for about 40 days with periodic sampling of the soil headspace gas and manual analysis of N₂O and CO₂ concentrations. Following each period of incubation, each chamber was vented to re-establish ambient atmospheric concentrations. At the end of the incubated period NO₃⁻ and NH₄⁺ concentrations within all the soil cores were determined (section 2.2.4.5).

5.1.2.2 Saturated soil conditions

The same procedure was used to determine the effect of faunal residues under saturated conditions. However, once the soil was pre-incubated at 15 °C for 72 hours and re-packed into 6 cores (3 controls and 3 amended with dead Earthworms: W1: 0.44 g; W2: 0.79 g; W3: 1.78 g), the soil cores were amended with de-ionized water (at 15 °C) before individual incubation. Sufficient water was added to fully saturate the soil cores, such that the surface was covered with 2-3 mm water.

5.1.3 Results and discussion

Neither the unsaturated or saturated soil cores were amended with nitrate at any point in the investigation. The gaseous emission rates presented in tables 5.1 and 5.2, were derived from the gradient of the cumulative emission calculated using regression analysis.

5.1.3.1 Unsaturated soil conditions: DFR treated and unamended soil cores

There was a significant difference in N₂O emission rates between the unsaturated DFR amended and unamended soil cores, the two treatments differed by 2-3 orders of magnitude (Fig. 5.1 a; table 5.1). Similarly, Aulakh *et al.*, (1991) and Christensen *et al.*, (1990 a) found differences of up to 2 orders of magnitude in N₂O emission rates from unsaturated soil amended and unamended with plant residues (see Appendix; no. 1 and 3). In this investigation the unamended cores (at 75 % F.C.) emitted N₂O at rates comparable to those observed in soils of similar moisture contents in earlier investigations (section 4.3). The N₂O emission rates from the unamended cores followed no apparent trend and were distinctly variable; however, this was negligible when compared to the rates of N₂O emissions from the DFR-amended cores.

In contrast to N₂O, the trend in CO₂ emission rates from both unamended and DFR amended unsaturated cores, were essentially constant throughout the investigation (Fig. 5.2 a; table 5.2). There was little variability in CO₂ emission rates from the unamended cores.

Unsaturated soil conditions: General effect of DFR treatments

The N₂O emission rates from the 3 DFR amended cores all followed a similar trend (Fig. 5.1 a; table 5.1); there was an initial 23 hour lag period prior to a sharp increase in N₂O emission rate over the next 98 hours, whereupon the rate declined but remained relatively constant for the remaining incubation period (121-960 h). The 23 hour time-lag was probably due to the time taken for the development of anaerobic conditions around the DFR or the *de-repression* of the reduction enzyme system (Dendooven and Anderson, 1995). The pattern of CO₂ production rates (Fig. 5.2 a; table 5.2) suggest that the lag time was not due to inhibition of microbial biomass activity during this period. The sharp increase in the N₂O emission rate from the DFR treated cores (23-121 h), by up to 3 orders of magnitude, and subsequent decline (121-960 h), is a similar trend to that reported by Aulakh *et al.*, (1991) and that found for the core containing the DFR described in section 4.3. However, the rate of N₂O emission from

the DFR containing core described in section 4.3 was substantially higher than the corresponding DFR-amended cores in this investigation, due to a higher soil water content and NO₃⁻ concentration.

The N₂O emission rates for each of the DFR amended aerobic cores (Fig. 5.1a), was fairly constant for the remaining incubation period (121-988 hours), and significantly greater than the N₂O emission rates from the unamended cores. The enhancement of N₂O emission rates with DFR amendment, supports the earlier finding that the DFR discovered in section 4.3, was responsible for the large rates of emission from one core.

Unsaturated soil conditions: Effect of increasing DFR mass on gaseous emissions

Throughout the incubation period, there was an apparent large increase in N₂O emission rate with increasing mass of DFR in unsaturated, aerobic soil (Fig. 5.1 a; table 5.1). This could simply be the result of increased amounts of C and N organic compounds and/or the increase in associated anaerobic volume. The CO₂ emission rates also appeared to increase with increasing mass of DFR (Fig. 5.2 a; table 5.2), but the increase was relatively small compared with the large increase in N₂O emissions. This suggests therefore, that DFR amendment imposed a *local* conditions effect within the unsaturated, aerobic soil that promoted denitrification. Similarly, Aulakh *et al.*, (1991) reported that the decomposition of a low C:N ratio legume residue, in an unsaturated soil, apparently increased denitrification through localized microbial activity.

Unsaturated soil conditions: residual N-concentration

The determination of NO₃⁻ and NH₄⁺ in each of the 6 unsaturated cores revealed significant changes in their concentration after incubation (table 5.3). Very little residual NH₄⁺ was present in any of the soil cores, suggesting that NH₄⁺ was probably nitrified as soon as it became available in the soil. Therefore ammonification was the rate limiting step for N₂O production in these aerobic soils. The unamended cores had

lower NO₃⁻ concentrations than those amended with DFRs; residual soil NO₃⁻ concentration also appeared to increase with increasing mass of DFR. (table 5.3).

5.1.3.2 Saturated soil conditions: DFR treated and unamended soil cores

The N₂O emission rates from the saturated cores are shown in Fig. 5.1 b and table 5.1. The saturated DFR amended cores also possessed 3 contrasting rates of N₂O emission over the incubation period. There was a substantial increase in N₂O emission rate (one order of magnitude) after 24 hours incubation for a period of 99 hours, whereupon the N₂O emission rate declined sharply. From 123 hours to the end of the incubation period, the soil apparently began to act as a sink and absorb N₂O from the ambient atmospheric pool.

There was an initial 24 hour lag period in the saturated unamended cores prior to the large increase in N₂O emission rate. The N₂O emission rate then remained relatively stable up to about 650 hours, whereupon it started to slowly decline. The N₂O emission rates from the saturated, unamended cores, were at least 1000 times greater than the corresponding unsaturated cores and about a factor of 10 greater, than the unsaturated DFR amended cores (table 5.1) in all but the initial 24 hour period. During the initial 24 hours the N₂O emission rates from the DFR amended saturated cores were 2-3 orders of magnitude greater, than the unamended controls. However, between 24 and 123 hours the difference reduced to about a factor of 4 (table 5.1). During the remaining incubation period (123-988 h), the unamended N₂O emission rates were about 1000 times greater than the DFR amended cores. These findings suggest that the rates of denitrification are limited in the unamended cores by the supply of available carbon, through the low but constant, mineralization of native soil organic matter. The DFR amended cores have enhanced N₂O emission due to the additional supply of different mineralizable organic carbon. Hence, the supply of available carbon whether native or amended, is a major factor influencing denitrification rates, especially in O₂ restricted soils, until the NO₃⁻ supply is exhausted.

It also appears that differences in organic matter composition lead to differences in denitrification and respiration rates.

Saturated soil conditions: General effect of DFR treatments

The dramatic reduction in N₂O emission rate from the saturated DFR amended cores after 123 hours may have been influenced by the increasing anoxic conditions, facilitated by the DFR, reducing any available NO₃⁻ to N₂. This suggestion is supported by the CO₂ data (Fig 5.2 b; table 5.2), which indicates considerably greater microbial activity in the DFR amended cores; emission rates from the DFR amended cores were double that from the unamended core rates. However, both the DFR amended and unamended cores respectively possess relatively constant emission rates throughout the duration of the incubation period, indicating stable microbial activity. The increased CO₂ rate may be due to the development of anaerobic fermenting microbes. The CO₂ emission rates from the saturated unamended cores are essentially the same as the unsaturated DFR amended and unamended cores.

N₂O emission rate increased with mass of DFR over the initial 123 hours in saturated conditions. However, this trend was not observed during the rest of the incubation period (123-960 hours) with all three DFR treated cores emitting little N₂O. The N₂O emissions from the three saturated unamended replicate cores were very similar to one another and throughout the total incubation period. The saturation of the cores eradicated any effect of a denitrification hotspot, which were prominent in the unsaturated replicates.

The total amount of N₂O emitted became proportionally less with increasing DFR mass, in both the unsaturated and saturated state, as a result of the decrease in DFR surface area relative to the total volume.

Saturated conditions: residual N-concentration

The determination of the NO_3^- and NH_4^+ concentrations of the saturated cores after the incubation period support earlier suggestions that the conditions within the DFR amended cores are very anaerobic (table 5.3). There was no apparent NO_3^- in the DFR amended cores, but there was considerable amounts of NH_4^+ which tended to increase with increasing mass of DFR. This shows that there was substantial mineralization of the DFR but no nitrification taking place. In the unamended saturated cores there was still NO_3^- present in the soil and was probably that remaining from the native NO_3^- concentration. The slightly enhanced NH_4^+ concentration in the unamended cores was probably derived from the ammonification of native soil organic matter, but due to the anoxic state of the soil this was not oxidised to NO_3^- .

Figure 5.1 Cumulative N_2O flux from soil cores re-packed with aggregates of the Wick series soil (< 2 mm diameter) at (a) 75 % F.C. and (b) under saturated conditions. Three cores are amended with dead Earthworms (W1, W2, W3) and three are unamended controls (C1, C2, C3).

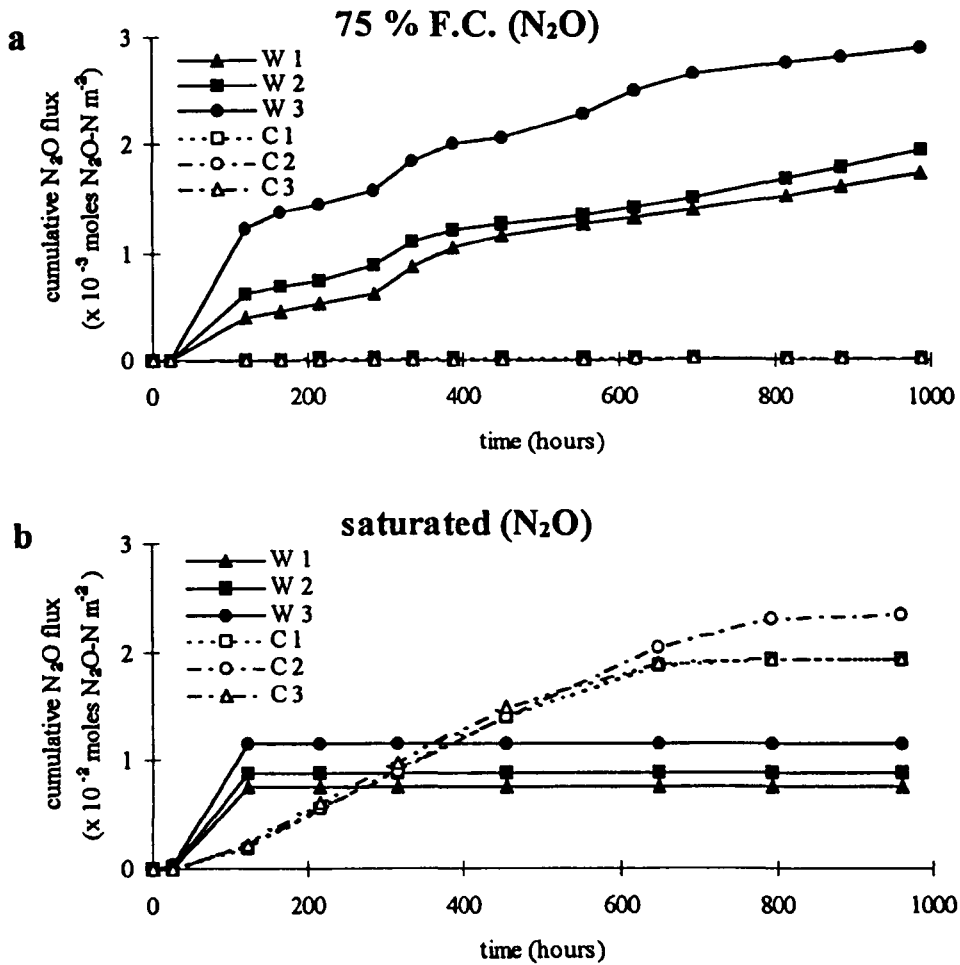


Figure 5.2 Cumulative CO_2 flux from soil cores re-packed with aggregates of the Wick series soil (< 2 mm diameter) at (a) 75 % F.C. and (b) under saturated conditions. Three cores are amended with dead Earthworms (W1, W2, W3) and three are unamended controls (C1, C2, C3).

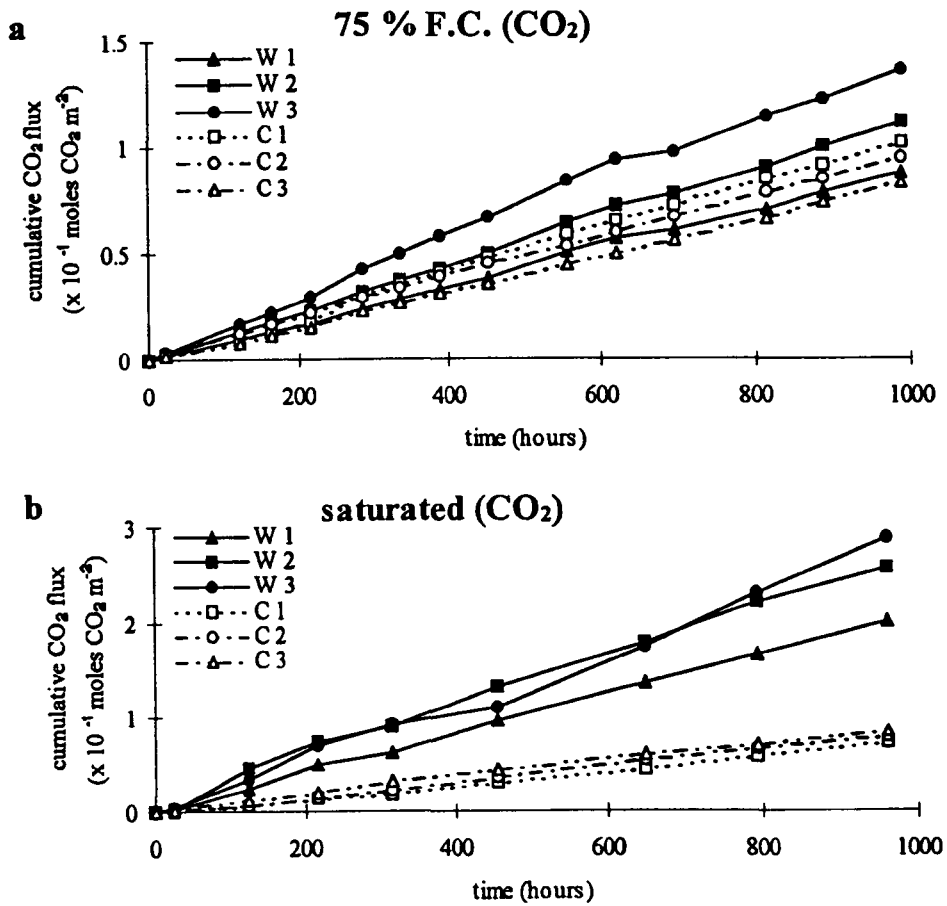


Table 5.1 Mean N₂O emission rates from cores re-packed with Wick series soil (< 2 mm diameter aggregates) at 75 % F.C.. Three cores were amended with dead Earthworms (W1, W2, W3) and three were unamended (C1, C2, C3).

Mean N ₂ O emission rate (x 10 ⁻⁷ moles N ₂ O-N m ⁻² h ⁻¹)						
unsaturated						
time (hours)	W1	W2	W3	control C1	control C2	control C3
0-23	0.05	0.32	0.84	-0.05	0.11	0.46
23-121	40.10	62.0	124.6	0.11	0.04	-0.03
121-988	15.77	14.97	20.53	0.21	0.14	0.25
saturated						
0-24	27.4	91.8	137.0	0.25	1.53	1.37
24-123	749.0	867.0	1120	189	191	215
123-960	0.15	-0.53	-0.22	216	273	211

Table 5.2 Mean CO₂ emission rates from cores re-packed with Wick series soil (< 2 mm diameter aggregates) at 75 % F.C.. Three cores were amended with dead Earthworms (W1, W2, W3) and three were unamended (C1, C2, C3).

Mean CO ₂ emission rate (x 10 ⁻⁴ moles CO ₂ m ⁻² h ⁻¹)						
unsaturated						
time (hours)	W1	W2	W3	control C1	control C2	control C3
0-23	0.81	1.10	1.37	0.82	1.02	0.69
23-121	0.81	1.00	1.34	0.84	1.00	0.72
121-988	0.90	1.14	1.38	1.06	0.94	0.86
saturated						
0-24	0.80	1.00	1.80	-0.19	0.95	1.08
24-123	2.16	4.45	2.91	0.61	0.32	0.88
123-960	2.03	2.52	2.93	0.79	0.89	0.85

Table 5.3 Concentration of NO₃⁻-N and NH₄⁺-N in 6 soil cores re-packed with aggregates of the Wick series (< 2 mm diameter) that were treated with (W1, W2, W3) and without (C1, C2, C3) dead Earthworms under saturated and unsaturated conditions after 40 days incubation.

Concentration of NO ₃ ⁻ -N and NH ₄ ⁺ -N (moles N m ⁻³ soil)				
treatment	unsaturated soil		saturated soil	
	NO ₃ ⁻ -N	NH ₄ ⁺ -N	NO ₃ ⁻ -N	NH ₄ ⁺ -N
W1	0.15	0	0	0.94
W2	0.20	0	0	1.93
W3	0.32	0	0	3.66
C1	0.09	0	0.12	0.15
C2	0.10	0	0.08	0.15
C3	0.10	0	0.10	0.15

(The ambient level of NO₃⁻ and NH₄⁺ in the soil prior to both saturated and unsaturated incubations was 1.93 and 0.04 moles N m⁻³ soil respectively.)

5.1.2 Method

Sub-samples (500 g) of Wick series soil (< 2 mm diameter aggregates) were re-packed into 24 cores (7.0 cm diameter and 13.0 cm in height), which were each fitted with a water access tube and manometer (section 2.2.2). Prior to core re-packing, the soil was pre-incubated at 15 °C for 72 hours, to achieve isothermal conditions and the soil water content adjusted to 75 % F.C. with distilled water (at 15 °C). The 24 cores were split into four equal groups; three of these were amended with DFRs and one group remained as a control. Two of the amended groups were amended with a total DFR mass of 1.0 g (W1) or 2.0 g (W2) respectively; each mass was split into two portions and located at depths of approximately 3 cm and 9 cm from the soil surface. The third treatment (W3) consisted of a DFR mass of 2.0 g positioned at a single depth of 3 cm from the core surface (the experimental configuration is schematically represented in Fig. 5.3). All 24 cores were individually incubated for a total of 37 days; the chamber atmosphere was regularly sampled to determine changes in N₂O and CO₂ concentration, via manual analysis (section 2.1.7). After an initial 7 day incubation, the cores were brought up to 100 % F.C. using a

5.2 EFFECT OF DISCRETE FAUNAL RESIDUES AND FLUCTUATING WATER TABLE ON N₂O FLUX

5.2.1 Introduction

In section 5.1 it was shown that the addition of DFRs to both saturated and unsaturated soil cores significantly affected the N₂O emission rate. This investigation is an expansion on the previous theme and looks at the effect of raising and lowering the water table on N₂O emission from soil, treated with variable amounts of DFR and with or without added NO₃⁻. Work has already been done to study the effect on denitrification of factors such as soil carbon content (Bowman and Focht, 1974), soil NO₃⁻ concentration (Blackmer and Bremner, 1978) and soil water content (Linn and Doran, 1984). However, work on the effect of combining these factors is limited.

5.2.2 Method

Sub-samples (500 g) of Wick series soil (< 2 mm diameter aggregates) were re-packed into 24 cores (7.0 cm diameter and 13.0 cm in height), which were each fitted with a water access tube and manometer (section 2.2.2). Prior to core re-packing, the soil was pre-incubated at 15 °C for 72 hours, to achieve isothermal conditions and the soil water content adjusted to 75 % F.C. with distilled water (at 15 °C). The 24 cores were split into four equal groups; three of these were amended with DFRs and one group remained as a control. Two of the amended groups were treated with a total DFR mass of 1.0 g (W1) or 2.0 g (W2) respectively; each mass was split into two portions and located at depths of approximately 3 cm and 9 cm from the soil surface. The third treatment (W3) consisted of a DFR mass of 2.0 g positioned at a single depth of 3 cm from the core surface (the experimental configuration is schematically represented in Fig. 5.3). All 24 cores were individually incubated for a total of 37 days; the chamber atmosphere was regularly sampled to determine changes in N₂O and CO₂ concentration, via manual analysis (section 2.1.7). After an initial 7 day incubation, the cores were brought up to 100 % F.C. using a

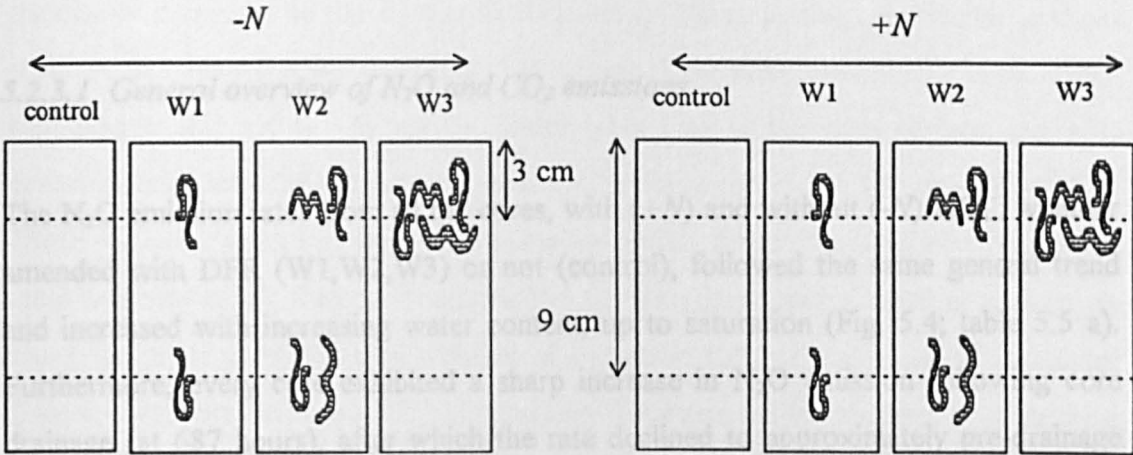
syringe to apply water evenly across the soil surface; half the cores (3) in each of the 4 groups were amended with distilled water alone (-N), while the remaining 3 cores in each group were amended with a KNO₃ solution (+N), equivalent to 150 kg NO₃⁻-N ha⁻¹. Once treated, the cores were incubated for a further 7 days. The soil water table was then sequentially raised to 1/2 way up the core and then to the core surface, followed by a drainage event which lowered the water table to approximately zero height. All these changes in water content were interspersed with a 7 day incubation period (the timing of each event is shown in table 5.4). The water table was raised and lowered using the water access tube and the height of the water table was determined with the attached manometer (section 2.2.2). At the end of the incubation the soil was analysed for both NO₃⁻ and NH₄⁺ concentrations (section 2.2.4.5).

Determination of N₂O trapped in soil water

Test tubes (20 cm³) were purged with high purity N₂ and stoppered with gas-tight *Suba-seals*. A 5 cm³ sample of the N₂-atmosphere from each test tube was then extracted with a syringe and replaced with a 5 cm³ sample of the drained water from each core. The water sample was extracted from the access tube, using a syringe, during the lowering of the core water table. This ensured that the water sample had not been exposed to the atmosphere. When the extracted water sample was injected into the test tube, a syringe filter (0.2 µm, cellulose acetate filter paper) was used to remove soil particles. The test tubes containing the water samples were then placed on a shaker for 48 hours (at 15 °C), to establish an equilibrium between the solution and gas phases. A sample of the test tube headspace was extracted with a syringe and manually injected into the GC, for determination of N₂O and CO₂ concentration. The total amount of N₂O and CO₂ in the solution phase was calculated from the equilibrium solution:gas ratio for each gas, calculated using the appropriate Bunsen coefficient, gas pressure and relative volumes of gas and solution (Davidson and Firestone, 1988).

5.2.3 Results and Discussion

Figure 5.3 Schematic of core configurations (described in section 5.2.2) of 2 main treatments, with (+N) and without (-N) NO₃⁻, each treatment contained 4 sub treatments including the control and the 3 DFR amendments (W1 (1.0 g), W2 (2.0 g), and W3 (2.0 g)).



levels. The rate of N₂O emission was also increased by the addition of DFR and NO₃⁻, but the response varied among treatment combinations. The mean rates of N₂O

Table 5.4 Sequence of events applied to each core as described in section 5.2.2 .

time (hours)	water status	Control	W1	W2	W3
0	75 % F.C.	6 replicates	6 replicates	6 replicates	6 replicates
184	100 % F.C (+/- KNO ₃)	3 replicates(+N) 3 replicates(-N)	3 replicates(+N) 3 replicates(-N)	3 replicates(+N) 3 replicates(-N)	3 replicates(+N) 3 replicates(-N)
350	50 % saturation	"	"	"	"
517	100 % saturation	"	"	"	"
687	core drainage	"	"	"	"
888	end of incubation	"	"	"	"

5.2.3 Results and Discussion

The results presented in table 5.5, were derived from regression analysis of gradients of the cumulative emissions illustrated in Figs. 5.4 and 5.5. Gaseous emission rates were compared using analysis of variance.

5.2.3.1 General overview of N₂O and CO₂ emissions

The N₂O emission rates from all the cores, with (+N) and without (-N) NO₃⁻, whether amended with DFR (W1,W2,W3) or not (control), followed the same general trend and increased with increasing water content, up to saturation (Fig. 5.4; table 5.5 a). Furthermore, every core exhibited a sharp increase in N₂O emission following core drainage (at 687 hours), after which the rate declined to approximately pre-drainage levels. The rate of N₂O emission was also increased by the addition of DFR and NO₃⁻, but the response varied among treatment combinations. The mean rates of N₂O emission from the control, W1 and W2 treatments were significantly different ($P < 0.05$) in both -N and +N treated soils.

In contrast to N₂O, there was relatively little variation in CO₂ emission rates with increasing soil water content (Fig. 5.5; table 5.5 b). However, there was a small increase in CO₂ emission rate in all cores, regardless of treatment, when the soil cores were drained. The rates of CO₂ emission increased with DFR addition, (control<W1<W2), up to 50 % core saturation. Generally, there was good agreement between replicate emission rates in each of the treatments for both gases (N₂O and CO₂).

5.2.3.2 Effect of soil water content on N₂O emission

The positive effect of increasing soil water content on N₂O emission from the treated cores is illustrated in Fig. 5.4. The rates of N₂O emission were considerably greater (up to 3 orders of magnitude in the case of the control treatment) under fully saturated conditions compared to the soils at field capacity. These findings are similar to those reported in section 5.1 and comparable to reports in the literature (Aulakh *et al.*, 1991; Bandibas *et al.*, 1994). When the water table was at the core surface, the N₂O emission rates from all treatments were similar (between 3-4 x 10⁻⁵ mol N m⁻² h⁻¹). These N₂O emission rates were approximately double those measured when the water table was only at half the core depth (table 5.5). This could be the result of an increase (by a factor of 2) in the total volume of anaerobic soil, or the result of a reduced distance between the saturated (N₂O-emitting) zone and the soil surface; thus reducing the likelihood of further reduction to N₂ prior to N₂O emission.

There was a rapid, short-term increase in N₂O emission rate in all the cores, by one order of magnitude, during the 24 hour period following the single drainage event (at 685 hours; Fig. 5.4). The N₂O flux at this time was between 1-5 x 10⁻⁴ moles N m⁻² h⁻¹. Due to the short time scale over which the increase in N₂O rate occurred, it seems unlikely that the rapid flux was the result of any change in microbial population or activity. The short lived rapid increase in N₂O emission rate was probably the result of aggregate *de-gassing*. Aggregate *de-gassing* may occur when the N₂O accumulation that occurs within aggregates under saturated conditions, rapidly diffuses into the (drained) *inter-aggregate* transmission pores when the water table is lowered. As the *inter-aggregate* pore space is no longer impeded by water, the N₂O in the *inter-aggregate* pores quickly diffuses through the air phase of the soil to the atmosphere, appearing as a rapid N₂O flux.

This process may have important implications in areas where land is frequently subjected to a fluctuating water table or intermittent flooding. In such areas it is likely that a far greater amount of N₂O may be emitted to the atmosphere, than in a

comparable aerobic soil. This may be a contributory factor to the N₂O *pulsing effect* observed during frequent rainfall (Corre *et al.*, 1995).

5.2.3.3 Effect of soil water content on CO₂ emission

The change in water content had little effect on CO₂ emission rates which, apart from the period immediately following core drainage, remained between 2-6 x 10⁻⁴ moles CO₂ m⁻² h⁻¹ (Fig. 5.5; table 5.5 b); this is similar to rates reported in previous sections (sections 4.4, 5.1). In contrast to N₂O, the CO₂ emission rates only increased slightly, when the soil water content was brought up to 100 % F.C., probably as a consequence of stimulating the aerobic microbial population. However, there were small reductions in the CO₂ emission rate from all cores when the water table was raised to 50 % of the core height and again when the cores were fully saturated, probably due to the impedance of CO₂ diffusion in water filled pores. There would also be a progressive suppression of the aerobic microbial population with a rise in soil water table.

As for the trend in N₂O emissions, there was a short lived (24 hours), increase in CO₂ emission rate from all cores when they were drained, whereupon they resumed their previous emission rates. The temporary increase (a factor of 3-5) was probably the result of the rapid diffusion from saturated aggregates via air-filled *inter-aggregate* pores. Relative to N₂O, it appears that aggregate *de-gassing* had a lesser effect on CO₂ emission. This may have been the result of greater CO₂ solubility in the soil solution, hence diffusion of CO₂ was less restricted by water filled *inter-aggregate* pores. CO₂ has a greater Bunsen absorption coefficient (1.0; Heys, 1966) than N₂O (0.74; Tiedje, 1982) at 15 °C. Furthermore, CO₂ in the soil solution exists not only as CO₂, but also in a hydrolysed dissociated form (e.g. HCO₃⁻, carbonic acid). Consequently the impact of draining the soil was less than it was on N₂O emission rates.

Figure 5.4 Cumulative N₂O flux from cores re-packed with aggregates from the Wick series soil (< 2 mm diameter) which were treated with DFR (W1,W2,W3) under variable soil water contents denoted as steps 1, 2, 3 and 4. a = unamended (-NO₃⁻) and b = amended (+NO₃⁻) with KNO₃.

1 = soil core at 100 % F.C.

2 = water table at half core depth

3 = water table at core surface

4 = core drained

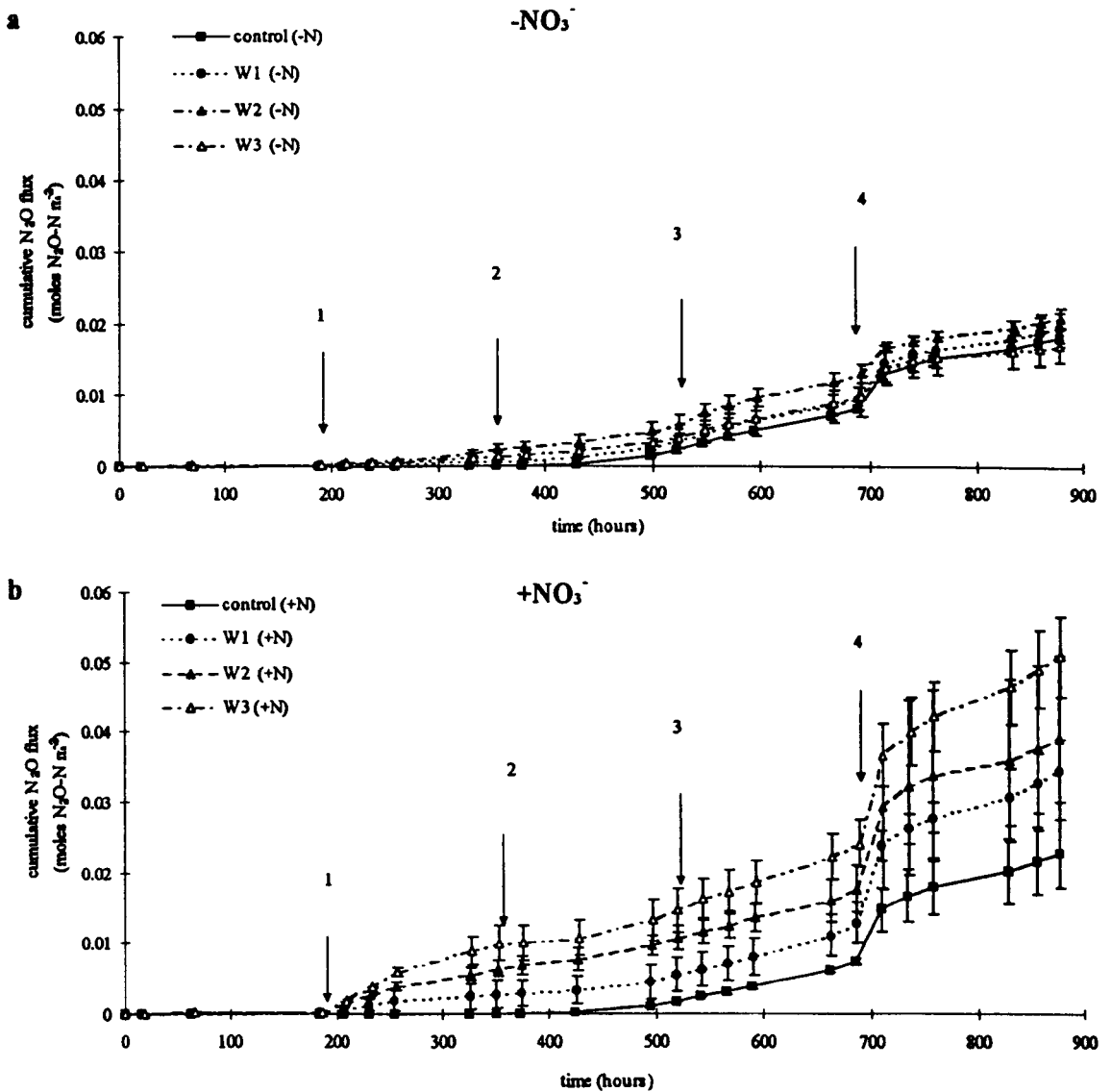


Figure 5.5

Cumulative CO_2 flux from cores re-packed with aggregates from the Wick series soil (< 2 mm diameter) which were treated with DFR (W1, W2, W3) under variable soil water contents denoted as steps 1, 2, 3 and 4. a = unamended ($-NO_3^-$) and b = amended ($+NO_3^-$) with KNO_3 .

1 = soil core at 100 % F.C.

2 = water table at half core depth

3 = water table at core surface

4 = core drained

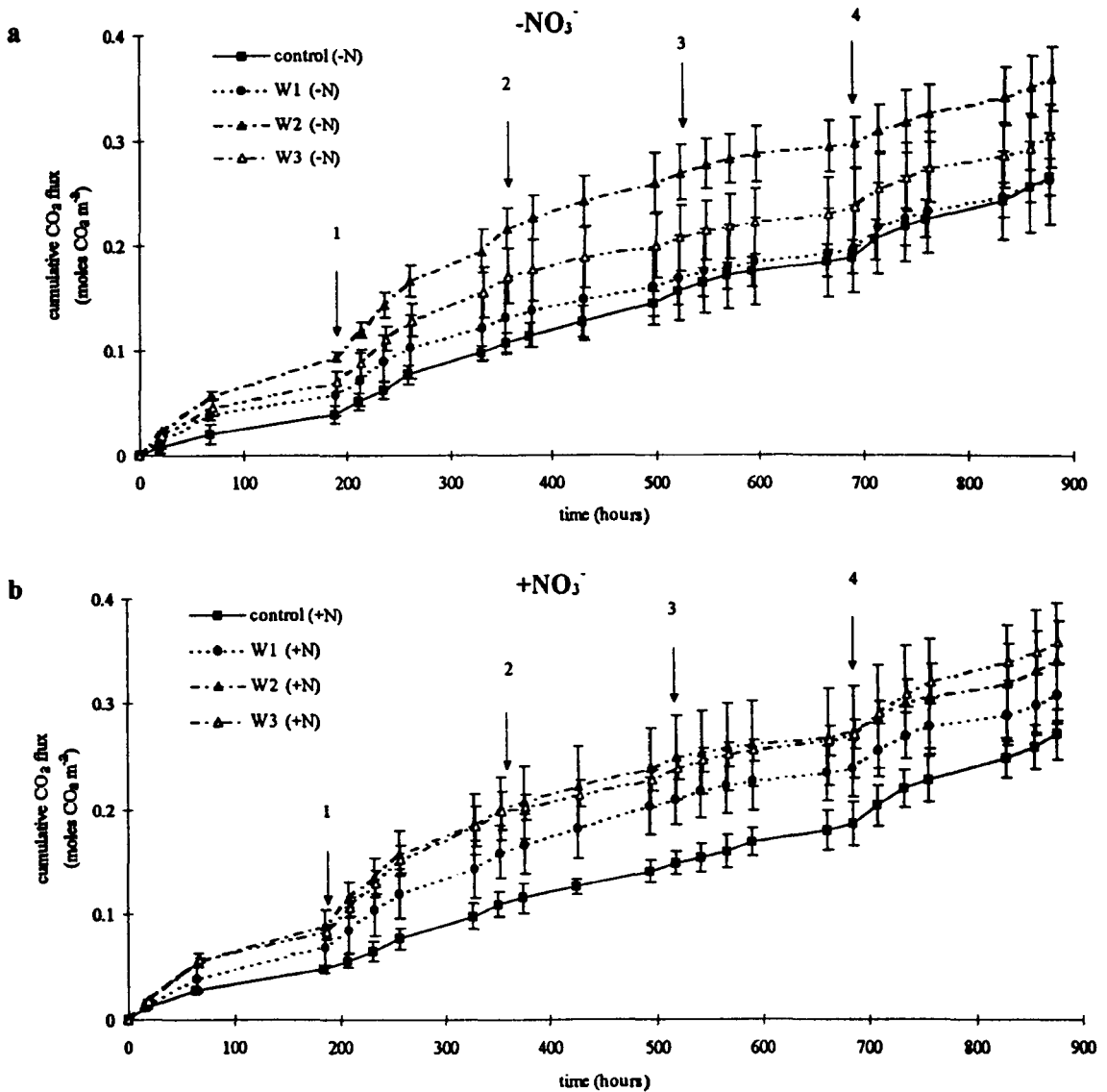


Table 5.5 Mean emission rates of (a) N₂O and (b) CO₂ from cores treated with and without both DFR (W1,W2,W3) and NO₃⁻ amendments during sequential raising and lowering of the soil water content. (Standard deviation in brackets).

a		N ₂ O flux rate (x 10 ⁻⁷ moles N ₂ O-N m ⁻² h ⁻¹)							
		without nitrate				with nitrate			
Time (h)		control	W1	W2	W3	control	W1	W2	W3
0-184		0.32	5.88	12.58	6.42	0.21	8.19	13.40	11.37
	75 % F.C.	(0.19)	(2.38)	(3.31)	(3.05)	(0.21)	(4.15)	(5.03)	(5.13)
184-350		1.45	28.39	122.35	72.60	0.965	149.3	344.7	579.3
	100 % F.C.	(0.82)	(14.03)	(33.95)	(39.76)	(0.19)	(109)	(67.39)	(167.8)
350-517		129.3	163.7	200.6	153.2	89.6	151.5	258.0	279.3
	1/2 SAT	(26.68)	(25.9)	(45.67)	(60.44)	(2.18)	(64.96)	(49.48)	(40.32)
517-685		336.4	354.8	397.1	332	345.6	440.4	407.4	552.7
	full SAT	(3.51)	(41.95)	(35.87)	(79.53)	(15.2)	(73.5)	(121.2)	(86.35)
685-709		2118	2138	1565	1705	3110	4675	5023	5559
	drained	(322.1)	(380.5)	(269.7)	(648.6)	(1272)	(363)	(3678)	(634.5)
709-876		296.7	292.3	244.69	182.6	444.6	586	526.9	793.5
	drained	(29.52)	(43.74)	(67.89)	(17.95)	(96.19)	(200)	(29.77)	(84.17)

b		CO ₂ flux rate (x10 ⁻⁴ moles CO ₂ m ⁻² h ⁻¹)							
		without nitrate				with nitrate			
Time (h)		control	W1	W2	W3	control	W1	W2	W3
0-184		2.19	3.42	5.36	4.07	2.74	3.98	5.25	4.96
	75 % F.C.	(0.56)	(1.08)	(0.23)	(0.57)	(0.16)	(1.03)	(0.79)	(0.31)
184-350		3.89	4.13	6.82	5.69	3.63	5.06	6.19	6.49
	100 % F.C.	(0.11)	(1.07)	(0.91)	(1.05)	(0.54)	(0.50)	(1.03)	(0.74)
350-517		2.85	2.15	3.08	2.16	2.33	3.07	2.90	2.37
	1/2 SAT	(0.36)	(0.24)	(0.58)	(0.34)	(0.34)	(0.14)	(0.62)	(0.44)
517-685		1.79	1.59	1.53	1.62	2.16	1.58	1.35	1.81
	full SAT	(0.34)	(0.13)	(0.13)	(0.45)	(0.57)	(0.21)	(0.47)	(0.23)
685-709		7.55	8.72	5.36	7.66	7.38	7.23	6.19	8.71
	drained	(1.48)	(0.95)	(0.81)	(1.30)	(0.92)	(0.87)	(2.16)	(1.98)
709-876		3.48	2.73	2.88	2.75	3.73	2.78	2.84	3.69
	drained	(0.37)	(0.90)	(0.66)	(0.32)	(0.73)	(0.73)	(0.54)	(0.54)

From first principles, an approximate value can be attributed to the amount of CO₂ as a proportion of the total carbonate in solution (T_c), assuming the Wick series soil has a pH 5.7 (section 2.2.3); where

$$T_c = [CO_2] + [HCO_3^-] + [H_2CO_3] + [CO_3^{2-}].$$

Therefore, from first principles;

$$\frac{CO_2}{T_c} = \frac{1}{1 + \frac{1}{Kh} + \frac{k1}{Kh(H^+)} + \frac{k1k2}{Kh(H^+)^2}}.$$

where $Kh = (CO_2/H_2CO_3)$; $k1 = (H_2CO_3)$; $k2 = (HCO_3^-)$.

$$\frac{CO_2}{T_c} = \frac{1}{1 + (1.67 \times 10^{-3}) + (0.209) + 5.86 \times 10^{-6}}$$

hence,

$$\frac{CO_2}{T_c} = \frac{1}{1.211} = 0.83$$

At pH 5.7, 83 % of the total carbonate in solution exists as CO₂, while the remaining 17 % exists in other hydrolysed forms.

5.2.3.4 Effect of DFR incorporation on N₂O emission

The rates of N₂O emission from soil cores were greatly enhanced with the incorporation of DFR (Fig. 5.4; table 5.5 a). The N₂O emission rates from the controls (no DFR) were subtracted from those of the DFR treatments (W1 and W2), for both NO₃⁻ amended and unamended cores, to clarify the effect of DFR amendment on N₂O emission rates (Fig. 5.6 a, b).

The incorporation of DFR in the soil, positively affected N₂O emission rates in all cores, under bulk aerobic conditions (75 % and 100 % F.C.), (Fig. 5.6 a, b). At 100 % F.C., the mean rates of N₂O emission from the 2 sets of controls (no DFR), only marginally increased and were about 1-2 orders of magnitude lower than the respective DFR treated cores (Fig. 5.4); in the case of (W2, +N) the mean N₂O emission rate was 3.5×10^{-5} moles N m⁻² h⁻¹, but only 9.7×10^{-8} moles N m⁻² h⁻¹ for the control (table 5.5 a). The ratio between N₂O emission rates of the control and the DFR treatments under the different soil water contents, is shown in Fig. 5.7. It reveals that the influence of DFR was greatest under bulk aerobic conditions (75 % and 100 % F.C.). Similar findings were reported by Aulakh *et al.*, (1991) in a comparison of control soils and soils amended with plant residues. It is likely that the DFR imposed a local demand for O₂ due to intense microbial activity, suggesting that N₂O production was primarily limited by availability of O₂. The N₂O emission rate in both NO₃⁻ amended and unamended states increased with increasing mass of DFR (W2 > W1), up to fully saturated conditions; suggesting that N₂O emission rates were limited by both NO₃⁻ and easily metabolizable carbon. Similar findings have been reported in the literature (Rosswall *et al.*, 1989; Aulakh *et al.*, 1991). In addition, mineralization of DFR-nitrogen could lead to an enhanced NO₃⁻ supply through local nitrification under bulk aerobic conditions, thus enhancing N₂O emission rates.

The N₂O emission rates from the different DFR treatments approached similar values when the water table was either at half the core depth or at the soil surface (table 5.5 a). The mean N₂O emission rate for the control, W1 and W2 under fully saturated conditions (with and without NO₃⁻), was between $3.4 - 4.4 \times 10^{-5}$ moles N m⁻² h⁻¹ (table 5.5 a); suggesting that DFR had much less effect on N₂O emission rates in saturated soil. Any local O₂-depleting effect of DFR would become irrelevant by the general increase in denitrification rate of the whole core under saturated conditions. In addition, the restriction imposed on N₂O diffusion by water filled pores, or a change in mineralization rate of the DFR under anoxic conditions, may have contributed this effect. It is shown in Fig. 5.6 (a, b) that after core drainage the DFR treatments had essentially a zero (W1) and a slightly depressive (W2) effect on the N₂O emission rates from the cores not amended with NO₃⁻, whereas in the NO₃⁻ amended cores both the

DFR treatments, had the same positive effect relative to the control. When the cores were drained, the DFR treatments provided conditions that favoured a greater N₂:N₂O ratio, however, this was suppressed by the high NO₃⁻ concentration of the +N treated cores.

N₂O produced from localized zones of intense denitrification (created by DFR) in unsaturated soil can diffuse out of the core unimpeded by water in the *inter-aggregate* pores. The amount of N₂O released from the unsaturated soil, would be emitted 10⁴ faster than an equivalent amount produced under saturated conditions. Additionally, the less time N₂O is retained in the soil, the less susceptible it is to further reduction, to N₂. Consequently, in unsaturated conditions, N₂O emitted from DFR treated cores amended with NO₃⁻, approached emission rates that are usually associated with fully saturated conditions due to the ease of diffusion.

It was clear from these investigations that Earthworms may play an important role in N₂O emission from soil. The contribution by Earthworms to N₂O emissions from soil, via their casts (Elliott *et al.*, 1990; Knight *et al.*, 1992; Parkin and Berry, 1994) and their effect on soil structure (Knight *et al.*, 1992) have been reported in the literature. However, there is no apparent record of the contribution from Earthworm decay, to N₂O emissions from soil. It has been reported in work by Knight *et al.*, (1992), that Earthworm populations can be as large as 500 m⁻², although there have been recordings of even larger populations (Lee, 1985). After periods of heavy rainfall Earthworms leave their flooded channels because of anoxia, or acidification of soil water in their channels, due to dissolved CO₂ (Lee, 1985) and travel towards the soil surface. At the surface, Earthworms may be killed by UV radiation (Lee, 1985). There is therefore a mechanism whereby periodic soil flooding coincides with increased levels of DFR in the topsoil. Hence Earthworm populations could significantly contribute to soil N₂O fluxes during periods of heavy rainfall and account for some of the spatial and temporal variability observed in field N₂O measurements.

Figure 5.7

Ratio of mean N_2O emission rates of control cores and DFR treatments (a) = unamended with ($-NO_3^-$) and (b) = amended ($+NO_3^-$) with KNO_3 . Cores were re-packed with aggregates from the Wick series soil (< 2 mm diameter). Time periods (x-axis) are denoted as steps 1, 2, 3, 4, 5 and 6, where:

1 = soil core at 75 % F.C. (0-184 h)

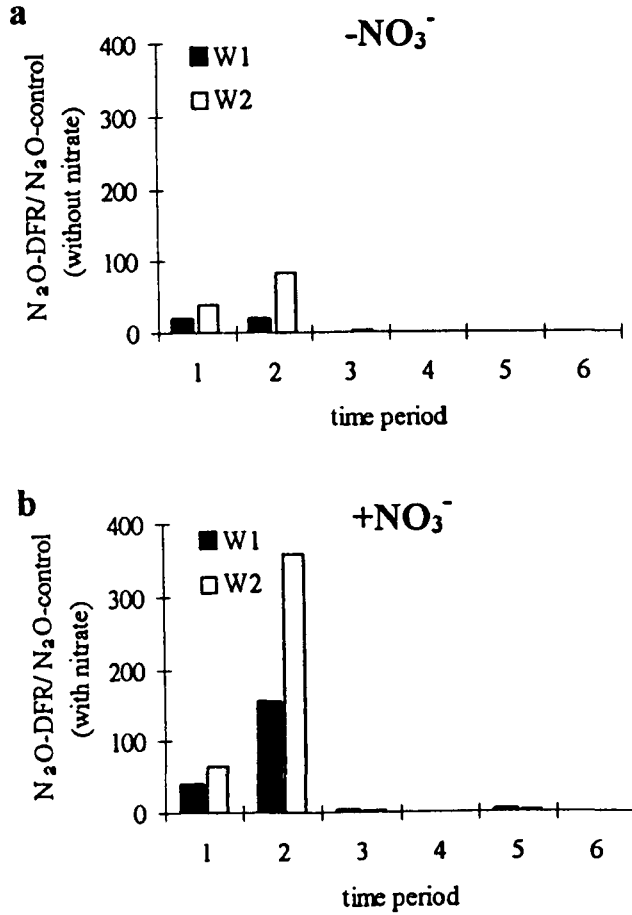
2 = soil core at 100 % F.C. (184-350 h)

3 = water table at 50% core depth (350-517 h)

4 = water table at core surface (517-685 h)

5 = core drained (685-709 h)

6 = core drained (709-876 h)



5.2.3.5 Effect of DFR incorporation on CO_2 emission

Although CO_2 emission rates were relatively unchanged by NO_3^- application, or an increase in water content, there were significant differences ($P > 0.05$) between the DFR treatments in both NO_3^- amended and unamended soil cores, up to the time of core drainage (Fig. 5.5). CO_2 emission rates increased with increasing DFR mass (control < W1 < W2), due to the stimulation of microbes by increased availability of organic carbon. This effect of DFR on CO_2 emission rates was also observed in section 5.1. The net effect of DFR on CO_2 emission rates (W1-control; W2-control) followed the same general trend (Fig. 5.8 a, b). CO_2 emission rates increased up to the point where the water table was raised to half the core height, but the incorporation of DFR appeared to have a slight net depressive effect on CO_2 emission rates after the cores were fully saturated. After the saturated cores were drained, the negative effect of DFR on CO_2 emission rates continued.

5.2.3.6 Effect of DFR position on N_2O emission

It was apparent from Fig. 5.4 (a, b) that in the NO_3^- amended state, W3 emitted more N_2O than W2 throughout the incubation period, regardless of the water table level, whereas the reverse occurred in cores unamended with NO_3^- . To clarify this complicated effect, the cumulative N_2O emission rates from W2 were subtracted from W3 and expressed as a % of the cumulative flux from W3 (Fig. 5.9 a). DFR placed deeper in the core may have less influence on the overall N_2O emission rate, as N_2O produced at depth may be reduced to N_2 during diffusion up the core. N_2O emission rates may therefore be mainly dependent on DFR nearer the soil surface. The greater the DFR mass, the more intense are the localized reducing conditions and the greater the demand for NO_3^- as an electron acceptor. Therefore in the NO_3^- -amended state, more N_2O was emitted in W3 than in W2. Furthermore, in the NO_3^- amended cores, N_2O reduction would be more inhibited by the higher NO_3^- concentration in the surface layers of the soil (Blackmer and Bremner, 1978). The cores without NO_3^- produced greater N_2O fluxes where the DFR was uniformly distributed throughout the volume

(W2). This was probably a consequence of a lower diffusional restriction on the supply of NO_3^- to the DFR under conditions of NO_3^- shortage (-N).

5.2.3.7 Effect of DFR position on CO_2 emission

The cumulative CO_2 flux from W2 was subtracted from the corresponding flux from W3, and expressed as % of the cumulative flux from W3, to demonstrate the effect of DFR positioning on CO_2 emission (Fig. 5.9 b). The relative changes in CO_2 emissions from both NO_3^- amended and unamended treatments were apparently unaffected by changes in water content throughout the incubation period. However, it was clear from the results that there was little difference between the CO_2 emissions of W2 and W3 within the NO_3^- amended cores. In the unamended state, W2 generally emitted significantly more ($P < 0.05$) CO_2 than W3. In the absence of NO_3^- the ratio of CO_2 fluxes remained fairly constant ($W2 > W3$), as suggested by the trend in Fig. 5.9 b, which is parallel to and below the x-axis (time). In the cores not amended with NO_3^- , due to the distribution of DFR, W2 was better able to utilize the supply of native NO_3^- than W3 (Fig. 5.9 b). Therefore, the net rate of denitrification and CO_2 production was greater from W2. However, there was little restriction on NO_3^- availability in cores amended with NO_3^- , therefore the denitrifying population in W2 and W3 were equally stimulated, thus producing similar respiration rates.

5.2.3.8 Effect of NO_3^- application on N_2O and CO_2 emission

It was apparent from Fig. 5.4 (a, b), that NO_3^- amendment clearly affected N_2O emission rates. However, to clarify the effect of NO_3^- addition on cumulative N_2O emission rates, the difference between the respective NO_3^- amended (Fig 5.4 b) and unamended (Fig. 5.4 a) treatments were calculated, the difference is shown in Fig. 5.10 a.

There was little difference between NO₃⁻ amended and unamended control cores (without DFR) as shown in Fig 5.10 a; hence the N₂O emission rates were dependent on both DFR and NO₃⁻ concentration, as suggested earlier. NO₃⁻ amendment (at field capacity) increased N₂O emission rates from all the DFR treated cores (W1, W2, W3), as it obviated any limitation on the supply of anaerobic oxidant. However, the application of NO₃⁻ appeared to have only a limited effect on N₂O emissions from DFR treated cores, when the water table was at half the core depth or at the soil surface (Fig. 5.10 a; table 5.5 a). This was probably the result of the water filled *inter-aggregate* pores alleviating the limitation on the supply of anaerobic oxidant, in the cores not amended with NO₃⁻. Additionally, the change in the mineralization rates of DFR under anaerobic conditions, may have contributed this effect. After core drainage (685-876 hours), NO₃⁻ amendment induced a positive increase in N₂O emission in all treatments, as it again assuaged any limitation on the supply of anaerobic oxidant.

It is clear from Fig. 5.5, that NO₃⁻ application had relatively little effect, if any, on CO₂ emission rates. This is confirmed in Fig. 5.10 b. Relative to N₂O, the differences in CO₂ emissions between unamended and NO₃⁻ amended cores were very small, with no apparent trends.

5.2.3.9 N₂O and CO₂ concentration in soil water

The concentrations of N₂O and CO₂ in the soil solution during the draining of the saturated cores, is shown in Fig. 5.11. For both N₂O and CO₂ there was some evidence of increased solution concentration with both NO₃⁻ and DFR addition; however this was a marginal effect. The concentrations were measured during a time when there was relatively little variation in rates of N₂O and CO₂ evolution. The W3 treatment without NO₃⁻, had an anomalously low concentration of N₂O within its soil water, which corresponded with its low N₂O emission rates.

The total amount of N_2O -N within the drained soil water was high, relative to the cumulative amount of N_2O -N emitted from the soil. The control cores emitted a total of about 8×10^{-5} moles N_2O -N, while W3 (+N) emitted about 2×10^{-4} moles N_2O -N, throughout the whole incubation period; the amount of N_2O -N within the soil water drained from the cores was about 5×10^{-5} moles N_2O -N. This illustrates the impeding nature of the water filled pores on N_2O diffusion from soil. In contrast, the amount of CO_2 impeded by the water filled pores appears to be minimal compared to that emitted from the soil. There was about 3×10^{-5} moles CO_2 within the drained soil water, while about 1.5×10^{-3} moles CO_2 were emitted from cores throughout the whole incubation period. However, this calculation does not include the amount of CO_2 that exists in the hydrolysed dissociated form (HCO_3^-); hence the amount of CO_2 in solution is greatly underestimated.

5.2.3.10 N and C balance

After the 36 day incubation period, the NO_3^- treated cores (+N) had a residual soil NO_3^- concentration that was about a factor of 10 greater than the -N cores (table 5.6). The residual soil NO_3^- concentration, regardless of sub-treatment, was almost the same for all NO_3^- treated cores and very similar for all the unamended cores. As expected, the NH_4^+ concentrations of both NO_3^- amended and unamended cores significantly increased with increasing mass of DFR. The residual NH_4^+ concentration in W3 was greater than W2 (table 5.6), for both NO_3^- amended and unamended treatments, due to the more intense localized reducing conditions of W3, which may restrict nitrification and hence, NH_4^+ loss.

Table 5.7, shows the approximate N-balance of the treatments investigated. The initial NO_3^- concentration includes that from the native soil and any applied as KNO_3 . The NO_3^- concentration in the soil water extracted at drainage was determined, in addition to the residual NO_3^- concentration in the soil after the 36 day incubation period. Also included in the N-balance, was the N emitted as N_2O to the atmosphere and the N_2O concentration within the drainage water. The N-balance revealed that the ratio

between the initial and residual amounts of NO_3^- , was approximately the same in both the NO_3^- amended and unamended treatments (table 5.7). This could indicate that the size of the denitrifying population was determined by the NO_3^- concentration. Although some of the NO_3^- may have been immobilized and/or organic matter mineralized during the incubation period, this would have had only a minor impact on the NO_3^- concentration within the +N treatments. Therefore it can be assumed that the vast amount of NO_3^- unaccounted for, was reduced to N_2 . DFR contained 10.5 % N (section 2.3) on a dry weight basis, therefore, assuming that the wet weight:dry weight ratio of the Earthworms was 6, the amount of N added, was approximately 1.5×10^{-3} (W1) or 3.0×10^{-3} (W2) moles N. However, this N would be in the form of proteins, which would need to be mineralized and nitrified to contribute to the N-balance.

The carbon content of the soils was only minimally increased by DFR treatment (table 5.8 b); W1 by about 1 % and W2 by about 2 %. This calculation assumed that the wet weight:dry weight ratio of the Earthworms was 6 and that the carbon content of the DFR, was 44 % of the Earthworm dry weight. The amount of C evolved as CO_2 , includes that from the drained soil solution (not including HCO_3^-), which was minimal relative to the total amount of organic carbon within the soil.

Figure 5.11 Concentration of (a) N_2O and (b) CO_2 in soil water drained from unamended and NO_3^- amended cores (including the control, W1, W2 and W3 sub-treatments).

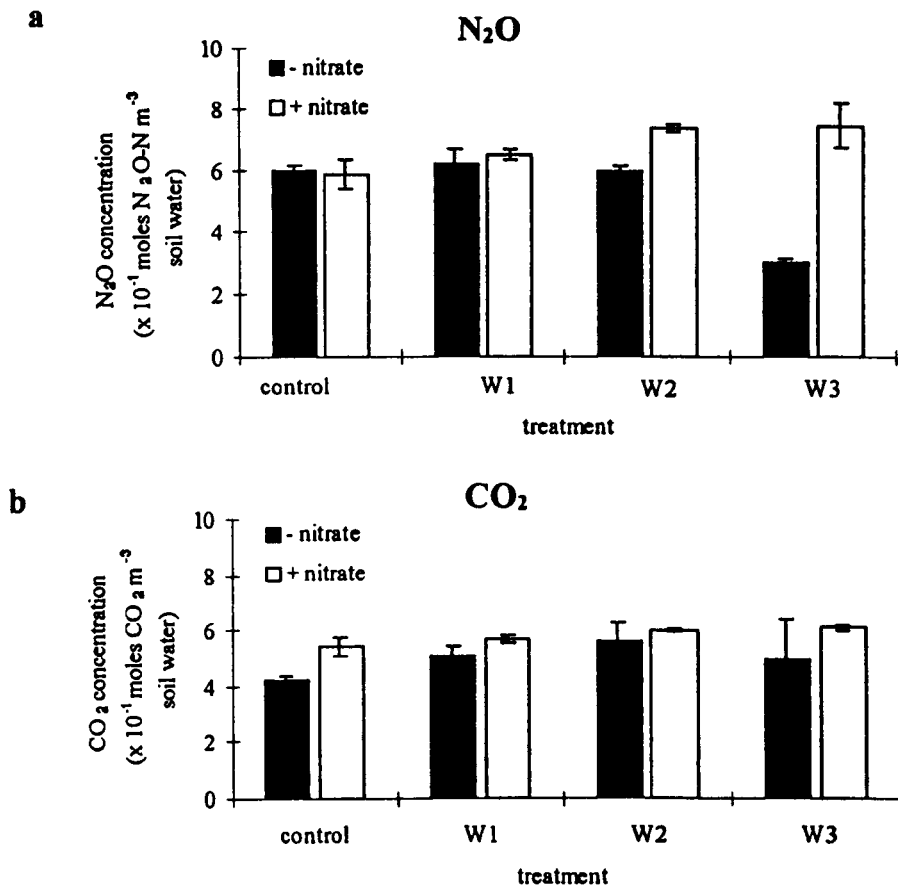


Table 5.6 Mean concentration of NO_3^- -N and NH_4^+ -N from replicated soil cores, re-packed with aggregates of the Wick series soil (< 2 mm diameter) after 36 days incubation at different soil water contents; The soils were treated with and without NO_3^- and with increasing mass of DFR (W1, W2, W3).

	without NO_3^- treatment		with NO_3^- treatment	
	NO_3^- concentration (mol NO_3^- -N m^{-3} soil)	NH_4^+ concentration (mol NH_4^+ -N m^{-3} soil)	NO_3^- concentration (mol NO_3^- -N m^{-3} soil)	NH_4^+ concentration (mol NH_4^+ -N m^{-3} soil)
control (SD)	0.39 (0.02)	0.12 (0.01)	3.80 (0.02)	0.08 (0.05)
W1 (SD)	0.49 (0.03)	0.25 (0.07)	3.70 (0.05)	0.20 (0.01)
W2 (SD)	0.50 (0.03)	0.47 (0.03)	3.81 (0.03)	0.32 (0.01)
W3 (SD)	0.39 (0.01)	0.53 (0.08)	3.78 (0.02)	0.50 (0.01)

Table 5.7 Measured fractions of N from each soil core treatments that had undergone a sequential raising and lowering of the soil water content.

	Amount of N ($\times 10^{-3}$ moles N)							
	without nitrate				with nitrate			
	control	W1	W2	W3	control	W1	W2	W3
initial amount of NO_3^-	0.49	0.49	0.49	0.49	6.74	6.74	6.74	6.74
residual amount of NO_3^-	0.32	0.36	0.35	0.30	3.49	3.33	3.55	3.72
amount of N as N_2O	0.11	0.12	0.12	0.09	0.13	0.18	0.20	0.25
missing N	0.06	0.01	0.02	0.10	3.12	3.23	2.99	2.77

Table 5.8 Measured fractions of C from each soil core treatment that had undergone a sequential raising and lowering of the soil water content.

	Amount of C ($\times 10^{-3}$ moles C)							
	without nitrate				with nitrate			
	control	W1	W2	W3	control	W1	W2	W3
amount of C in soil	500	500	500	500	500	500	500	500
amount of C added (DFR)	0	6.11	12.22	12.22	0	6.11	12.22	12.22
amount of C as CO_2	1.05	1.05	1.41	1.21	1.07	1.22	1.34	1.41

5.3 CONCLUSIONS

From these studies it was clear that Earthworm (DFR) decomposition in soil has considerable potential for significantly contributing to N₂O emission to the atmosphere. DFRs act as major environmental determinants for N₂O fluxes in aerobic soil, providing conditions for rapid denitrification. Unsaturated soil containing DFRs can emit N₂O at rates similar to those produced when unamended soil is saturated. However, in saturated soil, the effect of DFR on N₂O emissions was limited. The associated increase in N₂O flux with DFR addition under unsaturated conditions, supports the suggestion that the variable emission rates previously observed, may be the result of localized concentrations of mineralizable organic residues. In support of this, rates of N₂O emission appeared less variable under saturated conditions, due to the uniform anoxic conditions throughout the flooded core. Rates of N₂O emission were thus greatly affected by changes in the soil environment, while CO₂ emission rates were quite constant suggesting uniform microbial activity.

Large rates of N₂O were emitted following drainage of the saturated soil, however this effect was short lived (< 24 h). It is suggested therefore, that to assess the full potential for N₂O production from soil susceptible to fluctuations in the groundwater table or frequent flooding, it is not sufficient to consider the summation of 2 steady state fluxes (saturated and unsaturated). Frequent transitions between saturated and drained conditions may boost expected fluxes considerably.

Chapter 6: Soil Water Content And N₂O Flux

6.1 MODELLING THE EFFECT OF SOIL FLOODING ON N₂O FLUX RATES

6.1.1 Introduction

In previous sections (4.3 and 5.2), as expected, a positive trend in the rate of N₂O emissions was observed with increasing soil water content; this relationship has been widely reported throughout the literature (Linn and Doran, 1984; Klemetsson *et al.*, 1988; Schuster and Conrad, 1992). In sections 5.1 and 5.2, the difference between N₂O emission rates from unsaturated and saturated soil was shown to be up to three orders of magnitude. This study extends these findings and compares rates of N₂O and CO₂ emission from different sizes of soil aggregate (Wick series), while undergoing a process of progressive *wetting up*, to saturation. The study includes a comparison with two contrasting soils from Scotland: unclassified alluvium (sandy clay loam) and Winton soil series (clay loam). These two soils were used in trials conducted by other members of the TIGER 2 consortium and were found to differ considerably in their rates of N₂O emission. The N₂O fluxes observed from the following investigation was used to validate the predictive N₂O emission model described in section 3.2.

6.1.2 Methods

Two large replicate core containers (13.0 cm diameter and 16.3 cm height) were re-packed with aggregate sizes of either < 2 mm, 2-5 mm, 5-10 mm and 10-20 mm, from the Wick soil series (bulk density of 1.1 g cm⁻³). Prior to re-packing, the soil water content was adjusted to 75 % F.C., using a fine spray of de-ionized water (at 15 °C). The re-packed cores were pre-incubated at 15 °C for 72 hours to achieve isothermal conditions. Each replicate chamber, containing a single core was incubated at 15 °C

and both N₂O and CO₂ emission rates were determined by the automated GC method (section 2.1.6).

During the course of the incubation, the soil cores underwent further additions of de-ionized water (at 15 °C), to establish soil water contents equivalent to 83 %, 92 % and 100 % field capacity. Each increment of water was applied using a syringe, to ensure an even distribution across the soil surface; all these changes in water content were interspersed with a 72 hour incubation period. Only the initial water addition (to 83 % F.C.) to each core, included an amendment of KNO₃, equivalent to 100 kg N ha⁻¹. Once the soil cores had been incubated at 100 % field capacity for a period of about 4 days, water was applied to the base of the core via the water access tube (section 2.2.2) until the core was fully saturated. Throughout the whole of the incubation (both unsaturated and saturated periods), the replicate chambers were vented every 24 hours to attain ambient concentrations of atmospheric gases (section 2.1.2.3). Soil mineral N concentrations (NO₃⁻ and NH₄⁺) were measured before and after the incubation. This procedure was undertaken for each aggregate size of the Wick series soil and for the 2-5 mm aggregate size fraction of both the unclassified alluvium (sandy clay loam) and Winton soil series (clay loam) from Scotland.

Modelling N₂O flux from soil

The model described in section 3.2 was used to simulate N₂O emissions from soil cores with different aggregate sizes and at variable moisture contents. Other than the denitrification rate (k_1 , k_2) and the *inter*-aggregate tortuosity factor (f), which were obtained through the optimization facility in the *ModelMaker* package, the values attributed to model parameters (section 3) were based on literature values. The smallest aggregate diameter (< 2 mm), was used for the first simulation of N₂O emissions from the model soil whilst undergoing a transformation from unsaturated to saturated conditions (Fig. 6.7). However, despite a good correlation between the model simulation and the observed data ($R^2 = 0.90$), the running time was over 24 hours. This was because the *ModelMaker* software had difficulty dealing with the values generated in the denitrification-diffusion process, which differed by several

orders of magnitude. As time considerations were a limiting factor in the model simulations, the model described in section 3, was modified to enhance running time. The net rate of N_2O emission from the model soil, which was dependent on both the production rates ($k1$, $k2$; section 3.1.3.1) and consumption rates ($k3$, $k4$; section 3.1.3.1) of N_2O was altered. The reduction of N_2O to N_2 was made obsolete and the emission rate of N_2O was assumed to be dependent entirely on its production rate ($k1$, $k2$; section 3.1.3.1).

The model was therefore attributed with two different N_2O production rates for saturated ($k1$) and unsaturated ($k2$) conditions. However, to account for the development of anaerobic zones within different aggregate sizes in unsaturated conditions, $k2$ was optimized for each model aggregate size. By contrast, a single N_2O production rate was used for all model aggregate sizes under saturated conditions; $k1$ was optimized on cores with the smallest aggregate size (< 2 mm). These assumptions were in accordance with the observed pattern of emission reported later in this chapter. When the model was run for all the aggregate sizes, in both unsaturated and saturated conditions, the predicted rates of N_2O emission became smaller with increasing aggregate diameter (Fig. 6.8 a), contrary to the observed results. The unsaturated stage of the simulation appeared unaffected due to the individual optimization of $k2$, which accommodated this anomaly for each aggregate size. However, the predicted rates of N_2O emission in unsaturated conditions, also decreased with increasing aggregate size.

This anomaly was principally due to differences in the (model) path length for diffusion from the *intra*- to the *inter*-aggregate pore space with different aggregate sizes. As the model aggregates were assumed to have 4 shells of equal thickness, the shell thickness changed when the aggregate size was altered, changing the diffusion path length and thus producing erroneous concentration gradients. This modelling deficiency was overcome by attributing to the outer *shell* a constant thickness for all aggregate sizes. However, there was still a noticeable difference between the predicted and observed emissions of N_2O from the different aggregate sizes during saturated conditions, due to differences in aggregate surface area (Fig. 6.8 b). These differences were also

observed in unsaturated conditions, but were again accommodated by the individually optimized values of k_2 . There is a 15 fold difference between the specific surface area of the largest aggregate (10-20 mm diameter) and the surface area of an equivalent volume of the smallest aggregates (< 2 mm). Hence, an individual optimized value of k_1 was required for each aggregate size to correlate with the observed N₂O emissions during saturated conditions. It was clear from the observed data however, that the N₂O emission rate from the saturated Wick series soil was virtually constant regardless of aggregate size (table 6.1).

The apparent inadequacy of the model to accurately predict N₂O emissions from unsaturated and saturated conditions was related to the independent production of N₂O from each aggregate; whereas in reality the aggregates within a profile may become compacted forming larger anaerobic zones. The whole, saturated soil core volume, may act as a single entity, obviating any influence of aggregate size. To eradicate these short-comings, the model was modified once more. Gas movement was described as transfers between homogenous layers in the soil column rather than from individual aggregates into the inter-aggregate transmission pores. All the descriptions of diffusion between layers within the model soil and between the soil and atmosphere (described in section 3) remained the same, only the production of N₂O was altered. Production of N₂O was in the model layer compartments. The description of the rates k_1 and k_2 remained, but were re-optimized for each layer. To accommodate the influence of aggregate size on N₂O emissions under unsaturated conditions, k_2 was optimized for each size category (table 6.3) and a single, optimized rate (k_1) for all aggregate sizes was used in saturated conditions (table 6.3). The new model configuration was successfully used to simulate N₂O fluxes from different aggregate sizes from the Wick series soil (Fig. 6.1). The correlation between the observed and predicted results for all aggregate sizes was highly significant; < 2 mm ($R^2 = 0.999$; Fig. 6.1 a), 2-5 mm ($R^2 = 0.996$; Fig. 6.1 b), 5-10 mm ($R^2 = 0.996$; Fig. 6.1 c), and 10-20 mm ($R^2 = 0.990$; Fig. 6.1 d). In addition, good correlation's were established between observed and predicted N₂O emission rates for the Winton series ($R^2 = 0.972$; Fig. 6.3 a) and the alluvium soil ($R^2 = 0.992$; Fig. 6.3 b).

6.1.3 Results and discussion

The results shown in table 6.1 (a, b) were derived from the regression analysis of the mean gradients of the cumulative N₂O and CO₂ emissions from the incubated cores at different moisture contents (illustrated in Figs. 6.1-6.3). The observed and model-predicted cumulative N₂O emission for each aggregate size are presented in Figs. 6.1 and 6.3.

6.1.3.1 Gaseous emissions from different aggregate sizes (Wick series)

General overview

The pattern of N₂O emission from all the cores containing different aggregate sizes followed the same general trend and increased with soil water content up to saturation (Fig. 6.1; table 6.1 a). For all aggregate sizes, the N₂O emission rates from saturated soil were very similar and considerably greater than from unsaturated cores. By contrast, the CO₂ emission rates did not change with increasing soil water content; cumulative emission remained essentially linear throughout the incubation period (Fig. 6.2; table 6.1 b).

N₂O emission from different soil aggregate sizes under unsaturated conditions (Wick series)

The N₂O emission rates from the different aggregate sizes, were between 10⁻⁸ and 10⁻⁷ mol N m⁻² h⁻¹, in unsaturated conditions (similar to rates observed previously in sections 4.3 and 5.2). In the unsaturated state, there was a small increase in N₂O emission rate with increasing soil moisture content from each of the aggregate sizes and a general decrease with decreasing aggregate size (table 6.1 a). This is similar to earlier findings (section 4.1 and 4.3) and reports in the literature (Smith, 1980; Sexstone *et al.*, 1985 b; Arah and Smith, 1989). The evidence suggests that larger aggregates possess larger internal anaerobic zones due to the greater physical impedance on O₂ diffusion.

N₂O emission from different soil aggregate sizes under saturated conditions (Wick series)

There was little change in the rates of N₂O emission (sampled every 2 hours) for a period of about 24 hours immediately following saturation, however, after this period each aggregate size exhibited a significant increase in N₂O emission rate (Fig. 6.1; table 6.1 a). This increased rate remained virtually constant through to the end of the incubation period. The 24 hour lag period occurred in all aggregate sizes and may be the result of either the time taken to produce or activate the appropriate denitrifying enzymes or populations (Firestone and Tiedje, 1979), and/or the time required to remove the inhibitory effects of residual O₂ (Dendooven and Anderson, 1995).

The mean N₂O emission rates from all aggregate sizes in saturated conditions, were greater than the emission rates under unsaturated conditions by about 2-3 orders in magnitude; with rates of emission between 0.96 and 1.03 × 10⁻⁴ mol N m⁻² h⁻¹ (table 6.1 a). Comparable changes in N₂O emission rate, between unsaturated and saturated conditions have been reported in the literature (Klemmedtsson *et al.*, 1988; Aulakh and Doran, 1990; Aulakh *et al.*, 1991; Bandibas *et al.*, 1994); comparable examples are shown in the Appendix (no. 10-14). In saturated conditions, there was no apparent correlation between aggregate size and N₂O emission rate; there were very similar rates of N₂O emission for all the aggregate sizes. This is because denitrification occurs throughout the entire saturated soil core, rather than from discrete zones of anoxia which are dependent on the size of the aggregates under aerobic conditions.

CO₂ emission from different soil aggregate sizes under unsaturated and saturated conditions (Wick series)

In contrast to N₂O, the rates of CO₂ emission appeared to be unaffected by aggregate size and water content in both unsaturated and saturated conditions (Fig. 6.2; table 6.1 b). CO₂ emission rates were typically between 1-4 × 10⁻⁴ mol m⁻² h⁻¹, similar to previous observations (sections 4 and 5). There was a small reduction in CO₂ emission rates from all aggregate sizes during saturation, which was probably due to the inhibition of aerobic microbial activity.

Figure 6.1 Observed mean cumulative and model predicted N₂O flux from replicate gas-tight chambers containing a single core re-packed with (a) < 2 mm, (b) 2-5 mm, (c) 5-10 mm and (d) 10-20 mm aggregates of the Wick series soil. The cores were incubated under variable soil water contents, denoted as 1, 2, 3 and 4. (***) - $P < 0.05$.

1 = 83 % field capacity
2 = 92 % field capacity

3 = 100 % field capacity
4 = complete saturation

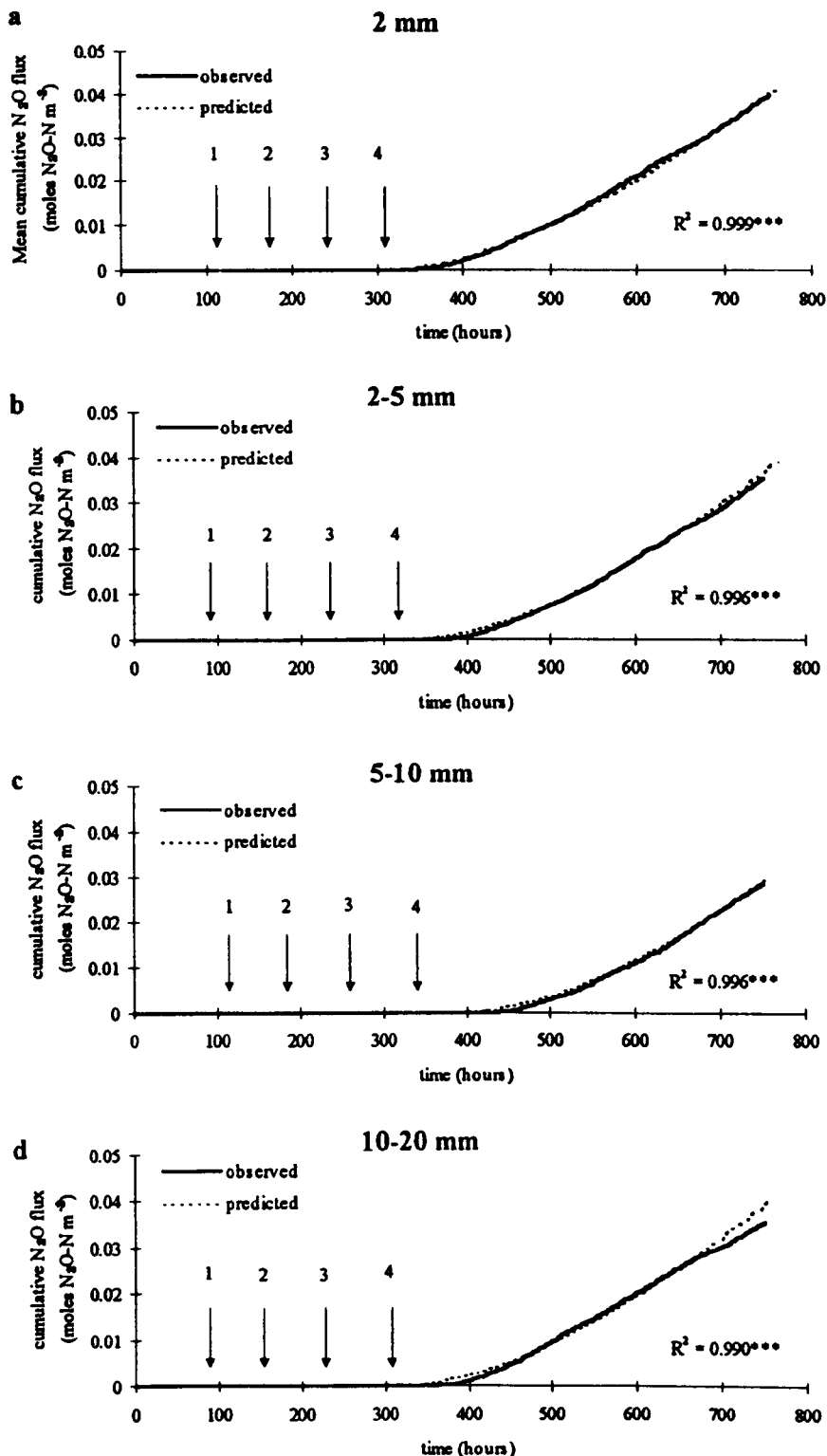


Figure 6.2 Observed mean cumulative CO₂ flux from replicate gas-tight chambers containing a single core re-packed with (a) < 2 mm, (b) 2-5 mm, (c) 5-10 mm and (d) 10-20 mm aggregates of the Wick series soil. The cores were incubated under variable soil water contents, denoted as 1, 2, 3 and 4.

1 = 83 % field capacity
2 = 92 % field capacity

3 = 100 % field capacity
4 = complete saturation

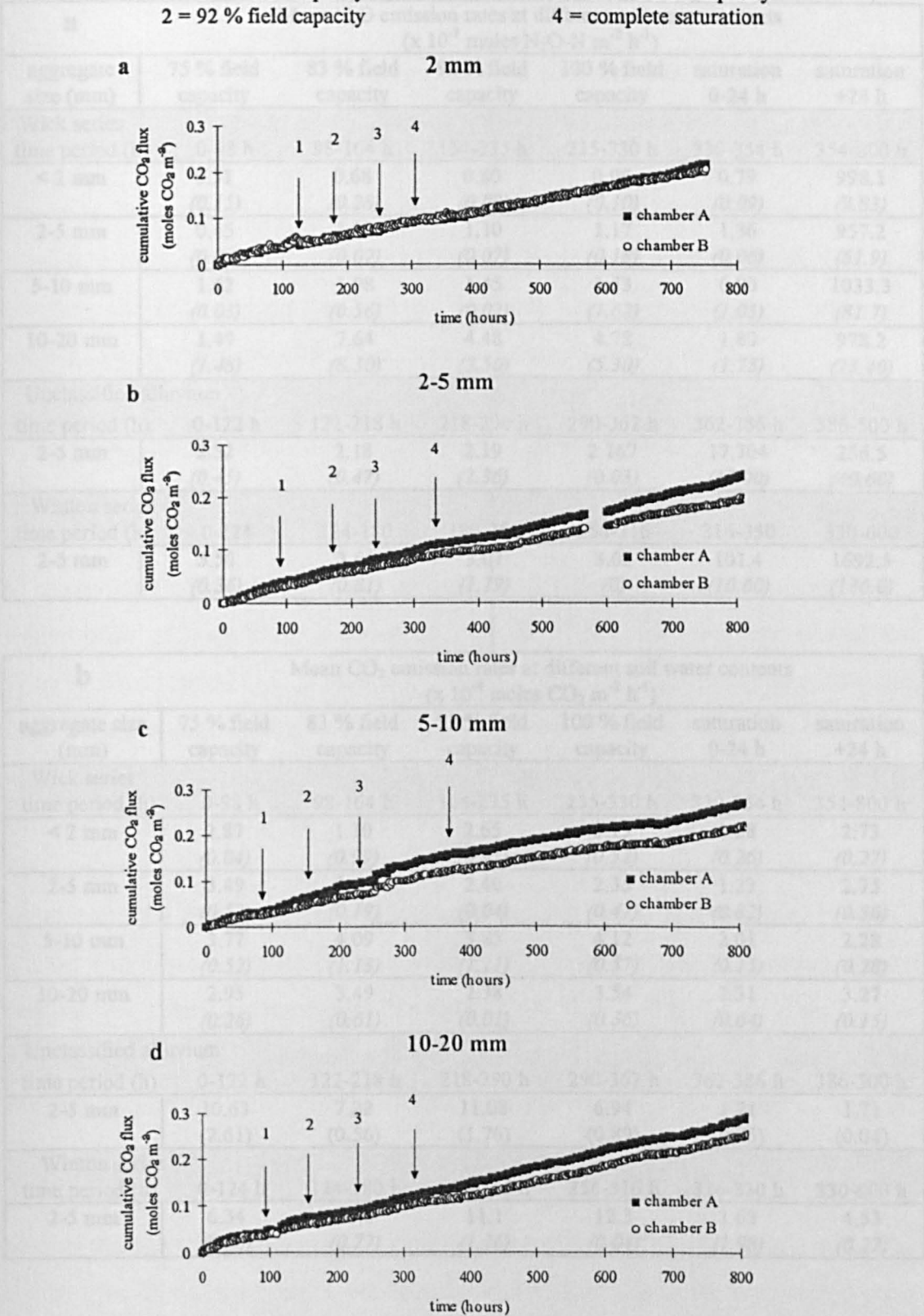


Table 6.1 Mean (a) N₂O and (b) CO₂ emission rates from 2 replicate chambers each containing a single core filled with one of four aggregate sizes, for 3 contrasting soils subjected to a progressive increase in soil water content.

a Mean N ₂ O emission rates at different soil water contents (x 10 ⁻⁷ moles N ₂ O-N m ⁻² h ⁻¹)						
aggregate size (mm)	75 % field capacity	83 % field capacity	92 % field capacity	100 % field capacity	saturation 0-24 h	saturation +24 h
Wick series						
time period (h)	0-98 h	98-164 h	164-235 h	235-330 h	330-354 h	354-800 h
< 2 mm	0.51 (0.15)	0.68 (0.28)	0.80 (0.09)	0.96 (0.10)	0.79 (0.09)	998.1 (9.83)
2-5 mm	0.45 (0.06)	1.02 (0.02)	1.10 (0.07)	1.17 (0.18)	1.36 (0.06)	957.2 (61.9)
5-10 mm	1.62 (0.03)	1.98 (0.56)	1.45 (0.02)	3.53 (1.62)	6.90 (1.03)	1033.3 (81.7)
10-20 mm	1.49 (1.48)	7.64 (8.30)	4.48 (3.50)	4.78 (5.30)	1.80 (1.73)	978.2 (23.40)
Unclassified alluvium						
time period (h)	0-122 h	122-218 h	218-290 h	290-362 h	362-386 h	386-500 h
2-5 mm	2.52 (0.45)	2.18 (0.47)	2.19 (2.36)	2.167 (0.03)	17.704 (13.00)	256.5 (40.60)
Winton series						
time period (h)	0-124	124-180	180-256	256-316	316-330	330-600
2-5 mm	5.50 (0.36)	3.66 (0.81)	3.07 (1.19)	3.02 (0)	101.4 (10.60)	1692.5 (136.0)

b Mean CO ₂ emission rates at different soil water contents (x 10 ⁻⁴ moles CO ₂ m ⁻² h ⁻¹)						
aggregate size (mm)	75 % field capacity	83 % field capacity	92 % field capacity	100 % field capacity	saturation 0-24 h	saturation +24 h
Wick series						
time period (h)	0-98 h	98-164 h	164-235 h	235-330 h	330-354 h	354-800 h
< 2 mm	2.87 (0.04)	1.10 (0.99)	2.65 (0.91)	3.15 (0.52)	1.28 (0.26)	2.73 (0.27)
2-5 mm	3.49 (0.52)	2.05 (0.19)	2.40 (0.04)	2.35 (0.47)	1.22 (0.82)	2.75 (0.36)
5-10 mm	3.77 (0.52)	4.09 (1.13)	3.85 (1.11)	4.12 (0.57)	2.01 (0.15)	2.28 (0.28)
10-20 mm	2.95 (0.26)	3.49 (0.61)	2.38 (0.01)	3.54 (0.36)	2.31 (0.64)	3.27 (0.15)
Unclassified alluvium						
time period (h)	0-122 h	122-218 h	218-290 h	290-362 h	362-386 h	386-500 h
2-5 mm	10.63 (2.61)	7.22 (0.56)	11.08 (1.76)	6.94 (0.89)	1.71 (0.05)	1.71 (0.04)
Winton series						
time period (h)	0-124 h	124-180 h	180-256 h	256-316 h	316-330 h	330-600 h
2-5 mm	6.34 (0.86)	14.3 (0.77)	11.1 (1.16)	12.3 (0.04)	1.63 (1.98)	4.53 (0.27)

6.1.3.2 Gaseous emissions from three contrasting soils -(Wick series, Unclassified alluvium and Winton series; 2-5 mm aggregate size range)

General overview

The N₂O emission rates from the unclassified alluvium and Winton series, both followed a similar trend to that shown by the Wick series and exhibited a substantial increase in N₂O emission rate upon saturation of the soil cores (Fig. 6.3; table 6.1 a). However, the rate of N₂O emission from the three contrasting soils under saturated conditions were significantly different: Winton > Wick > Alluvium soil (table 6.1). By contrast, the CO₂ emission rates from the three soils decreased upon saturation, although this was a minor effect relative to the change in N₂O emissions.

N₂O emission under unsaturated conditions from three contrasting soils -(Wick series, Unclassified alluvium and Winton series; 2-5 mm aggregate size range)

In unsaturated conditions, the N₂O emission rates from the three soils were all of a similar order of magnitude, at about 10⁻⁷ mol N m⁻² h⁻¹. However, the alluvial and Winton series emitted N₂O at rates about 2 and 3 times (respectively) greater than that from the equivalent aggregate size of the Wick series (table 6.1 a). The differences were most likely the result of the contrasting soil textures; the general trend in N₂O emission rates from the three different soils, reflect the fineness of the soil texture and its associated water holding capacity. The Winton series soil had the largest water content and the Wick series the smallest water content at 100 % field capacity (section 2.2.3). There was a positive linear correlation ($R^2 = 1.0$) between clay content of each soil and their respective mean N₂O flux rates at 100 % F.C. (Fig. 6.4 a). This positive relationship was strong throughout the unsaturated state. Similar findings were reported by Aulakh *et al.*, (1991). In addition, the trend in N₂O emissions from the three soils may have also been affected by their respective soil organic carbon contents. There was a positive relationship ($R^2 = 0.94$) between the organic matter content of each of the three soils (section 2.2.3) and their respective N₂O flux at 100 % F.C. (Fig. 6.4 b). Similarly, this positive relationship applied throughout the unsaturated state.

An increase in carbon content would be expected to enhance the general denitrification rate of the soil (Bowman and Focht, 1974; Christensen *et al.*, 1990 a).

In contrast to the general trend shown for N₂O emission rates from the unsaturated Wick series soil, the emission rates from both the alluvial soil and Winton series declined slightly with increasing soil water content, over the range of 75-100 % field capacity (table 6.1 a). This phenomenon was most likely the result of localized flooding of the surface layers of the finer textured soils upon each wetting event slightly impeding N₂O diffusion out of the soil.

N₂O emission under saturated conditions from the three contrasting soils -(Wick series, Unclassified alluvium and Winton series; 2-5 mm aggregate size range)

The alluvium and Winton series soils appeared to establish anaerobic conditions much more quickly than the Wick series (table 6.1 a). During the 24 hour period following saturation, the N₂O emission rate from the alluvial soil increased by one order of magnitude to about 1.8×10^{-6} mol N m⁻² h⁻¹, while the emission rate from Winton series increased by 2 orders of magnitude, to about 1×10^{-5} mol N m⁻² h⁻¹. During the same period, the mean N₂O emission rate from the Wick series increased by only a factor of 1.16, to 1.36×10^{-7} mol N m⁻² h⁻¹. The more rapid development of anoxic conditions was probably enhanced by the fine texture and the organic carbon content of the alluvium and Winton series soil, which would dictate the rate of O₂ diffusion and consumption (and hence denitrification). Additionally, there would be a greater number of pre-existing anaerobic sites with increasing fineness of soil texture; hence the time to establish a viable denitrifying population would be reduced.

Although the alluvium soil quickly established anaerobic conditions, the mean N₂O emission rate during the saturated period was 2.6×10^{-5} mol N m⁻² h⁻¹, which was about a factor of 4 lower than that from the Wick soil (Fig. 6.3 a; table 6.1 a). The Winton series however, emitted N₂O at a mean rate of about 1.7×10^{-4} mol N m⁻² h⁻¹, which was greater than the corresponding rate from the Wick series by a factor of about 1.8. The differences in N₂O emission rate from the three soils during fully

saturated conditions may have been related to soil pH. The N₂:N₂O ratio is increased during denitrification at higher pH values (Weier and Gilliam, 1986; Aulakh *et al.*, 1992). There was a negative linear correlation ($R^2 = 0.99$) between the pH (section 2.2.3) of the three soils and their respective mean N₂O flux rates, under saturated conditions (Fig. 6.5). Bandibas *et al.*, (1994) also found that maximum N₂O emissions were negatively correlated with pH under waterlogged conditions. Mean N₂O emission rates under waterlogged conditions reported by Bandibas *et al.*, (1994), were comparable to those from the three contrasting soils of the present study. The authors report soils of pH 5.7 and 6.3 emitting N₂O at rates of $5.26 \times 10^{-5} \text{ mol N m}^{-2} \text{ h}^{-1}$ and $1.41 \times 10^{-5} \text{ mol N m}^{-2} \text{ h}^{-1}$, respectively; the soils in this study emitted rates equivalent to $2.56 \times 10^{-5} \text{ mol N m}^{-2} \text{ h}^{-1}$ (alluvium, pH 6.4), $9.57 \times 10^{-5} \text{ mol N m}^{-2} \text{ h}^{-1}$ (Wick, pH 5.7) and $1.69 \times 10^{-4} \text{ mol N m}^{-2} \text{ h}^{-1}$ (Winton, pH 5.2). The two rates of N₂O emission from the literature expressed on a flux basis are an approximation.

CO₂ emission in unsaturated and saturated conditions from three contrasting soils - (Wick series, Unclassified alluvium and Winton series; 2-5 mm aggregate size range)

The mean CO₂ emission rates from the three soils, were relatively constant throughout the unsaturated incubation period (Figs. 6.2, 6.3 c, d; table 6.1 b). In unsaturated conditions, the alluvium and Winton series soils had a greater CO₂ production rate than the Wick series, by about a factor of 2-3, consistent with their higher soil organic matter content. The mean CO₂ emission rate for each of the three contrasting soils at 100 % F.C. correlated well ($R^2 = 0.89$) with percentage organic matter (Fig. 6.6 a); this strong relationship existed throughout the range of 75-100 % F.C..

In contrast to N₂O, the rates of CO₂ emission from the three soils under saturated conditions did not increase but either maintained a similar rate to that emitted in unsaturated conditions (Wick series) or declined (unclassified alluvium and Winton series) (Figs. 6.2, 6.3 c, d; table 6.1 b). There was a negative correlation ($R^2 = 0.94$) between the pH of the three soils and their respective mean CO₂ flux rates, under saturated conditions (Fig. 6.6 b). This may be a reflection of the denitrifying activity in each soil.

Figure 6.3 Observed and predicted cumulative N_2O (a and b) and observed CO_2 (c and d) emissions from replicate gas-tight chambers containing a single core re-packed with 2-5 mm size aggregates of the unclassified alluvium (a and c) and Winton series (b and d) soils. The soils were incubated under variable water contents denoted as 1, 2, 3 and 4. (***) = $P < 0.05$.

1 = 83 % field capacity
2 = 92 % field capacity

3 = 100 % field capacity
4 = complete saturation

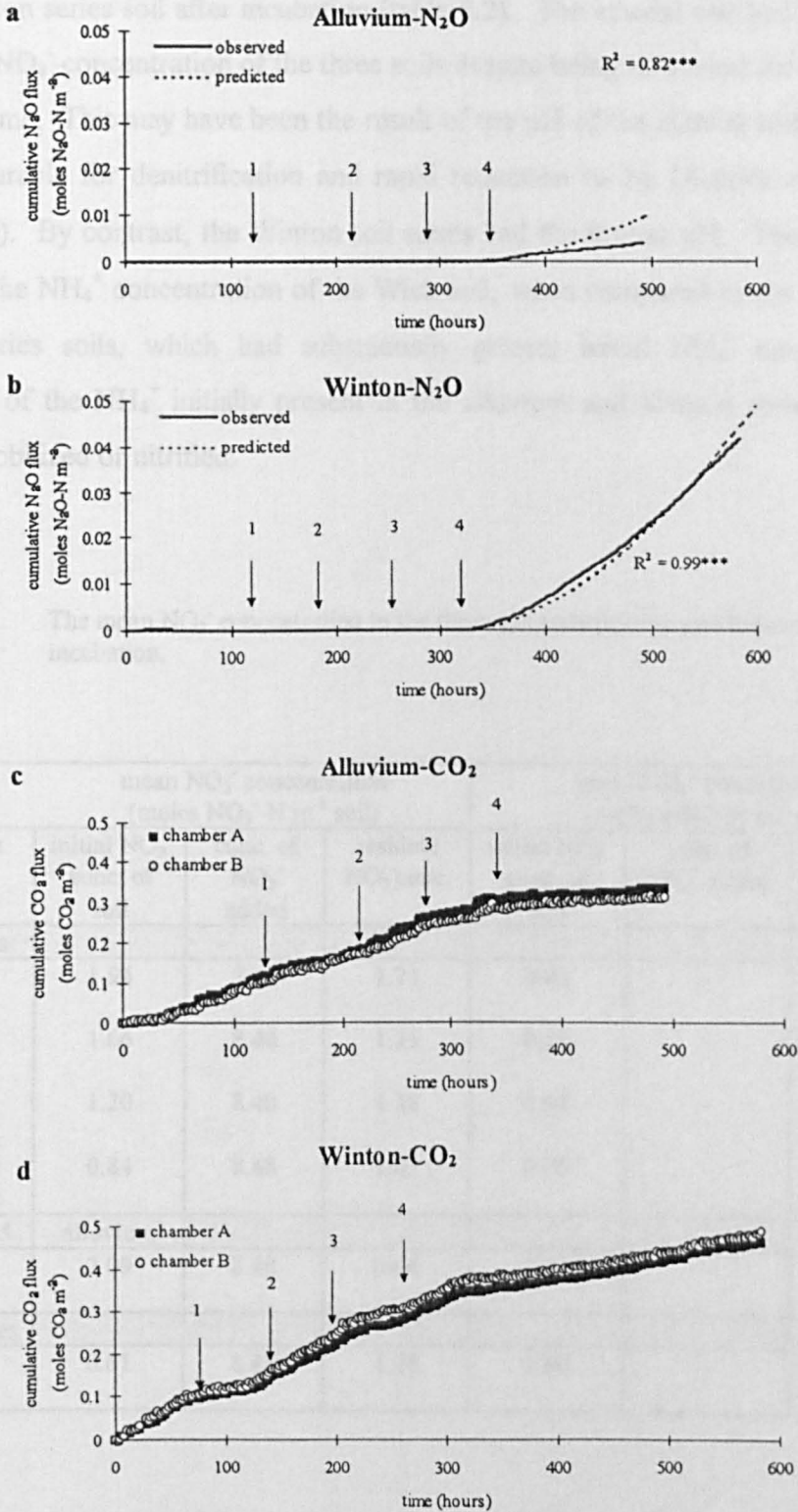


Figure 6.4 Relationship between N_2O flux rate from the three contrasting soils and (a) % clay and (b) % organic matter, at 100 % F.C.

Residual N -concentration

Virtually all of the NO_3^- applied to the Wick series and alluvium soil re-packed cores was lost over the incubation period but, half of the initial NO_3^- concentration remained in the Winton series soil after incubation (table 6.2). The alluvial soil had the smallest remaining NO_3^- concentration of the three soils despite being incubated for the shortest length of time. This may have been the result of the pH of the alluvial soil, which was most favourable for denitrification and rapid reduction to N_2 (Aulakh *et al.*, 1992; Tate, 1995). By contrast, the Winton soil series had the lowest pH. There was little change in the NH_4^+ concentration of the Wick soil, when compared to the alluvial and Winton series soils, which had substantially greater initial NH_4^+ concentrations. Almost all of the NH_4^+ initially present in the alluvium and Winton series soils was either immobilized or nitrified.

Table 6.2 The mean NO_3^- concentration in the three test soils prior to and following each incubation.

Aggregate size	mean NO_3^- concentration (moles NO_3^- -N m^{-3} soil)			mean NH_4^+ concentration (moles NH_4^+ -N m^{-3} soil)		
	initial NO_3^- conc. of soil	conc. of NO_3^- added	residual NO_3^- conc.	initial NH_4^+ conc. of soil	conc. of NH_4^+ added	residual NH_4^+ conc.
Wick series						
< 2 mm	1.94	8.48	1.71	0.05	-	0.01
2-5 mm	1.66	8.48	1.21	0.14	-	0.07
5-10 mm	1.20	8.48	1.18	0.04	-	0.03
10-20 mm	0.84	8.48	1.03	0.05	-	0.06
Unclassified						
2-5 mm	2.09	8.48	0.66	2.51	-	< 0.01
Winton series						
2-5 mm	0.61	8.48	4.25	1.80	-	< 0.01

Figure 6.4 Relationship between N_2O flux rate from the three contrasting soils and (a) % clay fraction and (b) % organic matter, at 100 % F.C..

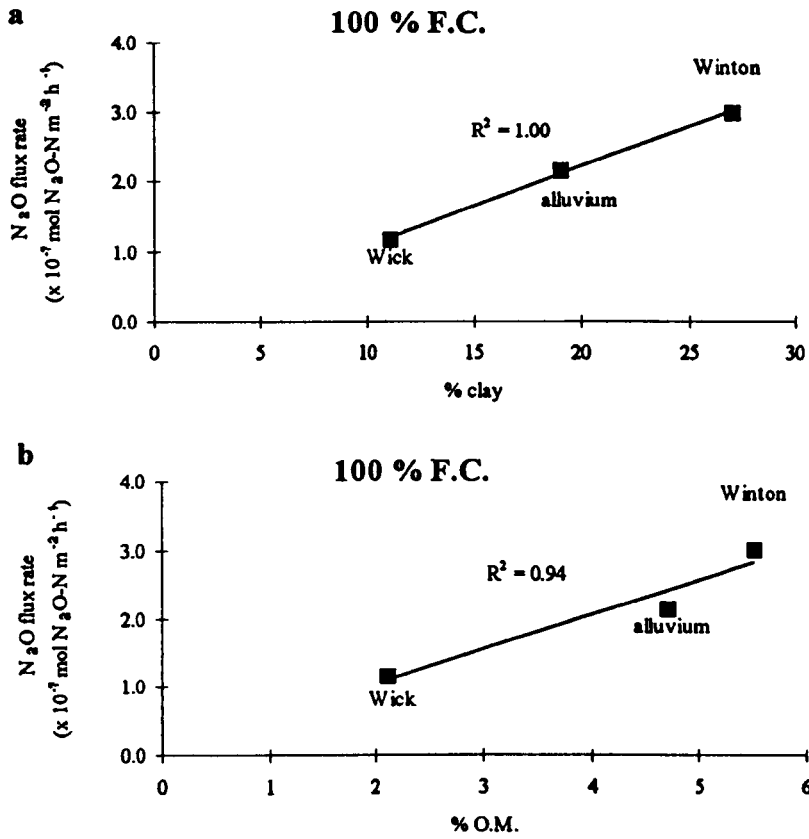


Figure 6.5 Relationship between N_2O flux rate from the three contrasting soils and pH in saturated conditions.

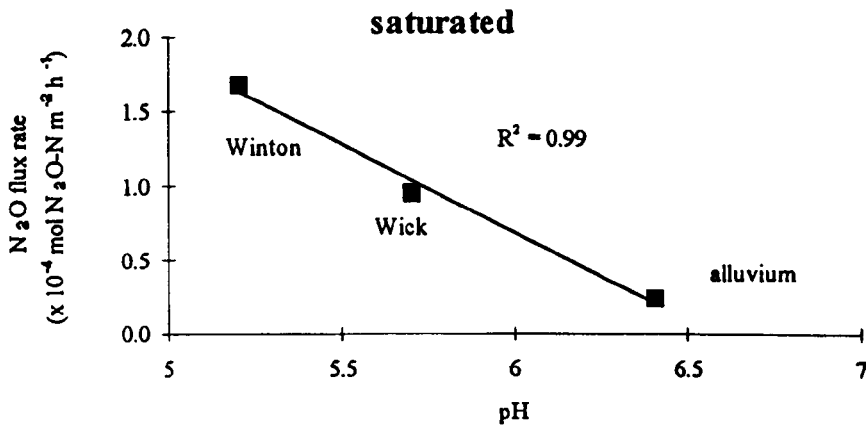


Figure 6.6 Relationship between CO_2 flux rate from the three contrasting soils and (a) % organic matter (at 100 % F.C.) and (b) pH (under saturated conditions).

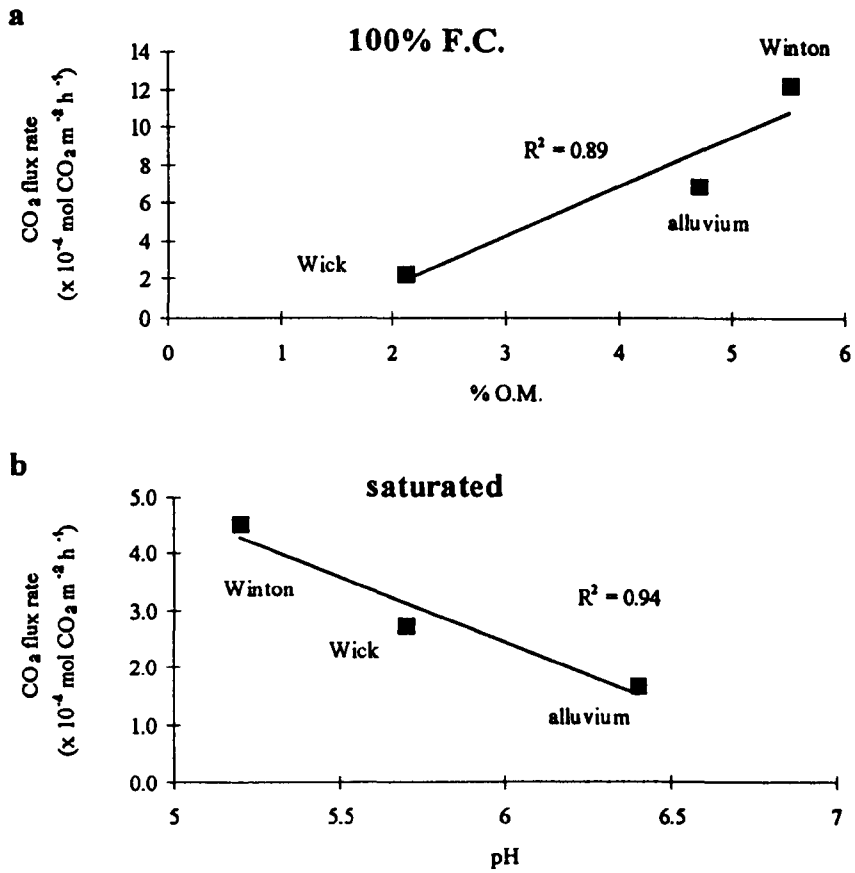


Figure 6.7 Observed and predicted cumulative N₂O flux from soil under unsaturated and saturated conditions. Arrow represents the point of saturation.

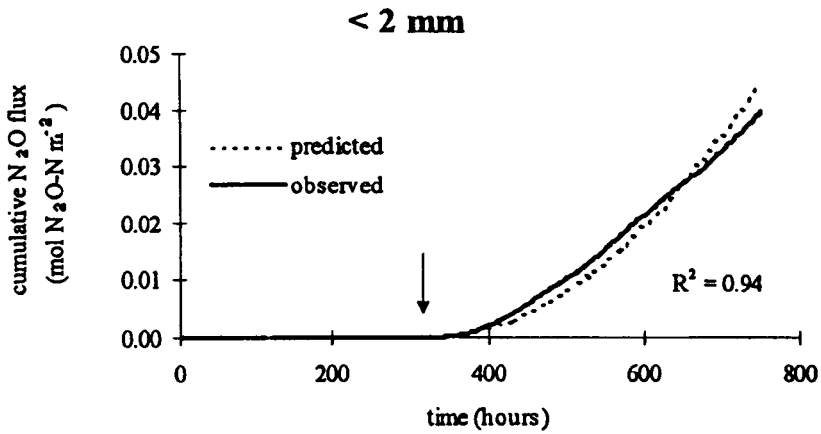


Figure 6.8 Example of predicted cumulative N₂O flux from soil under unsaturated and saturated conditions. The arrow represents the point of saturation. (a) = model predictions with aggregates constructed with a different outer shell thickness (25 % of aggregate radius), (b) = model predictions with aggregates constructed with the same outer shell thickness.

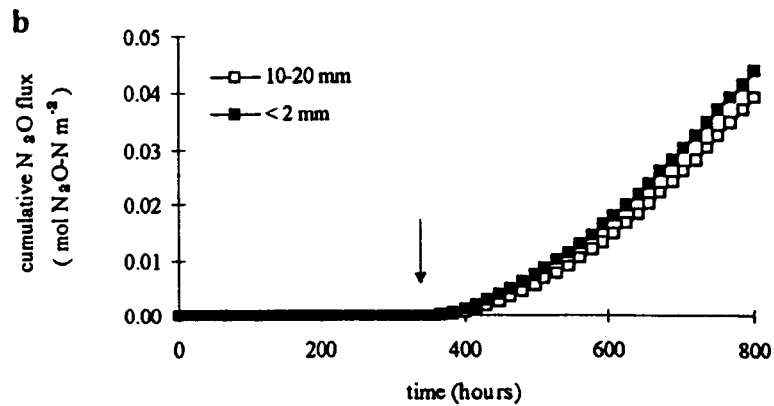
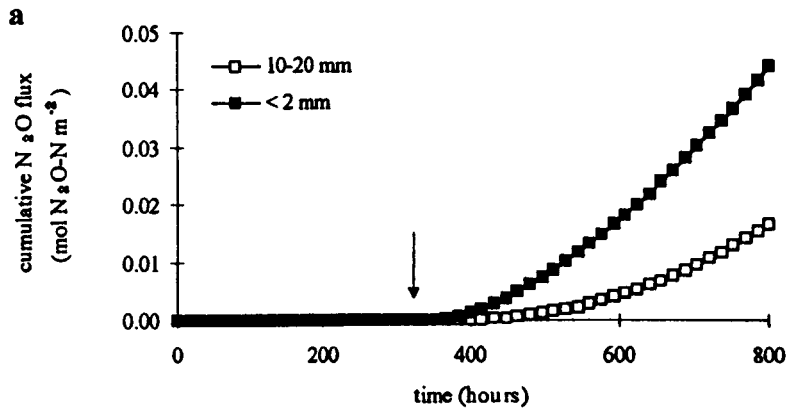


Table 6.3 Parameter values derived from the literature and generated by optimization of the model for each of the three test soils.

parameter	value	source
atmospheric concentration of N ₂ O (ppbv)	311	Houghton <i>et al.</i> , (1991)
Bunsen adsorption coefficient at 15 °C	0.743	Tiedje (1983)
Diffusion coefficient of N ₂ O (15 °C) in air (m ² s ⁻¹)	1.43 x 10 ⁻⁵	Leffelaar (1987)
Diffusion coefficient of N ₂ O (15 °C) in water (m ² s ⁻¹)	1.43 x 10 ⁻⁹	Russell (1988)
tortuosity factor, <i>f</i>	0.64	<i>optimized</i>

Wick series			
(all aggregate sizes)	<i>k1</i> (mol m ⁻³ s ⁻¹)	1.658 x 10 ⁻¹	<i>optimized</i>
(< 2 mm)	<i>k2</i> (mol m ⁻³ s ⁻¹)	6.192 x 10 ⁻⁸	<i>optimized</i>
(2-5 mm)	<i>k2</i> (mol m ⁻³ s ⁻¹)	4.70 x 10 ⁻⁸	<i>optimized</i>
(5-10 mm)	<i>k2</i> (mol m ⁻³ s ⁻¹)	8.692 x 10 ⁻⁸	<i>optimized</i>
(10-20 mm)	<i>k2</i> (mol m ⁻³ s ⁻¹)	2.222 x 10 ⁻⁷	<i>optimized</i>
Alluvium			
(2-5 mm)	<i>k1</i> (mol m ⁻³ s ⁻¹)	1.364 x 10 ⁻¹	<i>optimized</i>
	<i>k2</i> (mol m ⁻³ s ⁻¹)	1.225 x 10 ⁻⁸	<i>optimized</i>
Winton series			
(2-5 mm)	<i>k1</i> (mol m ⁻³ s ⁻¹)	7.00 x 10 ⁻¹	<i>optimized</i>
	<i>k2</i> (mol m ⁻³ s ⁻¹)	2.189 x 10 ⁻⁷	<i>optimized</i>

6.2 MODELLING THE EFFECT OF SOIL FLOODING AND DRAINAGE ON N₂O EMISSION RATES

6.2.1 Introduction

It has been previously shown (sections 5.2 and 6.1) that there was a substantial increase in the rate of N₂O emission upon saturation of each of the three contrasting soils; in some cases, up to 3 orders of magnitude. However, even greater rates of N₂O emission occurred following the draining of saturated soil cores (aggregate *de-gassing*, section 5.2). The aims of the following trial, were to determine whether the N₂O emission rate increased with volume of saturated soil and to ascertain the extent of the aggregate *de-gassing* event, during sequential lowering of the water table in the 3 test soils. The sequential flooding and drainage of the soil was expanded to evaluate whether the *de-gassing* effect diminished with repeated flooding and draining events. The N₂O fluxes observed were used to further validate the model soil.

6.2.2 Method

6.2.2.1 *Sequentially raising and lowering the soil core water table*

Two large replicate core containers (13.0 cm diameter and 16.3 cm height) were re-packed with a single aggregate size of 2-5 mm from the Wick series (bulk density of 1.1 g cm⁻³). Prior to re-packing, the soil water content was adjusted to 75 % F.C., using a fine spray of de-ionized water (at 15 °C). The re-packed cores were pre-incubated at 15 °C for 72 hours to achieve isothermal conditions throughout the core. Following the pre-incubation period, the soil water content was increased to 100 % F.C, via surface application of de-ionized water (at 15 °C), which included a KNO₃ amendment (100 kg N ha⁻¹). Each replicate chamber containing its single core was incubated for a total period of 50 days, at 15 °C, with both N₂O and CO₂ emission rates determined every 2 hours by the automated GC method (section 2.1.6). As for previous experiments, the replicate chambers were vented every 24 hours to re-

establish ambient atmospheric concentrations. After an initial 5 day incubation period, the soil water table was made to sequentially rise and fall in the soil cores using the water access tube; the height of the water table was monitored using the manometer (section 2.2.2). The water table was raised to 25 % core depth, 50 % core depth, 75 % core depth and then to the core surface, before sequentially declining in the reverse order. Each change in water table height was interspersed with about a 5 day incubation period. At the end of the 50 day incubation period, sub-samples were extracted from the soil for determination of NO_3^- and NH_4^+ concentrations. This procedure was also undertaken for the unclassified alluvium and Winton soil series.

6.2.2.2 Repetitive flooding and draining of soil on N_2O flux

Two large replicate core containers (13.0 cm diameter and 16.3 cm height) were re-packed with a single aggregate size (2-5 mm) of Wick series soil. The re-packed cores were treated exactly the same as described in section 6.2.2.1, except with respect to changes in the water table height. The soil core water table was repeatedly raised and lowered using the water access tube; the water table height was monitored by the attached manometer (section 2.2.2). The water drained from the soil cores was the same solution that was re-introduced to raise the height of the water table. Drained water was stored in gas tight, air free, 60 cm³ syringes (at 15 °C) prior to use for soil flooding. The repeated flooding and draining of the soil occurred over a period of about 90 days, the sequence of events is given in table 6.6. As for previous experiments the replicate chambers were vented every 24 hours to re-establish ambient atmospheric concentrations.

6.2.3 Results and discussion

6.2.3.1 N₂O and CO₂ emissions from soil cores affected by raising and lowering the water table.

General overview.

Figs. 6.9 and 6.10, illustrate the cumulative N₂O and CO₂ fluxes from the incubated soil cores, while table 6.4 shows the mean N₂O and CO₂ emission rates that correspond to each change in water table height. Table 6.4, includes both the mean rate for the immediate 24 hours after each change in water table height and the mean rate for the remaining time period at that water table level.

All three soils, exhibited some increase in N₂O emission rates as the water table approached the core surface and a rapid short-term increase in N₂O flux at each drainage stage (Fig. 6.9; table 6.4 a). By contrast, the mean CO₂ emission rate declined with an increase in core water table height and increased, as the water table was lowered (Fig. 6.10; table 6.4 b). However, relative to N₂O, the emission rates of CO₂ were only marginally affected by changes in water table height.

The effect of a progressive increase in water table height on N₂O emission.

The trends that were observed in the previous section (6.1) were apparent again. At zero water table height, the Winton series, Alluvium soil and Wick series emitted N₂O at rates 1.97×10^{-7} , 0.49×10^{-7} and $0.68 \times 10^{-7} \times 10^{-7}$ mol N m⁻² h⁻¹, respectively (table 6.4 a). The Winton series and alluvial soil established anaerobic conditions before the Wick series soil. Within 24 hours of raising the water table to 25 % soil core height, the mean N₂O emission rates for the Winton series, Alluvium soil and Wick series were about 40×10^{-7} , 13×10^{-7} and 1×10^{-7} mol N m⁻² h⁻¹, respectively (table 6.4 a). However, when the water table was 100 % core height in all three soils, the mean N₂O emission rates tended to follow the trend, Winton > Wick > Alluvium; this trend applied to each stage in the raising of the water table. The mean rates of N₂O emission

from the soils during the sequential increase in water table were generally of the order 10^{-5} to 10^{-4} mol N m⁻² h⁻¹ (table 6.4 a), similar to those reported in section 6.1, during fully saturated conditions. The N₂O emission rate increased with increasing water table height for all three soils but the increase in flux was small for the Wick series and alluvial soils (table 6.4 a) and was not proportional to the volume of saturated soil in the core. A smaller specific flux (mol kg⁻¹ h⁻¹) would be expected with increasing anoxic soil volume because an increased diffusion impedance, and hence residence time, allows greater reduction of N₂O to N₂.

In Wick series soil, there were small, short-term increases in N₂O emission rates during the 24 hour period immediately following an increase in water table height (Fig. 6.9 a; table 6.4 a). This feature was clearly seen when the cumulative N₂O trend was converted to point emission rates (Fig. 6.11). This could be the result of the rising water table effecting a mass movement of the soil atmosphere through the coarse texture. The alluvial soil only exhibited a short increase in N₂O emission rate, when the water table was raised to the core surface and the finer textured Winton series showed only a minimal increase during the same period (Fig. 6.11).

The mean N₂O emission rate for both the Wick series and the alluvium soil was lower when the water table was at the surface than when it was at 75 % of the core height (Fig. 6.9 a; table 6.4 a). This may have arisen because the soil slumped at 100 % saturation and so there was a film of water over the soil surface. The Wick series was more susceptible to slumping than the other two soils.

The effect of a progressive decrease in water table height on N₂O emission.

On each occasion when the water table was lowered, there was a rapid increase in the rate of N₂O emitted from each soil (Fig. 6.9; table 6.4 a), similar to that observed in section 5.2 (aggregate *de-gassing*). When the cumulative N₂O emission data were converted to point emission rates (Fig. 6.11), the effect of the draining events relative to the increase in water table height on N₂O emission was clearly illustrated. The three soils (6.11 a, b, c) each produced a very sharp increase in N₂O emission rate at the

time of each drainage event; the increased flux was very short lived, lasting only a few hours. In all three soils, the rates of N₂O emission were otherwise relatively constant. The maximum rates of N₂O emission from the Wick series and alluvium soil recorded after the drainage events, were of the order of 1×10^{-3} moles N m⁻² h⁻¹, while the maximum rate recorded from the Winton series was about 5×10^{-3} moles N m⁻² h⁻¹ (Fig. 6.11).

It can be seen from Fig. 6.9 and more clearly from Fig. 6.11, that there was no short term increase in N₂O flux from the Wick series soil when the water table was lowered for the first time (from the surface of the core to 75 % of the core height). This was due to the slumping of the soil aggregates, which had occurred to such an extent during saturated conditions, that water remained above the soil surface despite the initial core drainage sequence. When the water table was lowered further (75 % to 50 % core height), the short term flux due to aggregate *de-gassing* was observed.

Following the short term increase in flux after each drainage event, the N₂O emission rate returned to approximately the same order of magnitude as that emitted under fully saturated conditions, in each of the respective soils. Changes in the mean N₂O emission rates at each water table height (excluding the initial 24 hours following any change), appeared to be relatively minor from the Wick series and the alluvial soil (Fig. 6.13). By contrast, the Winton series emitted rates of N₂O that appeared to increase with the rise and fall of the water table (Fig. 6.13). The increase in rate from the Winton series during the progressive lowering of the water table, may be the result of the soil's fine texture restricting pore drainage due to capillary action. The water filled pores in the Winton series thus drained slower than those in the coarser textured soil, hence the N₂O emission rates appeared to increase with a lowering of the water table. However, the mean rates of N₂O emitted during the lowering of the water table (excluding *de-gassing* events) from all three soils, do not appear to be dependent on the saturated volume. The N₂O emitting zone was probably close to the surface of the core water table, below which N₂O was impeded by diffusion through the soil solution. The rates of N₂O emission during the lowering of the water table, including the rates from aggregate *de-gassing*, tended to follow the trend of Winton > Wick > Alluvium;

this is similar to previous trends seen under saturated conditions in this section and in section 6.1.

The effect of a progressive increase in water table height on CO₂ emission

In all three soils, there was a relatively small negative trend in CO₂ emission rates with increasing water table height (table 6.4 b) due to a progressive reduction in aerobic respiration and gas diffusion rate. When the water table was at the surface, the CO₂ emission rates for each of the three soils were similar to that attributed to the fully saturated cores in section 6.1 (about $2-4 \times 10^{-4}$ moles m⁻² h⁻¹). The mean CO₂ emission rates always followed the trend Winton > Alluvium > Wick (Fig. 6.10; table 6.4 b). The rates of CO₂ emission from each soil did not differ by more than a factor of 5, throughout the entire incubation period.

The effect of a progressive decrease in water table height on CO₂ emission

The draining of the soil facilitated the re-establishment of aerobic organisms, bringing about a general increase in the mean CO₂ emission rate (Fig. 6.10; table 6.4 b). The aggregate *de-gassing* events were small compared to the general emission rate of CO₂. This is seen clearly when the cumulative CO₂ emission data were transformed into rates (Fig. 6.12). Only the Winton series appeared to show any noticeable increase in CO₂ emission rate following drainage of the core.

Figure 6.9 Cumulative N_2O flux from (a) Wick series (b) Alluvium and (c) Winton series soil (cores re-packed with 2-5 mm diameter aggregates) incubated under a water table (WT) of variable height denoted as steps 1-7.

1 = WT at 25 % core height
 2 = WT at 50 % core height
 3 = WT at 75 % core height
 4 = WT at core surface

5 = WT at 75 % core height
 6 = WT at 50 % core height
 7 = WT at 25 % core height

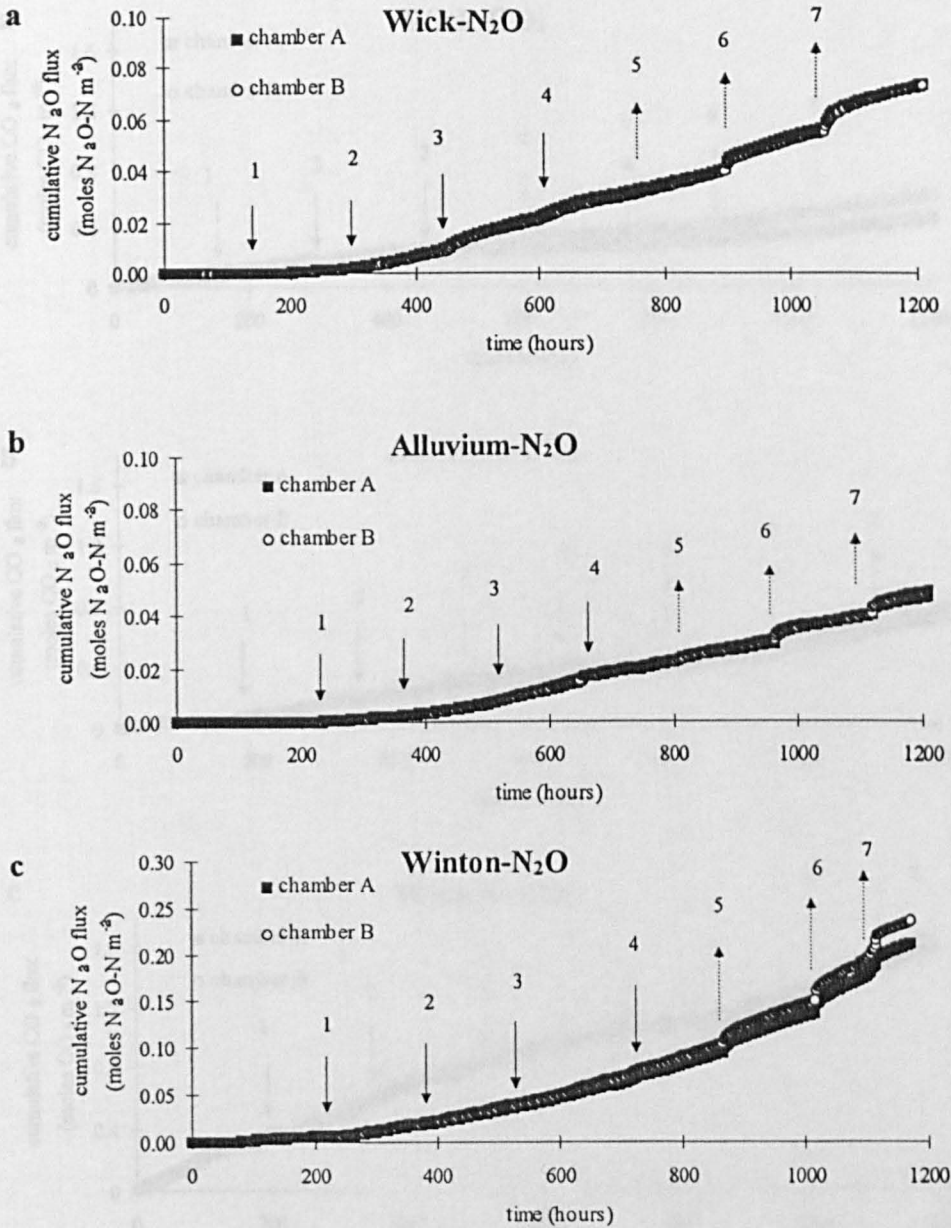


Figure 6.10 Cumulative CO₂ flux from (a) Wick series (b) Alluvium and (c) Winton series soil (cores re-packed with 2-5 mm diameter aggregates) incubated under a water table (WT) of variable height denoted as steps 1-7.

- | | |
|----------------------------|----------------------------|
| 1 = WT at 25 % core height | 5 = WT at 75 % core height |
| 2 = WT at 50 % core height | 6 = WT at 50 % core height |
| 3 = WT at 75 % core height | 7 = WT at 25 % core height |
| 4 = WT at core surface | |

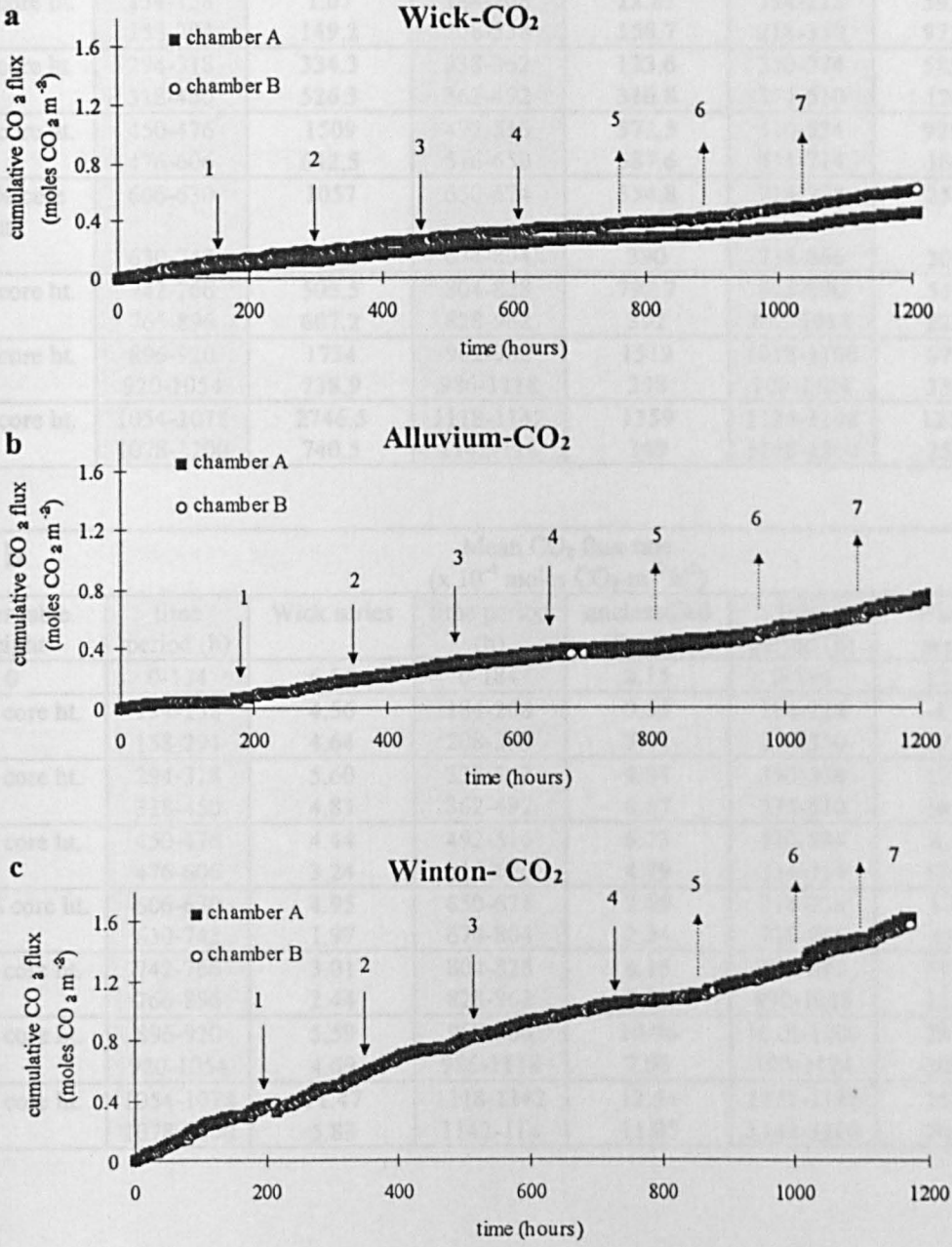


Table 6.4 Mean (a) N₂O and (b) CO₂ emission rate from cores re-packed with 3 different soils, that have undergone changes in core water table height.

a						
Mean N ₂ O flux rate (x 10 ⁻⁷ moles N ₂ O-N m ⁻² h ⁻¹)						
water table height	time period (h)	Wick series	time period (h)	unclassified alluvium	time period (h)	Winton series
0	0-134	0.68	0-184	0.49	0-194	1.97
25 % core ht.	134-158	1.07	184-208	12.83	194-218	39.75
	158-294	149.2	208-338	156.7	218-350	971.1
50 % core ht.	294-318	334.3	338-362	123.6	350-374	585.3
	318-450	526.3	362-492	316.8	374-510	1244
75 % core ht.	450-476	1509	492-516	572.5	510-534	979.7
	476-606	642.5	516-650	587.6	534-714	1665
100 % core ht.	606-630	1057	650-674	554.8	714-738	2570
	630-742	562.2	674-804	390	738-866	2064
75 % core ht.	742-766	505.5	804-828	792.7	866-890	5473
	766-896	607.2	828-962	392	890-1018	2226
50 % core ht.	896-920	1734	962-986	1519	1018-1100	6731
	920-1054	738.9	986-1118	398	100-1124	3310
25 % core ht.	1054-1078	2746.5	1118-1142	1359	1124-1148	12110
	1078-1200	740.5	1142-114	349	1148-1200	2598

b						
Mean CO ₂ flux rate (x 10 ⁻⁴ moles CO ₂ m ⁻² h ⁻¹)						
water table height	time period (h)	Wick series	time period (h)	unclassified alluvium	time period (h)	Winton series
0	0-134	6.56	0-184	2.15	0-194	17.40
25 % core ht.	134-158	4.56	184-208	9.53	194-218	-4.21
	158-294	4.64	208-338	7.61	218-350	17.23
50 % core ht.	294-318	5.60	338-362	4.94	350-374	17.86
	318-450	4.83	362-492	6.67	374-510	10.86
75 % core ht.	450-476	4.44	492-516	6.73	510-534	8.16
	476-606	3.24	516-650	4.79	534-714	10.35
100 % core ht.	606-630	4.95	650-674	2.69	714-738	6.46
	630-742	1.97	674-804	2.24	738-866	4.63
75 % core ht.	742-766	3.01	804-828	8.15	866-890	13.52
	766-896	2.44	828-962	5.29	890-1018	12.26
50 % core ht.	896-920	5.59	962-986	10.06	1018-1100	28.82
	920-1054	4.69	986-1118	7.93	100-1124	10.00
25 % core ht.	1054-1078	11.47	1118-1142	12.51	1124-1148	15.77
	1078-1200	5.83	1142-114	11.03	1148-1200	20.41

Residual N concentrations

The determination of the NO_3^- concentration in the three soils after the incubation revealed that about half of the total NO_3^- -N concentration (including that added as KNO_3) had been either denitrified or immobilized in both the Wick series and alluvial soils (Table 6.5). Virtually all the NO_3^- applied had been denitrified or immobilized in the Winton series. The greater loss from the Winton series reflects the greater total emission of N_2O , relative to the other soils. The NH_4^+ concentration of the Wick series appeared not to change, while the alluvium and Winton series showed a decline in NH_4^+ concentration over the incubation period (Table 6.5). This suggests that nitrification and immobilization occurred at a greater rate than mineralization in the finer textured soils; it would appear that in the Wick soil nitrification and immobilization processes may be equal to the mineralization rate.

Table 6.5 Mean NO_3^- and NH_4^+ concentration in the test soils prior to and following each incubation.

soil type	initial NO_3^- conc. of soil	conc. of NO_3^- added	residual soil NO_3^- conc.	initial NH_4^+ conc. of soil	conc. of NH_4^+ added	residual soil NH_4^+ conc.
Wick series	1.69	8.48	4.41	0.04	-	0.04
Alluvium	2.33	8.48	4.43	1.28	-	< 0.01
Winton series	1.77	8.48	0.91	1.50	-	0.42

Figure 6.11 N_2O emission rate from (a) Wick series (b) Alluvium and (c) Winton series soil (cores re-packed with 2-5 mm diameter aggregates) which have been incubated under a water table of variable height.

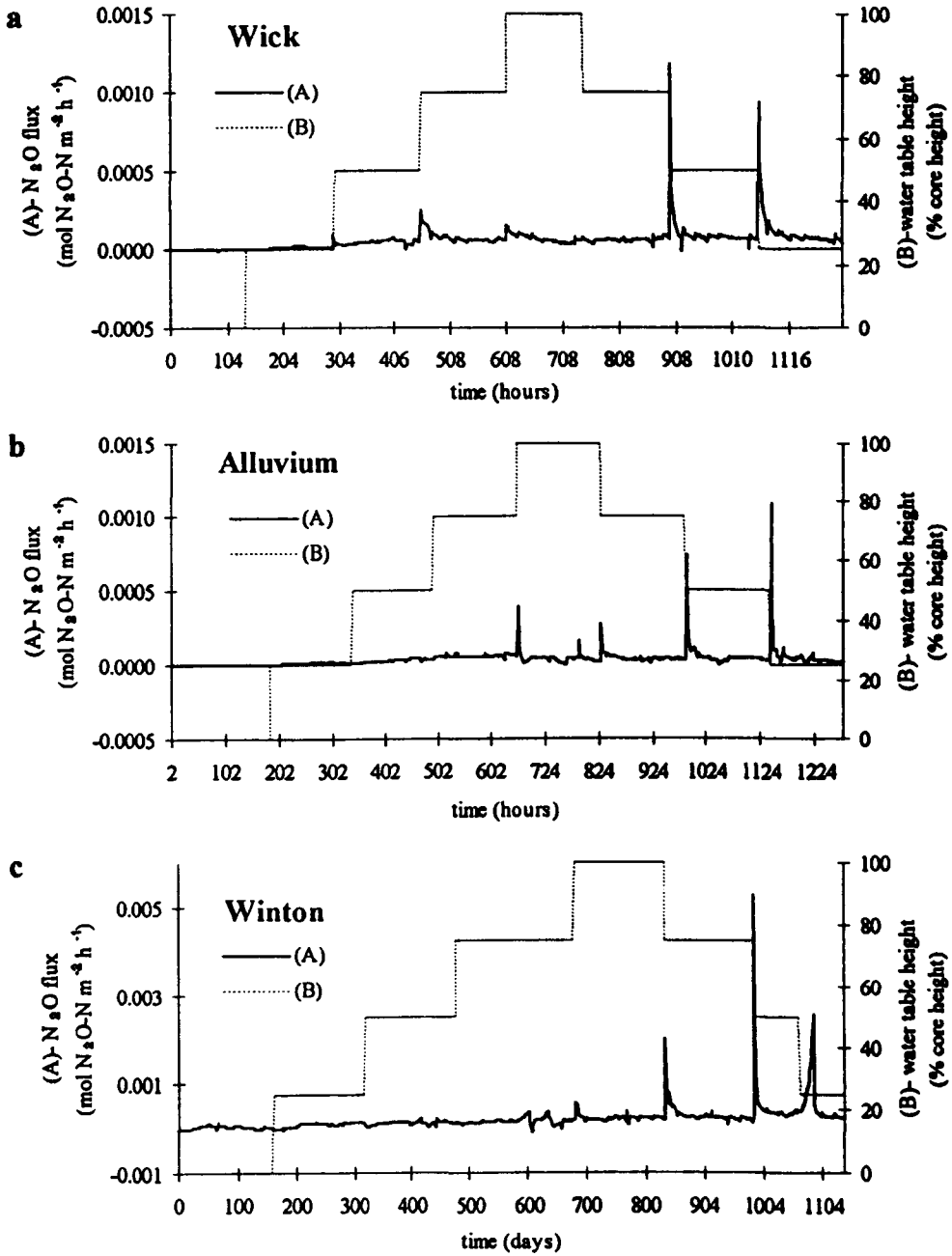


Figure 6.12 CO₂ emission rate from (a) Wick series (b) Alluvium and (c) Winton series soil (cores re-packed with 2-5 mm diameter aggregates) which have been incubated under a water table of variable height.

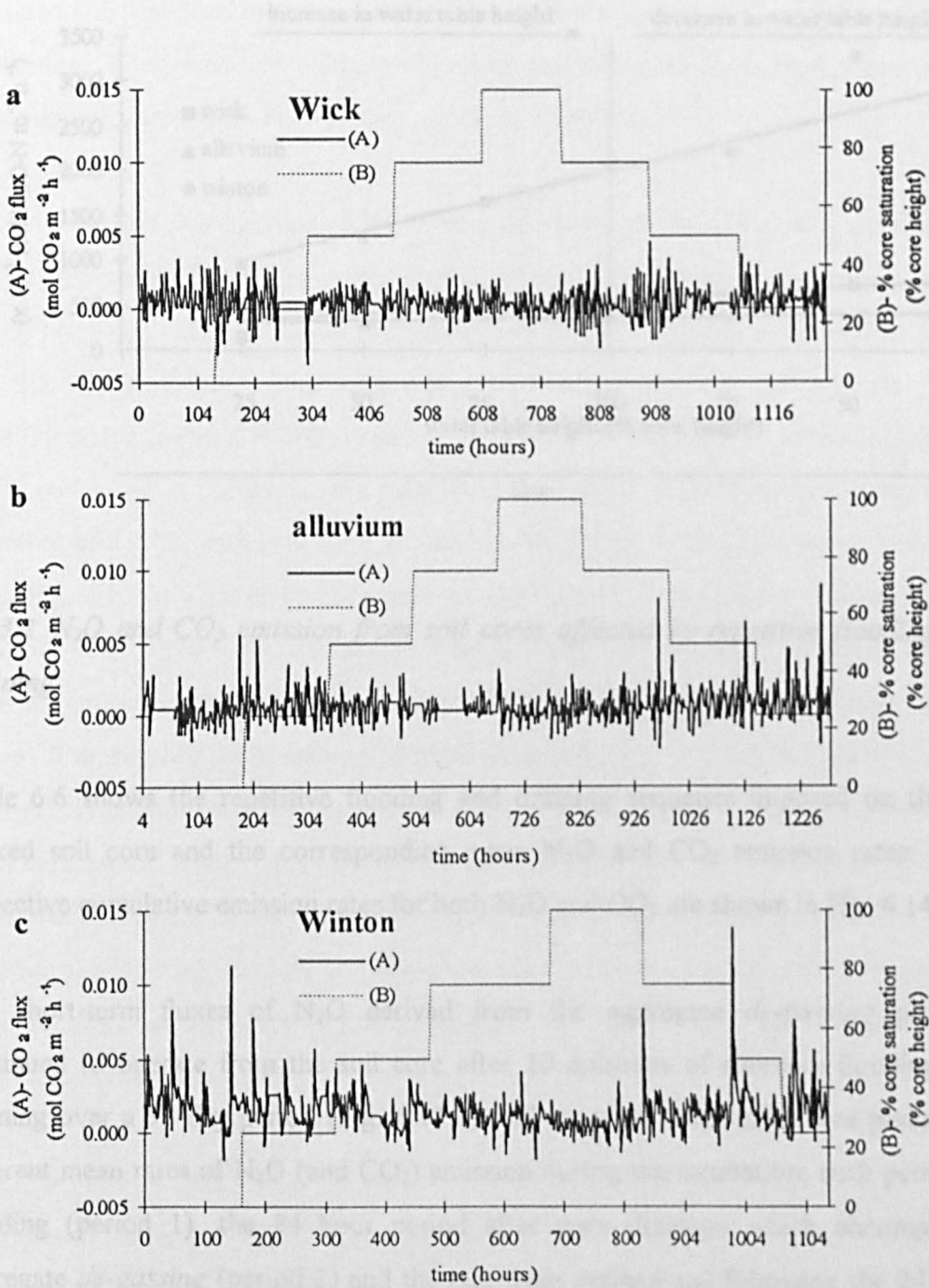
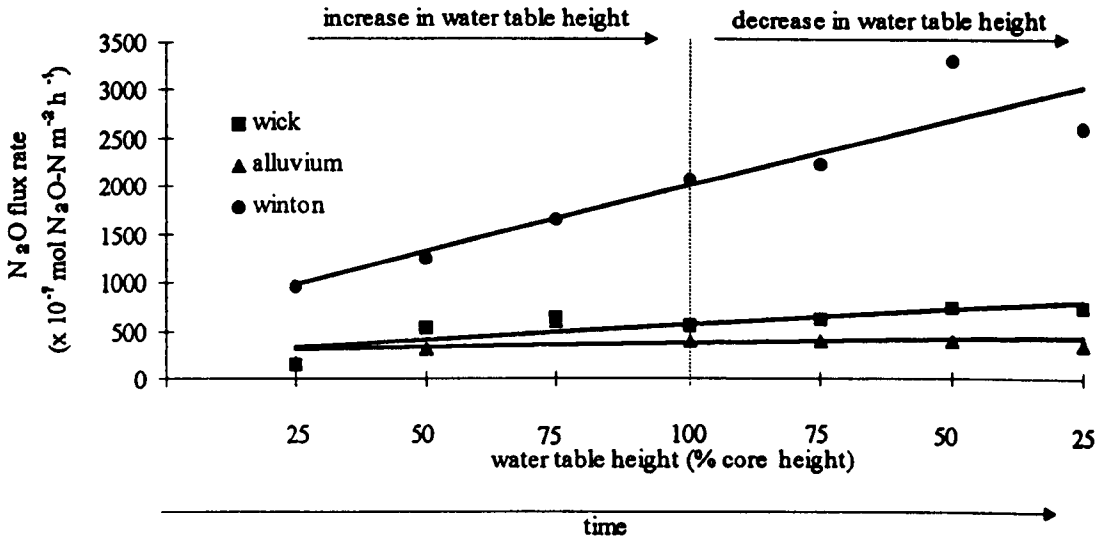


Figure 6.13 Mean N_2O emission rates at each stage during the progressive flooding and subsequent draining events (excluding the initial 24 hours after each change in water table height) for the three contrasting soils.



6.2.3.2 N_2O and CO_2 emission from soil cores affected by repetitive flooding and draining

Table 6.6 shows the repetitive flooding and draining sequence imposed on the re-packed soil core and the corresponding mean N_2O and CO_2 emission rates. The respective cumulative emission rates for both N_2O and CO_2 are shown in Fig. 6.14 a, b.

The short-term fluxes of N_2O derived from the aggregate *de-gassing* process, continued to operate from the soil core after 10 episodes of alternate flooding and draining over a 90 day period (Fig. 6.12 a). There were essentially three periods of different mean rates of N_2O (and CO_2) emission during the incubation; each period of flooding (period 1), the 24 hour period after core drainage which encompassed aggregate *de-gassing* (period 2) and the rate from drained soil following the 24 hour *de-gassing* period (period 3). The average of these mean rates during each period is expressed in table 6.6. The greatest mean rate of emission for both N_2O ($1.36 \times 10^{-4} \text{ mol N m}^{-2} \text{ h}^{-1}$) and CO_2 ($5.87 \times 10^{-4} \text{ mol m}^{-2} \text{ h}^{-1}$) occurred during period 2 (table 6.7).

The rates of emission for both N₂O and CO₂ during period 1, were always lower than period 3 (table 6.7). In the case of N₂O, this was because of air-filled *inter-aggregate* pores allowing rapid diffusion from residual pockets of anoxia within the soil core during period 3. By contrast, the greater rates of CO₂ in drained soil compared to saturated soil may also have been due to the re-establishment of the aerobic microbial population. There was little variation in mean emission rates for both gases at each of these periods (apart from N₂O on one occasion, at 560 h).

When the cumulative emissions of N₂O were expressed as rates (Fig. 6.15 a), the rapid short term fluxes of N₂O (*de-gassing*) that occurred with every drainage event were clearly observed. Similar to the rates observed during *de-gassing* episodes in section 6.1, the N₂O emissions were large and short-lived, lasting only a few hours. Apart from the drainage event at 560 hours, which gave a peak emission rate equivalent to $3 \times 10^{-3} \text{ mol N m}^{-2} \text{ h}^{-1}$, the emission rates from aggregate *de-gassing* were generally of the order of $6 \times 10^{-4} \text{ mol N m}^{-2} \text{ h}^{-1}$. Relative to N₂O (Fig. 6.15 a), the emission rates of CO₂ (Fig. 6.15 b) were essentially constant throughout the sequence of flooding as in previous trials. There was no apparent relationship between the N₂O emission rates from the *de-gassing* process and the extent of the time for which the soil was flooded (Fig 6.16 a), or with the duration of soil drainage (Fig. 6.16 b); this applied either with or without the anomalous (high) rate at 560 h. From Fig. 6.16 it seems that even a 24 h flooding period is enough to generate a maximal N₂O flush after draining (for 24 h). Also, the *de-gassing* flush seem unaltered despite frequent repetition (Fig. 6.15 a). Therefore, a diurnal flooding and draining cycle such as that occurring on beaches, tidal estuaries or in areas regularly irrigated may emit more N₂O than if these environments remained flooded.

The residual soil NO₃⁻ concentration determined after the incubation, was $1.57 \text{ mol NO}_3^- \text{-N m}^{-3}$, while the NH₄⁺-N concentration was $< 0.01 \text{ mol N m}^{-3}$, these were similar to the respective concentrations prior to incubation (2.26 and $0.03 \text{ mol N m}^{-3} \text{ soil}$). Once the added KNO₃ had been utilized in the soil core, the NO₃⁻ reduced during periods of flooding, was derived from nitrification during periods when the core was drained.

Figure 6.14 Cumulative (a) N_2O and (b) CO_2 flux from cores re-packed with aggregates from the Wick series soil (2-5 mm diameter aggregates) which have incubated during repetitive flooding and draining cycles (2 hours sampling rate).

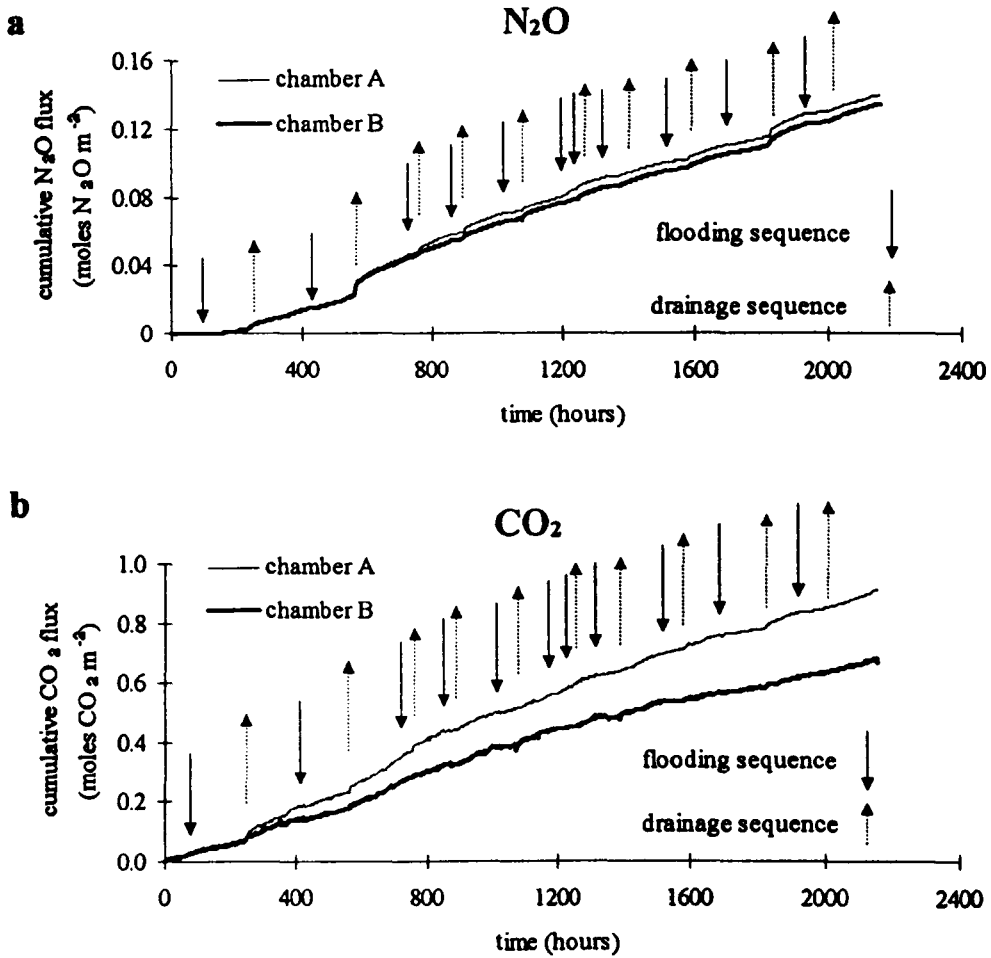


Figure 6.15 Rates of (a) N₂O and (b) CO₂ emission from cores re-packed with aggregates from the Wick series soil (2-5 mm diameter aggregates) which have incubated during repetitive flooding and draining cycles (2 hours sampling rate).

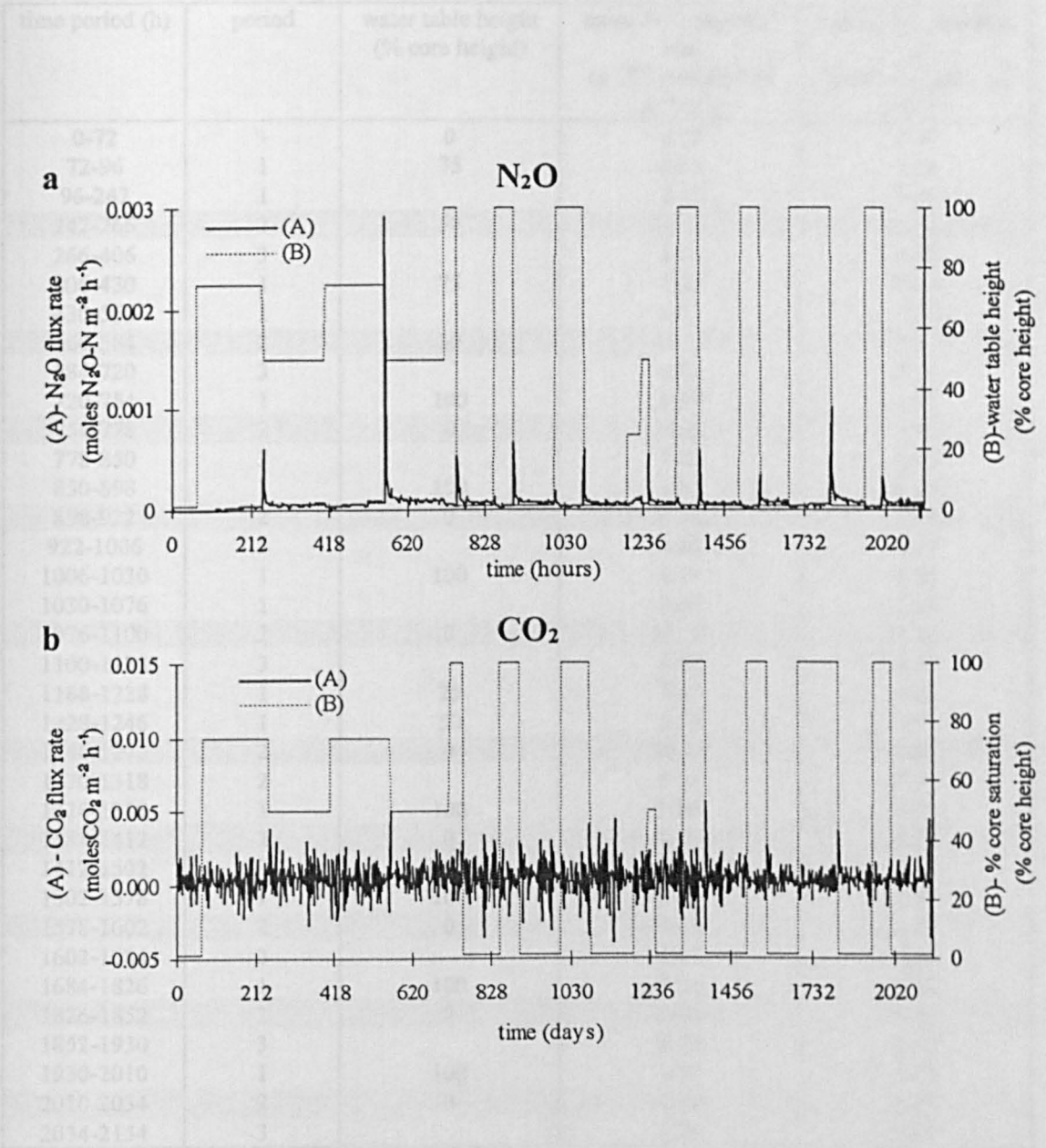


Table 6.6 Mean N₂O and CO₂ emission rates from cores re-packed with Wick series soil (2-5 mm diameter aggregates) that had undergone repetitive flooding and draining cycles (shaded areas represent the 24 hour period after the lowering of the water table).

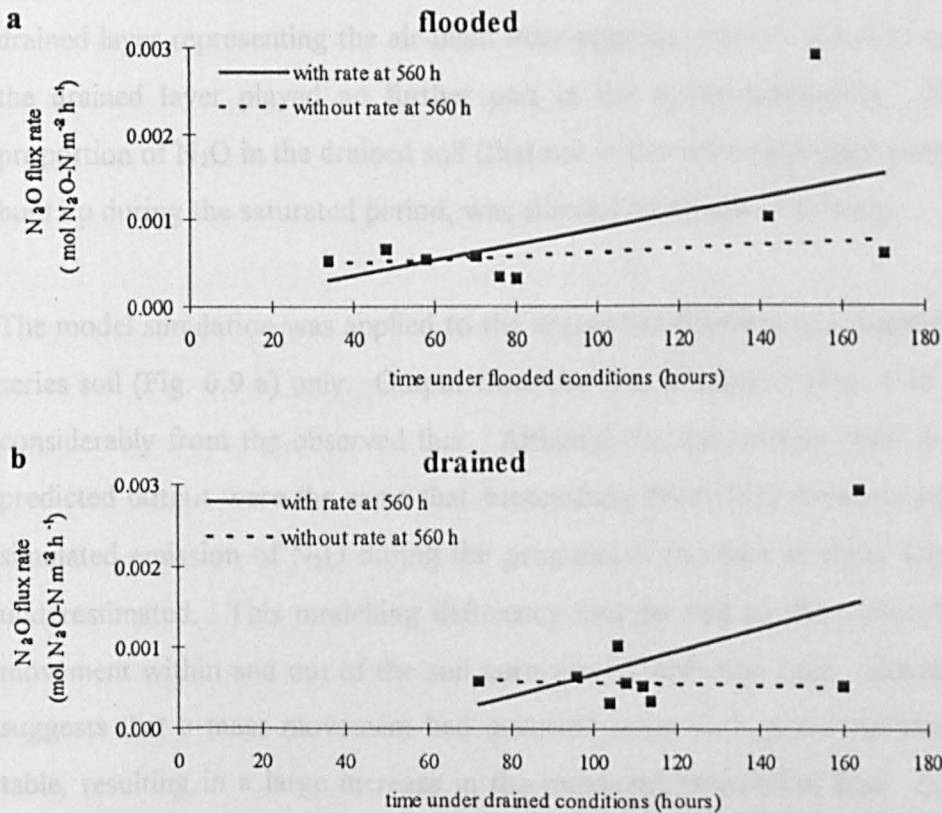
time period (h)	period	water table height (% core height)	mean N ₂ O emission rate ($\times 10^{-5}$ mol N ₂ O-N m ⁻² h ⁻¹)	mean N ₂ O emission rate ($\times 10^{-4}$ mol CO ₂ m ⁻² h ⁻¹)
0-72	-	0	0.27	3.87
72-96	1	75	0.03	2.75
96-242	1		2.16	2.46
242-266	2	50	10.61	9.91
266-406	3		5.08	4.69
406-430	1	75	2.89	0.16
430-560	1		5.67	3.30
560-584	2	50	30.19	8.17
584-720	3		8.84	5.94
720-754	1	100	4.97	4.83
754-778	2	0	14.11	5.92
778-850	3		7.02	4.93
850-898	1	100	3.21	0.45
898-922	2	0	12.80	5.82
922-1006	3		6.80	4.47
1006-1030	1	100	4.19	1.52
1030-1076	1		2.66	1.05
1076-1100	2	0	11.55	7.31
1100-1188	3		5.92	4.17
1188-1228	1	25	7.67	3.04
1228-1246	1	50	5.55	2.94
1246-1270	2	0	10.38	4.07
1270-1318	2		6.14	4.38
1318-1388	1	100	2.93	0.75
1388-1412	2	0	8.78	5.29
1412-1502	3		5.76	4.40
1502-1578	1	100	2.40	1.49
1578-1602	2	0	9.61	4.89
1602-1684	3		6.83	3.28
1684-1826	1	100	3.94	1.46
1826-1852	2	0	19.21	5.31
1852-1930	3		8.23	3.73
1930-2010	1	100	2.73	1.72
2010-2034	2	0	8.82	2.01
2034-2154	3		5.70	3.69

6.2.3.3 Modelling

Table 6.7 Mean of the average N_2O and CO_2 flux rates for the three periods defined during the repetitive flooding and draining of the soil. Periods 1, 2 and 3 represent flooded conditions, the 24 h following draining (encompassing *de-gassing*) and the remaining drained period, respectively

	period 1 (flooded)	period 2 (de-gassing)	period 3 (drained)
mean N_2O flux ($\times 10^{-5}$ mol N m^{-2} h^{-1}) (SD)	4.13 (1.70)	13.61 (6.61)	6.63 (1.18)
mean CO_2 flux ($\times 10^{-4}$ mol N m^{-2} h^{-1}) (SD)	2.18 (1.28)	5.87 (2.20)	4.37 (0.75)

Figure 6.16 Relationship between the peak emission rates of N_2O (y-axis) during the aggregate *de-gassing* events (period 2) and the time the core was (a) flooded (x-axis) and (b) drained (x-axis). The graphs include regression lines calculated with and without the anomalous rate that occurred at 560 h (outlier on figs a and b).



6.2.3.3 Modelling

The literature-derived and optimized parameters (table 6.3) applied in the previous simulations (Figs. 6.1, 6.3) were used, in an attempt to predict rates of N₂O emitted from a soil core undergoing a sequential rise and fall in the height of the water table (data from section 6.2).

Unsaturated conditions prevailed throughout the model layers at the start of the simulation; N₂O was produced at the rate k_2 and diffusion was through the air phase (D_a). As the water table rose up the model soil, the flooded layers were attributed an N₂O production rate, k_1 and the diffusion coefficient for N₂O movement in water (D_i). When the water table was lowered, each drained layer reverted to the parameters associated with unsaturated conditions (k_2 , D_a). To accommodate the lowering of the water table, a *drain* was incorporated into each of the four layers of the model soil. The *drain* facility was described by a simple flow equation, which only came into operation when each saturated model layer was drained. Invoking the *drain* established ambient atmospheric N₂O concentrations within the proportion of the drained layer representing the air-filled *inter*-aggregate pores; the N₂O extracted from the drained layer played no further part in the active simulation. The remaining proportion of N₂O in the drained soil (that not in the *inter*-aggregate pores), which had built up during the saturated period, was allowed to diffuse out freely.

The model simulation was applied to the sequential flooding and draining of the Wick series soil (Fig. 6.9 a) only. Output from the first simulation (Fig. 6.14 a, b) differed considerably from the observed flux. Although the parameters used to generate this predicted output were the same that successfully fitted N₂O fluxes in section 6.1, the simulated emission of N₂O during the progressive increase in water table height was underestimated. This modelling deficiency may be due to the assumption that N₂O movement within and out of the soil core was by diffusion only. However, Fig. 6.11 suggests that a mass movement had occurred upon each sequential rise in the water table, resulting in a large increase in the measured cumulative flux. Since events of N₂O mass movement were not accommodated within the model, the predicted output

was somewhat lower than that observed (Fig. 6.14 a). Furthermore, the model assumed that as each new section of the core attained saturated conditions (kI, D_s), the amount of N_2O (in solution) within each newly saturated zone was only equivalent to that in equilibrium with the ambient atmosphere. However, because water was introduced from below the N_2O concentration was certainly greater than ambient. Therefore each time the water table was raised the concentration gradient and hence flux between the top layer of each new saturated zone and the overlying unsaturated soil layer was underestimated. In reality, the concentration gradient between the top layer of each newly saturated zone and the corresponding overlying unsaturated layer would remain approximately the same with each rise in water table height. In the model, the amount of N_2O that had built up in previous saturated layers only diffused into the newly saturated layer.

The model was unable to accurately predict the N_2O flux during the *de-gassing* event, with N_2O emissions being greatly overestimated (Fig. 6.14 b). This model deficiency was unlikely to be the result of the simulated N_2O concentration within the saturated transmission pores, as it corresponded closely to the measured value in the drainage water. The predicted N_2O concentration just prior to drainage was 4.6 mol N m^{-3} water, while the actual N_2O concentration within the drainage water was measured at 2.1 mol N m^{-3} water (method described in section 5.2.2). Therefore this model deficiency was due to an over-simplification within the physical description of the *de-gassing* procedure. Rather than the whole soil layer *de-gassing* when drained, it may be that only a proportion of the soil volume was responsible for the short-term fluxes observed, due to the majority of soil pores being blocked by residual water. To illustrate this the model was modified to incorporate the assumption that *de-gassing* occurred within a depth of soil smaller than the depth of the drained layer; the number of identical layers within the soil core was therefore increased to 16. All other model principles and assumptions remained the same. When the model was re-run for the sequential rise and fall in water table height, it was assumed that during the lowering of the water table (from the soil surface to 75 % of the core height), that only the top 25 % of the drained layer volume underwent *de-gassing*. Hence, the volume *de-gassed* was a factor of 4 smaller than in previous model simulations (which used only 4 layers

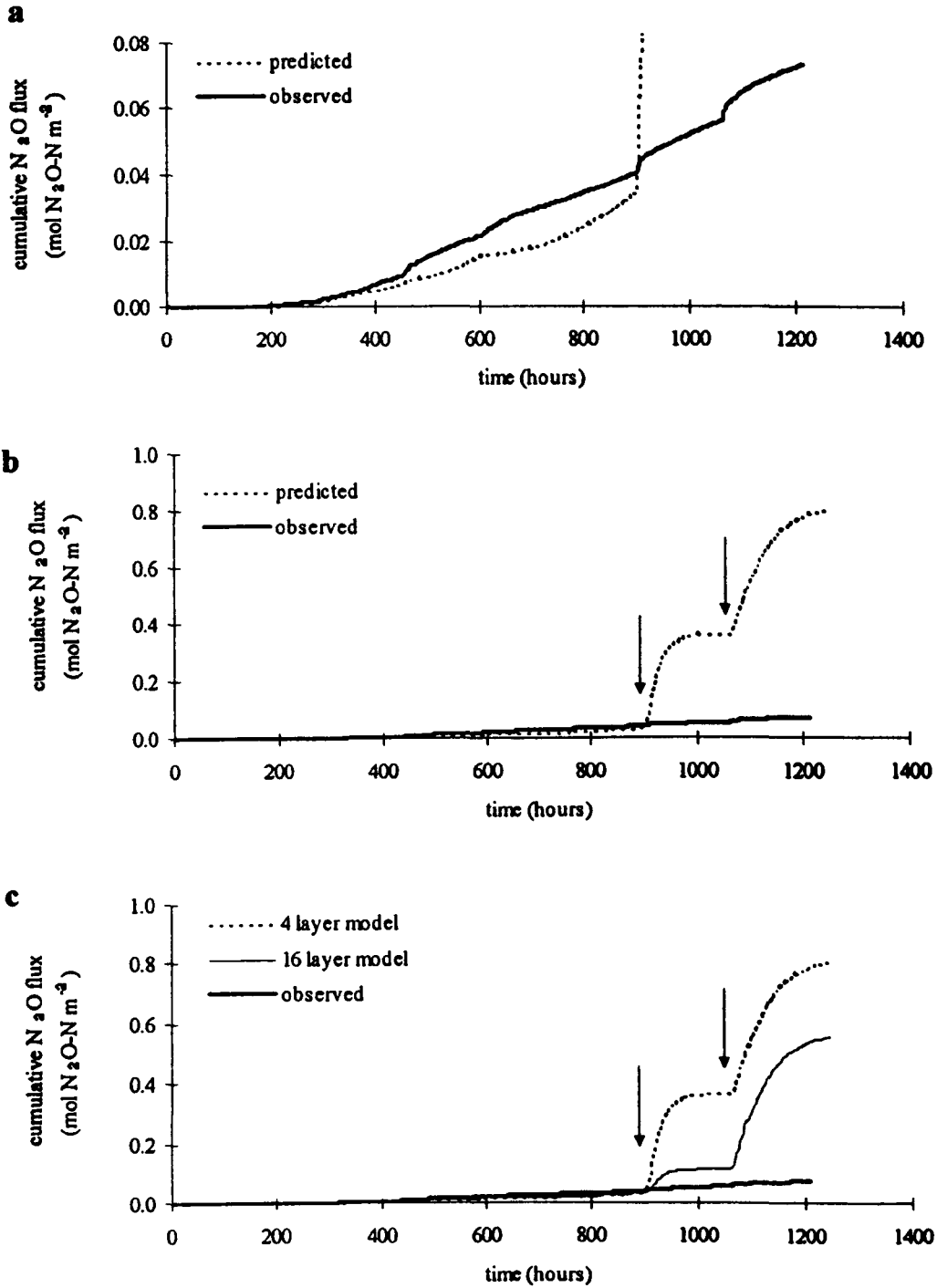
to describe the model soil). However, this assumption fails during the next draining sequence (75 % to 50 % core height) because all the layers above the second drained volume, which have not previously *de-gassed*, are also assumed to undergo *de-gassing* along with top 25 % of the second drained layer . Therefore the flux produced from the second drainage sequence is 4 times that of the first drainage step (Fig. 6.14 c.).

Consideration of the moisture release curve as a means of relating N₂O flux during *de-gassing* to air-filled porosity (as predicted by the relationship between the volumetric water content and matric potential; section 2.2.4.3) were also discounted. The assumption that only pores above a certain size facilitate *de-gassing* within a drained volume, would produce the same unrealistic increase in flux with each volume drained; for reasons described above where it was assumed that only the top layer of the drained zone *de-gasses*.

The proportion of the drained soil volume responsible for the flux during the first *de-gassing* event was tentatively estimated. The proportion of the measured amount of N₂O emitted during *de-gassing* relative to the modelled flux which assumed that the whole drained layer contributed to *de-gassing* approximates to 0.01 (Fig. 6.14 b). Therefore the equivalent proportion of the drained soil volume responsible for *de-gassing* is 1 %, which corresponds to a core layer thickness of 0.41 mm.

It seems likely that the disparity between the observed and predicted flux derived from *de-gassing* is dependent on both the volume of drained soil and the depth of the water table, which suggests a surface phenomenon depending in part on the continuity of pores. However, some of the disparity between the observed and predicted N₂O emissions may be due to a failing in the experimental procedure. As the draining of the core occurred outside the gas-tight chamber, it was possible that losses of N₂O to the atmosphere may have occurred, thus the observed data may be an underestimation of the true *de-gassing* flux. Future data acquisition, for experiments involving the raising and lowering of soil core water tables, may require adjustments in design and procedure; specifically, a method whereby the water table may be altered within the gas-tight chamber itself.

Figure 6.17 Observed and predicted cumulative N₂O fluxes from Wick series soil which has undergone a sequential rise and fall in the water table. (a) 4 layer model simulation (magnified) (b) 4 layer model simulation (full scale) (c) 4 and 16 layer model simulation. The arrows indicate time of drainage.



6.3 CONCLUSIONS

A 2 hour sampling rate enabled a comprehensive appraisal of the magnitude of peak N_2O emission rates, during changes in the soil environment. The increased frequency of measurements, highlighted the almost constant rate of N_2O emission under saturated conditions. Furthermore, the short-term increase in N_2O flux derived from aggregate *de-gassing* was found to occur over very short periods of time, in some instances, within 2 hours. The almost instantaneous increase in N_2O emission rate and the minimal change in CO_2 emission rates following *de-gassing*, strongly supports the assumption that the flux was physically derived and not of biological action. These *de-gassing* events were also found to occur in all three test soils, thus indicating the non-specificity of the process.

Although N_2O emission from unsaturated soil is influenced by aggregate size, under saturated conditions aggregate radius appears to have no effect at all, due to bulk core anoxia. However, the rate of N_2O and CO_2 emission from soil is affected by soil texture in both saturated and unsaturated conditions. Soil texture indirectly influences the soil's ability to supply carbon and NO_3^- and directly affects pore size, aggregation, water infiltration rates, water-holding capacity and aeration status of the soil. Emission rates of N_2O and CO_2 were influenced by different soil parameters. In unsaturated conditions gaseous emissions appeared to be affected by organic matter and clay content, while pH appeared to be the determining factor in saturated soils. The amount of clay and organic matter in unsaturated soil affected the N_2O emission rates by influencing diffusion and consumption of O_2 , respectively. When soil was saturated the entire system rapidly became anoxic and local variation in microbial respiration was of little importance, however, between soils, the pH determined the general denitrification rate.

The attempt to simulate N_2O emission using the results gained from these investigations was only partially successful. The model described in section 3 had to be altered to enable the predicted results to fit the observed emissions from soil that

was undergoing a transformation from unsaturated to saturated conditions. However, further deficiencies were found during simulations involving the sequential rise and fall in water table height. The inability of the model to correctly predict N₂O emissions under these conditions exposed gaps in knowledge and areas of future research regarding the short-term fluxes of N₂O from soil.

Summary

A system to continuously measure N₂O fluxes from soil at the laboratory scale was successfully developed. The automated soil headspace gas analyser system was found to be reliable and accurately identified short-term changes in N₂O emission rate. As expected, the rates of N₂O emission from soil were generally found to increase with concentration of soil NO₃⁻, soil water content and aggregate size (in unsaturated conditions only) in agreement with that reported in the literature (Weier *et al.*, 1993, VanCleemput *et al.*, 1994, Sexstone *et al.*, 1985 b, respectively).

Under unsaturated conditions, the variability in N₂O emissions may have been due to discrete organic residues; in one case Earthworm remains were responsible for the large variability between essentially identical re-packed soil cores. Similar studies (Parkin, 1987; Christensen *et al.*, 1990 a) have isolated vegetative residues in localized zones of soil as the source of large N₂O emissions. Earthworms have been found to positively influence gaseous N emissions by their cast development, their breakdown and excretion of residues and by their general amelioration of the soil matrix (Elliott *et al.*, 1990; Knight *et al.*, 1992; Parkin and Berry, 1994). However the effect of dead Earthworms (DFRs) on N₂O emissions in soil has not been previously investigated. The positive contribution on N₂O emission from DFR-amended soil, indicates the substantial effect that Earthworms can have on N₂O fluxes under certain environmental conditions. Earthworms, unlike plant material do not contain cellulose (Lee, 1985) and are therefore easily mineralized, thus creating localized zones of anoxia. Hence, the potential release of N₂O can be significant in soil conditions in which Earthworms proliferate.

Emissions of N₂O from the three test soils were greatly influenced by saturation and drainage cycles. In the field, the soil moisture content will vary considerably, after events of rainfall or frequent irrigation, where the surface layers of soil may become saturated for brief periods of time. In some instances, the surface layers of the soil may undergo many cycles of flooding and drainage, which on the evidence found here

can dramatically increase N₂O emission rates. Furthermore, the increases in N₂O flux following the drainage of saturated soils occurred almost instantaneously, but were short lived, in some cases lasting less than 2 hours. Hence, there is the potential for underestimating N₂O emissions, as these short-term fluxes can be easily missed during selective aggregative measurements in the field. The short-term flux of N₂O following rapid and intermittent flooding and drainage cycles is analogous to the effect of tidal movement on estuarine mud flats, intensively irrigated fields and frequent rainfall events in general.

It was evident from these trials, that a number of practices could be adopted to reduce N₂O emission from the soil to the atmosphere. A lower soil NO₃⁻ concentration will promote a greater conversion rate of N₂O to N₂, therefore the application of NO₃⁻ fertilizers should be at lower rates but more frequent. Additionally, if soil is to be amended with an easily decomposable carbon substrate (crop residues, manure), then this should also be carried out in low NO₃⁻ environments. However, in practice the energy required (and hence CO₂ produced) to carry out these proposals may well be greater than the reduction in the amount of N₂O emitted. In addition any extra costs will be met by the consumer of agricultural produce, which may not be politically acceptable.

The great uncertainty in the source strength in global inventories of N₂O (Houghton *et al.*, 1995) may be derived from underestimation of fluxes from the soil. Soil, whether in natural ecosystems or anthropogenically manipulated is by far the greatest source of N₂O (Bouwman, 1990). However, due to the variable nature of N₂O emission rates under different environmental conditions, there may be inaccuracies in taking representative flux measurements and extrapolating them into landscape or regional values. In addition, these investigations highlighted that soils of different textures also emit N₂O at different rates under different conditions. Hence, as the texture of soil can change considerably even at the field scale, it may be necessary to undertake a comprehensive analysis of N₂O emissions from distinct soil types under diverse environmental conditions in order to accurately quantify soil derived N₂O emissions.

Appendix

ref. no.	soil type (land use)	soil pH (H ₂ O)	soil conditions	mean N ₂ O flux (x 10 ⁻⁷ mol m ⁻² h ⁻¹)	reference
1	sandy loam	3.8	80 % F.C.	7.37 [*]	Christensen <i>et al.</i> , (1990 a)
2	sandy loam	3.8	100 % F.C.	108.6 [*]	Christensen <i>et al.</i> , (1990 a)
3	sandy loam	3.8	100 % F.C (+DFR) [†]	1810 [*]	Christensen <i>et al.</i> , (1990 a)
4	sandy loam	3.8	slurry	3789 [*]	Christensen <i>et al.</i> , (1990 a)
5	Mollic Albaqualfs	N/A	+ 5 mm rainfall	3.9	Corre <i>et al.</i> , (1993)
6	Mollic Albaqualfs	N/A	+ 10 mm rainfall	6.2	Corre <i>et al.</i> , (1993)
7	Mollic Albaqualfs	N/A	+ 20 mm rainfall	34	Corre <i>et al.</i> , (1993)
8	Mollic Albaqualfs	N/A	+ 40 mm rainfall	119	Corre <i>et al.</i> , (1993)
9	sandy	5.2	100 % F.C.	12.6 [*]	Bandibas <i>et al.</i> , (1994)
10	sandy	5.2	saturated	245 [*]	Bandibas <i>et al.</i> , (1994)
11	clay-sandy	6.1	100 % F.C.	76.6 [*]	Bandibas <i>et al.</i> , (1994)
12	clay-sandy	6.1	saturated	553 [*]	Bandibas <i>et al.</i> , (1994)
13	very heavy clay	7.4	100 % F.C.	89.8 [*]	Bandibas <i>et al.</i> , (1994)
14	very heavy clay	7.4	saturated	4016 [*]	Bandibas <i>et al.</i> , (1994)

ref. no.	soil type	soil pH (H ₂ O)	soil conditions	mean N ₂ O flux (x 10 ⁻⁷ mol m ⁻² h ⁻¹)	reference
15	sandy loam (grassland)	7	35 % moisture content 20 °C (-N)	437	VanCleemput et al., (1994)
16	sandy loam (grassland)	7	35 % moisture content 20 °C (+N)	1063	VanCleemput et al., (1994)
17	sandy soil	7.4	60 % WHC (-N,-C) 25 °C	13.4	Weier et al., (1993)
18	sandy soil	7.4	90 % WHC (-N,-C) 25 °C	73	Weier et al., (1993)
19	sandy soil	7.4	90 % WHC (+N,-C) 25 °C	202	Weier et al., (1993)
20	sandy soil	7.4	90 % WHC (+N,+C) 25 °C	7978	Weier et al., (1993)
21	silt loam	7.3	60 % WHC (-N,-C) 25 °C	23	Weier et al., (1993)
22	silt loam	7.3	90 % WHC (-N,-C) 25 °C	252	Weier et al., (1993)
23	silt loam	7.3	90 % WHC (+N,-C) 25 °C	392	Weier et al., (1993)
24	silt loam	7.3	90 % WHC (+N,+C) 25 °C	1517	Weier et al., (1993)
25	silt clay loam	6.5	60 % WHC (-N,-C) 25 °C	14	Weier et al., (1993)
26	silt clay loam	6.5	90 % WHC (-N,-C) 25 °C	133	Weier et al., (1993)
27	silt clay loam	6.5	90 % WHC (+N,-C) 25 °C	806	Weier et al., (1993)
28	silt clay loam	6.5	90 % WHC (+N,+C) 25 °C	12650	Weier et al., (1993)
29	gley soil	7	20 % moisture content 24 °C	26 ^P	Mulvaney and Kurtz (1984)
30	gley soil	7	50 % moisture content 24 °C	3857 ^P	Mulvaney and Kurtz (1984)
31	clay soil	6.4	Dec (7 °C)	mean = 7.1 peak = 321	Colbourn and Harper (1987)
32	clay soil	6.4	May (15 °C)	mean = 96 peak = 571	Colbourn and Harper (1987)

ref. no.	soil type	soil pH (H ₂ O)	soil conditions	N ₂ O flux (x 10 ⁻⁷ mol m ⁻² h ⁻¹)	reference
33	sandy loam	N/A	(+N) [†] (April)	72.5 ^m	Skiba <i>et al.</i> , (1994)
34	sandy clay loam (grass/lawn)	N/A	(+N) [†] (April)	11.1 ^m	Skiba <i>et al.</i> , (1994)
35	clay loam (grassland)	N/A	(+N) [†] (April)	234 ^m	Skiba <i>et al.</i> , (1994)
36	clay loam (grassland)	N/A	(+N) [†] (June)	0.03 ^m	Skiba <i>et al.</i> , (1994)
37	sandy loam (agricultural)	6.1	After heavy rainfall > 40mm (+N) 15 °C	1786 ^p	Hansen <i>et al.</i> , (1993)

* = converted from volumetric rate to flux; m = median emission rate; p = peak emission rate; N/A = not available

Bibliography

- Adel, A. (1938) Further details in the rock salt prismatic solar spectrum. *Astrophysics Journal*, 88, 186-188.
- Adel, A. (1939) Note on the atmospheric oxides of nitrogen. *Astrophysics Journal*, 90, 627-628.
- Alexander, M. (1977) *Introduction to soil microbiology* (2nd Edition) Wiley and Sons, New York.
- Allison, F.E. (1955) The enigma of soil nitrogen balance sheets. *Advances in Agronomy*, 7, 213-250.
- Ambus, P. (1993) Control of denitrification enzyme activity in a streamside soil. *FEMS Microbiology Ecology*, 102, 225-234.
- Ambus, P. and Christensen, S. (1993) Denitrification variability and control in a riparian fen irrigated with agricultural drainage water. *Soil Biology and Biochemistry*, 25, 915-923.
- Ambus, P. and Christensen, S. (1995) Spatial and seasonal nitrous-oxide and methane fluxes in Danish forest-ecosystems, grassland-ecosystems, and agro-ecosystems. *Journal of Environmental Quality*, 24, 993-1001.
- Arah, J.R.M. and Smith, K.A. (1989) Steady state denitrification in aggregated soils: a mathematical model. *Journal of Soil Science*, 40, 139-149.
- Arah, J.R.M., Crichton, I.J. and Smith, K.A. (1993) Denitrification measured directly using a single inlet mass spectrometer and by acetylene inhibition. *Soil Biology and Biochemistry*, 25, 233-238.
- Arnold, P.W. (1954) Loss of nitrous oxide from soil. *Journal of Soil Science*, 5, 116-128.
- Aulakh, M.S., Rennie, D.A. and Paul, E.A. (1982) Gaseous nitrogen losses from cropped and summer-fallowed soils. *Canadian Journal of Soil Science*, 62, 187-195.
- Aulakh, M.S., Rennie, D.A. and Paul, E.A. (1984 a) Gaseous nitrogen losses from soils under zero-till as compared with conventional-till management systems. *Journal Environmental Quality*, 13, 130-136.
- Aulakh, M.S., Rennie, D.A. and Paul, E.A. (1984 b) Acetylene and N-Serve effects upon N₂O emissions from NH₄⁺ and NO₃⁻ treated soils under aerobic and anaerobic conditions. *Soil Biology and Biochemistry*, 16, 351-356.

- Aulakh, M.S. and Doran, J.W. (1990) Effectiveness of acetylene inhibition of N₂O reduction for measuring denitrification in soils of varying wetness. *Communications in Soil Science and Plant Analysis*, 21, 2223-2243.
- Aulakh, M.S., Doran, D.T., Walters, and Power, J.F. (1991) Legume residues and soil water effects on denitrification in soils of different textures. *Soil Biology and Biochemistry*, 23, 1161-1167.
- Aulakh, M.S., Doran, D.T. and Mosier, A.R. (1992) Soil Denitrification-Significance, Measurement and Effects of Management. *Advances in Soil Science*, 18, 2-57.
- Avalakki, U.K., Strong, W.M. and Saffigna, P.G. (1995) Measurement of gaseous emissions from denitrification of applied ¹⁵N. 3. Field measurements. *Australian Journal of Soil Research*, 33, 101-111.
- Badr, O. and Probert, S.D. (1993) Environmental impacts of atmospheric nitrous oxide. *Applied Energy*, 44, 197-231.
- Bailey, L.D. (1976) Effects of temperature and root on denitrification in a soil. *Canadian Journal of Soil Science*, 56, 79-87.
- Bailey, L.D. and Beauchamp, E.G. (1973) Gas chromatography of gases emanating from a saturated soil system. *Canadian Journal of Soil Science*, 53, 122-124.
- Bandibas, J., Vermoesen, A., Degroot, C.J. and VanCleemput, O. (1994) The effect of different moisture regimes and soil characteristics on nitrous-oxide emission and consumption by different soils. *Soil Science*, 158, 106-114.
- Banin, A. (1986) Global budget of N₂O: The role of soils and their change. *The Science of the Total Environment*, 55, 27-38.
- Beauchamp, E.G., Bergstrom, D.W. and Burton, D.L. (1996) Denitrification and nitrous oxide production in soil fallowed or under alfalfa or grass. *Communications in Soil Science and Plant Analysis*, 27, 87-99.
- Bergstrom, D.W., Tenuta, M., and Beauchamp, E.G. (1994) Increase in nitrous-oxide production in soil induced by ammonium and organic-carbon. *Biology and Fertility of Soils*, 18, 1-6.
- Betlach, M.R. and Tiedje, J.M. (1981) Kinetic explanation for accumulation of nitrite, nitrite oxide and nitrous oxide during bacterial denitrification. *Applied Environmental Microbiology*. 42, 1074-1084.
- Blackmer, A.M., Baker, J.H. and Weeks, M.E. (1974) A simple gas chromatographic method for separation of gases in soil atmospheres. *Soil Science Society of America Proceedings*, 38, 689-690.
- Blackmer, A.M. and Bremner, J.H. (1977) Gas chromatographic analysis of soil atmospheres. *Soil Science Society of America Journal*, 41, 908-912.

- Blackmer, A.M. and Bremner, J.H. (1978) Inhibitory effect of nitrate on reduction of N_2O to N_2 by soil micro-organisms. *Soil Biology and Biochemistry*, 10, 187-191.
- Blok, K. and De Jager, D. (1994) Effectiveness of non- CO_2 greenhouse gas emission reduction technologies. *Environmental Monitoring and Assessment*, 31, 17-40.
- Blosl, M. and Conrad, R. (1992) Influence of an increased pH on the composition of the nitrate-reducing microbial populations in an anaerobically incubated acidic forest soil. *Applied Microbiology*, 15, 624-627.
- Bouwman, A.F., (1990) Exchange of greenhouse gases between terrestrial ecosystems and the atmosphere. In *Soils and the Greenhouse Effect*, pp 61-127 (Ed. Bouwman, A.F.) Wiley, Chichester.
- Bouwman, A.F., Fung, I., Matthews, E. and John, J. (1993) Global analysis of the potential for N_2O production in natural soils. *Global Biogeochemical Cycles*, 7, 557-597.
- Bowden, R.D., Melillo, J.M., Steudler, P.A. and Aber, J.D. (1991) Effects of nitrogen additions on annual nitrous-oxide fluxes from temperate forest soils in the north-eastern united-states. *Journal of Geophysical Research-Atmospheres*, 96, 9321-9328.
- Bowman, R.A. and Focht, D.D. (1974) The influence of glucose and nitrate concentrations upon denitrification rates in a sandy soil. *Soil Biology and Biochemistry*, 6, 297-301.
- Breitenbeck, G.A., Blackmer, A.M. and Bremner, J.M. (1980) Effects of different nitrogen fertilizers on emission of nitrous oxide from soil. *Geophysical Research Letters*, 7, 85-88.
- Bremner, J.M. and Blackmer, A.M. (1978) Nitrous oxide emission from soils during nitrification with fertilizer nitrogen. *Science*, 199, 295-296.
- Bremner, J.M. and Blackmer, A.M. (1981) Terrestrial nitrification as a source of atmospheric nitrous oxide. In *Denitrification, Nitrification and atmospheric nitrous oxide*, pp. 151-170 (Ed. Delwiche, C.C.) Wiley and Sons, New York.
- Bremner, J.M., Breitenbeck, G.A. and Blackmer, A.M. (1981) Effect of nitrapyrin on emission of nitrous oxide from soil fertilized with anhydrous ammonia. *Geophysical Research Letters*, 8, 353-356.
- Bronson, K.F., Mosier, A.R. and Bishnoi, S.R. (1992) Nitrous-oxide emissions in irrigated corn as affected by nitrification inhibitors. *Soil Science Society of America Journal*, 56, 161-165.

- Bruggemann, D.A.G. (1935) The calculation of various physical constants of heterogeneous substances. I. The dielectric constants and conductivities of mixtures composed of isotopic substances. *Ann. Physik*, 24, 636-664.
- Burford, J.R. (1969) Single sample analysis of N₂-N₂O-CO₂-Ar-O₂ mixtures by gas chromatography. *Journal Chromatography Science*, 7, 760-762.
- Burton, D.L. and Beauchamp, E.G. (1985) Denitrification rate relationships with soil parameters in the field. *Communications in Soil Science and Plant Analysis*, 16, 539-549.
- Burton, D.L. and Beauchamp, E.G. (1994) Profile nitrous-oxide and carbon-dioxide concentrations in a soil subject to freezing. *Soil Science Society of America Journal*, 58, 115-122.
- Chalk and Smith (1983) Chemodenitrification. In *Gaseous loss of nitrogen from plant soil systems*, Developments in Soil Science vol.9, pp. 65-89 (Eds. Freney, J.R. and Simpson, J.R.). Martinus Nijhoff/Dr.W.Junk Publishers, The Hague.
- Chen, D.L., Freney, J.R., Mosier, A.R. and Chalk, P.M. (1994) Reducing denitrification loss with nitrification inhibitors following pre-sowing applications of urea to a cotton-field. *Australian Journal of Experimental Agriculture*, 34, 75-83.
- Cho, C.M. and Mills, J.G. (1979) Kinetic formulation of the denitrification process in soil. *Canadian Journal of Soil Science*, 59, 249-257.
- Christensen, S., Simkins, S. and Tiedje, J.M. (1990 a) Spatial variation in denitrification dependency of activity centres on the soil environment. *Soil Science Society of America Journal*, 54, 1608-1613.
- Christensen, S., Simkins, S. and Tiedje, J.M. (1990 b) Temporal patterns of soil denitrification: their stability and causes. *Soil Science Society of America Journal*, 54, 1614-1618.
- Cicerone, R.J., Shetter, J.D., Stedman, D.H., Kelly T.J. and Liu, S.C. (1978) Atmospheric N₂O, measurements to determine its sources, sinks and variations. *Journal of Geophysical Research*, 83, 3042-3050.
- Clay, D.E., Molina, J.A.E., Clapp, C.E. and Linden, D.R. (1985) Nitrogen-tillage-residue management. 2. Calibration of potential rate of nitrification by model simulation. *Soil Science Society of America Journal*, 49, 322-325.
- Clayton, H., Arah, J.R.M. and Smith, K.A. (1994) Measurement of nitrous-oxide emissions from fertilized grassland using closed chambers. *Journal of Geophysical Research-Atmospheres*, 99, 16599-16607.

- Cochran, V.L., Elliott, L.F. and Papendick, R.I. (1981) Nitrous oxide emissions from a fallow field fertilized with anhydrous ammonia. *Soil Science Society of America Journal*, 45, 307-310.
- Colbourn, P. and Harper, I.W. (1987) Denitrification in drained and undrained arable clay soil. *Journal of Soil Science*, 38, 531-539.
- Colbourn, P (1993) Limits to denitrification in two pasture soils in a temperate maritime climate. *Agricultural Ecosystem Environment*, 43, 49-68.
- Conrad, R., Seiler, W. and Bunse, G. (1983) Factors influencing the loss of fertilizer nitrogen in the atmosphere as N₂O. *Journal of Geophysical Research*, 88, 6709-6718.
- Coolman, R.M. and Robarge, W.P. (1995) Sampling nitrous oxide emissions from humid tropical ecosystems. *Journal of Biogeography*, 22, 381-391.
- Corfee-Morlott, J., Schwengels, P. and Lurding, S. (1994) National GHG inventories: recent developments under the IPCC/OECD joint programme. *Environmental Monitoring and Assessment*, 31, 41-52.
- Corre, M.D., Vankessel, C., Pennock, D.J. and Solohub, M.P. (1995) Ambient nitrous-oxide emissions from different landform complexes as affected by simulated rainfall. *Communications in Soil Science and Plant Analysis*, 26, 2279-2293.
- Coyne, M.S., Gilfillen, R.A. and Blevins, R.L. (1994) Nitrous-oxide flux from poultry-manured erosion plots and grass filters after simulated rain. *Applied and Environmental Quality*, 23, 831-834.
- Crank, J., McFarlane, N.R., Newby, J.C., Paterson, G.D. and Pedley, J.B. (1981) *Diffusion processes in environmental systems*. Macmillan Press Ltd., London.
- Crutzen, P.J. (1994) Global budgets for non-CO₂ greenhouse gases. *Environmental Monitoring and Assessment*, 31, 1-15.
- Currie J.A. (1960) Gaseous diffusion in porous media: 2. Dry granular materials. *British Journal of Applied Physics*, 11, 318-323.
- Currie J.A. (1961) Gaseous diffusion in porous media. 3. Wet granular materials. *British Journal of Applied Physics*, 12, 275-281.
- Davidson, E.A. and Firestone, M.K. (1988) Measurement of nitrous oxide dissolved in soil solution. *Soil Science Society of America Journal*, 52, 1201-1203.
- Davidson, E.A. (1992) Sources of nitric-oxide and nitrous-oxide following wetting of dry soil. *Soil Science Society of America Journal*, 56, 95-102.

- Davidson, E.A. and Schimel, J.P. (1995) Microbial processes of production and consumption of NO, N₂O and CH₄. In *Biogenic Trace gases: Measuring Emissions from soil and water*. pp 327-353 (Eds. Matson, P.A. and Harriss, R.C.). Blackwell Scientific.
- Dendooven, L. and Anderson, J.M. (1994) Dynamics of reduction enzymes involved in the denitrification process in pasture. *Soil Biology and Biochemistry*, 26, 1501-1506.
- Dendooven, L. and Anderson, J.M. (1995) Use of a least square optimization procedure to estimate enzyme characteristics and substrate affinities in the denitrification reactions in soil. *Soil Biology and Biochemistry*, 27, 1261-1270.
- Dibb, J.E., Rasmussen, R.A., Mayewski, P.A. and Holdsworth, G. (1993) Northern hemisphere concentrations of methane and nitrous oxide since 1800: results from Mt. Logan and 20D ice cores. *Chemosphere*, 27, 2413-2423.
- Dickinson, R.E. and Cicerone, R.J. (1986) Future global warming from atmospheric trace gases *Nature*, 319, 109-115.
- Dorland, S. and Beauchamp, E.G. (1991) Denitrification and ammonification at low temperatures. *Canadian Journal of Soil Science*, 71, 293-303.
- Dowdell, R.J. and Smith, K.A. (1974) Field studies of the soil atmosphere II. Occurrence of nitrous oxide. *Journal of Soil Science*, 25, 231-238.
- Dowdell, R.J. and Webster, C.P. (1984) A lysimeter study of the fate of fertilizer nitrogen in spring barley crops grown on a shallow soil overlying chalk: denitrification losses and the nitrogen balance. *Journal of Soil Science*, 35, 183-190.
- Drury, C.F., McKenney, D.J. and Findlay, W.I. (1992) Nitric-oxide and nitrous-oxide production from soil - water and oxygen effects. *Soil Science Society of America Journal*, 56, 766-770.
- Eggington, G.M. and Smith, K.A. (1986) Losses of nitrogen by denitrification from a grassland soil fertilized with cattle slurry and calcium nitrate. *Journal of Soil Science*, 37, 69-80.
- Elliott, P.W., Knight, D. and Anderson, J.M. (1990) Denitrification in Earthworm casts and soil from pastures under different fertilizer and drainage systems. *Soil Biology and Biochemistry*, 22, 601-605.
- Eichner, M. (1990) Nitrous oxide emissions from fertilized soils: Summary of available data. *Journal of Environmental Quality*, 19, 272-280.
- Eriksen, A.B. and Holtanhartwig, L. (1993) Emission-spectrometry for direct measurement of nitrous-oxide and dinitrogen from soil. *Soil Science Society of America Journal*, 57, 738-742.

- Fillery, I.R.P. (1983) Biological Denitrification. In *Gaseous loss of nitrogen from plant soil systems*, Developments in Soil Science vol. 9, pp. 33-64 Martinus Nijhoff/Dr. W. Junk Publishers, The Hague.
- Firestone, M.K. and Tiedje, J.M. (1979) Temporal change in nitrous oxide and dinitrogen from denitrification following onsets of anaerobiosis. *Applied Environmental Microbiology*, 38, 673-679.
- Firestone, M.K., Smith, M.S., Firestone, R.B. and Tiedje, J.M. (1979) The influence of of nitrate, nitrite and oxygen on the composition of the gaseous products of denitrification in soil. *Soil Science Society of America Journal*, 43, 1140-1144.
- Firestone, M.K., Firestone, R.B. and Tiedje, J.M. (1980) Nitrous oxide from soil denitrification: Factors controlling its biological production. *Science*, 208, 749-751.
- Firestone, M.K. and Davidson, E.A. (1989) Microbiological basis of NO and N₂O production and consumption in soil. In *Exchange of trace gases between terrestrial ecosystems and the atmosphere*, pp. 7-21 (Eds. Andreae, M.O. and Schimel, D.S.) John Wiley and Sons.
- Flessa, H. and Beese, F. (1995) Effects of sugar-beet residues on soil redox potential and nitrous-oxide emission. *Soil Science Society of America Journal*, 59, 1044-1051.
- Flessa, H., Dorsch, P. and Beese, F. (1995) Seasonal variation of N₂O and CH₄ fluxes in differently managed arable soils in southern Germany. *Journal of Geophysical Research-Atmospheres*, 100, 23115-23124.
- Focht, D.D. (1974) The effect of temperature, pH, and aeration on the production of nitrous oxide and gaseous nitrogen- a zero-order kinetic model. *Soil Science*, 118, 173-179.
- Focht, D.D., Voloras, N. and Letey, J. (1980) Use of interfaced gas chromatography-mass spectrometry for detection of concurrent mineralization and denitrification in soil. *Journal Environmental Quality*, 9, 218-223.
- Folorunso, O.A. and Rolston, D.E. (1985) Spatial variability of field measured denitrification gas fluxes. *Soil Science Society of America Journal*, 48, 1214-1219.
- Foth, H.D. (1978) *Fundamentals of Soil Science* (6th Edition), Wiley, Chichester.
- Freney, J.R., Denmead, O.T. and Simpson J.R. (1979) Nitrous oxide emission from soils at low moisture contents. *Soil Biology and Biochemistry*, 11, 167-173.
- Garciaplazaola, J.I., Becerril, J.M., Arreseigor, C., Gonzalezmurua, C. and Aparicotejo, P.M. (1993) The concentration of *Rhizobium-meliloti* to soil denitrification. *Plant and Soil*, 157, 207-213.

- Germon, J.C. (1985) Denitrification in cropped soils. *Fertilizers and Agriculture*, 89, 3-13.
- Ghoshal, S. and Larsson, B. (1975) Gas chromatographic studies on soil denitrification. 1. An isothermic separation method for evolved gases using *carbosieve-B* as the packing. *Acta Agriculture Scandinavia*, 25, 275-280.
- Goodroad, L.L. and Keeney, D.R. (1984) Nitrous-oxide production in aerobic soils under varying pH, temperature and water-content. *Soil Biology and Biochemistry*, 16, 39-43.
- Grant, R.F. (1991) A technique for estimating denitrification rates at different soil temperatures, water contents and nitrate concentrations. *Soil Science*, 152, 41-52.
- Grant, R.F., Nyborg, M. and Laidlaw, J.W. (1993 a) Evolution of nitrous-oxide from soil. 1. Model development. *Soil Science*, 156, 259-265.
- Grant, R.F., Nyborg, M. and Laidlaw, J.W. (1993 b) Evolution of nitrous-oxide from soil. 2. Experimental results and model. *Soil Science*, 156, 266-277.
- Grant, R.F. (1995) Mathematical-modelling of nitrous-oxide evolution during nitrification. *Soil Biology and Biochemistry*, 27, 1117-1125.
- Greenwood, D.J. (1961) The effect of oxygen concentration on the decomposition of organic material in soil. *Plant and Soil*, 14, 360-376.
- Groffman, P. M. (1991) Ecology of nitrification and denitrification in soil evaluated at scales relevant to atmospheric chemistry. In *Microbial production and consumption of greenhouse gases: methane, nitrogen oxides and halomethanes*, pp. 201-217 (Eds. Rogers, J.E. and Whitman, W.B.) American Society for Microbiology, Washington, DC.
- Groffman, P.M. and Turner, C.L. (1995) Plant productivity and nitrogen gas fluxes in a tall-grass prairie landscape. *Landscape Ecology*, 10, 255-266.
- Hansen, S., Maehlum, J.E. and Bakken, L.R. (1993) N₂O and CH₄ fluxes in soil influenced by fertilization and tractor traffic. *Soil Biology and Biochemistry*, 25, 621-630.
- Hao, W.M., Wofsey, S.C., McElroy, M.B., Beer, J.M. and Togan, M.A. (1987) Sources of atmospheric nitrous oxide from combustion. *Journal of Geophysical Research*, 92, 3098-3104.
- Hargreaves, K.J., Skiba, U., Fowler, D., Arah, J.R.M., Wienhold, F.G., Klemetsson, L. and Galle, B. (1994) Measurement of N₂O emission from fertilized grassland using micrometeorological techniques. *Journal of Geophysical Research-Atmospheres*, 99, 16569-16574.

- Hauck, R.D. (1971) Quantitative estimates of nitrogen cycle processes: Concept and review. In *Nitrogen-15 Soil-Plant studies*, IAEA, Vienna, Austria.
- Hauglustaine, D.A., Granier, C., Brasseur, G.P. and Megie, G. (1994) The importance of atmospheric chemistry in the calculation of radiative forcing on the climate system. *Journal of Geophysical Research*, 99, 1173-1186.
- Hayhurst, A.N. and Lawrence, A.D. (1992) Emissions of nitrous oxide from combustion sources. *Progress in Energy Combustion*, 18, 529-552.
- Haynes, R.J. (1986 a) Origin, distribution and cycling of nitrogen in terrestrial ecosystems. In *Mineral nitrogen in the plant soil system*, pp. 127-165 (Ed. Haynes, R.J.) Academic Press Inc..
- Haynes, R.J. (1986 b) Nitrification In *Mineral nitrogen in the plant soil system*, pp. 127-165 (Ed. Haynes, R.J.) Academic Press Inc..
- Haynes, R.J. and Sherlock, R.R. (1986) Gaseous losses of nitrogen. In *Mineral nitrogen in the plant soil system*, pp. 242-302 (Ed. Haynes, R.J.) Academic Press Inc..
- Heys, H.L. (1966) *Physical Chemistry* (3rd Edition). G.G. Harrap and Co. Ltd. London.
- Hilton, B.R., Fixen, P.E. and Woodward, H.J. (1994) Effects of tillage, nitrogen placement, wheel compaction on denitrification rates in the corn cycle of a corn-oats rotation. *Journal of Plant Nutrition*, 17, 1341-1357.
- Hillel, D. (1982) *An Introduction to Soil Physics*. Academic Press, New York.
- Houghton, J.T, Jenkins, G.J. and Ephraums, J.J. (1990) *Climate change: The IPCC scientific assessment*, Intergovernmental Panel on Climate Change. Cambridge University Press, Cambridge.
- Houghton, J.T. (1991) Scientific Assessment of climate change. In *Climate change, Science, Impacts and Policy. Proceedings of the second world climate conference*. pp. 23-44 (Eds. Jager, J. and Ferguson, H.L.) Cambridge University Press, Cambridge.
- Houghton, J.T., Callander, B.A. and Varkey, S.K. (1992) *Climate change 1992: The supplementary report to the IPCC Scientific Assessment*. Cambridge University Press, Cambridge.
- Houghton, J.T. Callander, B.A. and Varkey, S.K. (1995) *Climate Change 1994: Radiative forcing of climate change*. Cambridge University Press, Cambridge.
- Hulgaard, T. and Dam-Johansen, K. (1992) Nitrous oxide sampling, analysis and emission measurements from various combustion systems. *Environmental Progress*, 11, 302-309.

- Hutchinson, G.L., Guenzi, W.D. and Livingstone, G.P. (1993) Soil water controls on aerobic soil emission of gaseous nitrogen oxides. *Soil Biology and Biochemistry*, 25, 1-9.
- IFA: (1992) Nitrogen fertilizer statistics 1986/87 to 1990/91, Information and market research service, A/92/147, *International Fertilizer Industry Association*, Paris, France.
- Johnsson, H., Klemetsson, L., Nilsson, A. and Svensson, B.H. (1991) Simulation of field scale denitrification losses from soils under grass ley and barley. *Plant and Soil*, 138, 287-302.
- Kaplan, W.A. and Wofsey, S.C. (1985) The biogeochemistry of nitrous oxide: a review. *Advances in Aquatic Microbiology*, 3, 181-207.
- Keeney, D.R., Fillery, I.R. and Marx, G.P. (1979) Effect of temperature on gaseous N products of denitrification in soil. *Soil Science Society of America Journal*, 43, 1124-1128.
- Keeney, D.R., Sahrawat, K.L. and Adams, S.S. (1985) Carbon-dioxide concentration in soil - effects on nitrification, denitrification and associated nitrous-oxide production. *Soil Biology and Biochemistry*, 17, 571-573.
- Keller, M., Veldkamp, E., Weitz, A.M. and Reiners, W.A. (1993) Effect of pasture age on soil trace gas emissions from a deforested area of Costa Rica. *Nature*, 365, 244-246.
- Khalil, M.A.K. and Rasmussen, R.A. (1989) Climate induced feedback's for the global cycles of methane and nitrous oxide. *Tellus*, 41B, 554-559.
- Khalil, M.A.K. and Rasmussen, R.A. (1992) The global sources of nitrous oxide. *Journal of Geophysical Research*, 97, 14651-14660.
- Klemetsson, L., Svensson, B.H. and Rosswall, T. (1987) Dinitrogen and nitrous-oxide produced by denitrification and nitrification in soil with and without barley plants. *Plant and Soil*, 99, 303-319.
- Klemetsson, L., Svensson, B.H. and Rosswall, T. (1988) Relationships between soil-moisture content and nitrous-oxide production during nitrification and denitrification. *Biology and Fertility of Soils*, 6, 106-111.
- Klemetsson, L., Simkins, S., Svensson, B.H., Johnsson, H. and Rosswall, T. (1991) Soil denitrification in three cropping systems characterised by differences in nitrogen and carbon supply. II. Water and NO₃⁻ effects on the denitrification process. *Plant and Soil*, 138, 273-286.
- Knight, D., Elliott, P.W., Anderson, J.M. and Scholefield, D. (1992) The role of Earthworms in managed permanent pastures in Devon, England. *Soil Biology and Biochemistry*, 24, 1511-1517.

- Knowles, R. (1981 a) Denitrification. In *Terrestrial Nitrogen cycles, Ecology Bulletin (Stockholm)* 3, 315-329.
- Knowles, R. (1981 b) Denitrification. In *Soil Biochemistry*, pp. 323-369 Vol. 5. (Eds. Paul, E.A. and Ladd, J.M.). Marcel Dekker, New York.
- Knowles, R. and Blackburn, T.H. (1993) *Nitrogen isotope techniques*. Academic Press Ltd., London.
- Koskinen, W.C. and Keeney, D.R. (1982) Effect of pH on the rate of gaseous products of denitrification in a silt loam soil. *Soil Science Society of America Journal*, 46, 1165-1167.
- Kostina, N.V., Stepanov, A.L. and Umarov, M.M. (1994) Study of the complex of nitrous oxide-reducing micro-organisms in the soil. *Eurasian Soil Science*, 26, 81-87.
- Kralova, M., Masscheleyn, P.H., Lindau, C.W. and Patrick jr, W.H. (1992) Production of dinitrogen and nitrous-oxide in soil suspensions as affected by redox potential. *Water Air and Soil Pollution*, 61, 37-45.
- Kroeze, C. (1994) Nitrous oxide and global warming. *The Science of the Total Environment*, 143, 193-209.
- Lashof, D.A. and Ahuja, D.R. (1990) Relative contributions of greenhouse gas emissions to global warming. *Nature*, 344, 529-531.
- Lee, K.E. (1985) *Earthworms: their ecology and relationship with soils and land use*. Academic Press, London.
- Leffelaar, P.A. (1979) Simulation of partial anaerobiosis in a model soil in respect to denitrification. *Soil Science*, 128, 110-120.
- Leffelaar, P.A. (1988) Dynamics of partial anaerobiosis, denitrification and water in a soil aggregate: Simulation. *Soil Science*, 146, 427-444.
- Leffelaar, P.A. and Wessel, W. (1988) Denitrification in a homogenous, closed system: Experiment and simulation. *Soil Science*, 146, 335-349.
- Letey, J., Valoras, N., Hadas, A. and Focht, D.D. (1980 a) Effect of air filled porosity, nitrate concentration and time on the ratio of $N_2O:N_2$ evolution during denitrification. *Journal Environmental Quality*, 9, 227-321.
- Letey, J., Valoras, N., Hadas, A. and Focht, D.D. (1980 b) Effect of pre-incubation treatment on the ratio of $N_2O:N_2$ evolution during denitrification. *Journal Environmental Quality*, 9, 323-335.

- Letey, J., Valoras, N., Focht, D.D. and Ryden, J.C. (1981) Nitrous oxide production and reduction during denitrification as affected by redox potential. *Soil Science Society of America Journal*, 45, 727-730.
- Leuenberger, M. and Siegenthaler, U. (1992) Ice-age atmospheric concentration of nitrous oxide from an Antarctic ice core. *Nature*, 360, 449-451.
- Li, C.S., Frolking, S., and Frolking, T.A. (1992 a) A model of nitrous-oxide evolution from soil driven by rainfall events. 2. Model applications. *Journal of Geophysical Research-Atmospheres*, 97, 9777-9783.
- Li, C.S., Frolking, S., and Frolking, T.A. (1992 b) A model of nitrous-oxide evolution from soil driven by rainfall events. 1. Model structure and sensitivity. *Journal of Geophysical Research-Atmospheres*, 1992, 97, 9759-9776.
- Linn, D.M. and Doran, J.W. (1984) Aerobic and anaerobic microbial populations in no-till and ploughed soil. *Soil Science Society of America Journal*, 48, 794-799.
- Lloyd, D. (1993) Aerobic denitrification in soils and sediments: from fallacies to facts. *TREE*, 8, 352-355.
- Machida, T., Nakazawa, T., Fujii, Y., Aoki, S. and Watanabe, O. (1995) Increase in the atmospheric N₂O concentration during the last 250 years. *Geophysical Research Letters*, 22, 2921-2924.
- Malhi, S.S. and McGill, W.B. (1982) Nitrification in 3 Alberta soils-effect of temperature, moisture and substrate concentration. *Soil Biology and Biochemistry*, 14, 393-399.
- Martikainen, P.J. and Deboer, W. (1993) Nitrous-oxide production and nitrification in acidic soil from a Dutch coniferous forest. *Soil Biology and Biochemistry*, 25, 343-347.
- Martikainen, P.J., Lehtonen, M., Lang, K., Deboer, W. and Ferm, A. (1993) Nitrification and nitrous-oxide production potentials in aerobic soil samples from the soil-profile of a Finnish coniferous site receiving high ammonium deposition. *FEMS Microbiology Ecology*, 13, 113-121.
- Masscheleyn, P.H., Delune, R.D. and Patrick jr, W.H. (1993) Methane and nitrous oxide emissions from laboratory measurements of rice soil suspension: effect of soil oxidation-reduction status. *Chemosphere*, 26, 251-260.
- Mateju, V., Cizinska, S., Krejci, J. and Janoch, T. (1992) Biological water denitrification- a review. *Enzyme and Microbiology Technology*, 14, 170-183
- Matson, P.A. and Vitousek, P.M. (1990) Ecosystem approaches to the development of a source budget for N₂O from moist tropical forests. *Bioscience*, 40, 667-671.

- McCarty, G.W. and Bremner, J.M. (1993) Factors affecting the availability of organic carbon for denitrification of nitrate in subsoils. *Biology and Fertility of Soils*, 15, 132-136.
- McConnaughey, P.K. and Bouldin, D.R. (1985 a) Transient microsite models of denitrification: I. Model development. *Soil Science Society of America Journal*, 49, 886-891.
- McConnaughey, P.K. and Bouldin, D.R. (1985 b) Transient microsite models of denitrification: II. Model results. *Soil Science Society of America Journal*, 49, 891-895.
- Mehran, M. and Tanji, K.K. (1974) Computer modelling of nitrogen transformations in soils. *Journal of Environmental Quality*, 3, 391-396.
- Miller, L.J., Coutlakis, M.D., Oremland, R.S. and Ward, B.B. (1993) Selective inhibition of ammonium oxidation and nitrification-linked N₂O formation by Methyl Fluoride and Dimethyl Ether. *Applied and Environmental Microbiology*, 59, 2457-2464.
- Molina, J.A.E., Clapp, C.E., Shaffer, M.J., Chichester, F.W. and Larson, W.E. (1983) NCSOIL, a model of nitrogen and carbon transformations in soil: description, calibration and behaviour. *Soil Science Society of America Journal*, 47, 85-91.
- Monaghan, R.M., and Barraclough, D. (1993) Nitrous-oxide and dinitrogen emissions from urine-affected soil under controlled conditions. *Plant and Soil*, 151, 127-138.
- Montieth, J.L. and Unsworth, M.H. (1990) *Principles in Environmental physics*, (2nd Edition), Arnold, London.
- Mosier, A.R. and Mack, L. (1980) Gas chromatographic system for precise rapid analysis of nitrous oxide. *Soil Science Society of America Journal*, 1121-1123.
- Mosier, A.R., Parton, W.J. and Hutchinson, G.L. (1983) Modelling nitrous oxide evolution from cropped and native soils. In *Environmental Biogeochemistry, Ecological Bulletin*, 35, pp. 229-241. (Ed. Hallberg, R.) Stockholm.
- Mosier, A.R. and Parton, W.J. (1985) Denitrification in a short-grass prairie, a modelling approach. In *Planetary Ecology* pp. 441-451 (Eds. Caldwell, D.E., Brierley, J.A. and Brierley, C.L.) Van Nostrand Reinhold Co., New York.
- Mosier, A.R., Guenzi, W.D. and Schweizer, E.E. (1986) Soil losses of dinitrogen and nitrous oxide from irrigated crops in north-eastern Colorado. *Soil Science Society of America Journal*, 50, 344-348.
- Mosier, A.R. and Schimel, D.S. (1991) Influence of agricultural nitrogen on atmospheric methane and nitrous oxide. *Chemistry and Industry*, (December) 874-877.

- Mulvaney, R.L. and Kurtz, L.T. (1982) A new method for determination of ^{15}N labelled nitrous oxide. *Soil Science Society of America Journal*, 46, 1178-1184.
- Mulvaney, R.L. and Kurtz, L.T. (1984) Evolution of dinitrogen and nitrous oxide from nitrogen -15 fertilized soil cores subjected to wetting and drying cycles. *Soil Science Society of America Journal*, 48, 596-602.
- Mulvaney, R.L. and Vanden Heuvel, R.M. (1988) Evaluation of ^{15}N tracer techniques for direct measurement of denitrification in soil: IV. Field studies. *Soil Science Society of America Journal*, 52, 1332-1337.
- Mummey, D.L., Smith, J.L. and Bolton, H. (1994) Nitrous-oxide flux from a shrub-steppe ecosystem - sources and regulation. *Soil Biology and Biochemistry*, 26, 279-286.
- Murakami, T., Owa, N. and Kumazawa, K. (1986) A new method for simultaneous determination of the amount of N_2O evolved from soil and its ^{15}N abundance. *Soil Science and Plant Nutrition*, 32, 503-510.
- Myrold, D.D., Elliott, L.F., Papendick, R.I. and Campbell, G.S. (1981) Water potential and water content characteristics of wheat straw. *Soil Science Society of America Journal*, 45, 329-333.
- Myrold, D.D. and Tiedje, J.M. (1985) Establishment of denitrification capacity in soil: effects of carbon, nitrate and moisture. *Soil Biology and Biochemistry*, 17, 819-822.
- Nommik, H. (1956) Investigations on denitrification in soil. *Acta Agriculture Scandinavia*, 6, 195-228.
- Nommick, H. and Larsson, K. (1989) Measurements of denitrification rate in undisturbed soil cores under different temperature and moisture conditions using ^{15}N tracer technique. 2. Factors affecting denitrification. *Swedish Journal of Agricultural Research*, 19, 35-44.
- Nye, P.H. and Tinker, P.B. (1977) *Solute movement in the soil-root system*. Studies in Ecology vol. 4. Blackwell Scientific Publications, Oxford.
- Ohyama, T. and Kumazawa, K. (1987) Characteristics of nitrate respiration of isolated soybean bacteroids. *Soil Science and Plant Nutrition*, 33, 69-78.
- Olivier, J.G.J. (1993) Working group report. Nitrous oxide emissions from fuel combustion and industrial processes. A draft methodology to estimate national inventories. In *Proceedings of the international workshop methane and nitrous oxide: Methods in national emission inventories and options for control*, pp. 347-361 (Ed. Vanamstel, A.M.) Amersfoort, The Netherlands.

- Olivier, J.G.J., Bouwman, A.F., Vandermaas, C.W.M. and Berdowski, J.J.M. (1994) Emission database for global atmospheric research (EDGAR). *Environmental Monitoring and Assessment*, 31, 93-106.
- Page, A.L., Miller, R.H. and Keeney, D.R. (1982) *Methods of Soil Analysis. Part 2. Chemical and Microbiological Properties*. 2nd Edition. No. 9 Agronomy, American Society of Agronomy, Madison, USA.
- Parkin, T.B. and Tiedje, J.M. (1984) Application of a soil core method to investigate the effect of oxygen concentration on denitrification. *Soil Biology and Biochemistry*, 16, 331-334.
- Parkin, T.B. (1987) Soil microsites as a source of denitrification variability. *Soil Science Society of America Journal*, 51, 1194-1199.
- Parkin, T.B., Starr, J.L. and Meisinger, J.J. (1987) Influence of sample size on measurement of soil denitrification. *Soil Science Society of America Journal*, 51, 1492-1501.
- Parkin, T.B. and Meisinger, J.J. (1989) Denitrification below the crop rooting zone as influenced by surface tillage. *Journal of Environmental Quality*, 18, 12-16.
- Parkin, T.B. and Robinson, J.A. (1989) Stochastic models of soil denitrification. *Applied Environmental Microbiology*, 55, 72-77.
- Parkin, T.B. and Berry, E.C. (1994) Nitrogen transformations associated with Earthworm casts. *Soil Biology and Biochemistry*, 26, 1233-1238.
- Parton, W.J., Mosier, A.R. and Schimel, D.S. (1988) Rates and pathways of nitrous oxide production in a short-grass steppe. *Biogeochemistry*, 6, 45-48.
- Paul, J.W., Beauchamp, E.G. and Zhang, X. (1993) Nitrous oxide and nitric oxide emissions during nitrification from manure-amended soil in the laboratory. *Canadian Journal of Soil Science*, 73, 539-553.
- Payne, W.J. (1973) Reduction of nitrogenous oxides by micro-organisms. *Bacteriology Review*, 37, 409-452.
- Powlson, D.S., Saffigna, P.G. and Kragtcoottaar, M. (1988) Denitrification at sub-optimal temperatures in soils from different climatic zones. *Soil Biology and Biochemistry*, 20, 719-723.
- Powlson, D.S. (1993) Understanding the nitrogen cycle. *Soil Use and Management*, 9, 86-94.
- Press, W.H., Flannery, B.P., Teukolsky, S.A. and Vetterling, W.T (1986) *Numerical Recipes*, Cambridge University Press, Cambridge.

- Ramanathan, V., Callis, L., Cess, R., Hansen, J., Saksen, I., Kuhn, W., Lacis, A., Luther, F., Mahlman, J., Reck, R. and Schlesinger, M. (1987) Climate-chemical interactions and effects of changing atmospheric trace gases. *Reviews of Geophysics*, 25, 1441-1482.
- Rasmussen, R.A., Krasnec, J. and Pierott, I.D. (1976) N₂O analysis in the atmosphere via electron capture gas chromatography. *Geophysical Research Letters*, 3, 615-618.
- Robertson, G.P. and Tiedje, J.M. (1987) Nitrous-oxide sources in aerobic soils - nitrification, denitrification and other biological processes. *Soil Biology and Biochemistry*, 19, 187-193.
- Robertson, G.P. (1989) Nitrification and denitrification in humid tropical ecosystems: potential controls on nitrogen retention. In *Mineral nutrients in tropical forest and savannah ecosystems*, (Ed. Procter, J.) Blackwell Scientific, Oxford.
- Robertson, K., Klemedtsson, L., Axelsson, S. and Rosswall, T. (1993) Estimates of denitrification in soil by remote sensing of thermal emission at different moisture levels. *Biology and Fertility of Soils*, 16, 193-197.
- Robertson, L.A. and Kuenen, J.G. (1984) Aerobic denitrification: a controversy revived. *Archives of Microbiology*, 139, 351-354.
- Robertson, L.A. and Kuenen, J.G. (1988) Heterotrophic nitrification in *Thiosphaera pantotropha*- O₂ uptake and enzyme studies. *Journal of General Microbiology*, 134, 857-863.
- Robertson, L.A. and Kuenen, J.G. (1990) Combined heterotrophic nitrification and aerobic denitrification in *Thiosphaera pantotropha* and other bacteria. *International Journal of General and Molecular Biology*, 57, 139-152.
- Rodhe, H. (1990) A comparison of the contribution of various gases to the greenhouse effect. *Science*, 248, 1217-1219.
- Rodriguez, M.B. and Giambiagi, N. (1995) Denitrification in tillage and no-tillage Pampean soils- relationships among soil-water, available carbon and nitrate and nitrous oxide production. *Communications in Soil Science and Plant Analysis*, 26, 3205-3220.
- Rolston, D.E., Hollman, D.L. and Toy, D.W. (1978) Field measurement of denitrification. I. Flux of N₂ and N₂O. *Soil Science Society of America Journal*, 42, 863-869.
- Rosswall, T., Bak, F., Baldocchi, D., Cicerone, R.J., Conrad, R., Ehhalt, D.H., Firestone, M.K., Galbally, I.E., Galchenko, V.F., Groffman, P., Papen, H., Reeburgh, W.S. and Sanhueza, E. (1989) Group report: What regulates production and consumption of trace gases in ecosystems: Biology or physiochemistry? In *Exchange of trace gases between terrestrial ecosystems*

and the atmosphere, pp. 73-95, Life Sciences Research Report 47, Wiley, Interscience.

Rudaz, A.O., Davidson, E.A. and Firestone, M.K. (1991) Sources of nitrous-oxide production following wetting of dry soil. *FEMS Microbiology Ecology*, 85, 117-124.

Russell, E.W. (1988) *Soil conditions and plant growth* (10th Edition), Longmans, London.

Ruz-Jerez, B.E., White, R.E. and Ball, P.R. (1994) Long term measurement of denitrification in three contrasting pastures grazed by sheep. *Soil Biology and Biochemistry*, 26, 29-39.

Ryden, J.C., Lund, L.J. and Focht, D.D. (1978) Direct in-field measurement of nitrous oxide flux from soils. *Soil Science Society of America Journal*, 42, 731-737.

Ryden, J.C., Lund, L.J. and Focht, D.D. (1979) Direct measurement of denitrification loss from soils, I. Laboratory evaluation of acetylene inhibition of nitrous oxide reduction. *Soil Science Society of America Journal*, 43, 104-110.

Sabaty, M., Gans, P. and Vermeglio, A. (1993) Inhibition of nitrate reduction by light and oxygen in *Rhodobacter sphaeroides* forma sp. *denitrificans*. *Archives of Microbiology*, 159, 153-159.

Sahrawat, K.L., and Keeney, D.R. (1986) Nitrous oxide emission from soils. *Advances in Soil Science*, 4, 103-148. Springer Verlag, New York.

Schiller, C.L. and Hastie, D.R. (1994) Exchange of nitrous oxide within the Hudson Bay lowland. *Journal of Geophysical Research*, 99, 1573-1588.

Schimel, D.S. and Potter, C.S. (1995) Process modelling and spatial extrapolation. In *Biogenic Trace gases: Measuring Emissions from soil and water*. pp 358-381 (Eds. Matson, P.A. and Harriss, R.C.). Blackwell Scientific.

Schuster, M. and Conrad, R. (1992) Metabolism of nitric-oxide and nitrous-oxide during nitrification and denitrification in soil at different incubation conditions. *FEMS Microbiology Ecology*, 101, 133-143.

Seech, A.G. and Beauchamp, E.G. (1988) Denitrification in soil aggregates of different sizes. *Science Society of America Journal*, 52, 1616-1621.

Seiler, W. and Conrad, R. (1981) Field measurements of natural and fertilizer induced N₂O release rates from soils. *Journal Air Pollution Control Ass.*, 31, 767-772.

Sexstone, A.J., Parkin, T.B. and Tiedje, J.M. (1985a) Temporal response of soil denitrification rates to rainfall and irrigation. *Science Society of America Journal*, 49, 99-103.

- Sexstone, A.J., Revsbech, N.P., Parkin, T.B. and Tiedje, J.M. (1985b) Direct measurement of oxygen profiles and denitrification rates in soil aggregates. *Science Society of America Journal*, 49, 645-651.
- Shoun, H., Kim, D., Uchiyama, H. and Sugiyama, J. (1992) Denitrification by fungi. *FEMS Microbiology Letters*, 94, 277-282.
- Skiba, U., Smith, K.A. and Fowler, D. (1993) Nitrification and denitrification as sources of nitric-oxide and nitrous-oxide in a sandy loam soil. *Soil Biology and Biochemistry*, 25, 1527-1536.
- Skiba, U., Fowler, D. and Smith, K.A. (1994) Emissions of NO and N₂O from soils. *Environmental Monitoring and Assessment*, 31, 153-158.
- Smith, C.J., Wright, M.F. and Patrick jr., W.H. (1983) The effect of soil redox potential and pH on the reduction and production of nitrous oxide. *Journal Environmental Quality*, 12, 186-188.
- Smith, C.J. and Patrick jr, W.H. (1983) Nitrous oxide emission as affected by alternate anaerobic and aerobic conditions from soil suspensions enriched with ammonium sulphate. *Soil Biology and Biochemistry*, 15, 693-697.
- Smith, K.A. and Dowdell, R.J. (1973) Gas chromatographic analysis of the soil atmosphere: Automatic analysis of gas samples for O₂, N₂, Ar, CO₂ and C₁-C₄ hydrocarbons. *Journal Chromatographical Science*, 11, 655-658.
- Smith, K.A. (1980) A model of the extent of anaerobic zones in aggregated soils and its potential application to estimates of denitrification. *Journal of Soil Science*, 31, 263-277.
- Smith, K.A. and Arah, J.R.M. (1990) Losses of nitrogen by denitrification and emissions of nitrogen oxides from soils. Proceedings of the Fertilizer Society, No. 299, 1-34.
- Smith, K.A., Clayton, H., Arah, J.R.M., Christensen, S., Ambus, P., Fowler, D., Hargreaves, K.J., Skiba, U., Harris, G.W., Wienhold, F.G., Klemedtsson, L. and Galle, B. (1994 a) Micrometeorological and chamber methods for measurement of nitrous-oxide fluxes between soils and the atmosphere - overview and conclusions. *Journal of Geophysical Research-Atmospheres*, 99, 16541-16548.
- Smith, K.A., Scott, A., Galle, B., and Klemedtsson, L. (1994 b) Use of a long-path infrared gas monitor for measurement of nitrous-oxide flux from soil. *Journal of Geophysical Research-Atmospheres*, 99, 16585-16592.
- Smith, K.A., Clayton, H., McTaggart, I.P., Thomson, P.E., Arah, J.R.M., and Scott, A. (1995) The measurement of nitrous-oxide emissions from soil by using chambers. *Philosophical Transactions of The Royal Society of London; Series A-Physical Sciences And Engineering*, 351, 327-337.

- Smith, M.S. and Parsons, L.L. (1985) Persistence of denitrifying enzyme activity in dried soils. *Applied and Environmental Microbiology*, 49, 316-320.
- Somerfield, R.A., Mosier, A.R. and Musselman, R.C. (1993) CO₂, CH₄ and N₂O flux through a Wyoming snowpack and implications for global budgets. *Nature*, 361, 140-142.
- Stayley, T.E., Caskey, W.H. and Boyer, D.G. (1990) Soil denitrification and nitrification potentials during the growing season relative to tillage. *Soil Science Society of America Journal*, 54, 1602-1608.
- Stephens, G.L. and Tjemkes, S.A. (1993) Water vapour and its role in the Earth's greenhouse. *Australian Journal of Physics*, 46, 149-166.
- Svensson, B.H., Klemedtsson, L., Simkins, S., Paustian, K. and Rosswall, T. (1991) Soil denitrification in three cropping systems characterized by differences in nitrogen and carbon supply. *Plant and Soil*, 138, 257-271.
- Tate, R.L. (1995) Denitrification. In *Soil Microbiology*, pp. 334-358. John Wiley and Sons, New York.
- Taylor, J.A. (1992) A global 3 dimensional lagrangian tracer transport modelling study of the sources and sinks of nitrous oxide. *Mathematics and Computers in simulation*, 33, 597-602.
- Thomsen, J.K., Iversen, J.J.L. and Cox, R.P. (1993) Interactions between respiration and denitrification of *Thiosphaera pantotropa* in continuous culture. *FEMS Microbiology Letters*, 110, 319-324.
- Tiedje, J.M., Sorensen, J. and Chang, Y.Y.L. (1981) Assimilatory and dissimilatory nitrate reduction: perspectives and methodology for simultaneous measurement of several nitrogen cycle processes. In *Terrestrial Nitrogen Cycles*. 33, pp. 31-342 (Eds. Clark, F.E. and Rosswall, T.) Ecological Bulletin (Stockholm).
- Tiedje, J.M. (1982) Denitrification. In *Methods of Soil Analysis, Part 2*. 2nd Edition, pp. 1011-1026 (Eds. Page, A.L., Miller, R.H. and Keeney, D.R.). American Society of Agronomy, Madison.
- Tisdale, S.L., Nelson, W.L. and Beaton, J.D. (1985) *Soil Fertility and Fertilizers*, (4th Edition), Macmillan, London.
- Van Cleemput, O., Abboud, S. and Baert, L. (1988) Denitrification and interaction between its intermediate compounds. In *Nitrogen Efficiency in Agricultural Soils*, pp. 302-311 (Eds. Jenkinson, D.S. and Smith, K.A.) Elsevier Applied Science, New York.
- Van Cleemput, O., Vermoesen, A., Degroot, C.J. and Van Ryckeghem, K. (1994) Nitrous-oxide emission out of grassland. *Environmental Monitoring And Assessment*, 31, 145-152.

- Van Veen, J.A. and Frissel, M.J. (1979) Mathematical modelling of nitrogen transformations in soil. In *Modelling nitrogen from farm wastes*, pp. 133-157 (Ed. Gasser, J.F.K.) Applied Science Publication Ltd. London.
- Webster, E.A. and Hopkins, D.W. (in press) Nitrogen and isotope ratios of nitrous oxide emitted from soil and produced by nitrifying bacteria. *Biology and Fertility of Soils*, In Press.
- Webster, E.A. and Hopkins, D.W. (in press) Contributions from different microbial processes to N₂O emission from soil under different water regimes. *Biology and Fertility of Soils*.
- Weier, K.L. and Gilliam, J.W. (1986) Effect of acidity on denitrification and nitrous-oxide evolution from Atlantic coastal-plain soils. *Soil Science Society of America Journal*, 50, 1202-1205.
- Weier, K.L., Doran, J.W., Power, J.F. and Walters, D.T. (1993) Denitrification and the dinitrogen nitrous-oxide ratio as affected by soil-water, available carbon, and nitrate. *Soil Science Society of America Journal*, 57, 66-72.
- Wentworth, W.E., Chen, E. and Freeman, R. (1971) Thermal electron attachment to nitrous oxide. *Journal Chemistry and Physics*, 55, 2075-2078.
- Wiehnhold, F.G., Welling, M. and Harris, G.W. (1995) Micrometeorological measurement and source region analysis of nitrous oxide fluxes from an agricultural soil. *Atmospheric Environment*, 29, 2219-2227.
- Willison, T.W. and Anderson, J.M. (1991) Dicyandiamide as an inhibitor of denitrification in coniferous forest soils. *Soil Biology and Biochemistry*, 23, 605-607.
- White, R.E. (1981) *Introduction to the principles and practice of Soil Science*. Blackwell Scientific Publications, Oxford.
- Wild, (1993) Soils, the atmosphere, global warming and ozone depletion. In *Soils and the environment: An introduction*, pp. 211-232. Cambridge University Press, Cambridge.
- Wiljer, J. and Delwiche, C.C. (1954) Investigations on the denitrification process in soil. *Plant and Soil*, 5, 155-169.